Purification of Free Chondroitin Sulphate Chains and Their Effects on Chondrogenesis of BMSCs

Jingyi Feng

MBBCh, MCh, MSc

A thesis submitted for the degree of Doctor of Philosophy

Cardiff University

January 2025

Table of Contents

Abstract

Background

Cartilage defects can occur in various anatomical locations. Since articular cartilage has limited repair capacity, tissue engineering aims to restore it by mimicking its mature cell and matrix structure. Chondroitin sulphate (CS) has shown promise due to its role in replicating native cartilage extracellular matrix (ECM) and supporting chondrocyte function or stem cell chondrogenesis. The aims of this project were to develop and optimise strategy for CS purification from bovine articular cartilage, and to investigate the effects of CS on chondrocyte phenotype and bovine bone marrow stem cell (bBMSCs) chondrogenesis.

Methods

Bovine *metacarpophalangeal* joint cartilage was employed to extract proteoglycans by 4M guanidine-HCl and density gradient centrifugation. Alkaline treatment using sodium borohydride ($NaBH_4$), released CS from aggrecan core protein. Further purification by anion-exchange chromatography and size-exclusion chromatography was conducted to separate CS from other molecules. Purified CS was analysed by glyco-analyses and proton nuclear magnetic resonance (^{1}H-NMR) to determine the sulphation pattern. The effects of different concentrations of CS on chondrocyte phenotype was determined in 2D and 3D agarose cultures systems. This was extended to study the effect of CS chains on the chondrogenesis of bBMSC in monolayer, 2% agarose constructs and the Transwell^{TM} system. RT-PCR was employed to examine chondrogenic gene marker expression, including *col2a1*, *sox-9* and *acan*. Immunohistochemical staining was utilised to evaluate ECM composition.

Results

CS was isolated from bovine cartilage with purity of 96.47±1.90% (chondroitinase ABC digestion method) and 87% (carbazole reaction) where CS-4 was the predominant constituent, comprising 78.3% of purified CS. Purified CS facilitated chondrocyte *sox-9* gene expression significantly (10-fold, $p<0.001$) on 0.1μg/cm^2 CS-coated substrate. Chondrogenesis of bBMSCs was improved with the addition of 100μg/ml CS in chondrogenic medium by enhancing ECM deposition and the expression of *sox-9* on both monolayer (2.2-fold, $p<0.05$) and the Transwell^{TM} system (3.7-fold, $p<0.001$).

Conclusion

This thesis optimised a methodology to purify high-quality CS (predominantly CS-4) from bovine cartilage and demonstrated its role in enhancing ECM deposition and *sox-9* expression in chondrocytes and BMSCs. The findings highlight CS as a promising biochemical cue for cartilage tissue engineering and regenerative medicine.

Acknowledgements

First and foremost, I would like to express my deepest gratitude to my supervisors, Dr. Emma Blain and Prof. Clare Hughes. Their invaluable support, guidance, and encouragement have been the pillars that helped me reach this stage. The journey of pursuing a PhD has been anything but easy, but from them, I not only learned the principles of scientific research but also experienced significant personal growth. In this place far from home, they have witnessed every step of my progress and provided care and support in all aspects of my life.

I am also immensely thankful to Dr. Sophie Gilbert, Dr. Paul White, Yixin Wang (Zoe), Dr. Ryan Jones, and Dr. Irina Guschina. Your companionship and assistance throughout this journey have been invaluable. Whenever I encountered challenges in my research, your timely advice and guidance made even the toughest obstacles seem manageable.

I would like to express my sincere gratitude to Professor Fuchuan Li, Professor Wenshuang Wang and their team at China National Glycoengineering Research Centre based at Shandong University, for their generous assistance in the determination of the purity and analysis of my CS samples. The support was instrumental to the progress of this project, and I deeply appreciate their time, expertise, and kind collaboration.

To my family and friends, thank you all for surrounding me with love, for your constant encouragement, patience, and understanding. Thank you to my husband, Dun, meeting you in Cardiff, 5000 miles away from our home cities, has been the most beautiful chapter of this journey. Together, we completed our PhDs and grew ourselves, supported each other, and shared our love and motivation every step of the way. Finally, I want to express my deepest appreciation to my mother, Jinfeng Li. She raised me on her own since I was 4 years old, pouring her endless love and patience into supporting every decision I made. Her guidance and unwavering understanding have shaped me into the person I am today, and I am proud to be her daughter.

Abbreviations

ACAN: Aggrecan

ACE: Angiotensin-Converting Enzyme

ACI: Autologous Chondrocyte Implantation

ACS: Acute Coronary Syndrome

ADAMTS: A Disintegrin and Metalloproteinase with Thrombospondin Motifs

AGE: Advanced Glycation End-products

ANOVA: Analysis of Variance

AP: Alkaline Phosphatase

ARC: Apoptosis-Related Cysteine Protease

BCA: Bicinchoninic Acid

BCIP: 5-Bromo-4-Chloro-3-Indolyl Phosphate

BMP: Bone Morphogenetic Protein

BMSC: Bone Marrow Stem Cells

BSA: Bovine Serum Albumin

CAIA: Collagen Antibody-Induced Arthritis

CFU: Colony-Forming Unit

COL: Collagen

COMP: Cartilage Oligomeric Matrix Protein

CPC: Cetylpyridinium Chloride

CS: Chondroitin Sulphate

CTAB: Cetyltrimethylammonium Bromide

DMEM: Dulbecco's Modified Eagle's Medium

DMMB: Dimethylmethylene Blue

DMSO: Dimethyl Sulfoxide

DNA: Deoxyribonucleic Acid

DPX: Dibutylphthalate Polystyrene Xylene

DS: Dermatan Sulphate

DSHB: Developmental Studies Hybridoma Bank

DTT: Dithiothreitol

ECM: Extracellular Matrix

EDTA: Ethylenediaminetetraacetic Acid

ELISA: Enzyme-Linked Immunosorbent Assay

ERK: Extracellular Signal-Regulated Kinase

ESC: Embryonic Stem Cells

FACS: Fluorescence-Activated Cell Sorting

FAK: Focal Adhesion Kinase

FBS: Foetal Bovine Serum

FDA: Fluorescein Diacetate in Acetone

FGF: Fibroblast Growth Factor

FITC: Fluorescein Isothiocyanate

FN: Fibronectin

FTIR: Fourier-Transform Infrared Spectroscopy

GAG: Glycosaminoglycan

HA: Hyaluronic Acid

HBSS: Hank's Balanced Salt Solution

HIF-1α: Hypoxia-inducible factor-1 alpha

HPLC: High-Performance Liquid Chromatography

HS: Heparan Sulphate

HSC: Hematopoietic Stem Cells

HYAL: Hyaluronidase

IBMX: Isobutylmethylxanthine

IGD: Immunoglobulin Domain

IGF: Insulin-Like Growth Factor

IHC: Immunohistochemistry

IL: Interleukin

ITS: Insulin-Transferrin-Selenium

KS: Keratan Sulphate

LPS: Lipopolysaccharide

LTD: Long-Term Depression

MAPK: Mitogen-Activated Protein Kinase

MEM: Minimal Essential Medium

MMP: Matrix Metalloproteinase

MRI: Magnetic Resonance Imaging

MSC: Mesenchymal Stem Cells

MTT: Methyl Thiazolyl Tetrazolium

MW: Molecular Weight

NBT: Nitro Blue Tetrazolium

NC: Negative Control

NMR: Nuclear Magnetic Resonance

NO: Nitric Oxide

OA: Osteoarthritis

OPG: Osteoprotegerin

PAGE: Polyacrylamide Gel Electrophoresis

PBS: Phosphate-Buffered Saline

PCL: Polycaprolactone

PFA: Paraformaldehyde

PG: Proteoglycan

PI: Propidium Iodide

PLGA: Poly(Lactic-co-Glycolic Acid)

PMSF: Phenylmethylsulfonyl Fluoride

PNPX: para-nitro-phenyl- b-xyloside

PTOA: Post-Traumatic Osteoarthritis

PVDF: Polyvinylidene Fluoride

RANK: Receptor Activator of Nuclear Factor κB

RANKL: Receptor Activator of Nuclear Factor κB Ligand

RGD: Arginine-Glycine-Aspartate

RNA: Ribonucleic Acid

ROS: Reactive Oxygen Species

RT-PCR: Real Time – P0lymerase Chain Reaction

SD: Standard Deviation

SDS: Sodium Dodecyl Sulphate

SOX: SRY-Box Transcription Factor

SYSADOA: Symptomatic Slow-Acting Drugs for Osteoarthritis

TGF: Transforming Growth Factor

TLR: Toll-Like Receptor

TNF: Tumour Necrosis Factor

Chapter 1

General Introduction

1.1 Tissue Engineering Approaches for Articular Cartilage Repair

Articular cartilage damage is a significant cause for osteoarthritis (OA) and a major clinical problem, bringing a huge economic burden to society. Since cartilage is an avascular tissue with limited self-repairing capacity, injuries often progress to joint degeneration if left untreated. Tissue engineering offers innovative approaches to regenerate or repair damaged cartilage by combining cells, signalling factors and biomaterials (Chung and Burdick, 2008).

1.2 Articular Chondral Defect

Articular chondral defects such as osteochondral dissecans can often lead to early onset of post-traumatic osteoarthritis (PTOA) and early treatment intervention using autologous chondrocyte implantation (ACI) has in part been successful in treating such disorders so preventing or further delaying PTOA (Section 1.3). The procedure involves implantation of chondrocytes into a cartilage defect, chondrocytes are harvested from a low-weight-bearing region of the patient's own joint followed by *in vitro* expansion. This tissue-engineering strategy has been applied in clinics for several decades, with two great advantages: autologous chondrocytes are used to reduce the immune or infection complications, and the process of *in vitro* chondrocyte culture minimises the defects of donor sites (Minas et al., 2014). However, this method fails to guide the synthesis and organisation of the matrix after implantation which is thought to be one of the primary reasons for unsatisfying outcomes. Matrix-induced autologous chondrocyte implantation (MACI) inherits the benefits of ACI but involves seeding chondrocytes onto collagen membranes (Marlovits et al., 2012) to offer better structural support for cellular growth. Nevertheless, little improved efficacy is observed among the patients after MACI than those after ACI (Zeifang et al., 2010), so more clinical trials and basic research are necessary to identify their performance. HA-based scaffolds are also demonstrated to maintain the phenotype of chondrocytes and promote the synthesis of collagen with many studies reporting hyaline-like cartilage deposition examined a year after implantation (Grigolo et al., 2002); however, this HA-based method needs a longer recovery time before extensive weight-bearing. Although the scaffold-based ACI approach for cartilage repair is

approved by some European countries and the Food and Drug Administration (FDA) in US, comparative studies with long-term follow up are still needed to understand the benefits and drawbacks (Makris et al., 2015). More effort is also required to explore the utilisation of various scaffold materials and seeding cells, as well as the optimal ratio of them.

Recent studies demonstrate that utilising mesenchymal stem cells (MSCs) (refer to Section 1.4.2) and induced pluripotent stem cells (iPSCs) for cartilage regeneration shows promise (Wang et al., 2024, Chang et al., 2020). Advances in stem cell biology and differentiation protocols are key to developing effective treatments. Engineering biocompatible scaffolds that mimic the native ECM and support chondrocyte growth and differentiation is a critical area of research. Integrated with this are innovations in 3D printing and nanotechnology which aim to enhance scaffold design to produce hyaline-like cartilage for transplantation.

1.3 Post-traumatic Osteoarthritis (PTOA)

PTOA is a form of secondary OA that develops after joint injury, such as ligament tears, meniscal damage, or direct cartilage trauma, which is a top cause of disability globally (Dilley et al., 2023). Unlike primary OA, PTOA often affects younger, active individuals and progresses more rapidly. PTOA mainly remains asymptomatic after injury, however, the biomechanical effects occur immediately after the injury on the whole joint, including meniscus, ligament, synovial tissue, cartilage and subchondral bone (Olson et al., 2012).

Injury to articular cartilage results in compromised structural integrity and mechanical functionality of cartilage. The dysregulation manifests as an imbalance in ECM homeostasis, leading to progressive degradation of collagen fibres and proteoglycans (PGs), which are critical for maintaining the load-bearing capacity and resilience of cartilage. This process underpins conditions such as primary osteoarthritis (OA) and secondary PTOA.

The development and progression of OA involves many inflammatory molecules, cytokines and signalling pathways. Matrix degradation products from fibronectin,

decorin or collagen bind to integrin and toll like receptors (TLR), initiating intracellular signalling pathways via nuclear factor-κB (NF-κB), to upregulate the expression of proinflammatory cytokines such as interleukin-1 (IL-1), -6, -8 and matrix metalloproteinases (MMPs). A disintegrin and metalloproteinase with thrombospondin motif (ADAMTS), further destroying the ECM (Loeser, 2014). Fibronectin fragments (FN-f) can be produced by transitory or long-term overloading; therefore, they are recognised as important mediators of cartilage ECM damage (Hwang et al., 2015). Integrins and TLRs can also bind with FN-fs, leading to the activation of NF-κB and downstream cascades, boosting the production and activity of MMPs, nitric oxide (NO) and prostaglandin E2 (PGE2) (Kim et al., 2006). Moreover, FN-fs are demonstrated to augment the formation of cartilage oligomeric matrix protein (COMP) (a marker for ECM turnover) and the degradation of collagen-binding molecules (Johnson et al., 2004).

Non-physiological or immoderate loads also have an influence on cartilage metabolism, which results in disruption to the balance of anabolism against catabolism, with activated enzyme activity leading to the degradation of structural components. Excessive load is defined by several important factors, including the frequency of the force applied, the peak stress and the duration of the loading period (Sauerland et al., 2003). If one or more factors exceed the normal range, cartilage damage occurs. At the onset of damage, the content of PGs distinctly declines whilst collagen synthesis elevates, but there is a shift from collagen type II to collagen type I expression (Lahm et al., 2010). Collagen type I is mainly situated in the subchondral bone and it cannot interact with PGs well, which consequently undermines the resilience of cartilage and its ECM structure when collagen type I levels increase (Poole et al., 2002, Martel-Pelletier et al., 2008). A few studies have discovered the thickness of cartilage increases following overloading compared to physiological loading as a result of the hyperproliferation of chondrocytes that produce more PGs to compensate – but this makes cartilage more susceptible to compression forces and internal damage (Henao-Murillo et al., 2021). When sustained non-physiological load is applied, levels of collagen synthesis decrease. Even though this trend cannot be examined or detected at an early stage (Figure 1.1B), the fibrillation of cartilage and visible fissures appear afterwards (Nam et al., 2011). Both the articular cartilage and

the subchondral bone can be degraded over a period of years as shown in figure 1.1C and 1.1D.

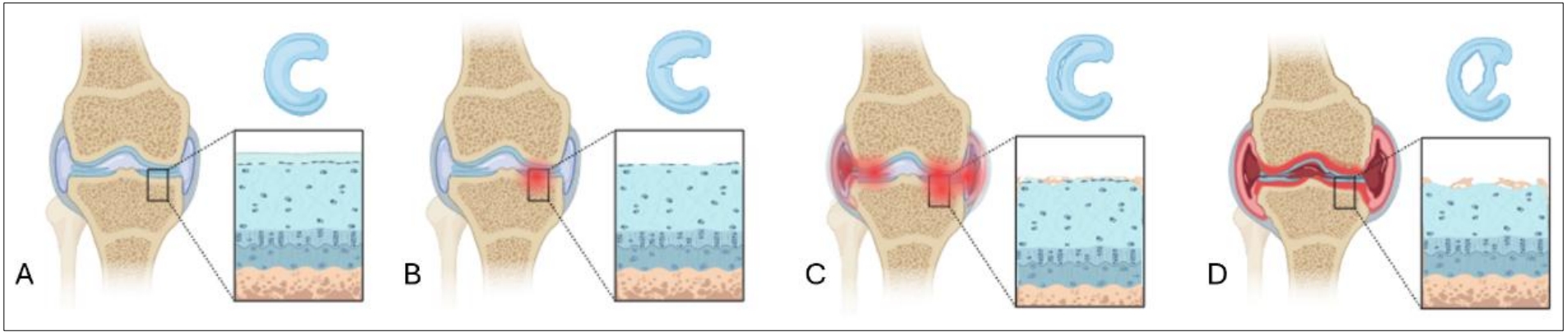

Figure 1.1 Schematic illustration of the development of OA. *The healthy cartilage (A) can withstand the load and provide smooth surface that allows the joint surfaces to move interrupted over one another. Due to certain factors including aging, obesity and injury, the cartilage damage and minimum disruption happens (B). The cartilage starts to break down with the release of enzymes from chondrocytes (C). Joint-space narrows and the gaps in the cartilage can expand until they reach the bone (D). The exposure of the underlying subchondral bone results in sclerosis, followed by reactive remodelling changes that lead to the formation of osteophytes. The joint space is progressively reduced over time and considerable amount of cartilage is lost, bringing worse and worse pain and stiffness to the patients.*

1.4 Cells

Natural healing or tissue engineered options for healing of articular cartilage requires understanding of chondrocytes, chondroprogenitors and bone marrow derived mesenchymal stem cells in the next few sections these cell types will be discussed.

1.4.1 Chondrocyte

Chondrocytes are a highly specialised and differentiated cell found exclusively in cartilage. They derive from foetal pluripotent mesenchymal stem cells that grow and form densely aggregated chondrogenic progenitor cells in the presence of diverse chondrogenic growth factors and signals (chondrification). When the progenitor cells are exposed to these molecules and/or other stimuli, mature chondrocytes arise. Although chondrocytes normally take up a relatively small percentage of cartilage mass (approximately 1-10% of total tissue volume) (Bhosale and Richardson, 2008), chondrocytes are the sole cell type existing in healthy cartilage tissue and are responsible for the homeostasis of the tissue i.e. production and destruction of the ECM. Chondrocytes are embedded in the matrix that they secrete, with the matrix exhibiting a concentric arrangement around the chondrocytes since the matrix is secreted in a successive manner. Each chondrocyte is situated in an oblong cavity surrounded by the ECM, called lacunae, which is built by a single cell. However, when undergoing mitotic division, up to eight cells can be found in a lacuna (Sapra., 2021). On account of the avascular character of cartilage, chondrocytes metabolise under low oxygen tension where they produce energy through anaerobic glycolysis and lactic acid is generated (Gale et al., 2019).

Following cell division, the phenotype of chondrocytes begins to change, and the cells turn into hypertrophic chondrocytes, referred to as a terminally differentiated status. As hypertrophy starts, the chondrocytes enlarge, up to 20-fold in size (Hallett et al., 2021), and synthesise collagen type X instead of collagen type II (Wu et al., 2021) (Figure 1.2). Finally, they transition into an osteo-lineage and express bone matrix components (Tsang et al., 2015), which is the process of endochondral ossification.

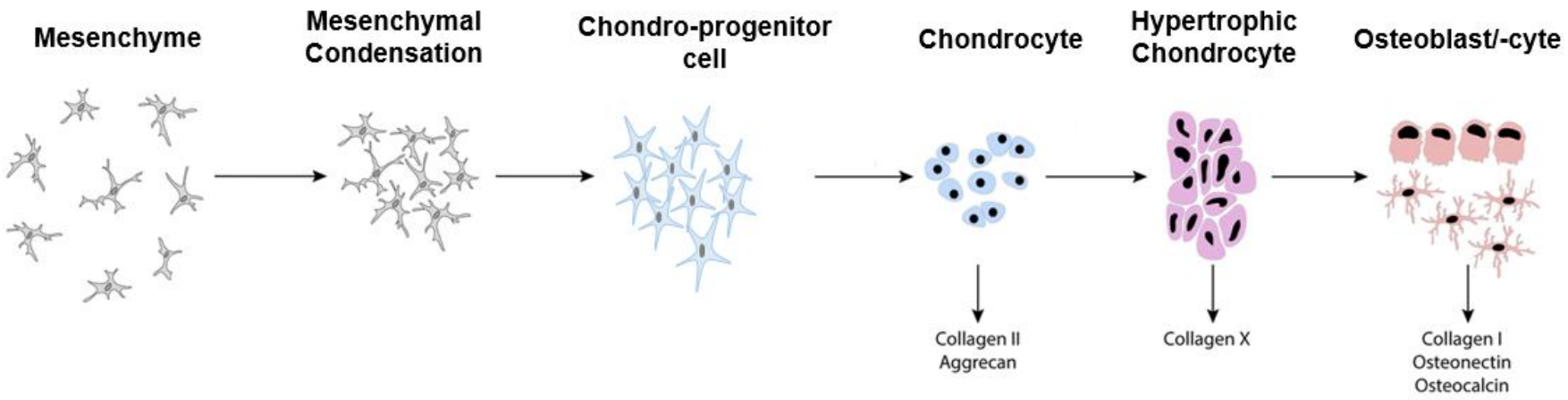

Figure 1.2 The fate of MSCs to chondrocytes. *Pluripotent mesenchymal stem cells condense and multiply into chondro-progenitor cells, which subsequently develop into chondrocytes (primarily in foetal period). Chondrocyte is the sole kind of cell in cartilage and secrete cartilage matrix components. Following numerous cell divisions, the phenotype of chondrocytes is further differentiated into osteoblasts/cytes (mainly in adulthood) (Adapted from Gillis (2019)).*

1.4.1.1 Chondrocyte Behaviour and Phenotypic Plasticity

Chondrocytes are essential for maintaining the articular cartilage tissue's structural and functional integrity through their synthesis and turnover of ECM components. The study of chondrocyte behaviour and phenotypic plasticity has gained significant attention due to its implications for cartilage development, repair and disease (Tallheden et al., 2003). Phenotypic plasticity refers to the ability of chondrocytes to change their phenotype in response to environmental cues, including hypertrophy, dedifferentiation, trans-differentiation, which has profound implications for cartilage biology and is crucial for cartilage development, repair, and adaptation to pathological conditions (Sommer, 2020). Chondrocytes exhibit remarkable phenotypic plasticity, allowing them to adapt to various physiological and pathological conditions by altering their phenotype. Their cellular behaviours include proliferation, matrix synthesis, response to mechanical stimuli, etc. (Zheng et al., 2021).

In the growth plate during development, chondrocytes undergo proliferation, contributing to the longitudinal growth of bones. The regulation of chondrocyte proliferation is controlled by signalling pathways such as the Indian hedgehog (Ihh)/parathyroid hormone-related protein (PTHrP) axis and fibroblast growth factor (FGF) signalling (Minina et al., 2002). Chondrocytes are responsible for producing the ECM components, primarily type II collagen and aggrecan, which provide the structural framework and mechanical properties of cartilage. The anabolic activity of chondrocytes is influenced by growth factors such as TGF-β and IGF-1 (Wu et al., 2024a). During growth plate development, hypertrophic chondrocytes orchestrate the calcification of cartilage and its subsequent vascular invasion, leading to bone formation, which is termed as endochondral ossification, where chondrocytes undergo hypertrophy, characterised by increased cell size and the expression of type X collagen and MMPs (Sun and Beier, 2014). Hypertrophic chondrocytes facilitate cartilage calcification and subsequent replacement by bone.

Chondrocytes are highly responsive to mechanical loading, which is crucial for maintaining cartilage health. They transduce mechanical stimuli through integrins (e.g., integrin α5β1), mechanosensitive ion channels, and primary cilia, triggering cytoskeletal rearrangements and downstream biochemical events (Loeser, 2014,

Dieterle et al., 2021). Moderate, cyclic mechanical loading promotes anabolic activity by stimulating ECM synthesis, enhancing cartilage strength and resilience, and even exerting anti-inflammatory effects via HDAC6-dependent pathways associated with primary cilia elongation (Jia et al., 2023). In contrast, excessive or abnormal loading—whether due to injury, obesity, or other factors—can induce catabolic responses that upregulate matrix-degrading enzymes such as MMPs and aggrecanases, ultimately leading to ECM degradation and chondrocyte apoptosis (Charlier et al., 2019). Additionally, in response to injury or in-vitro culture conditions, chondrocytes can dedifferentiate, losing their cartilage-specific phenotype in favor of a fibroblast-like morphology characterized by reduced synthesis of type II collagen and aggrecan with a concomitant increase in type I collagen production (Wang et al., 2022a). Under certain pathological conditions, such as osteoarthritis, chondrocytes may also transdifferentiate into other cell types or acquire a hypertrophic-like phenotype, further contributing to cartilage degradation and disease progression (Wang et al., 2022a).

1.4.1.2 Regulation of Chondrocyte Activity

Chondrocytes play a pivotal role in maintaining the structure and function of cartilage tissue through their ability to synthesise and degrade ECM components. The regulation of chondrocyte activity is crucial for cartilage development, repair, and disease progression since they are responsible for synthesising and remodelling key ECM components, such as type II collagen and PGs, which are essential for cartilage's load-bearing and shock-absorbing properties. The regulation of chondrocyte activity is a highly dynamic process influenced by a combination of mechanical, biochemical, and environmental cues, ensuring cartilage homeostasis under normal physiological conditions and driving cartilage degeneration in pathological states.

Biochemical signals from the local joint environment tightly regulate chondrocyte activity. Growth factors, such as TGF-β and IGF-1, stimulate ECM synthesis and promote cartilage repair (Goldring et al., 2008). Conversely, inflammatory cytokines, like IL-1β and TNF-α, trigger catabolic pathways, increasing the production of MMPs and pro-inflammatory mediators (Chadda and Puthucheary, 2024). The balance between anabolic and catabolic signals is critical for maintaining cartilage

homeostasis (figure 1.3), and its disruption leads to pathological conditions such as OA (Mueller and Tuan, 2011). The molecular marker crosstalk network of diverse signalling pathways, amongst TGF-β/Smad, Wnt/β-catenin, RANK/RANKL/OPG and MAPK pathways, is the basis of OA development and they can also become the treatment targets of OA drug (Zhou et al., 2020).

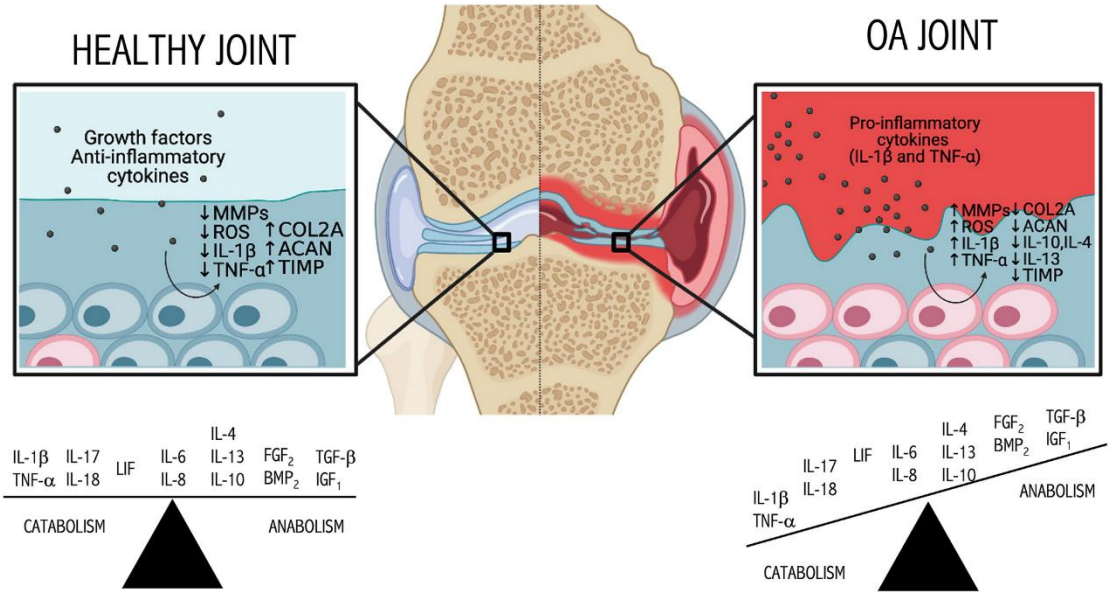

Figure 1.3 Regulation of cartilage health by biochemical signals. *In healthy articular cartilage, regulatory proteins, e.g. TGF-β and IGF-1, involved in chondrocyte metabolism primarily promote anabolic activities. Chondrocytes typically remain in a quiescent state with minimal turnover, maintaining a stable balance between anabolic and catabolic processes. However, during the onset of OA, this equilibrium is disrupted by an increase in pro-inflammatory cytokines, such as 1β and TNF-α (Segarra-Queralt et al., 2022).*

The unique avascular, aneural, and hypoxic environment of articular cartilage influences chondrocyte behaviours. Hypoxia-inducible factor-1 alpha (HIF-1α) plays a pivotal role in adapting chondrocytes to low oxygen levels by promoting the synthesis of ECM components and inhibiting apoptosis (Guo et al., 2022). As for nutrient availability mediated by synovial fluid diffusion, it also affects chondrocyte metabolism and ECM production (An et al., 2022). Due to being located deeper in cartilage, chondrocytes are more susceptible to oxygen and glucose deprivation compared to the cells in other anatomical locations, which can lead to reduced ECM production and low self-repair (Housmans et al., 2022).

Aging is also a vital factor for cartilage health and chondrocyte behaviours, which is highly related to primary OA. With aging, chondrocytes exhibit reduced anabolic activity and increased senescence, impairing their ability to maintain the ECM of collagen and PGs (Li et al., 2013c). This dysregulation is characterised by a shift toward a catabolic phenotype, exacerbating cartilage degeneration and predisposing joints to OA (Jørgensen et al., 2017). Additionally, environmental and biochemical factors such as chronic low-grade inflammation further disrupt the balance between anabolic and catabolic processes in aged cartilage. In disordered cartilage, the dysregulation of chondrocyte activity plays a central role in cartilage degradation, where pro-inflammatory cytokines like IL-1β and TNF-α promote catabolic pathways in chondrocytes, leading to increased production of MMPs and aggrecanases that degrade the ECM (Segarra-Queralt et al., 2022). Understanding the regulatory mechanisms of chondrocytes is crucial for developing therapeutic strategies to halt or reverse chondral disorder progression.

1.4.2 Bone Marrow Mesenchymal Stem Cells

1.4.2.1 BMSCs Classification and Characterisation

Bone marrow stem cells (BMSCs) are a heterogeneous population of cells with remarkable potential for self-renewal and differentiation, playing a crucial role in tissue regeneration and repair. These stem cells are broadly categorised into hematopoietic stem cells (HSCs) and mesenchymal stem cells (MSCs), each with distinct characteristics and functions. The classification and characterization of BMSCs are fundamental for understanding their biology and therapeutic potential (Bonnet, 2003).

MSCs can proliferate extensively while maintaining their multipotency. MSCs can differentiate into cells of mesodermal origin, such as bone, cartilage, and fat cells (Kuroda et al., 2011). They typically express markers such as CD73, CD90, and CD105, and lack hematopoietic markers like CD34 and CD45 (Ghazanfari et al., 2017). The surface markers of MSCs are often used to authenticate and classify the stem cells harvested from bone marrow in the lab, via fluorescence-activated cell sorting (FACS) (Zheng et al., 2018). Colony-forming assays are also used to evaluate

the clonogenic potential of BMSCs by assessing their ability to form colonies *in vitro*, where fibroblast colony-forming unit (CFU-F) assays are specifically used for MSCs (Robey et al., 2014). Differentiation assays are also performed to test the multipotency of BMSCs (Robey et al., 2014) into osteoblasts, chondrocytes, and adipocytes, which is the strategy we employed to authenticate MSCs primarily isolated in current study.. Besides, the plastic-adherent ability of MSCs is also commonly applied to the isolation of them.

The classification and characterisation of BMSCs have significant implications for both basic research and clinical applications. Understanding the properties of MSCs is essential for developing stem cell-based therapies for a range of conditions of tissue engineering, which highlights their significance in regenerative medicine and offering insights into future research directions (Kwon et al., 2018).

1.4.2.2 Application of BMSCs in Cartilage Regeneration

Cartilage injuries and degenerative diseases, including OA, present significant clinical challenges due to the limited self-repair capacity of cartilage tissue. In recent years, the application of BMSCs in cartilage regeneration has emerged as a promising therapeutic strategy, owing to the unique properties of these cells to enhance tissue repair and restore function. Embryonic stem cell (ESC) was a prevalent option for tissue engineering and regeneration but fewer researchers are using ESCs at present because of their potential risk of tumorigenicity and teratoma (Ben-David and Benvenisty, 2011). The immune exemption characteristic and lower adverse effects also indicate the superiority of MSCs compared to other stem cells. Under the influence of specific growth factors and mechanical stimuli, BMSCs can differentiate into chondrocytes producing ECM components (Harrell et al., 2019).

Apart from the capacity of BMSCs to differentiate into chondrocytes stimulated by diverse growth factors, BMSCs also can release trophic factors that enhance the regenerative capacity of resident chondrocytes, stimulate ECM synthesis, and modulate immune responses to create a pro-repair environment (Qing et al., 2011). BMSCs were reported to downregulate the growth of T lymphocytes and suppress the synthesis of PGE_2 and other pro-inflammatory molecules (Bouffi et al., 2010). BMSCs produce exosomes that are engaged in regulatory B cell-mediated IL-10

secretion to enhance joint cartilage lesion repair (Wu et al., 2022). The extracellular vesicles (EVs) from human BMSCs were also reported to inhibit inflammation-related genes expression, especially IL-1β, and promote expression of chondrogenic genes, such as *COL2A1*, restraining early OA development and cartilage damage (Liu et al., 2018). BMSCs possess immunomodulatory properties that can reduce inflammation and prevent further cartilage damage, which is particularly beneficial in inflammatory joint diseases (Kwon et al., 2022).

The various application approaches of BMSCs explored in the last decades for cartilage regeneration make their clinical treatment feasible. BMSCs can be directly injected into the affected joint, where they migrate to the site of injury and contribute to tissue repair through differentiation and paracrine signalling. A randomised, double-blinded controlled study has demonstrated efficacy of BMSC use in alleviating joint pain and discomfort to improve joint mobility (Gupta et al., 2016). Treatment of OA using autologous BMSCs injections together with dexamethasone was confirmed by MRI to repair and promote growth of knee cartilage and meniscus (Iijima et al., 2018); range of motion and pain scores were also improved after 3 months of injections (Iijima et al., 2018). BMSCs can be genetically modified to overexpress specific growth factors, anti-inflammatory cytokines or specific proteins, enhancing their regenerative potential and providing a targeted therapeutic approach for cartilage repair. Chen et al. (2016) discovered chondromodulin-1 (Chm-1) was a chondrogenic phenotype-related gene and it is expressed at a high level in chondrocytes; hence, they employed an adenovirus to transduce BMSCs with Chm-1 before these modified BMSCs, constitutively expressing Chm-1, were applied to engineer cartilage *in vivo*. Genetically modified human BMSCs were found to promote a good chondrogenic phenotype by histological assays in the engineered cartilage. Upregulated expression of *TGF-β* by recombinant adeno-associated viral vector-mediated gene transfer was also reported to promote the chondrogenesis of primary BMSCs with increased production of *cartilage matrix* via SOX-9 pathway (Frisch et al., 2014).

BMSCs are combined with biocompatible scaffolds and growth factors that mimic the native ECM, providing structural support and enhancing cell viability and differentiation. These scaffolds can be implanted into cartilage defects to promote

regeneration; for example, BMSCs have been encapsulated into silk fibroin/chitosan scaffolds supplemented with nerve growth factor to repair articular cartilage defects in rabbit knees, with the constructs promoting chondrogenic repair in cartilage lesion sites (Zhang et al., 2024). Lu et al. (2018) modified self-assembling peptide (SAP) RADA16-I (RAD, Ac-(RADA)4-NH2) with the addition of functional peptide sequence PFS (PFSSTKT). Then BMSCs were embedded into the SAP/PFS scaffold for *in-vitro* culture and implanted them into rabbit knee cartilage defect, the composite hydrogel scaffold enhanced the recruitment of MSCs with $CD29^{+}/CD90^{+}$ double positive markers after 7 days and increased the cartilage-associated gene markers, including *acan* and *col2a1*. The results of micro-CT and MRI confirmed the cartilage defects have been fully repaired by the tissue similar to surrounding native cartilage after 3 months post-surgery.

1.5 Articular Cartilage

An understanding of articular cartilage structure and function is central to design of tissue engineered intervention. The following sections review the current literature in this area.

1.5.1 Articular Cartilage and its Features

Articular cartilage (AC) refers to a very thin connective tissue layer (typically 2-4mm thick in humans) covering the end of bones of diarthrodial articulation (Guo et al., 2024), and is a specialised type of hyaline cartilage. The principal function of articular cartilage is to provide a lubricated and smooth surface for joint articulation, as well as to increase the transmission of load to underlying subchondral bone with a low-friction coefficient. Mature articular cartilage does not have nerves, lymphatics or blood vessels, but unlike other cartilage tissues which depend on nutrient diffusion from the outer perichondrium, articular cartilage relies on nourishment from synovial fluid in the joint capsule that is continuous with the periosteum of joint bones and surrounds the articulating surfaces. AC receives nutrition from synovial fluid by either diffusion that is a slow process, or via convection which is a more effective way. The latter method provides a theoretical foundation for the finding that moderate

compression and movement of joints facilitates the production of synovial fluid as well as the nourishment of chondrocytes – the only cell type in AC (Eckstein et al., 2006).

1.5.2 Major Constituents of Articular Cartilage Extracellular Matrix

The ECM is a complex 3-dimensional network of extracellular molecules and inorganic minerals. It supports the chondrocytes embedded within it both structurally and biochemically so that cells can perform their normal physiological role, based on the expression and proportion of these components in the tissue. In cartilage, the ECM does not only segregate it from other tissues, but also contributes a paramount role in cell communication, cell adhesion and dynamic cellular behaviours (Gao et al., 2014). In addition, Cai and colleagues (2020) also found that the stiffness and elasticity of the ECM has the potential to guide the cross-talk between chondrocytes in cartilage via regulating the expression of fibronectin and transmembrane receptor connexin (Cx43); this is meaningful as it demonstrates the importance of the ECM constituents and corresponding stiffness in regulating the processes of cartilage healing, fibrosis, cell migration and gene expression.

1.5.2.1 Water

Water accounts for as much as 80% of cartilage mass; a small volume exists in the chondrocytes as cytoplasm to ensure basic metabolism, a third is resident amongst the collagen fibrils, while the remaining other half is present in the pore space of the ECM (Maroudas et al., 1991). Water performs as a solvent to dissolve inorganic ions and active molecules, as well as a reactor to initiate and control various biochemical reactions. Water is critical to achieve the viscoelastic properties of cartilage; the water flows through the cartilage ECM enabling the tissue to withstand compressive loads (Yamabe et al., 2017), where the interstitial water is pressurised to support most of the applied load. The biphasic behaviour and osmotic pressure will be further introduced in following sections.

1.5.2.2 Collagen

The most abundant collagen in articular cartilage is type II, a fibril-forming collagen which can be visualised as rod-like fibrils under an electron microscope. It is a fibrillar collagen synthesised by chondrocytes in articular cartilage, which forms the structural backbone of cartilage, providing tensile strength and structural integrity. The molecular structure of type II collagen is characterised by a triple helix, consisting of three alpha-1 (II) chains. This helical structure allows it to form strong, rope-like fibrils that are crucial for the mechanical properties of cartilage. AC comprises type II collagen accounting for approximately 90-95% of the total collagen content, making it the predominant collagen type (Miosge et al., 2004). The collagen fibrils form a dense network that provides tensile strength and contributes to the tissue's ability to resist shear forces (Zeng et al., 2019). This network also helps maintain the shape and resilience of the cartilage, which is essential for counteracting the swelling forces in cartilage to achieve its load-bearing function (Zimmerman et al., 2021), a phenomenon referred to as the Donnan effect.

Type II collagen forms heterotypic fibril through interactions with type IX (Kadler et al., 2008) and Type XI. Collagen type IX is a non-fibrillar collagen predominantly found in cartilage, where it associates with the surface of type II collagen fibrils. It is composed of three alpha chains: alpha-1 (IX), alpha-2 (IX), and alpha-3 (IX) (Sun et al., 2020). This collagen type plays a critical role in the ECM by stabilising the collagen fibril network and facilitating interactions between collagen fibres and other matrix components (Diab et al., 1996). Type IX collagen acts as a bridge between collagen fibrils and proteoglycans, contributing to the tensile strength and resilience of cartilage (He and Karsdal, 2016), which is essential for maintaining the structural integrity of cartilage and ensuring its ability to withstand mechanical stress. Type XI collagen is also essential for regulating the fibril size and spacing of type II collagen fibrils and maintaining the structural organisation of the ECM (Sophia Fox et al., 2009). Hence, the interaction between type II, type IX and type XI collagen plays a significant role in ensuring the proper formation and function of cartilage. This heterotypic network contributes to the tissue's mechanical strength, load distribution, and resistance to compressive and tensile forces (Alcaide-Ruggiero et al., 2021).

1.5.2.3 Proteoglycans and Glycosaminoglycans

Proteoglycans (PGs) are essential components of the cartilage ECM, contributing to its biomechanical properties and resilience (Alcaide-Ruggiero et al., 2023). These macromolecules consist of a core protein to which multiple glycosaminoglycan (GAG) chains are covalently attached. The most abundant PG in cartilage is aggrecan, which plays a crucial role in maintaining cartilage hydration and mechanical integrity (Knudson and Knudson, 2001). Further introduction about PGs in articular cartilage will be given in section 1.6.

GAGs are long, linear polysaccharides composed of repeating disaccharide units, which carry negative charges due to sulphate and carboxyl groups (Perez et al., 2023). Major GAGs in cartilage include chondroitin sulphate (CS) and keratan sulphate (KS). These GAGs attract and retain water within the matrix, creating an osmotic swelling pressure that allows cartilage to resist compressive forces (Zimmerman et al., 2021). Section 1.7 will give more introduction about GAGs in articular cartilage.

The interaction between aggrecan and hyaluronic acid, facilitated by link proteins, forms large proteoglycan aggregates that enhance cartilage's ability to absorb mechanical loads. This water-retaining capacity is vital for cartilage’s viscoelastic behaviour, enabling it to distribute compressive forces efficiently (Bayliss et al., 2000).

Any imbalance in PG composition or degradation of GAGs, as seen in OA, leads to a loss of hydration and reduced mechanical performance, ultimately contributing to cartilage degeneration (Gauci et al., 2017).

1.5.3 Structural and Biochemical Composition of Articular Cartilage

The sparsely distributed chondrocytes are surrounded by the dense matrix mainly consisting of water, collagen and proteoglycans (PGs). Together with collagen fibrils, mainly collagen type II throughout articular cartilage tissue along with collagen type VI, IX and XI, chondrocytes are organised into multiple zones in AC without anatomical boundary—the superficial zone, the middle zone, the deep zone and the calcified zone, each with specific cellular arrangements and ECM compositions

tailored to its mechanical demands. In different zones, chondrocytes exhibit diverse morphology and behaviours, and diverse collagen fibril alignment.

The superficial zone represents 10%-20% of cartilage volume, and it is the outermost layer and plays a critical role in the mechanical strength of cartilage by withstanding mechanical forces experienced at the joint surface, including shear stress and tensile forces, whilst providing protection and maintenance for deeper zones (Poole et al., 2001). This zone is primarily composed of type II collagen with the presence of minor collagens, particularly types IX and XI that interact with type II collagen to stabilise the fibrillar network, and type VI collagen aiding in cell-matrix communication. The type II collagen fibrils in the superficial layer are small in diameter and organised parallel to the articular surface, and they are packed tightly with flattened chondrocytes embedded within (Figure 1.4 SZ) (Killen and Charalambous, 2020). Type XI collagen integrates into type II collagen fibrils, controlling the diameter and ensuring uniform fibril size (Alcaide-Ruggiero et al., 2021). Type VI collagen are present in the pericellular matrix of chondrocytes in cartilage and provide additional support in cell-matrix interactions (Pullig et al., 1999). Furthermore, lubricin, also known as superficial-zone protein, is primarily found in the cartilage surface and topmost layer, contributing to reducing friction and wear at the joint surface (Jay and Waller, 2014).

In the underlying layer referred to as the middle zone, chondrocytes are less abundant and more spherical in shape. This zone takes up 40%-60% of the cartilage depth, containing obliquely arranged thicker and larger collagen type II fibrils, where type XI collagen regulates type II collagen fibrillogenesis (Sophia Fox et al., 2009). Type IX collagen is discovered in this zone as a cross-linker between type II collagen and other molecules to maintain cartilage integrity (Diab et al., 1996). Cartilage oligomeric matrix protein is expressed to stabilise matrix components (Posey et al., 2018). As for the deep zone, representing the other 30% of cartilage volume, it is characterised by the highest PG concentration, the lowest water content, and the thickest collagen type II fibrils that are aligned perpendicular to the joint surface, so this zone consequently offers the greatest resistance to compressive forces. Chondrocytes are typically aligned parallel to the collagen type II fibrils yet perpendicular to the cartilage surface, and in columnar orientation (Wang et al.,

2022b). The calcified zone is continuous with the deep zone, where chondrocytes are extremely rare and are hypertrophic in the calcified zone. The ECM consists of network-forming collagen, type X collagen, which is mainly expressed in hypertrophic chondrocytes and anchor to subchondral bone to facilitate endochondral ossification (Shen, 2005). The main function of the calcified zone is to secure cartilage to the underlying bone, which it does by anchoring the collagen fibrils in the deep zone of cartilage to the subchondral bone. Moreover, it also participates in providing resistance to compressive forces.

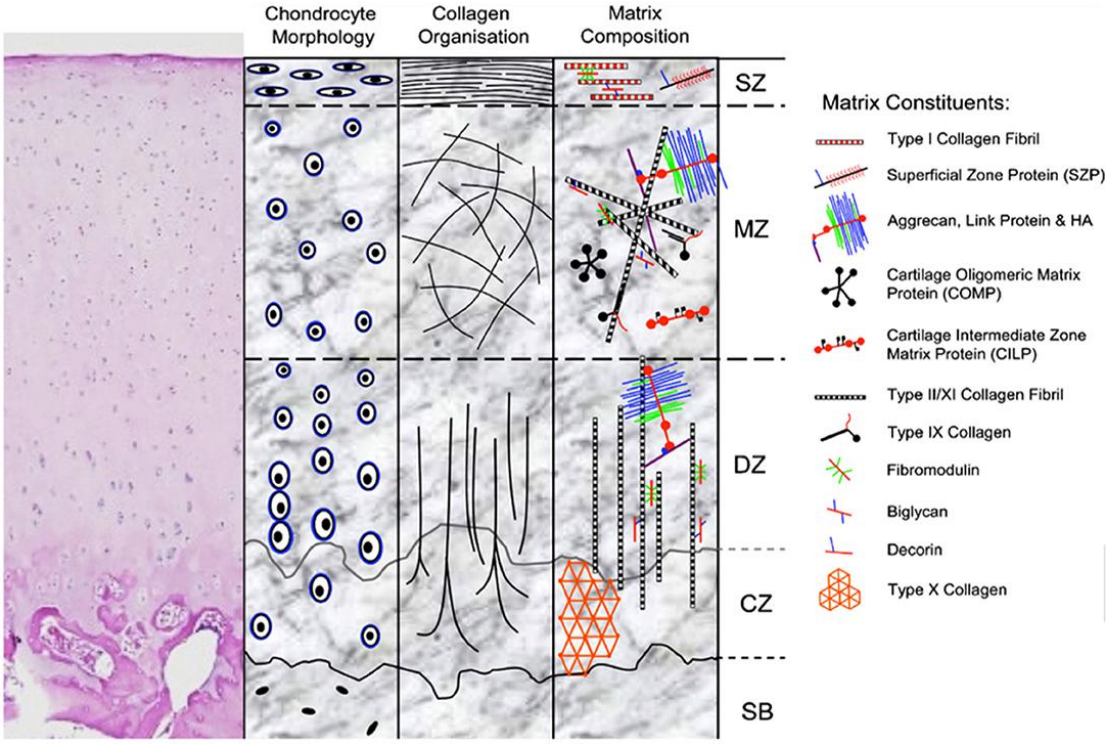

Figure 1.4 A cross-sectional Haematoxylin and Eosin (H&E) stain and schematic diagram of healthy articular cartilage structure. *This shows the arrangement of chondrocytes, the collagen fibril organisation and matrix composition in the four histological zones: superficial zone (SZ), middle zone (MZ), deep zone (DZ), calcified zone (CZ) of articular cartilage (Francis et al., 2018).*

Apart from depth-dependent zonal differences in structure and ECM constituents, each zone is further categorised into three regions based on the proximity of the chondrocytes with the collagen fibril architecture — referred to as the pericellular, territorial and interterritorial region — each with specific compositional and functional characteristics (Figure 1.5).

The pericellular region is most adjacent to chondrocytes as its name implies, where PGs (e.g. syndecan), along with some glycoproteins (e.g. fibronectin) and non-collagenous proteins (e.g. CD44), are major components; ECM molecules in this region are important in initiating signal transduction pathways in response to load. The territorial region contains abundant collagen fibrils which contribute to cartilage resiliency and capability of load bearing. The interterritorial region is the largest one and the a forementioned organisation of collagen bundles in each zone is primarily determined by this region. Additionally, given the enrichment of PG in this region, the interterritorial region contributes most to the biomechanical properties of cartilage (Sophia Fox et al., 2009).

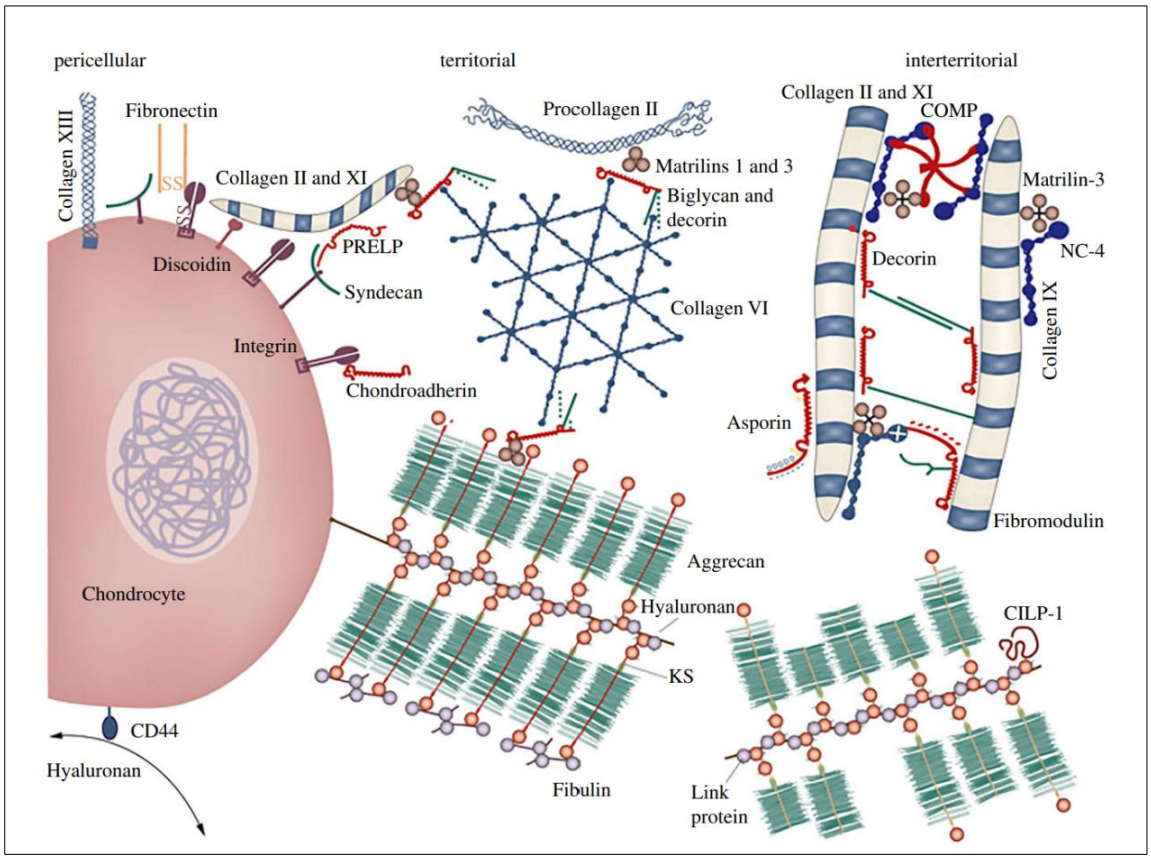

Figure 1.5 Schematic for the relative position and composition of three matrix regions in articular cartilage—pericellular, territorial and interterritorial region as it spans away from the chondrocytes respectively *(Lindahl, 2015). The pericellular matrix (left), immediately surrounding the chondrocytes, is rich in proteoglycans and serves as a biochemical and mechanical interface. The territorial matrix (middle), enclosing the collagen fibrils for structural support. The interterritorial matrix (right), located further from the chondrocytes, has a more dispersed collagen fibre arrangement and contributes to the overall mechanical properties of the cartilage.*

1.5.4 Mechanical Properties of Articular Cartilage

The mechanical properties of AC are essential for its function, as they allow the cartilage to withstand substantial loads, distribute stress, and provide a low-friction surface for joint articulation. Understanding these mechanical properties is crucial for comprehending how cartilage performs under physiological conditions and how it responds to injury and degenerative diseases such as OA. The collagen and PGs provide the cartilage with its characteristic properties: viscoelasticity, compressive stiffness, tensile strength, and low frictional resistance.

One of the defining mechanical features of articular cartilage is viscoelasticity, which allows it to exhibit both elastic and viscous behaviour under loading. This property enables the cartilage to absorb shock and dissipate energy, protecting the underlying bone and maintaining joint function. The interplay between the fluid phase (water and soluble ions) and the solid phase (collagen and proteoglycans) within the ECM is key to this viscoelastic behaviour (Desrochers et al., 2012). The fluid phase depends on the flow of interstitial fluid and the flow of synovial fluid through cartilage. Once mechanical loading is applied onto the joints, the interstitial fluid pressure increases immediately, resulting in the interstitial fluid escape from the ECM (Sophia Fox et al., 2009), but the tissue deformation happens in a time-dependent way since the fluid cannot flows out through the ECM instantaneously (Eschweiler et al., 2021). When the loading is eased, the interstitial fluid flows back to the cartilage. Solid phase contributes to the compressive stiffness, enabling cartilage to bear and distribute loads across the joint surface. This stiffness is primarily due to the negative electrostatic repulsion forces between interstitial fluid and proteoglycan aggregates, where their mutual repulsion of negative charges of the glycosaminoglycan chains leads to the PG molecules swelling and spreading. With the compression, the PG aggregates are pressed closer together, which intensifies the negatively repulsive force and conveys the compressive stiffness to the cartilage, thereby the collagen network provides additional structural support, ensuring that the cartilage maintains its shape and function under load (Sun et al., 2016).

AC also exhibits a unique biomechanical property known as Donnan pressure, which arises due to the presence of negatively charged PGs within the cartilage matrix (Zimmerman et al., 2021). These charged molecules attract positively charged

counterions, leading to an osmotic pressure difference between the cartilage and surrounding fluid (Zeng et al., 2019). This phenomenon plays a crucial role in maintaining cartilage hydration, providing resistance to compressive forces, and facilitating nutrient exchange. Donnan pressure contributes significantly to the functional integrity of articular cartilage, ensuring its ability to withstand mechanical loads and support joint mobility. Understanding this mechanism is essential for studying cartilage biomechanics and developing treatments for degenerative conditions such as osteoarthritis (Eschweiler et al., 2021).

Tensile strength, provided by the the heterotypic fibrils of type II, IX and XI collagen, is essential for withstanding the tensile forces that occur during joint movement to balance Donnan osmotic swelling. The orientation and their intermolecular cross-linking vary across the depth of the cartilage (Aspden and Hukins, 1989), contributing to its ability to resist shear and tensile stresses.

Low frictional resistance is critical for joint lubrication and smooth movement, the coefficient of friction can be as low as 0.001 under physiological pressure (An et al., 2022). Lubricin, a type of PG, also known as proteoglycan 4, exists in the synovial fluid and the surface of AC to antagonise abnormal cellular adhesion and overgrowth (Lee et al., 2018), leading to a significant reduce of friction coefficient (Waller et al., 2013). Furthermore, some molecules, including HA and phospholipids, are regarded as lubricants for joint movement (Sorkin et al., 2013, Radin et al., 1970).

1.6 Proteoglycans

Proteoglycans (PG) are composed of a core protein to which are covalently attached repeating disaccharide units called glycosaminoglycans (GAGs) (Figure 1.6a), the total mass of which represents 10-15% of cartilage wet weight (Mankin and Lippiello, 1971). The disaccharide structure and sulphation pattern determine four classes of GAGs: chondroitin sulphate/dermatan sulphate (CS/DS), keratan sulphate (KS), heparin/heparan sulphate and HA; the number and composition of GAG chains further classify the diverse PG types.

Proteoglycans can link to other PGs, such as HA to form large molecular weight aggregates e.g. aggrecan, or attach to proteins, like collagen to support the ECM architecture. Non-aggregating PGs, including decorin and fibromodulin, are much smaller than aggrecan but maintain important roles in collagen fibrillogenesis and the interaction between fibres (Burton-Wurster et al., 2003). Biglycan, another small PG, is believed to interact with collagen type VI in the immediate vicinity of chondrocytes as a prerequisite for assembly of collagen type VI beaded filament (Rajasekaran et al., 2020), thereby implicating its involvement in mechanotransduction. There is also some evidence that biglycan might be a mediator of cartilage ageing (Barreto et al., 2015).

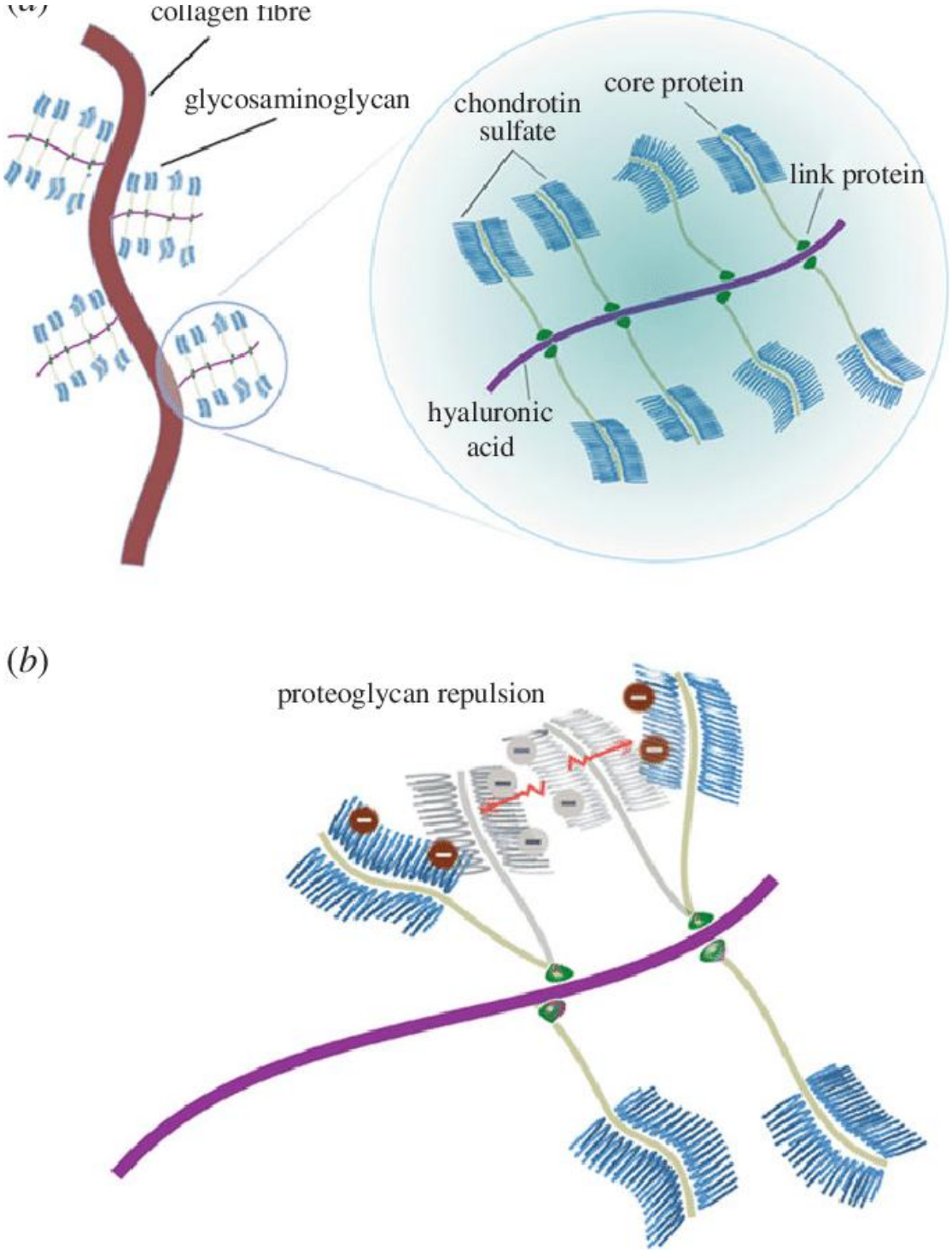

Figure 1.6 Schematic representation of cartilage ECM networks. *PGs composed of GAGs and core proteins can be attached to HA via link protein, which exists in the intrafibrillar space among collagen fibrils (a) to maintain tissue integrity and function mechanical duties. PG chains separate from one another due to charge repulsion (b) to increase the available space and maximise biomechanical properties(Manzano et al., 2015).*

1.6.1 Aggrecan

Aggrecan is the major proteoglycan in cartilage and contains chondroitin sulphate (CS) and keratan sulphate (KS) attached to the core protein with a bottlebrush-like shape. As one of the members of the lectican family who all have highly conserved globular domains while the extended regions are less well conserved (Doege et al., 1991), the aggrecan core proteins typically have three globular domains which are abbreviated as G1, G2 and G3 from N-terminal to C-terminal, respectively. From G2 to G3, KS and CS chains are attached, forming a relatively short KS-enriched region and a longer CS-enriched region (Figure 1.7). Although each core protein has the potential to interact with tens even hundreds of GAG molecules, these GAGs extend out from the core protein separately from each other due to repulsion charge (Figure 1.6b), serving as one mechanism of cartilage for withstanding stress and shear forces with the interactions with collagen network and other ECM components (Cavalcante et al., 2005). Furthermore, they enable cartilage hydration since they possess a high affinity for water and attraction to cations (Mattson et al., 2017). It is found mainly non-covalently bind to HA to form large multi-molecular aggregates stabilised by a link protein (Figure 1.7). These aggregates are of high hydrophilicity and negative-charged density, which are enriched in the interterritorial matrix in cartilage.

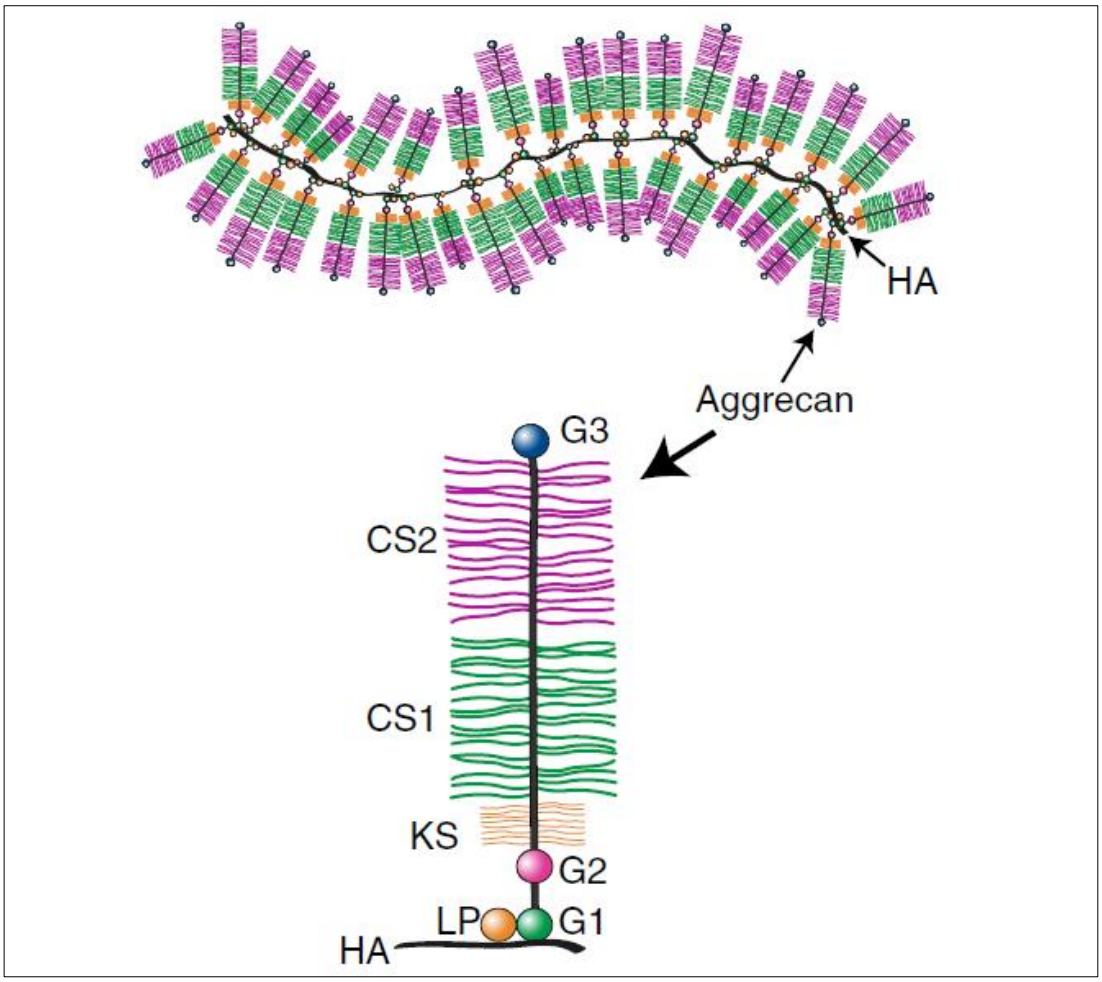

Figure 1.7 Schematic figure for structure of aggrecan and HA complex. *Globular domain 1 (G1) of aggrecan links to HA via link protein (LP), KS-rich domain and 2 CS-rich domains lies between globular domain 2 (G2) and globular domain 3 (G3) domains.(Roughley and Mort, 2014).*

1.6.2 Lubricin

The maintenance of joint function and cartilage integrity is crucial for mobility and overall musculoskeletal health. The low-friction environment in articular cartilage is maintained by a complex interaction of structural components within the cartilage matrix and synovial fluid. Among these, lubricin, also known as proteoglycan 4 (PRG4), plays a pivotal role in cartilage lubrication and protection. Structurally, lubricin consists of mucin-like domain in the middle with hydrophilic oligosaccharides extending out from core protein between two somatomedin B-like (SMB) domains in one end and a hemopexin-like (PEX) domain in the other end (Figure 1.8 A). These terminal domains interplay with other molecules in cartilage ECM or synovial fluid, for example, lubricin synergises and connects with HA in synovial fluid to enhance joint lubrication and maintain synovial fluid viscosity to ensure smooth articulation.

Lubricin is primarily synthesised by synovial fibroblasts and superficial zone chondrocytes. It is heavily glycosylated and able to form a hydrophilic boundary layer over the articular cartilage surface (Figure 1.8 B, C and D) to reduce friction in articulation, especially under conditions of high shear and low load (Jay and Waller, 2014). The presence of lubricin prevents the apoptosis of chondrocytes by protecting the superficial layer when cartilage is subject to mechanical wear and enzymatic degradation (Waller et al., 2013). Roggio et al. (2023) found that lubricin inhibits the adhesion of synovial cells, proteins and inflammatory molecules to cartilage surface, which mitigates the risk of joint inflammation and cartilage fibrosis.

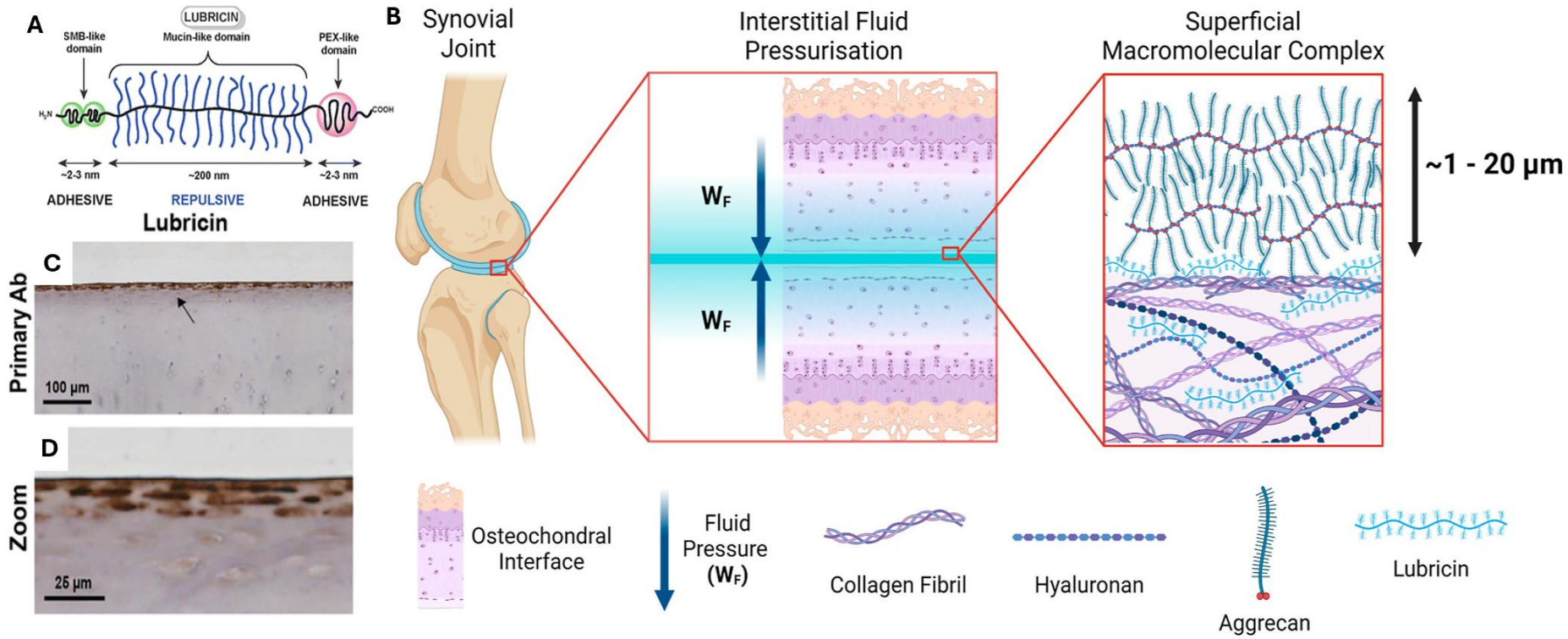

Figure 1.8 Structure and localisation of lubricin in articular cartilage. *[A] Schematic representation of lubricin's molecular structure with SMB-like, mucin-like domain and PEX-like domains. [B] Schematic illustration of lubricin localisation within the joint and its distribution on the surface and in the topmost layer of articular cartilage. [C] and [D] Immunohistochemical staining of lubricin in joint tissue sections demonstrating its presence in the superficial zone of articular cartilage.*

1.6.3 Small Leucine-rich Proteoglycans

Small leucine-rich proteoglycan (SLRP) is a family of PGs characterised by harbouring relatively small (36-42kDa) protein core and leucine-rich repeat (LRR) domains (Farrán et al., 2018). They are classified into several subfamilies based on sequence homology and functional properties, such as decorin, biglycan, fibromodulin and lumican, etc.

Decorin is a critical and abundant SLRP consisting of a CS or dermatan sulphate GAG chain at its N-terminus, which involved in collagen fibrillogenesis and ECM assembly (Gubbiotti et al., 2016). It binds to collagen type I and II fibrils, regulating their diameter and spacing, which is essential for maintaining the tensile strength of cartilage (Chen and Birk, 2013). Additionally, decorin exerts regulatory effects on aggrecan aggregation by increasing the adhesion between aggrecans and between aggrecan and collagen II fibrils, herein, cartilage aggrecan network integrity and its biomechanical functions can be modulated by decorin (Han et al., 2019). Decorin has also been reported to regulate the activity of MMPs and inhibit excessive ECM degradation, studies showing that decorin-null mice exhibit accelerated cartilage degradation and increased susceptibility to OA (Chery et al., 2021).

Biglycan is another important SLRP that plays a role in matrix assembly and cellular signalling. It binds to growth factors such as BMPs and TGF-β, influencing cartilage development, homeostasis and repair (Wu et al., 2016). Biglycan is also involved in inflammatory response regulation, interacting with TLRs to mediate immune signalling. Its deficiency can result in abnormal ECM organisation and increased susceptibility to cartilage degradation (Roedig et al., 2019).

Fibromodulin primarily functions in collagen fibril organisation and mechanical resilience (Kalamajski et al., 2016). It binds to collagen fibrils, influencing their alignment and diameter, which is essential for cartilage biomechanical properties. Fibromodulin also regulates MMP activity and immune response, preventing excessive collagen degradation (Zhao et al., 2023). Its reduced expression has been associated with weakening of cartilage structure and increased degradation in osteoarthritic joints (Monfort et al., 2006). Additionally, fibromodulin is involved in

the regulation of oxidative stress within cartilage, reducing reactive oxygen species (ROS) levels and protecting chondrocytes from apoptosis (Zeng-Brouwers et al., 2020).

Lumican contributes to collagen network stabilisation and hydration in cartilage. It regulates the spacing and organisation of collagen fibrils, ensuring optimal load-bearing capacity (Barreto et al., 2020). Lumican also interacts with cell surface receptors, integrin α2β1, to modulate mechanotransduction, chondrocyte behaviour and prevent premature matrix breakdown (Brézillon et al., 2013). Its dysregulation has been linked to increased ECM degradation and loss of cartilage integrity in OA since lumican mediate TLR-4 involved inflammation activation (Barreto et al., 2018).

1.7 Glycosaminoglycans

Glycosaminoglycans (GAGs), previously known as mucopolysaccharides, are negatively charged polysaccharides composed of repeating disaccharide units. From terminology, the ‘glyco-’ and ‘aminoglycan’ describes the two constituents of the disaccharides. The ‘glyco-’ refers to the uronic acid (glucuronic acid or iduronic acid) or galactose, and the ‘aminoglycan’ means hexosamine, including glucosamine and galactosamine. Both the variation of the pairs of monosaccharides and the degree of sulphation, determine the major categories of GAGs, including HA, heparin/heparan sulphate, chondroitin sulphate/dermatan sulphate, and keratan sulphate (Ghiselli, 2017).

The modification of GAGs occurs in and around the Golgi apparatus. The GAGs are subject to covalent linkage to anchor proteins/core protein after their sulphation, whereby the PGs form. The tetra-saccharide linker between the GAG and PG connects to the amino acid residue of the core protein, mainly serine residues. Three types of carbohydrate-protein linkages have been discovered in the connective tissue PGs so far: (1) an O-glycosidic linkage between xylose and serine hydroxyl groups; (2) an O-glycosidic linkage between N-acetyl-galactosamine and the hydroxyl groups of serine or threonine; and (3) an N-glycosylamine linkage between N-acetylglucosamine and the amide group of asparagine. The first linkage type is

commonly found in CS, DS, heparin, and HS; the second in skeletal KS-II (keratan sulphate II); and the third in corneal KS-I (keratan sulphate I) (Prydz, 2015).

1.7.1 Chondroitin Sulphate

Chondroitin sulphate pertains to a class of glycosaminoglycans with sulphation and alternating units of glucuronic acid (GlcA) and N-acetyl galactosamine (GalNAc) (Figure 1.9). Each CS heteropolysaccharide can comprise more than one hundred monosaccharides that can be sulphated at varying positions and to different extents. CS can be O-sulphated at the C2, C4 and C6 positions into isomers (Sugahara et al., 2003) and they are respectively termed as CS-A (chondroitin-4-sulphate), CS-C (Chondroitin-6-sulphate), CS-D (chondroitin-2,6-sulphate), CS-E (chondroitin-4,6-sulphate) according to their mono- or disulphate positions (refer to figure 1.8). The CS-B is a misnomer because its glucuronic acid moiety is epimerised to iduronic acid (IdUA) that is sulphated at C2; at the same time, the sulphated C4 of N-acetyl galactosamine exists as well. Hence, the CS-B is considered a member of the dermatan sulphate group instead.

CS is widely distributed in the cartilage ECM and exist as a major component of PGs primarily aggrecan, which is involved in cell communication to regulate cell proliferation, adhesion and cell division (Ogawa et al., 2012).

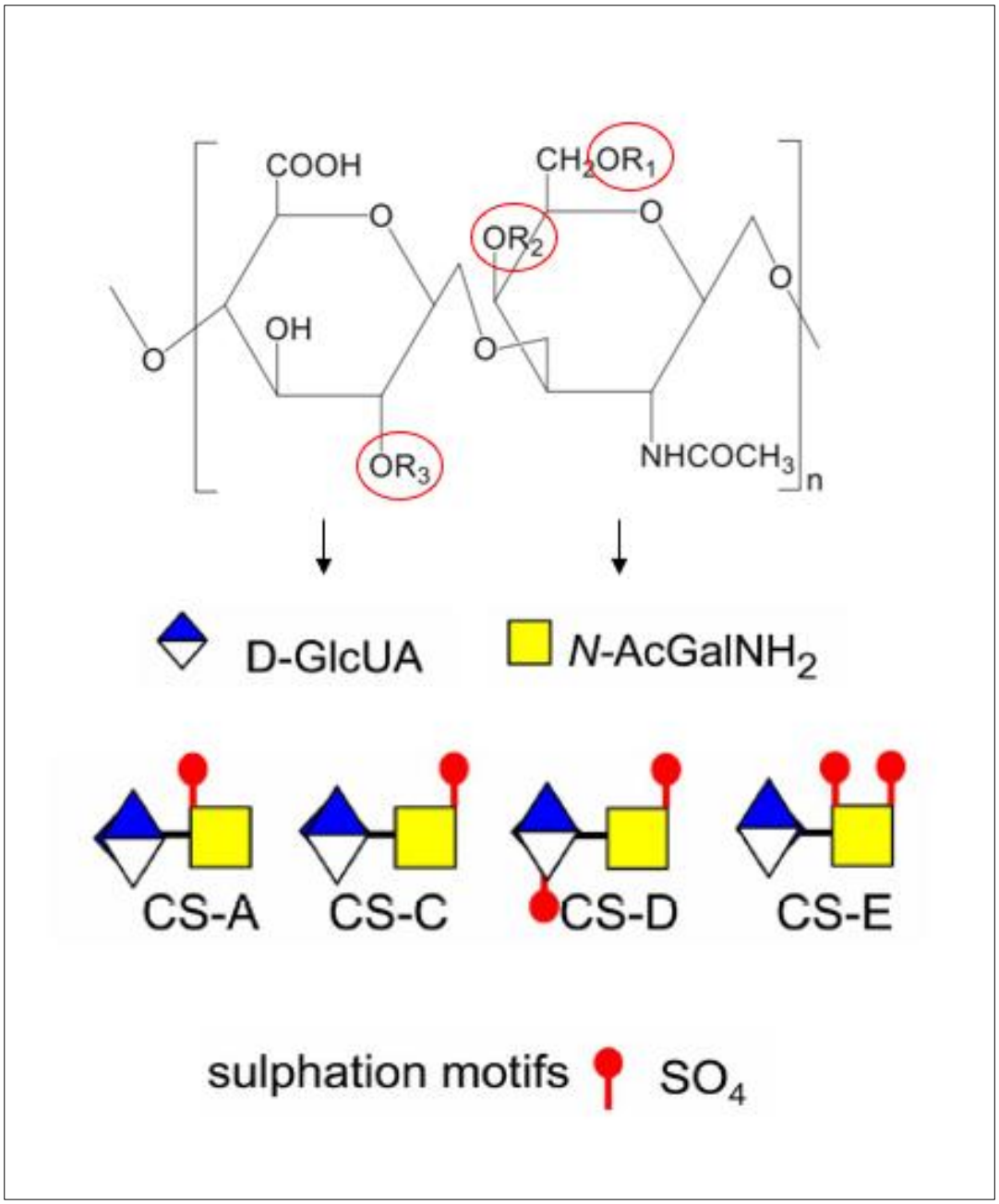

Figure 1.9 The structure of a repeating disaccharide unit in CS molecules. *R_1, R_2 and R_3 are the carbon position where the sulphation always happens. When sulphation happens at R_1, it is called CS-C, and CS-A when R_2 (modified and combined from (Bishnoi et al., 2016) and (Hayes et al., 2018a)).*

In 1980s, Caterson et al. (1983) generated, refined, and partially characterised distinct monoclonal antibodies, such as 3B3, 4C3, 6C3, and 7D4, etc, which specifically recognise native sulphation patterns in CS and dermatan sulphate (DS) chains. These sulphated motifs are divided based on their structure and sulphation position with specific features of 4C3, 6C3, 7D4, 3B3(-/+) and 2B6(-/+) shown in figure 1.10. Both our laboratory and others have investigated the localisation and biochemical structure of some of these sulphation motif epitopes within the oligosaccharide segments of CS/DS GAG chains. All these motifs can be recognised by specific antibodies (Caterson, 2012), which have been utilised to detect the stem cell niche (Hayes et al., 2016) and interfere with foetal joint development (Shu et al., 2013). As interest in stem cell-based therapies began to grow, many studies discovered that the precise spatio-temporal expression patterns of CS GAG sulphation motifs in various cartilage-related biological contexts, including 3B3 involved in chick normal skeletal tissue formation and maintenance (Caterson et al., 1990c), and 6C3 and 7D4 expression significantly increased several months after the onset of musculoskeletal diseases (Lin et al., 1998).

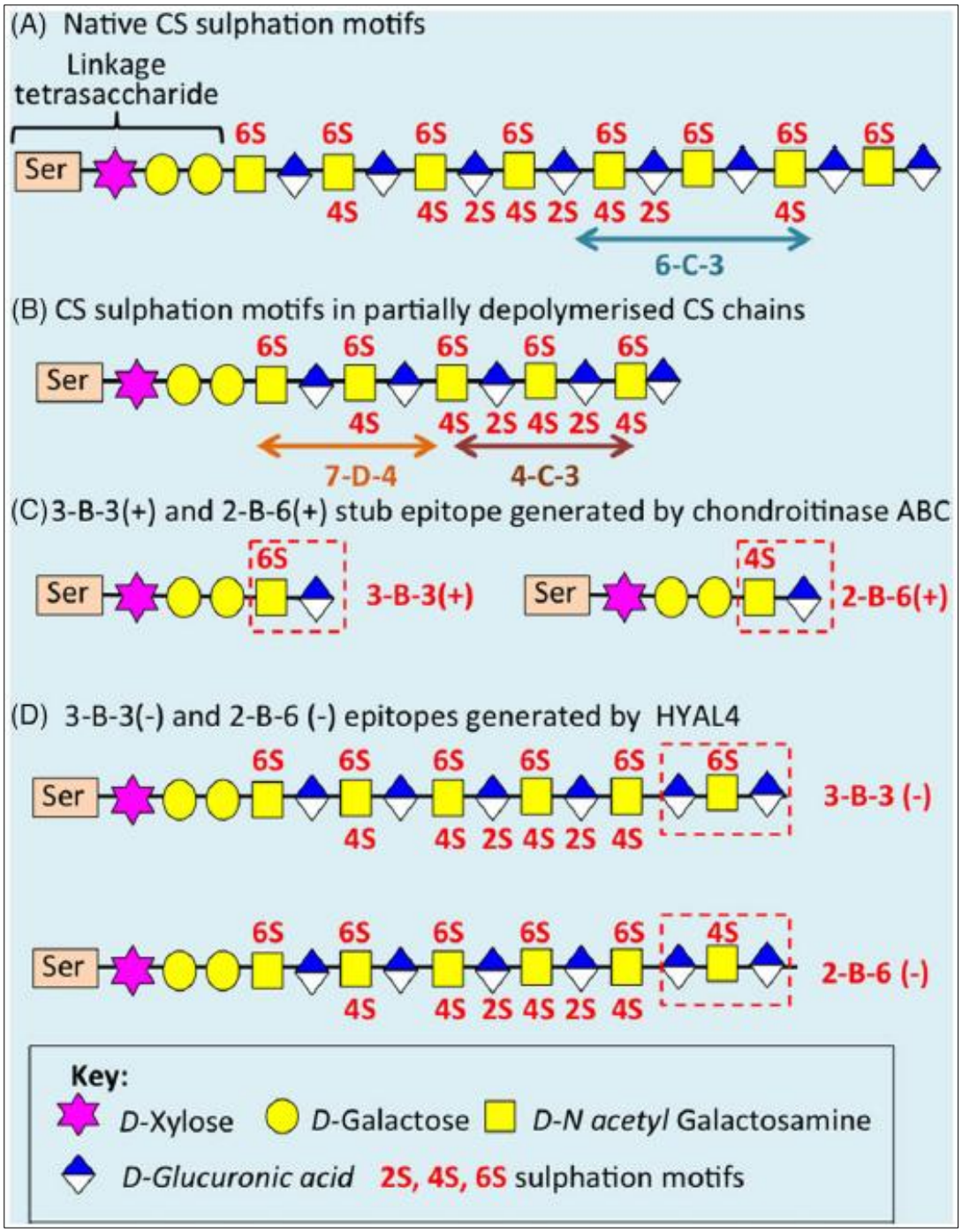

Figure 1.10 Chondroitin sulphate molecular structure and sulphation position. *CS links to core protein through an O-glycosidic linkage between xylose and serine hydroxyl groups. (A) CS with 3-B-3(-) and 6-C-3 motifs. (B) 7-D-4 and 4-C-3 exposed after CS partial digestion by chondroitinase ABC. (C) 3-B-3(+) or 2-B-6 (+) mapped by CS complete digestion. (D) 3-B-3(+) or 2-B-6 (+) generated by hyaluronidase (HYAL 4) (Hayes et al., 2018b).*

1.7.2 Keratan Sulphate

Keratan sulphate (KS) is another notable constituent in cartilage. Compared with CS in terms of composition, the KS building block comprises the repeating disaccharide units of N-acetyl-β-glucosamine (GlcNAc) and galactose (Gal) rather than uronic acid. This structural feature makes KS the only type of GAG that does not have acidic residues unless the sulphation provides acidic components to KS (Funderburgh, 2002). Although the GlcNAc subunit is the one that is sulphated more often, both of these sugar units can be 6-O-sulphated (Pomin et al., 2012). All the KS chains are a mixture of non-sulphated (Gal-GlcNAc), mono-sulphated (Gal-GlcNAc6S), and di-sulphated (Gal6S-GlcNAc6S) disaccharides (Figure 1.11). According to the different linkage to proteins, KS are classified into KS I, KS II and KS III. KS I was first found in the cornea and is N-linked to asparagine residues, while KS II was initially isolated from skeletal tissue and is O-linked to serine (Ser) or threonine (Thr) (Brown et al., 1996). KS III was first isolated from mouse brain tissue (Krusius et al., 1986) and is O-linked to a Ser/Thr residue on the core protein via a single mannose as shown in figure 1.11 (Caterson and Melrose, 2018). KS can be identified by monoclonal antibody 5D4 through its Gal6S-GlcNAc6S epitope (Bertolotto et al., 1998).

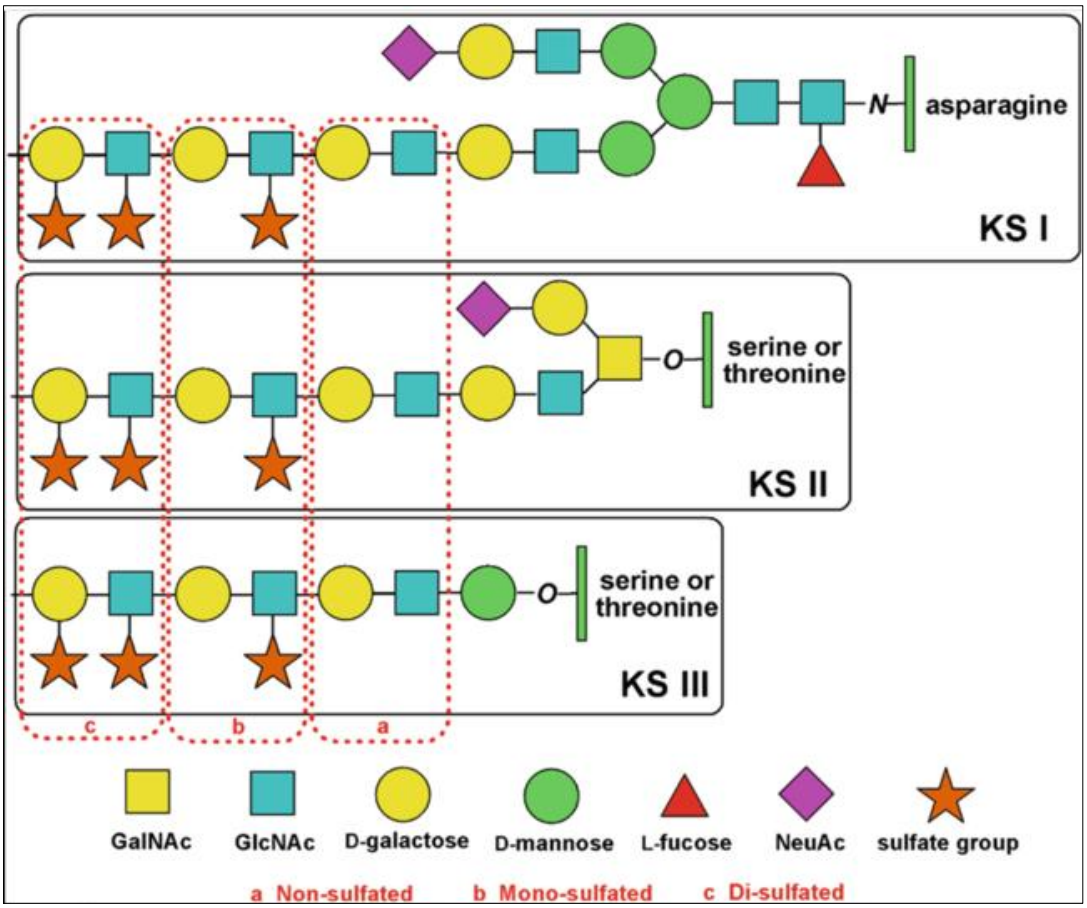

Figure 1.11 Schematic diagram of the molecular structure and sulphation of KS I, KS II and KS III. *The linkages of KS subtypes include N-glycosylamine linkage between N-acetylglucosamine and the amide group of asparagine for KS I and O-glycosidic linkage between N-acetyl-galactosamine and the hydroxyl groups of serine or threonine for KS II and KS III. The sulphation occurs to GlacNAc (6S) more often when mono-sulphated (Bedini et al., 2019).*

1.7.3 Advances in Chondroitin Sulphate Research

1.7.3.1 Advances in Purification of Chondroitin Sulphate

CS is the most abundant GAG in cartilage where it contributes to compressive load bearing properties by attracting cations and water. Furthermore, it has also been discovered that CS exerts joint-related healing, including anti-inflammation (Ronca et al., 1998, Iovu et al., 2008, Legendre et al., 2008), antioxidation (Ofman et al., 1997, Zhu et al., 2018a), and anti-apoptosis (Ju et al., 2015) properties. Recently, scientific interest and clinical needs for cartilage repair have focused on CS to behave as a beneficial biomaterial for cartilage regeneration (Wang et al., 2007, Uzieliene et al., 2023). The optimisation and exploration of methods for CS extraction and purification date back to the 1950s; cartilage is the most common animal source used and includes extraction of CS from cartilage sourced from terrestrial (Sundaresan et al., 2018) and marine animals (Sim et al., 2007). CS is most abundant on aggrecan making it a good source of material; the first step for isolation of CS is the extraction of PGs, mainly aggrecan from various forms of cartilage. The principle of the classic method consists of four steps: I. Chemical alkaline hydrolysis of cartilage with concentrated guanidine hydrochloride (GuHCl), sodium hydroxide (NaOH), urea; II. Degradation of core protein; III. Exclusion of proteins and peptides and recovery of CS; IV. Purification of CS (Shi et al., 2014). The first step is regarded as the extraction of PGs, and the last two steps are processes of CS purification.

The methods of PG extraction from cartilage have been explored for more than half a century (Hascall and Sajdera, 1969). In the seminal publication by Hascall and Sajdera (1969), PGs were extracted from bovine nasal cartilage using 4M GuHCl followed by equilibrium centrifugation in caesium chloride (CsCl) under associative and/or dissociative conditions. More than 95% of hexuronate was pooled at the bottom fraction whilst the PGs recovered from the top fraction accounted for less than 3% of the weight of protein-polysaccharides.

Alkaline treatment is applied to cleave the carbohydrate-protein linkage, which results from the alkali lability of the bonds linking the hydroxyamino acids, serine and threonine (Montreuil, 1980). With the presence of borohydride, a peeling reaction can

be prevented by avoiding the cleavage of newly released reducing terminals in alkaline treatment (Bienkowski and Conrad, 1984).

Recently, the philosophy of some methodologies has started to employ enzymes in the core proteins digestion before CS purification, which will be further discussed in Chapter 6. Proteases such as pronase, papain and trypsin have been used to hydrolyse cartilage and proteins (Michelacci and Horton, 1989), followed by chemical treatments to release the GAG chains. Vázquez et al. (2018) used alcalase to degrade the cartilage followed by two chemical treatments separately, either alkaline treatment or hydroalcoholic alkaline treatment, and membrane purification; they reported optimal conditions for proteolysis as 52.9ºC at pH 7.31. After the chemical treatments, purities of CS were brought up to more than 80% and 90%, respectively as determined by ^{1}H-NMR.

Mechanical energy can also be transferred into chemical energy for the degradation of polymers to extract CS. Since it is a solvent-free process, it is believed as the most eco-friendly method. Wang and Tang (2009) reported a rapid method for the purification of CS. Shark cartilage was mechanically dissociated into powder and then mixed with solid alkali reagent, which 3% NaCl solution diffused into, followed by being acidified to pH 6.0 to harvest the insoluble parts until the CS products were obtained with the purity of more than 95%. Ultrasound has also been used as a mechanical force to enhance solvent penetration into tissue samples, during the process air bubbles are formed increasing the pressure and temperature further enhancing penetration and solubilisation of proteoglycans embedded in tissue samples. 37kHz ultrasound-assisted extraction and hydroalcoholic alkaline treatment were employed to extract CS from squid cartilage at 52ºC for 46 mins compared with conventional extraction with 3% NaOH. The final CS products was 82.3% purity with 23.7% yield (Yang et al., 2021).

To further purify CS from other glycosaminoglycans, differences in charge density and solubility in organic solvent of the various GAGs have been utilised. Such methods include electrophoresis, precipitation with quaternary ammonium reagents and anion-exchange column chromatography, all based on the different charge density of the different GAGs. Quaternary ammonium reagents, including cetyltrimethylammonium bromide (CTAB) and cetylpyridinium chloride (CPC), can

combine with negatively charged GAG chains forming quaternary ammonium salts that are barely soluble in water to precipitate, which can be employed for purification of sulphated PGs/GAGs (Cleland and Sherblom, 1977). Column chromatography is another highly specific tool to purify CS from PG-GAG complexes with the bioactivities and structure of CS protected. Krichen et al. (2018c) enzymatically hydrolysed the cartilage from smooth hound with alcalase and precipitated CS with 0.5% (w/v) CPC solution. The lyophilised precipitate was loaded onto a DEAE-cellulose anion-exchange resin and eluted with a linear gradient of NaCl from 50mM to 2M, which brought the purity of CS up to more than 70%.

Selective precipitation of CS in organic solvent takes advantage of the solubility of CS in organic solvent, and ethanol is the most used solvent with a cheap price and little environmental harm. Ethanol precipitation also can be applied after anion-exchange chromatography for the eluates (Ogawa et al., 2012). Sequential precipitation with ethanol was also employed by Volpi (1996), 0.1 to 2.0 volumes of ethanol or methanol was added into the GAGs mixture sample and the sample was stored at 4 ºC for 24 hours after every 0.1 volume was added. The precipitates were harvested separately for further analysis. Methanol failed to separate CS from dermatan sulphate so these both were pooled at 0.8 to 1.6 volumes of methanol. However, it is reported that 100% CS was isolated with volumes higher than 0.8, whilst it is heparan sulphate that was precipitated at about 0.4 volume of ethanol (Kim et al., 2021).

The extraction and purification of CS is the fundamental step for its application into future research attempts and clinical translation. It is desirable to obtain purer CS with less environmental influences and more convenient procedures so that the known and potential functions of CS and its inner mechanisms can be unveiled.

Table 1.1 CS purification protocol associated literature summary

Extraction protocol	Origin	CS Purity achieved (%)	Reference
4M GuHCl, density gradient centrifugation, pH extraction (mainly PG level molecules extracted)	Bovine nasal cartilage	95% (including PG complex)	(Hascall and Sajdera, 1969)
β-elimination, DEAE-cellulose and Sepharose CL6B chromatography	Hepatocyte cell line	70%-80% (predominantly HS)	(Bienkowski and Conrad, 1984)
3M GuHCl, papain digestion, ethanol precipitation, gel filtration	Shark cartilage	84%	(Michelacci and Horton, 1989)
Alcalase digestion, alkaline-alcoholic precipitation, membrane purification	Shark cartilage	81%-97%	(Vázquez et al., 2018)
Mechanical digestion, NaCl solution purification	Shark cartilage	95%	(Wang and Tang, 2009)
Ultrasound-assisted extraction, hydroalcoholic alkaline treatment	Squid cartilage	82.3%	(Yang et al., 2021)
Alcalase digestion, CPC precipitation, DEAE-cellulose chromatography	Smooth hound cartilage	70%	(Krichen et al., 2018b)
Ethanol precipitation	Mice cartilage	-	(Ogawa et al., 2012)

1.7.3.2 Function and Application of Chondroitin Sulphate in Cartilage Biology

CS has gained substantial interest since it is widely recognised for its crucial role in maintaining joint health, but it is still controversy over whether CS plays a positive role, despite plenty of clinical studies have discovered that targeted administration of CS can more effectively improve joint health by reducing symptoms and adverse events (Brito et al., 2023, Ruiz-Romero et al., 2025, Simental-Mendía et al., 2018). The joint protective function of CS is mainly explained by the following two mechanisms: (1) CS can enhance anabolic metabolism of cartilage as an essential constitute of cartilage and synovial fluid; (2) CS elicits anti-inflammatory effects by dampening inflammation-induced catabolism.

CS is a key component of the cartilage ECM and contributes significantly to the structural integrity, elasticity, and shock-absorbing properties of cartilage (Section 1.7.1). Its unique molecular structure allows it to interact with other ECM components, such as collagen and HA, to form PGs like aggrecan, which are essential for cartilage function (Hardingham and Fosang, 1992). Guan et al. (2022) utilised a monosodium iodoacetate-induced knee arthritis rat model and administrated CS (100mg/kg) as a dietary supplement regularly for 2 weeks. Histo-morphological evaluation revealed that CS supplementation increased chondrocyte proliferation and the secretion of type II collagen.

As an anti-inflammation factor in ECM of AC, CS has shown to inhibit IL-1β induced NF-κB nuclear translocation in chondrocytes to enhance chondrocyte proliferation and metabolic activity, leading to ECM synthesis, cartilage homeostasis and inflammation modulation (Vallières and du Souich, 2010). Cho et al. (2004) also reported CS can decrease the IL-6 in serum and relieve joints inflammation and oedema after its oral administration to type II collagen-induced arthritis mice at 300mg/kg. These findings were endorsed by Campo et al. (2008) who observed similar chondro-protective outcomes in LPS-treated chondrocytes and in an *in vivo* murine collagen-induced OA model. CS also exerts joint protection by inhibiting the inflammation-induced expression of MMP and aggrecanases, which cause the enzymatic degradation of cartilage ECM in conditions like OA (Jung et al., 2019). Hsu et al. (2022) treated chon-001 chondrocyte cell line in a 3D Transwell^{TM} model with CS in the culture medium by various concentrations (0, 100, 200, 400, 800, or

1600 μg/mL) of CS for 48 h or 72 h. Western blot results demonstrated the increased expression of type II collagen and zymographic assays reported the suppression of MMP-9 and MMP-2 activities.

CS has been found to play a critical role in chondrocytes signalling, which heavily impacts on OA pathophysiology. Jung et al. (2019) discovered that degradation of CS in cartilage can increase NO production, oxidative stress, and expression of MMP-13 and ADAMTS-5 by TLR2 and TLR4 signalling pathways. By employing inhibitor assays, it was found that CS degradation products function as damage-associated molecules and can activate pathways downstream of TLRs, including MAP kinases, NF-κB, NO and STAT3 signalling. When 5% (w/v) CS was loaded into a hydrogel and implanted into a rabbit joint cartilage defect, it was shown to repair 2-4mm cartilage defects and integrate with surrounding tissue with a 2-month recovery by suppressing Wnt/β-catenin signalling pathway in the later stages (Wu et al., 2024b).

As described above, CS elicits various responses and can significantly impact cartilage metabolism, hence it has been listed as a systematic slow-acting drug for OA, which can alleviate pain and improve joint mobility (Zhu et al., 2018b). Oral administration of CS at 60.38mg/kg to an OA rabbit model (cranial cruciate ligament transection constructed) for 84 days modulated ECM synthesis by promoting the expression of gene markers, including aggrecan and collagen type II (Mariné-Casadó et al., 2024). In a clinical study where OA patients with disease severity grade of 2–3 based on Kellgren–Lawrence radiographic scoring were given 1200mg CS dietary supplement for 24 months, CS improved knee joint health with qualitative MRI results showing reduced synovial thickness in the medial suprapatellar bursa and joint swelling (Pelletier et al., 2016). CS has also been suggested to have disease-modifying effects by slowing the progression of cartilage degradation. Its ability to inhibit catabolic enzymes and promote anabolic activities in chondrocytes supports this therapeutic potential. Reginster and Veronese (2021a) reviewed the evidence to figure out the role of highly purified CS in the treatment of OA, when they found CS is safe and effective for OA treatment and delay the course of OA.

Intra-articular injections of CS or CS-containing formulations are being explored as a potential OA treatment through the delivery of high concentrations of CS directly to the affected joint, enhancing its therapeutic efficacy in cartilage repair and pain relief.

Yang et al. (2024b) developed an injectable CS-containing hydrogel which was designed for porcine 7mm-diameter haemophilic articular cartilage defects, and it was found to alleviate inflammation and regulate macrophage M2 polarisation via NF-κB signalling in. This study demonstrates the effectiveness of a CS-containing hydrogel in quick haemostasis, immunomodulation and chondrogenic regeneration.

CS is often used in combination with other nutraceuticals, such as HA, to achieve synergistic effects. This combination therapy is believed to provide enhanced joint protection, reduce inflammation, and promote cartilage health more effectively than either compound alone (Mariné-Casadó et al., 2024). CS was combined with collagen type II into a scaffold which encapsulated synovium-derived mesenchymal stem cells and used to chondrogenic culture for 3 weeks, found to promote the chondrogenesis confirmed by tissue staining and chondrogenic gene markers, including BMP-7 (Yang et al., 2023).

1.7.3.4 Application of Chondroitin Sulphate in Cartilage Engineering

Cartilage engineering is a rapidly advancing field aimed at developing innovative strategies to repair or regenerate damaged cartilage. The application of CS in cartilage engineering leverages its unique biochemical properties to support chondrocyte/stem cell function and promote cartilage ECM formation (Sharma et al., 2022). CS favours chondrocyte proliferation and promotes their differentiation into mature chondrocytes, essential for effective cartilage repair (Hsu et al., 2022). It also helps maintain the chondrogenic phenotype by preventing dedifferentiation. For example, CS was coated onto polycaprolactone (PCL) electrospun nanofibrous scaffolds and films before application to induce the chondrogenic differentiation of human dental pulp stem cells (hDPSC). The hDPSCs presented a higher proliferation rate in CS-containing films and showed better viability and chondrogenic differentiation capacity on CS-containing scaffolds (Eldeen et al., 2024a).

The hydrophilic nature of CS helps maintain scaffold hydration, which is essential for nutrient diffusion and waste removal (Rasoulianboroujeni et al., 2018). Additionally, CS contributes to the mechanical strength of scaffolds, mimicking the natural properties of native cartilage. CS was incorporated with agarose to create a porcine chondrocyte scaffold, and the presence of CS brought a 4- to 5-fold improvement in

mechanical properties compared to agarose gels without CS (Ingavle et al., 2012). CS also improved the biocompatibility and cellular viability by providing a more relevant and beneficial micro-environment for cellular signalling. CS-containing scaffolds closely mimic the native cartilage ECM, facilitating the organisation and deposition of new matrix by chondrocytes. This leads to the formation of tissue that closely resembles native cartilage in both structure and function. CS was introduced into highly porous polymer scaffolds for osteogenesis of a mouse pre-osteoblast cell line MC3T3-E1 and maintenance of chondrogenic phenotype in primary rat chondrocytes. After a 21-day *in vitro* culture, it was found that CS stimulates cell adherence, survival ability, proliferation, differentiation and ECM formation (Behere et al., 2024). CS also enhances the production of key ECM components, such as type II collagen and aggrecan, which are crucial for the structural and functional integrity of engineered cartilage (Sechriest et al., 2000).

Incorporating CS into scaffolds enhances their biocompatibility and bioactivity. CS-modified scaffolds provide a more natural and conducive environment for chondrocytes, promoting cell attachment, proliferation and differentiation. Janipour et al. (2024) fabricated biofilms with CS and gelatin and encapsulated Wharton's jelly MSCs into the films. The films demonstrated excellent mechanical strength and stability, better swelling ratio and induced chondrogenesis with the formation of chondrocyte lacunae on the 30^{th} day. Modified CS was integrated into a microcarrier before the injection into surgical method induced mice joints where CS was found to enhance the scaffold bioactivities by improving recruitment of stem cell exosomes with a 3-day culture, collagen type II production and repression of inflammation (Yang et al., 2024a).

CS possesses anti-inflammatory properties that can reduce inflammation and catabolic activity in damaged cartilage. This is particularly beneficial in treating conditions such as osteoarthritis, where inflammation plays a significant role in cartilage degradation. Zhou et al. (2017) incorporated 6wt.% CS with silk fibroin to create a bio-scaffold for human chondrocytes. The adhesion, proliferation and migration assay results demonstrated its advantageous biocompatibility, and the CS-containing scaffold performed better in maintaining chondrocyte phenotype compared with the control group. Furthermore, the CS-containing scaffold was found to suppress the

inflammatory response in rabbit OA model induced by a full-depth cylindrical cartilage defect, generating better neo-tissue and integrity. CS-based scaffolds embedded with MSCs upregulated immunosuppression-related molecules, including NO, prostaglandins, etc. When they were implanted subcutaneously into heathy adult Lewis rats, reduced infiltration of leukocytes was detected after 24 hours, showing the anti-inflammatory characteristics of CS (Corradetti et al., 2016).

1.8 Hypothesis

Cartilage lesions and defects often occur in many anatomical locations affecting the physical movement, physiological function and psychological well-being of people of all ages, gender and ethnicity. As articular cartilage has extremely limited ability for repair and restoration, it is expected that tissue engineering approaches can adequately repair cartilage defects using a biomimetic recapitulating the mature cell and matrix structure of cartilage. To address these challenges, the incorporation of biomimetic molecules -- chondroitin sulphate, has emerged as a promising strategy, given its critical role in replicating the native cartilage ECM and promoting chondrocyte function or stem cell chondrogenesis. This leads to the hypothesis that **the *ex-vivo* production of a biological environment containing cartilage extracellular matrix macromolecules (i.e. GAGs) along with autologous cells (chondrocytes/BMSCs), cultured in chondrogenic environment, can be used as an initial implant for the subsequent regeneration and integration of newly repaired cartilage in human patients needing cell implantation treatments.**

1.8.1 Experimental Aims

The overall aim of my PhD is to (i) develop and/or refine existing methodologies to improve the purity of native chondroitin sulphate extracted from articular cartilage and (ii) utilise the purified CS in the construction of 3D scaffolds to facilitate the regeneration of articular cartilage in patients that would benefit from surgical intervention. Specific aims include:

Chapter 3 - to explore and optimise methods for the purification of free chondroitin sulphate molecules from bovine articular cartilage. This will involve investigating purification techniques to achieve high purity levels of free CS chains whilst maintaining its structural integrity.

Chapter 4 - to investigate the impact of CS-coated substrates on the behaviour, viability and phenotype of chondrocytes to assess the potential of CS-coated surfaces in enhancing the chondrocytes' responses in 2D environment.

Chapter 5 - to explore the effects of a CS-containing medium on the chondrogenic differentiation of BMSCs in Transwell^{TM} system, evaluating how CS concentrations influence key markers of chondrogenesis, the mature chondrocyte phenotype and extracellular matrix production.

Collectively, these aims will assess the role of CS in promoting or modulating cell behaviours, both in mature chondrocytes and BMSCs, and determine its potential as a bioactive supplement in chondrocyte/stem cell-based cartilage tissue engineering. The findings are expected to contribute to optimizing culture conditions for enhancing cartilage regeneration strategies.

Chapter 2

Materials and Methods

2.1 Materials

All materials were obtained from Sigma-Aldrich (Southampton, UK) unless otherwise stated and were of analytical grade or above. All molecular biology plasticware, filter tips and reagents were DNase and RNase free. All experiments conducted had 6 technical replicates (n = 6) and three independent repeats (N=3) performed unless otherwise stated.

2.2 Proteoglycan Extraction

2.2.1 Source of Tissue

Articular cartilage tissue was obtained from the *metacarpalphalyngeal* joints of young (3 weeks old) and old (18 months old) bovine animals following slaughter (F Drury & Sons abattoir, Swindon). Feet were scrubbed to remove extraneous material and disinfected using microsol (diluted 1:50), prior to removal of the skin. The *metacarpalphalyngeal* joint was opened using a sterile blade and full-depth cartilage explants removed to a petri dish.

2.2.2 Extraction of Proteoglycans

Bovine articular cartilage (BAC) extracts were obtained as previously published (Theocharis et al., 2002) and kindly provided by Prof. Clare Hughes (School of Biosciences, Cardiff University). PGs were extracted from the articular cartilage of young and old bovine animals by mild stirring, for 24 hours at 4°C, with 10 volumes of extraction buffer (4M guanidine-hydrochloric acid (GuHCl), 0.05M sodium acetate (NaAc), pH 5.8). Immediately prior to use, protease inhibitors were added, including 5mM benzamidine, 0.1M 6-aminocaproic acid, 10mM Ethylenediaminetetraacetic acid (EDTA) and 0.5mM phenylmethyl-sulphonyl fluoride (PMSF). The extraction mixture was filtered, and the filtrate dialysed against 10 volumes of distilled water at 4°C so that the concentration of GuHCl was 0.4M. Dialysed extracts were aliquoted and used for the purification of PGs.

2.3 Purification of Proteoglycans and Glycosaminoglycans

2.3.1 Partial Purification of Proteoglycans and Glycosaminoglycans by Caesium Chloride Density Gradient Centrifugation

2.3.1.1 Associative caesium chloride density gradient centrifugation

The density of extracts (Section 2.2.2) was adjusted to 1.5g/ml by adding caesium chloride (CsCl) before transferring into 25ml centrifugation tubes. Associative density gradient centrifugation was performed for prepared extracts at 8°C (Beckman L-60 centrifuge, 8×25ml 50Ti fixed angle rotor) at 120,000 g for 48 hours. After centrifugation, the gradient was divided into three equal fractions as follows: bottom 8.3ml fraction (A1, density>1.58g/ml), middle 8.3ml fraction (A2, density 1.44-1.58g/ml) and top 8.3ml fraction (A3, density<1.44g/ml). Fractions were dialysed against 2-3 changes of distilled water, followed by dialysis overnight against 10 volumes of 0.15M sodium chloride (NaCl) containing protease inhibitor cocktail (Section 2.2.2). The distribution of GAGs and protein in associative gradient fractions was determined using the dimethylmethylene blue (DMMB) assay (Section 2.16.2) and bicinchoninic acid (BCA) assay (Section 2.16.3). A1 fractions were enriched with aggrecan/link protein/HA complex and were stored at -20°C for future use.

2.3.1.2 Dissociative Caesium Chloride Density Gradient Centrifugation

The BAC-D1D1 fraction was kindly gifted by Professor Clare Hughes (School of Biosciences, Cardiff University). Briefly, a 4M GuHCl extract was adjusted to a density of 1.5g/ml with CsCl. Dissociative centrifugation was performed at 100,000 g at 8°C for 48 hours. Gradients were equally divided into D1, D2 and D3 fractions from the bottom to top respectively. The D1 fraction was mixed with 8M GuHCl containing 2X protease inhibitor cocktail (Section 2.2.2) and CsCl to a density of 1.5g/ml for a second round of density gradient centrifugation at 100,000 g, 8°C for 48 hours. Then the sample was equally divided into three parts as D1D1, D1D2 and D1D3 from bottom to top respectively. The BAC-D1D1 fraction was dialysed against 2-3 changes of distilled water, followed by dialysis overnight against 10 volumes of 0.15M NaCl containing protease inhibitor cocktail (Section 2.2.2).

BAC-A1D1 was prepared from the A1 fraction (Section 2.3.1.1). After associative centrifugation, the A1 fraction was adjusted to 4M GuHCl by the addition of 8M GuHCl containing 2X protease inhibitor cocktail (Section 2.2.2). CsCl was added to a density of 1.5g/ml. Centrifugation was performed at 120,000 g at 8˚C for 48 hours after which individual tubes were equally divided into three parts as A1D1, A1D2 and A1D3 from bottom to top respectively. The BAC-A1D1 fraction was dialysed against 2-3 changes of distilled water, followed by dialysis overnight against 10 volumes of 0.15M NaCl containing protease inhibitor cocktail (Section 2.2.2). BAC-A1D1 fractions were stored at -20℃ for future use.

2.3.2 Alkaline β-elimination, Cetylpyridinium Chloride Precipitation and Ethanol Precipitation

GAG chains in Aggrecan (A1 or A1D1) (1- 5 mg total GAG amount) were released from any remaining protein core/peptide fragments by treatment with an equivalent volume of 1M sodium hydroxide (NaOH) and incubated at room temperature overnight. A volume of 1M acetic acid, equivalent to the initial A1 fraction volume, was added before dialysing against water (dialysis membrane (Repligen, USA) with pore size of 1000-dalton) overnight.

After dialysis, samples were spun in the SC210A concentrator (Savant, USA) overnight. The freeze-dried samples were reconstituted in 1ml of 50mM sodium sulphate (Na_2SO_4) and 10% (w/v) cetylpyridinium chloride (CPC) solution added dropwise until a dense precipitate formed. Samples were centrifuged at 500g for 5 minutes at 8℃ to separate the CPC salt from the supernatant which was subsequently discarded. The salt precipitate was washed with 4ml of 0.05% (w/v) CPC solution twice to remove ions, before being dissolved in 1ml of 80% (v/v) propan-1-ol to form a solution. This solution was added to 100µl of 5M NaAc and a drop of acetic acid to lower the pH until the solution went cloudy. Then 5 volumes of cold ethanol were added to precipitate the sodium salt of the GAG chains as a dense white precipitate, and the mixture left at 4℃ overnight. Samples were centrifuged at 500 g for 20 minutes at 8℃, before drying the precipitate at room temperature overnight and reconstituting in 0.1M NaCl solution as needed.

2.3.3 Modified Alkaline β-elimination

Aggrecan (A1 or A1D1) (1- 5 mg total GAG amount) was lyophilised (Edwards High Vacuum, UK) overnight, and then reconstituted in a minimal volume of freshly prepared alkaline borohydride reagent (0.3M sodium borohydride ($NaBH_4$) in 0.4M NaOH) in the fume hood. The reaction mix was incubated for 24 hours at room temperature without a cap to ensure release of hydrogen gas generated by the reaction. 2M HCl was added to the solution until the pH of the solution was 0 (monitored using pH paper), converting excess borohydride to hydrogen gas. 1M NaOH was added to obtain a pH between 6-8 measured using pH paper or a pH meter. The resultant sample was then desalted using a PD-10 Desalting column (Cytiva, UK). Briefly, columns were equilibrated with approximately 25ml deionised water, β-eliminated samples were loaded in a final volume of 2.5 ml and eluted with 10-12 ml of deionised water collected as 1 ml fractions. GAG concentration in each fraction was determined using the DMMB assay (Section 2.15.2).

2.4 Purification of Chondroitin Sulphate using Gel Filtration Chromatography

A Superose 6 column (10/300) (Cytiva, UK) was connected to the AKTA chromatography system (AKTA Pure) and equilibrated in 2 column volumes of 0.1M NaCl buffer (10mM Tris-HCl, pH 7.4). Lyophilised samples were reconstituted in 0.1M NaCl buffer (10mM Tris-HCl, pH 7.4), filtered through 0.2µm filters and loaded into the sample loop for delivery onto the column. The sample was isocratically eluted with 1.5 column volumes of 0.1M NaCl (10mM Tris-HCl, pH 7.4). Eluant was monitored at 280nm and 215 nm (Protein andpeptide).1 ml fractions were collected and analysed for GAG and protein content using the DMMB (Section 2.15.2) and BCA assay (Section 2.15.3), respectively.

2.5 Purification of Chondroitin Sulphate using Anion-exchange Chromatography

Samples were filtered through 0.2µm filters and loaded onto a DEAE anion exchange column (Hi-trap Q, 5ml; GE Healthcare, Sweden) connected to an AKTA Pure, pre-equilibrated with 0.1M NaCl (10mM Tris-HCl, pH 7.4). The column was washed with

three volumes of 0.1M NaCl and then eluted with a linear gradient of 0.1M-3M NaCl (10mM Tris-HCl, pH 7.4) (8 column volume). The absorbance of samples under the wavelength of 280nm and 215nm was transformed into plots using Matlab (R2021a).

2.6 Glycosaminoglycan Analysis

2.6.1 Determination of the Purity of Purified Chondroitin Sulphate

The purified CS sample was quantified by the carbazole reaction following published methods (Bitter and Muir 1962). The protein and nucleic acid contents of the purified CS were quantified using a NanoDrop One microUV-Vis spectrophotometer (ThermoFisher, USA) at 280nm and 495nm. These experiments were carried out in the National Glycoengineering Research Centre at Shandong University, China.

2.6.2 Enzyme Analysis of Purified Chondroitin Sulphate

To investigate whether the CS preparation contained other GAG impurities such as DS and Hep/HS, 10 μg of purified CS and CS standards with known purity (purified from shark cartilage by National Glycoengineering Research Centre at Shandong University, China) were treated at 37℃ for 4 h with chondroitinase AC (10 mU) (GlycoSciTech Co, Ltd, China), chondroitinase B (10 mU) (GlycoSciTech Co, Ltd, China), and a mixture of Hepases I, II and III (4 mU each) (GlycoSciTech Co, Ltd, China), respectively, the enzymes used in this experiment are listed in Table 2.1.

The enzymatic products generated by chondroitinase AC, chondroitinase B, and Hepases were analysed using gel filtration chromatography on a Superdex^{TM} Peptide 10/300 GL column (GE Healthcare) eluted with 0.2 M NH_4HCO_3 at a flow rate of 0.4 mL/min for 60 min with monitoring at 232 nm by a UV detector (Shimadzu Co., Ltd., Kyoto, Japan).

In this study, the purity of the CS preparation was determined using an external standard approach as previously published (Kinoshita and Sugahara, 1999). CS standards with different purities peak areas in chromatography profile was used to

establish a linear relationship between disaccharide unit amount and peak area with Matlab (R2021a). The best fitting line and function determined the amount of disaccharide produced by enzyme digestion in CS preparation.

Table 2.1 Enzymes employed in this project

Enzyme	Origin	CAS No.
Chondroitinase AC	Flavobacterium heparinum	9047-57-8
Chondroitinase B	Flavobacterium heparinum	52227-83-5
Chondroitinase ABC	Proteus vulgaris	9024-13-9
Heparinase I	Bacteroides stercoris	9025-39-2
Heparinase II	Sphingomonas	149371-12-0
Heparinase III	Pseudomonas aeruginosa	37290-86-1

2.6.3 Disaccharide Composition Assay of Purified Chondroitin Sulphate

To determine the disaccharide composition of the CS, 1μg of CS sample was treated with 5mU Chondroitinase ABC (GlycoSciTech Co, Ltd, China) for 12 hours and then heated in boiling water for 10 mins and cooled in ice-cold water for 10 mins. With a 15-min centrifugation at 15,000 g, the supernatants were kept and labelled with 2-aminobenzamide in the presence of sodium cyanoborohydride reagents as described previously (Bigge et al. 1995), and the free 2-aminobenzamide was eliminated by chloroform. Then the product was analysed by anion exchange HPLC on YMC-Pack PA-G (250 × 4.6 mm, YMC Co., LTD., Japan) eluted with a linear gradient of NaH_2PO_4 (16 mM to 460 mM) at a flow rate of 1 mL/min over 60 min. Monitoring was performed through a fluorescence detector with excitation and emission

wavelengths of 330 nm and 420 nm, and standard CS/DS unsaturated disaccharides were applied for qualitative and quantitative purposes. Online monitoring and data analysis were performed using the software LC solution version 1.25 (SHIMADZU, Japan) (Li et al., 2010b).

2.6.4 Nuclear Magnetic Resonance (NMR) Spectroscopy Analysis for Purified Chondroitin Sulphate

To confirm the structural characteristics, 20mg of lyophilised CS preparation was exchanged with D_2O 3 times and finally dissolved in 0.5 mL of D_2O inside a 5 mm NMR tube. The one-dimensional (1D) ^1H NMR spectrum was acquired with 32 scans ranging from 1 to 11 ppm. The NMR experiments were performed on an Agilent DD2 600 (Agilent Technologies Inc., US) operating at a proton frequency of 600 MHz; data were analysed on MestReNova 9.0.1 (Mestrelab Research S.L, Spain).

2.7 Primary Isolation of Bovine Chondrocytes

Articular cartilage was extracted from the *metacarpalphalyngeal* joints of 7-day-old bovine calves as previously described (Section 2.1). Full-depth cartilage slivers were incubated in Hanks' balanced salt solution (HBSS) (Life Technologies Ltd, UK) containing 400U/ml penicillin, and 400 µg/ml streptomycin (PS) (Thermo, UK), with three 15 minutes washes. The cartilage was subsequently washed in 100U/ml PS-HBSS prior to enzymic digestion. 25ml of filter sterilised 0.1% (w/v) pronase (from *Streptomyces griseus*) solution (in Dulbecco's modified eagle medium/F12 (DMEM) (Gibco, UK) containing 100U/ml PS and 5% (v/v) fetal bovine serum (FBS) (Thermo, UK)) was used to digest the cartilage matrix from each bovine *metacarpalphalyngeal* joint for 40 minutes with mild agitation at 37°C, 5% CO_2 in a humidified atmosphere. Following pronase removal, 0.04% (w/v) type II collagenase from *Clostridium histolyticum* (Gibco, UK: in DMEM/F12 with 100U/ml penicillin, and 100 µg/ml streptomycin and 5% (v/v) FBS) was employed to break down cartilage collagen matrix with agitation at 37°C (5% CO_2). After overnight digestion, the medium containing the chondrocytes was filtered through a 40µm cell strainer (Corning, UK) and centrifuged at 1000 rpm for 5 minutes before the supernatant was discarded. The

chondrocyte pellet was resuspended in DMEM/F12 (50 ug/ml ascorbate-2-phosphate, 100U/ml PS, 1% (v/v) insulin-transferrin-selenium (ITS) (Gibco, UK) and cell number determined by cytometry prior to seeding.

2.8 Chondrocyte Culture with Exogenous Chondroitin Sulphate

2.8.1 Chondrocyte Culture on Different Concentration of Purified Chondroitin Sulphate Substrate

Purified CS was diluted with 80% saturated 4.2M ammonium sulphate to generate final CS coating concentrations of 0μg/cm^2 (control), 0.1μg/cm^2, 0.25μg/cm^2, 0.5μg/cm^2, 1μg/cm^2 and 5μg/cm^2. The diluted CS solutions were filtered through a 0.2μm filter, 500μl of each coating solution was added to appropriate wells in triplicate of a 24-well plate and stored at 4°C overnight. Coating buffer was carefully aspirated, and plates washed with sterile phosphate buffered saline (PBS, pH 7.4) five times prior to chondrocyte seeding at 1×10^6 cells/well. Plates were cultured at 37°C (5% CO_2) for 5 days. Chondrocytes were observed under a light microscope (EVOS core; Invitrogen, UK) (magnification of 100× and 200×); medium was changed every three days. 1ml of TRIzol™ was added to each well prior to subsequent analysis as described in section 2.17 and stored at -80°C.

2.8.2 Chondrocyte Culture in CS-Containing Agarose Hydrogel

A 4% (w/v) agarose solution was made up using low gelling point Type VII agarose (Sigma) and 1X PBS before autoclaving; the solution was subsequently cooled to 37°C. An equivalent volume of 2×10^6 cell/ml bovine chondrocyte suspension was mixed well with the warm agarose solution at 37°C in a 60mm petri dish so that a 10mm thick hydrogel was formed and set (equating to approximately 14 ml of both cell suspension and agarose solution). An 8mm-diameter biopsy punch (Integra, USA) was employed to cut the hydrogel into plugs, which were subsequently transferred into 24-well plates and cultured with 1ml chondrogenic medium. Hydrogels were cultured at 37°C, 5% CO_2 for 1 week and underwent Live/Dead assays.

2.8.3 Live/Dead Assay for Chondrocytes-embedded Hydrogels

Cell viability in the hydrogel plugs was determined using the live/dead assay. Chondrogenic medium was removed before addition of 1 ml of freshly prepared fluorescent live/dead staining solution (0.16% (v/v) 5mg/ml fluorescein diacetate (FDA) in acetone, 1% (v/v) 2mg/ml propidium iodide (PI) in PBS, phenol red free medium) to each well. Plates were returned to the incubator, protected from light (in foil) and the hydrogel plugs incubated for 30mins in the dark. Staining solution was removed, and the plugs washed 3 times with 1X PBS. Hydrogel plugs were cut through the middle perpendicularly to the plane of the two bases, and 1ml of 1X PBS added to each well to prevent dehydration. Bovine chondrocytes viability in hydrogel plugs was visualised using an Olympus IX71 inverted microscope with red (633nm) and green (488nm) filters.

2.9 Culture of Bovine Bone Marrow Stem Cells

2.9.1 Primary Isolation of Bovine Bone Marrow Stem Cells

Bovine bone marrow was obtained from the metacarpal bones of 7-day-old calves following slaughter (F Drury & Sons abattoir, Swindon). Feet were scrubbed to remove extraneous material with multi-purpose detergent (VWR international, UK) prior to removal of the skin. Metacarpal bone was cut using a sterile hacksaw into three parts and immediately transferred into an air-flow cabinet. Using a sterile spatula and spoon, bone marrow was scooped out and transferred into a 100mm petri dish. 10-15 ml of minimum essential medium α (α-MEM) (Gibco, UK) was added into each dish and mixed well with the bone marrow. The resulting suspension was sequentially filtered through 2 × 60μm metal cell strainers and a 40μm cell strainer. The filtrate was transferred into a 50 ml Falcon tube and centrifuged at 1000 g for 10mins at 37°C (Boeco U-32R, Hettich Zentifugen-D-78532, Germany). The resultant pellet was resuspended with growth medium (α-MEM culture medium containing 10% (v/v) FBS (Gibco, UK), 100U/ml Penicillin and 100μg/ml streptomycin (Thermo, UK)); the cells were seeded into T75 flasks at 2×10^4 cells/cm^2 and incubated at 37°C in a humidified atmosphere containing 5% CO_2. After 4-days of culture, non-adherent

cells were removed by washing with α-MEM culture medium and the adherent bovine bone marrow stem cells (bBMSCs) cultured for a further 2 days forming small colonies (Passage 1). The cell culture medium was changed every three days.

2.9.2 Passaging bBMSCs Cultures

At 80%-90% confluence, BMSCs were passaged. Briefly, culture medium was removed, and the cells were washed with 1X PBS. 5 ml of 0.05% (v/v) trypsin-EDTA (Gibco, UK) was added, and plates were incubated at 37˚C for 5 minutes or until they became detached and rounded. Culture medium (10X volume of trypsin) was added into the flasks to terminate the reaction. The solution was transferred into a 50ml Falcon tube and cells pelleted by centrifugation at 200 g for 5 minutes at 37°C. The resultant pellet was resuspended in α-MEM (as Section 2.9.1) and a cytometer was used to count cells prior to reseeding in new T225 flasks at a density of 1×10^4 cells/cm^2 or as per experimental requirements.

2.9.3 Cryopreservation of bBMSCs

Passage 3 bBMSCs were cryopreserved to maintain a stock of readily available cells. Following each passage, cell pellets were resuspended in freezing medium (9:1 FBS:dimethyl sulphoxide (DMSO) (Fisher Scientific, UK)) in vials containing 1×10^6 bBMSCs per 1 ml of freezing medium. Cryovials were kept in propan-2-ol filled Mr. Frostys (Nalgene, USA) for 24 hours for slow cooling to -80°C before transfer to a liquid nitrogen tank for long term storage.

2.9.4 Thawing bBMSCs

Cells stored in cryovials were transferred out from liquid nitrogen storage and placed upright in a 37°C incubator promptly until the cell suspension was thawed completely. Cells were transferred into a 50ml Falcon tube and resuspended in 10ml warm α-MEM. The cell suspension was centrifuged at 200 g for 5 minutes and supernatant discarded; the resultant cell pellet was re-suspended in 10ml of warm culture media

and seeded at the required cell density. The medium was changed after 24 hours to remove dead cells and debris.

2.10 Osteogenic Differentiation of bBMSCs

2.10.1 Osteogenic Differentiation of bBMSCs

For the analysis of osteogenic differentiation potential, passage 3 bBMSCs were seeded at 1×10^4 cells/cm^2 in 6-well plates. At 80%-90% confluency, cells were cultured with osteogenic differentiation medium (DMEM (Gibco, UK), 10% (v/v) FBS, 10nM dexamethasone, 0.1mM ascorbate acid-2-phosphate, 1mM sodium pyruvate, 10mM β-glycerophosphate, 100U/ml PS) and incubated at 37°C, 5% CO_2 and 95% oxygen for 21 days. The control group cells were seeded at the same density but cultured with α-MEM growth medium only for 21 days. The medium of both groups was changed every 3 days. On day 21, cells were processed for further analysis (Section 2.10.2).

2.10.2 Identification of Osteogenic Differentiation of bBMSCs by Alizarin Red S Staining

Medium was removed, cells were washed with 1X PBS twice and fixed with 4% (w/v) paraformaldehyde for 45 minutes at room temperature. Paraformaldehyde was removed and cells washed twice with distilled water. Cells were immersed in a solution of 40mM alizarin red S (pH 4.1) for 40 minutes, subsequently washed with sterile distilled water until the excess stain was removed, left to dry and observed by light microscopy (EVOS core; Invitrogen, UK).

2.11 Adipogenic Differentiation of bBMSCs

The adipogenic potential of bBMSCs was assessed; briefly, bBMSCs were seeded into 6-well plates at a density of 1×10^4 cells/cm^2 in α-MEM proliferation medium (Section 2.9.1). At 80-90% confluency, adipogenic medium (DMEM, 10% (v/v) FBS,

0.1mM indomethacin, 1μM dexamethasone, 500μM 3-Isobutyl-1-methylxanthine (IBMX), 10μg/ml insulin, 1mM sodium pyruvate, 100U/ml PS) was added and cells maintained at 37°C, 5% CO_2. Equivalent control cultures were maintained in α-MEM proliferation medium only for 21 days. The medium was changed every three days and lipid staining (Section 2.11.2) was carried out after 21-days in culture.

2.11.1 Identification of Adipogenic Differentiation of bBMSCs by Oil Red O Staining

Medium was removed, cells washed with 1X PBS twice and fixed with 4% (w/v) paraformaldehyde for 45 minutes at room temperature. After two washes with distilled water, 60% (v/v) isopropanol was added into each well and incubated for 5 minutes to improve the specificity of the dye for neutral lipids. Cell layers were subsequently immersed in a solution of oil red O (0.18% (w/v) oil red O, 60% (v/v) isopropanol) for 15 minutes. The staining solution was removed and cells washed with distilled water to remove excess stain. 1X PBS was added into each well before the cells were observed under a light microscope.

2.12 Chondrogenic Differentiation of bBMSCs

For the chondrogenic differentiation of bBMSCs, passage 3 cells were seeded in Eppendorf tubes at a density of 1×10^6 cells/pellet following centrifugation at 3000rpm for 10 minutes at 37°C. Cells were cultured with chondrogenic differentiation medium (DMEM, 0.1mM ascorbate acid-2-phosphate, 0.1μM dexamethasone, 1% (v/v) ITS, 1.25mg/ml BSA, 10ng/ml recombinant transforming growth factor β-3 (TGF-β_3: Peprotech, UK), 1mM sodium pyruvate, 100U/ml PS) for 28 days. The medium was changed every 2-3 days.

2.12.1 Paraffin Sectioning of Chondrogenic Pellets

At day 28, the pellets were fixed with 4% (w/v) paraformaldehyde (PFA) for 45 minutes at room temperature and then transferred into 70% ethanol. Paraffin

embedding and sectioning (5µm) was carried out by the Cardiff University Bioimaging Hub.

2.12.2 Identification of Chondrogenic Differentiation of bBMSCs by Toluidine Blue Staining

Sections were deparaffined with two changes of xylene (4 minutes each) and rehydrated through a decreasing ethanol series (100%, 100%, 90%, 70%, 4 mins each) before a final rinse with tap water for 5 minutes. Toluidine blue solution (0.1% in distilled water) was applied to cover each section for 1 minute then rinsed with tap water until clear. Excess liquid was removed from the sections using filter paper and transferred to an incubator at 37℃ for 30-60 minutes to dry. Sections (slides) were then twice clarified in xylene prior to addition of DPX mountant and coverslip.

2.12.3 Imaging

After the completion of staining, images were captured using a Leica DMRB upright brightfield microscope (magnification of 50X, 100X, and 200X) and a Jenoptic Progres SpeedXT core3 colour digital camera with Progres CapturePro software at Cardiff University Bioimaging Research Hub.

2.13 Chondrogenesis and Analysis of bBMSCs in CS-containing Medium on Monolayer

2.13.1 Chondrogenesis of bBMSCs in CS-containing Medium on Monolayer

Purified CS (Section 2.5) was diluted in either growth medium (Section 2.9.1) or chondrogenic medium (Section 2.12.1) to a final concentration of 100µg/ml. The CS-containing media were sterilised by filteration through a 0.2µm filter. bBMSCs were resuspended in a) control growth medium (without CS), b) with CS-containing growth medium (with 100µg CS per ml of growth medium) c) control chondrogenic medium (without CS) or d) CS-containing medium (with 100µg CS per ml of chondrogenic

medium) and plated into 12- well plates at 1×10^6 cells per well in quadruplicate. Plates were cultured at 37℃ (5% CO_2) for 14 days. Cells were then observed under a light microscope (EVOS core; Invitrogen, UK) and images taken every day over the 14 days culture period; medium was changed every three days. Analysis was carried out as described in sections 2.13.2.

2.13.2 Alcian Blue Staining and Quantitative Analysis for bBMSCs Chondrogenesis in CS-containing Medium on Monolayer

After 14 days of culture, bBMSCs were washed with PBS and fixed with 4% PFA for 1 hour at room temperature. 1ml of Alcian Blue solution (50mg alcian blue dye in 1ml 8M guanidine and 19ml of 18mM sulphuric acid-0.25% Triton X-100) was applied to each well for a 15-minute incubation period at room temperature. With removal of stain, PBS was used to rinse each well to get remove excess stain. The plate was observed, and images were taken using a mobile phone Xiaomi 13 Ultra (Xiaomi, China). The quantitative analysis of Alcian Blue staining on chondrogenesis of bBMSCs in CS-containing medium was conducted as previously published (Kawato et al., 2012). After Alcian Blue staining (Section 2.13.2), 4M GuHCl was employed to extract stains by overnight incubation at 4℃. With room temperature equilibration, the absorbance was measured at 600nm using a plate reader (BMG LABTECH, UK).

2.14 Chondrogenesis of bBMSCs in Agarose Hydrogel

2.14.1 Establishment of bBMSCs-embedded Hydrogel Constructs

As previously described (Section 2.8.2), 8mm diameter 2% agarose constructs containing 2×10^6/ml bBMSCs were generated, transferred into 24-well plates and cultured with 1ml chondrogenic medium. Hydrogels were cultured at 37℃, 5% CO_2 for 1 week and underwent Live/Dead assays.

2.14.2 Live/Dead Assay for bBMSCs-embedded Hydrogels

Cell viability in the hydrogel plugs was determined using the live/dead assay as previously described (section 2.8.3). Following staining, constructs were then cut through the middle perpendicularly to the plane of the two bases, and 1ml of 1X PBS added to each well to prevent dehydration. bBMSC viability in hydrogel plugs was visualised using an Olympus IX71 inverted microscope with red (633nm) and green (488nm) filters as described in section 2.8.3.

2.15 Chondrogenesis of bBMSCs in Transwell™ System

2.15.1 Chondrogenesis of bBMSCs using Transwell™ System in Medium Containing Chondroitin Sulphate Concentration Gradient

3rd passage bBMSCs were resuspended at 6×10^7/ml using DMEM containing 100U/ml penicillin, and 100µg/ml streptomycin, a 100µl volume was pipetted evenly onto the dry Transwell™ inserts (MilliQ) in a 24-well plate and the plate centrifuged at 200g for 5 mins. Chondrogenic medium was made up as Section 2.12.1 freshly with(out) the addition of purified CS for control group (no addition of purified CS), low concentration CS treatment group (10µg/ml) and high concentration CS treatment group (100µg/ml). 1ml of chondrogenic medium was added to the outside of the insert of each well and incubated at 37ºC, 5% CO_2 in a humidified chamber; medium with or without CS was replenished every 2 days and Transwell™ bBMSCs cultured for 6 weeks.

2.15.2 Paraffin Sectioning of Transwell™ Constructs and histological staining of ECM

After 6 weeks of Transwell™ culture, 4% (w/v) PFA was applied to the Transwell™ membrane overnight at 4°C. Each membrane was removed from the Transwell™ inserts and stored in 70% ethanol at 4°C until paraffin embedding and sectioning (5µm) was carried out by the Cardiff University Bioimaging Hub. Paraffin embedded

sections were deparaffinised and stained with Toluidine Blue (Section 2.12.2) and haematoxylin and eosin (H&E) by Cardiff University Bioimaging Hub.

2.15.3 Trichrome Staining

Sections were deparaffinised and rehydrated as previously described (section 2.12.2) and stained with Trichrome Stain (Abcam, UK). Sections were incubated for 60 mins at 60℃ with preheated (60℃) Bouin's Fluid to fix the sample, cooled for 10 mins followed by successive washes in tap then distilled water until the sections were completely clear. The sections were stained with Weigert's Iron Hematoxylin (equal parts of Weigert's A and Weigert's B) for 5 mins to stain the nuclei and rinsed with running tap water for 2 mins. Biebrich Scarlet/Acid Fuchsin Solution was used to stain sections for 15 mins to stain the proteins, and excess stain was removed with distilled water. The sections were then differentiated in Phosphomolybdic/Phosphotungstic Acid Solution to remove red staining from collagens until the collagen was not red and directly incubated with Aniline Blue Solution for 10 mins to stain collagens. After a rinse with distilled water, Acetic Acid Solution (1%) was applied to the sections for 5 mins to adjust pH and enhance dye binding specificity. Dehydration was achieved by increasing the concentration gradient of ethanol (75%, 95%, 100%, 100%, 4 minutes each) and twice in xylene (4 minutes each) followed by mounting with DPX. Imaging of the sections was carried out using a Leica DMRB brightfield photomicroscope at 100X and 200X.

2.15.4 Immunohistochemical Staining

Paraffin embedded sections were deparaffinised and rehydrated as previously described (Section 2.12.2). To block endogenous peroxidase activity, sections were incubated with 1% (v/v) H_2O_2 in methanol for 40 mins. To unmask epitopes and to improve antibody penetration, sections were treated with 40 mU/ml chondroitinase ABC (ChABC) for 1 hour at 37℃ (in 50 mM Tris, 60mM sodium acetate, pH 8.0), before treatment with 0.1% (w/v) pepsin (in 0.1 M acetic acid) for 1 hour at 37℃. Sections were treated with 1 mg/ml bovine testicular hyaluronidase in PBS at 37℃

for 1 hour to reduce the density of extracellular matrix. Between each enzyme treatment, 1X PBS containing 0.1% (v/v) Tween-20 (PBS/T) was employed to remove the previous enzyme treatment. To avoid non-specific antibody binding, sections were incubated with BLOXALL blocking solution (Vector Laboratories) for 10 mins before the sections were blocked with horse serum (Vector Laboratories) for 20 mins. Primary antibodies raised against collagen types I, II, VI and X were employed to detect collagen deposition (Table 2.2) with 1X PBS and mouse IgG or rabbit IgG as positive control, mouse joint sections gifted by Dr. Sophie Gilbert as positive controls, respectively. Sections were incubated in primary antibody overnight at 4°C.

After a 5 minutes wash with 1X PBS/T, sections were incubated with horse anti-mouse/rabbit IgG secondary antibody (Vector Laboratories) for 30 mins at room temperature. Following repeated washes in 1X PBS/T, VECTASTAIN Elite ABC reagent (Vector Laboratories) was employed to incubate sections for 30 mins before washing with Tween 20/PBS for 5 mins. ImmPACT DAB EqV solutions were mixed in a 1:1 ratio and applied to the sections for appropriate time until visible colour was produced. Sections were rinsed with tap water before undergoing sequential dehydration by increasing concentration gradient ethanol (75%, 95%, 100%, 100%, 4 minutes each) and twice xylene (4 minutes each) washes followed by mounting with DPX. Imaging of the sections was carried out using a Leica DMRB brightfield photomicroscope at 100X and 200X.

Table 2.2 List of primary antibodies used for immunohistochemical staining

Antibody	Type	Cat. No.	Dilution	Source/reference
COL-I	Goat monoclonal, IgG		1:100	Gifted by Prof. Vic Duance. S Li (PhD Thesis)
CIIC1	Chicken monoclonal, IgG	Ab528164 (DSHB, USA)	1:5	(Nandakumar and Holmdahl, 2005)
COL-VI	Rabbit monoclonal, IgG	Ab182744 (Abcam, UK)	1:250	(Corano Scheri et al., 2023)
COL-X	Rabbit monoclonal, IgG		1:1	Gifted by Klaus Von Der Mark. (Girkontaité et al., 1996)

2.16 Biochemical Assays

2.16.1 MTT Assay

At different time points depending on the experimental objectives, 3-[4,5-dimethylthiazol-2-yl]-2,5-diphenyltetrazolium bromide assay was conducted to examine cell viability. 0.1 volumes of 12mM Thiazolyl Blue Tetrazolium Bromide (MTT) solution, prepared according to the manufacturer's instructions with sterile PBS, was added to each well. After 4 hours, the mixture of medium and MTT solution was removed, an equivalent volume of dimethyl sulfoxide (DMSO) added to each well and mixed well with the formazan crystals. After a 10-minute incubation period, the absorbance of each well was measured at a wavelength of 570nm using a plate reader (BMG LABTECH, UK).

The viability of cells in the treated group was normalised to untreated control and expressed as a percentage before plotting.

2.16.2 DMMB Assay

Sulphated GAGs (sGAGs) content was measured using the dimethylmethylene blue (DMMB) assay (Little et al., 1990). Freshly prepared shark chondroitin-6-sulphate standards (10-40µg/ml) were added along with experimental samples, in triplicate, on a 96-well plate (CoStar, UK). The absorbances were read using a plate reader (BMG LABTECH, UK) at a wavelength of 525 nm immediately after 200µl of DMMB solution (16µg/ml 1,6-dimethylmethylene blue, 1% (v/v) ethanol, 29.5mM NaOH, 0.35%(v/v) formic acid) was added to each well. The absorbances of standards were used to produce a calibration curve in Matlab (R2021a). The line of best fit determined the concentration of sGAGs in the samples. Samples which produced absorbances out of the range of standards were diluted, re-assayed and the results scaled up accordingly.

2.16.3 BCA Assay

Pierce™ BCA assay kit (ThermoFisher, UK) was employed to measure the concentration of proteins in size exclusion fractions. Albumin Standards (BSA) with a concentration range 0µg/ml -2000µg/ml (0µg/ml, 25µg/ml, 125µg/ml, 250µg/ml, 500µg/ml, 750µg/ml, 1000µg/ml, 1500µg/ml, 2000µg/ml) were diluted from a stock concentration of 2mg/ml Albumin Standard as reference. 25µl of each standard and size-exclusion fraction (in duplicate) was added into each well of a 96-well plate. Then 200µl of the BCA working reagent (50:1, Reagent A: B from the assay kit) was pipetted into each well and mixed thoroughly on a plate shaker for 30 seconds. The plate was protected from light and incubated at 37°C for 30 minutes. The plate was cooled to room temperature before the absorbance was measured at 562nm on a plate reader (BMG LABTECH, UK). The absorbances of standards were used to produce a linear calibration curve in GraphPad Prism 9, from which the concentration of protein in the unknown samples were determined.

2.16.4 Direct ELISA Assay

Enzyme-linked immunosorbent assay (ELISA) was employed to detect CS GAG motifs in fractions from anion exchange or gel chromatography with the monoclonal antibodies 7D4, 6C3, 4C3, 3B3(-) and KS antibody 5D4 (Figure 2.1).

Samples (fractions) were prepared at a concentration of 2µg/ml sGAGs as measured using the DMMB assay in either coating buffer (Tris/Saline/Azide (TSA) buffer (50mM TRIZMA, 200mM NaCl, 0.02% (w/v) sodium azide, 0.05% (v/v) Tween, 0.4% HCl, pH 7.4) (whole PGs) or in 80% saturated 4.2M ammonium (free GAG chains). 100µl of each sample (fraction) was added to wells of a 96-well plate (ThermoFisher, Denmark) and left overnight at 4°C. Samples were removed and wells blocked with 100µl of 5% (w/v) BSA/TSA at 37°C for 1 hour. Plates were washed once with TSA (250µl per well), and 100µl primary antibody (Table 2.3) was added to appropriate wells with a 1-hour incubation at 37°C. Wells were washed with TSA 4 times and 100µl of alkaline phosphatase (AP)-conjugated anti-mouse secondary antibody (Promega, UK) diluted 1:5000 in 1% (w/v) BSA/TSA was added and incubated at 37°C for 1 hour. Wells were washed with TSA 6 times; 2 tablets of alkaline phosphatase substrate was dissolved in 10ml of DEA buffer (2.56% (w/v) magnesium chloride ($MgCl_2$), 9.6% (v/v) Diethanolamine, pH 9.8), 100µl was added to each well and incubated for 1 hour at 37°C, prior to recording of absorbance readings at 405nm using a plate reader (BMG LABTECH, UK).

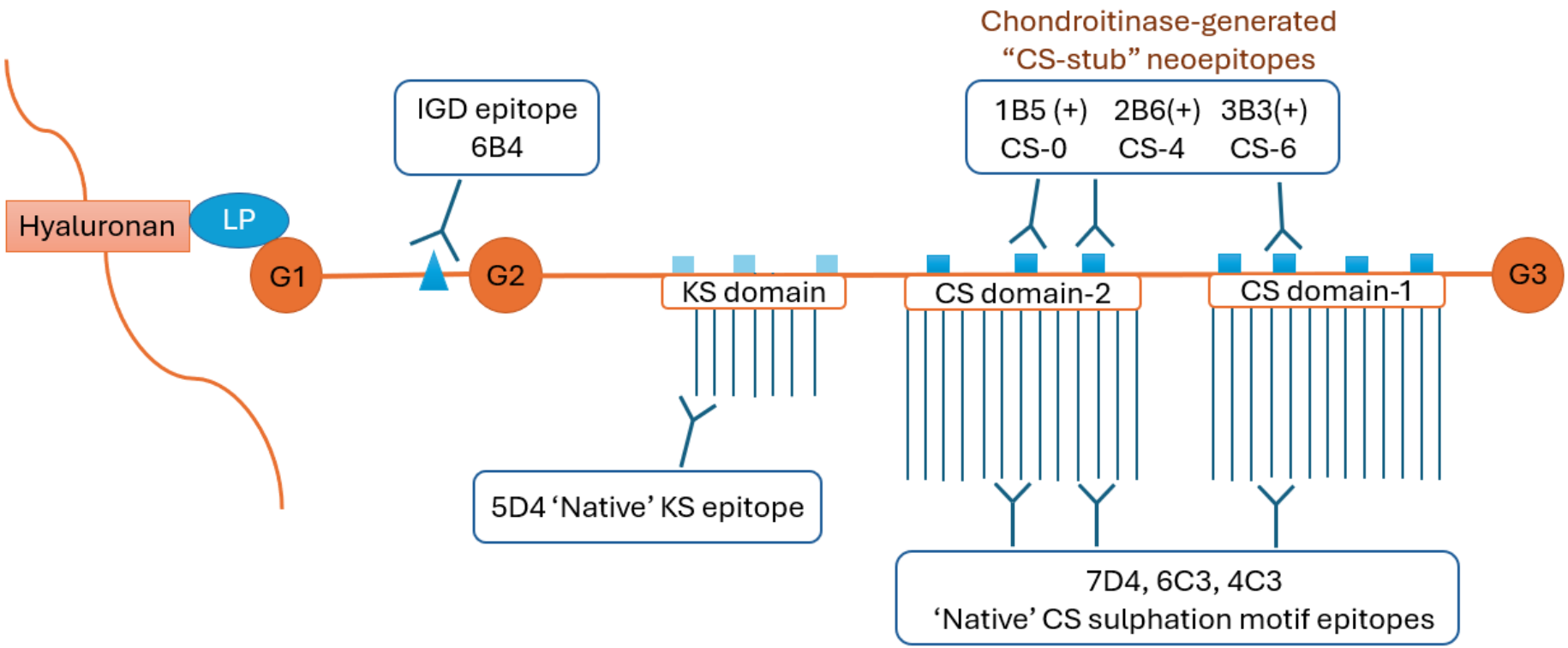

Figure 2.1 Monoclonal antibodies against metabolites of aggrecan. *Native CS epitopes include 7D4, 6C3 and 4C3. CS subtypes of CS-0, CS-4 and CS-6 can be digested by chondroitinase and generate neoepitopes of 1B5(+), 2B6(+) and 3B3(+). KS presents native 5D4 motif.*

Table 2.3 Primary antibodies used in the ELISA including clone isotype, molecular epitope detected and the dilution used.

Antibody (dilution)	**Clone (isotype)**	**Specificity**	**Source/references**
7D4 (1:5)	M (IgM_κ)	Distinct native CS/DS sulphation motif epitope occurring towards linkage region of CS chains	In house; (Caterson et al., 1990a)
6C3 (1:100)	M (IgM_κ)	Unidentified CS/DS sulphation motif epitope occurring towards non-reducing terminus of CS chains	In house; (Caterson, 2012)
4C3 (1:1)	M (IgM_κ)	Distinct, as yet unidentified, native CS sulphation motif epitopes occurring towards linkage region.	In house; (Cortes et al., 2009)
2B6 (1:5)	M (IgG_κ)	4-sulphated unsaturated disaccharide “stubs” (CS-4)	In house; (Couchman et al., 1984)
6B4 (1:1)	M (IgG_κ)	Linear amino acid sequence (394EPEEPFTFAPEI406) present in the interglobular domain (IGD) of aggrecan	In house; (Caterson et al., 2000)
CS-56 (1:200)	M (IgM_κ)	Chondroitin sulphate types A and C (not B, dermatan sulphate)	Gifted by Dr. Jim Ralphs; (Ohnishi et al., 2023)
5D4 (1:100)	M (IgM_κ)	Native KS linear di-sulphation motif epitope occurring towards non-reducing terminus of KS chains	In house; (Hayes and Melrose, 2020)

2.16.5 Competitive ELISA Assay

Microtiter plates were coated overnight at 4˚C with 100 µl of aggrecan (BAC-D1D1) at a concentration of 5µg/ml GAG in BAC-D1D1 diluted in coating buffer as described in Section 2.16.4. Coating solution was discarded, and wells were blocked in 5% (w/v) BSA/TSA for 1 hour at 37°C. After washing once with TSA buffer, BAC-D1D1 was diluted into sGAGs concentration of 0µg/ml, 0.5µg/ml, 1µg/ml, 2µg/ml, 5µg/ml, 7.5µg/ml, 10µg/ml and 20µg/ml as standards and 100 µl of a set of pre incubated standards were added in triplicate to appropriate wells. 100 µl of samples for analysis were also added to appropriate wells. The plate was incubated at 37°C for 1 hour, solutions were discarded, and plates washed 4 times with TSA buffer. 100µl of a 1:5000 dilution of alkaline phosphatase (AP)-conjugated anti-mouse secondary antibody (Promega, UK) (in 1% (w/v) BSA/TSA) was added and the plates incubated at 37°C for 1 hour. Wells were washed with TSA for 6 times followed by addition of 100µl DEA buffer (2 alkaline phosphatase substrate tablets in 10ml DEA buffer as described in section 2.16.4) for 1 hour at 37°C. Absorbances were recorded at a wavelength of 405nm and used to plot a standard curve to determine inhibition of binding of the unknown samples.

2.16.6 Barium Acetate Gel Electrophoresis and Alcian Blue Staining for the Detection of β-eliminated Glycosaminoglycans.

PG and GAG samples were visualised on 0.5% (w/v) agarose gels made up in 40mM barium acetate buffer (40mM barium acetate, pH 5.8 with 1M acetic acid, stored at 4°C). The solution was micro-waved to dissolve the agarose completely and when sufficiently cooled the warm solution was poured into an 8×10cm gel cassette. A comb was placed about 1cm from the edge of the gel generating 5mm wells for sample loading. The gel was allowed to set at room temperature for approximately 40 minutes followed by transfer to the electrophoresis tank filled with PDA buffer (50mM 1,2-diaminopropane (PDA), pH 9 with glacial acetic acid). 10µg GAG per sample with 20% (v/v) cresol red solution (0.1mg/ml cresol red dye in distilled water)

and 20% (v/v) glycerol were loaded into the wells. Electrophoresis was performed for 3.5 hours at 50mA in an electrophoresis tank (Anachem).

8×10cm nitrocellulose membrane (Amersham, Germany) was derivatised with freshly prepared 1% (w/v) CPC (in 30% (v/v) 2-propanol) for 5 minutes and incubated in 150mM NaCl solution for 15 minutes. The membrane was rinsed several times in 150mM NaCl to remove the excess CPC. The blotting sandwich was assembled as follows: Whatman 3mm filter paper was placed on a glass plate, two ends of which were immersed in a reservoir of transfer buffer (100mM Tris-acetate buffer, pH 7.3 with glacial acetate acid) allowing the migration of the buffer from the two sides to the top side of the blotting sandwich. The agarose gel was carefully placed on the filter paper and the detergent-treated NC membrane, placed on top of the gel followed by three pieces of filter paper and two sponges soaked with transfer buffer. Bubbles were removed using a roller. Finally, 5 layers of absorbent paper tissue were put on top of the blotting sandwich and stabilized by placing a 500-gram weight on top. The capillary blotting was performed overnight at room temperature.

Membranes were submerged in freshly prepared Alcian Blue solution (50mg alcian blue dye in 1ml 8M guanidine and 19ml of 18mM sulphuric acid-0.25% Triton X-100) for about 20 minutes, rinsed with 150mM NaCl and further destained using 150mM NaCl until bands were visible. Membranes were scanned using an EPSON PERFECTION V750 PRO scanner.

2.16.7 SDS-PAGE and Western Blotting

2.16.7.1 SDS-PAGE Electrophoresis

10µg GAG was diluted 1:1 with 2x sample buffer (125mM tris-HCl, pH 6.8, containing 4% (w/v) sodium dodecyl sulphate (SDS), 20% (w/v) glycerol; 0.01%(w/v) bromophenol blue) and boiled for 5 minutes at 100°C. Samples were loaded onto 4-12% (or 4-20%) Tris-glycine gradient gels (nUView, USA) and separated in SDS running buffer (25mM trizma, pH 8.4;192mM glycine, 0.01% (w/v) SDS) using gel electrophoresis; gels were run at 180 volts for about 60 minutes (until the bromophenol blue sample buffer reached the end of the gel). The molecular weight of

separated molecules was sized against Precision PlusProtein^{TM} Standards (Bio-Rad, UK). Samples were subsequently transferred to nitrocellulose membranes (Whatman, UK) using SDS transfer buffer (25mM trizma, pH 8.1-8.4;192mM glycine, 20%(v/v) methanol) at 20 volts overnight.

2.16.7.2 Western Blotting

For Western blot analysis, nitrocellulose membranes were blocked in 5% (w/v) BSA/TSA for 1 hour at room temperature, with gentle agitation, followed by probing the membranes with the primary antibodies diluted in 1% (w/v) BSA/TSA (Table 2.3), at room temperature for 1 hour. Blots were rinsed with TSA buffer for 3×10 minutes before a 1-hour incubation with an alkaline phosphatase conjugated anti-mouse secondary antibody (Promega, UK) (1:7500 dilution in 1% (w/v) BSA/TSA) at room temperature. After a further 3×10 minutes washes in TSA, the immunoblots were incubated with an alkaline phosphatase substrate (100mM tris-HCl, 100mM NaCl, 5mM $MgCl_2$, pH 9.8) containing 0.66% (v/v) nitro blue tetrazolium (NBT) (Promega, UK) and 0.33% (v/v) 5-bromo-4-chloro-3-indoylphosphate (BCIP) for 10-50 minutes at room temperature or until optimal colour development of immuno-positive bands was achieved. This analysis was used to determine the biochemical and macromolecular status of the A1 aggrecan core protein.

2.16.8 Dot Blotting

To eliminate the potential loss of GAGs in membrane transfer in Western blotting and achieve better GAGs epitope detection, dot blotting was employed to detect GAGs. 5µl of samples (fractions) were pipetted onto a nitrocellulose membrane and air dried for approximately 30-60 minutes. Subsequent blotting steps were carried out as previously described (Section 2.16.7.2).

2.17 Gene Marker Expression using Real-time Quantitative Polymerase Chain Reaction (RT-qPCR)

2.17.1 RNA Isolation using RNeasy Mini Kits

RNA was isolated using the Qiagen RNeasy Mini Kit (Qiagen, Germany) according to the manufacturer's protocol. In brief, 0.2ml of 1-bromo-3-choloropropane (Sigma-Aldrich, Dorset, UK) was added to thawed samples containing 1ml TRIzol™-Reagent and left for 15mins at room temperature before centrifugation at 10,000 g for 15mins at 4°C (Boeco, U-32R, Hettich Zentifugen-D-78532, Germany). The upper RNA containing aqueous phase was carefully transferred to a new sterile Eppendorf tube and an equal volume of 70% ethanol (EtOH) added to each sample and mixed, followed by transfer of approximately 800µl of sample/EtOH mixture into the Qiagen RNeasy kit spin column which was then spun at 7,000 g for 15sec at 4ºC. The flow through was discarded and the above step was repeated for the remaining sample/EtOH mixture. 700µl of Buffer RW1 was added to each spin column before spinning at 7,000 g for 15sec at 4ºC; the flow through was discarded followed by the transfer of a spin column to a new collection tube. Residual buffer was removed prior to the addition of 500µl of Buffer RPE to the spin columns, then the columns were centrifuged for 15sec at 7,000 g at 4ºC with the flow through discarded. Another 500µl of Buffer RPE was added to spin columns before spinning at 7,000 g for 2mins. The spin column was dried by centrifugation at full speed for 2mins before air-drying for 15mins to allow the evaporation of EtOH. 30µl of RNase free water was added directly to the spin column membrane and centrifuged at 7,000 g for one minute to elute and collect RNA which was stored at -80°C.

2.17.2 RNA Isolation by 2-propanol Precipitation

RNA was also isolated using modifications of the methodology as described previously (Blain et al., 2003). Briefly, 1ml of TRIzol™ reagent was added to chondrocyte monolayers and transferred to sterile microcentrifuge tubes after which 200 µl of 1-bromo-3-chloropropane was added. Tubes were shaken vigorously for 15 seconds and left to stand for 10 minutes at room temperature before centrifugation at

10,000 g for 15 mins at 4°C (Boeco U-32R, Hettich Zentifugen-D-78532, Germany). The upper aqueous phase containing RNA was transferred to a new RNase-free 1.5 mL Eppendorf tube and a 1:1 volume of 2-propanol (Sigma-Aldrich, Dorset, UK) added to precipitate RNA at -20°C overnight. Tubes were centrifugated at 10000rpm for 10 mins at 4°C to pellet the RNA. The supernatant was removed by pipetting and 1mL of 75% EtOH added to wash the pellet before centrifugation at 7,000 g for 5mins at 4°C. The supernatant was removed, and the RNA pellet was air dried for 15-30 mins before addition of 26µl nuclease free water.

2.17.3 Removal of Genomic Contaminants

Genomic DNA was removed by performing a DNase treatment whereby 2 Units/µL DNase (Invitrogen, UK) and 3µl 10X DNase buffer were added to the RNA and incubated at 37°C for 30 mins. 0.1 volumes of DNase inactivation reagent (Invitrogen, UK) was added to the RNA solution to remove impurities, salts and other contaminants followed by centrifugation at 7,000 g for 2 mins at room temperature. Pure RNA was transferred to a new Eppendorf tube and stored at -80°C.

2.17.4 Measurement of RNA Quality and Quantity

The purity (A260:A280 ratio) and concentration (ng/µl) of RNA samples was quantified using the Nanodrop^{s} Lite Spectrophotometer (Thermo Scientific^{TM}, ThermoFisher Scientific, Paisley, UK). The instrument was cleaned with lens tissue, blanked against 1µl of nuclease free water, cleaned again before placing 1µl of each sample on the sensor. An A260:A280 ratio of between 1.8 and 2 was considered as sufficiently pure RNA for further analysis.

2.17.5 Reverse Transcription of RNA

cDNA was synthesised as described previously (Blain et al., 2003) with a few modifications. 200ng of RNA was added to 250ng of random primers (Promega, Southampton, UK) and 100µM dNTPs and made up to 20µl with nuclease free water.

Components were then incubated at 60°C for 5mins to promote annealing of primers to template RNA in a Techne^{TM} TC-3000 Thermal cycler (Bibby Scientific Ltd, UK) before cooling on ice. A reverse transcription (RT) master mix comprising 6 µl 5x 1st Strand buffer (250mM Tris pH 8.3, 375mM KCl, 25mM $MgCl_2$), 30mM DTT, 20U recombinant RNasin RNase inhibitor (Promega, Southampton, UK) and 20U Superscript IV^{TM} reverse transcriptase was prepared. 10µl of the RT master mix was added to 20µl of RNA/random primer/dNTPs mixture followed by incubation at 23°C for 10mins prior to incubation for 50mins at 50°C to allow extension of nucleotide sequences, then 15mins at 70°C to inactivate the reactions using a Techne^{TM} TC-412 Thermal cycler (Bibby Scientific Ltd, UK).

2.17.6 RT-qPCR

Real time-quantitative polymerase chain reaction (RT-qPCR) was utilised to quantify gene expression by fluorescent DNA binding dye SYBR Green. The dye is able to intercalates into double-stranded DNA, and the fluorescence is measured and recorded at the end of each cycle in an AriaMx Real-Time qPCR machine (Agilent Technologies, Cheshire, UK).

1µl of cDNA was added to 19µl of a qPCR reaction mix made up of 7.8µl nuclease free water, 1X Brilliant III Ultra-fast SYBR Green qPCR master mix (Agilent Technologies, Cheshire, UK), 200nM gene specific forward and reverse primers (Table 2.4). The resulting 20µl reaction volume was placed in a 96-well plate, allowing the polymerase chain reaction to happen under the following cycling conditions; heating at 95°C for 3mins for one cycle to activate DNA polymerase, before performing 40 cycles of denaturation at 95°C for 15sec and incubation at 60°C for 30 sec to allow the annealing of primers to template DNA and extension of nucleotide sequences. One more cycle of incubation at 95°C for 1min, 65°C for 30sec and 95°C for 1 minute was performed to generate standard melting curves.

Following amplification, melting curve analysis was carried out on individual samples where a single peak representing amplification of a single product was acceptable, where the intensity of emission fluorescence is proportional to the amount of cDNA template since SYBR Green only fluoresces when bound to DNA. Threshold cycle

values (C_T) of relevant genes were compared to stably expressed housekeeping genes, and the relative gene expression was calculated using the $\Delta\Delta C_T$ method (Livak and Schmittgen, 2001).

2.17.7 Selection of Housekeeping Genes

A set of candidates housekeeping genes, including *gapdh*, *18s*, *ywhaz*, *sdha*, *ppia*, *hprt1*, *rpl4*, were selected based on previous literature and studies. The primers were all designed and gifted by Lekau Dintwa (Table 2.4). The expression of housekeeping genes was measured by RT-qPCR as described in section 2.17.6. C_T values of housekeeping genes were then analysed by an online tool, RefFinder, which ranks all genes based on the geometric mean of four algorithms of geNorm, NormFinder, BestKeeper and ΔC_T method. The most stable housekeeping gene was selected for normalisation in subsequent gene expression analyses by the $\Delta\Delta C_T$ method.

Table 2.4 Primer information of housekeeping gene and cartilage gene markers

Gene	**Accession number**	**Forward primer sequence 5'-3'**	**Reverse primer sequence 5'-3'**	**Reference**
gapdh	NM_001034034	TGTCTCCTGCGACTTCAACAGCG	CACCACCCTGTTGCTGTAGCCAAAT	(Darling and Athanasiou, 2005)
sdha	NM_175814	GATGTGGGATCTAGGAAAAGGCCTG	ACATGGCTGCCAGCCCTACAGA	(Anstaett et al., 2010)
ywhaz	NM_174814	CTGAGGTTGCAGCTGGTGATGACA	AGCAGGCTTTCTCAGGGGAGTTCA	(Anstaett et al., 2010)
18s	NR_036642	GCAATTATTCCCCATGAACG	GCCTCACTAAACCATCCAA	(Frye et al., 2005)
ppia	NM_178320	GGTGGTGACTTCACACGCCATAATG	CTTGCCATCCAACCACTCAGTCTTG	(Anstaett et al., 2010)
hprt1	NM_001034035	TAATTATGGACAGGACCGAACGGCT	TTGATGTAATCCAACAGGTCGGCA	(Anstaett et al., 2010)

rpl4	NM_001014894	TTTGAAACTTGCTCCTGGTGGTCAC	TCGGAGTGCTCTTTGGATTTCTGG	(Anstaett et al., 2010)
acan	NM_173981.2	CAGCCAGGCCACCCTAGAG	GGGTGTAGCGCGTGGAGAT	(L. Dintwa, unpublished)
col-2a1	NM_001001135.3	AGCAGGTTCACATATACCGTTCTG	CGATCATAGTCTTGCCCCACTT	(L. Dintwa, unpublished)
sox-9	XM_024981096.1	TGAAGATGACCGACGAGCAGG	CCGCTTCTCGCTCTCGTTCAG	(L. Dintwa, unpublished)

2.18 Statistical Analysis

All biochemical data are presented as mean ± SD and analysed using a parametric two-way ANOVA test (GraphPad Prism 9). The normality of data distribution was assessed using the Shapiro-Wilk test and visually inspected using Q-Q plots. Homogeneity of variance was tested using Levene's test to ensure the assumptions for parametric tests were met. If assumptions were violated, appropriate non-parametric tests were used. To compare the means of more than two data sets, Dunnett post-hoc test was performed. For the qPCR data, each normally distributed gene was tested for significant differences using 2-way ANOVA test to determine differences between every CS-containing group and CS free control group. Statistical differences were considered significant at P values <0.05 and represented on figures as $*/^{\#}$, $**/^{\#\#}$ and $***/^{\#\#\#}$ denoting $p < 0.05$, 0.01, 0.001 respectively.

Chapter 3

Purification and Characterisation of Free Chondroitin Sulphate from Bovine Cartilage

3.1 Introduction

The identification of CS motifs 7D4, 6C3, and 4C3 in PGs associated with stem cells highlights their potential role in modulating growth factor (e.g. TGF-β1) interactions crucial for chondrocyte phenotype maintenance and differentiation of BMSCs into the chondrogenic lineage (Goude et al., 2014). These CS motifs have been shown to be transiently and spatially regulated during tissue morphogenesis, influencing cellular differentiation and ECM organisation. The presence of 7D4, 6C3, and 4C3 epitopes in developing musculoskeletal tissues, including articular cartilage and the intervertebral disc, suggests their involvement in chondrogenic processes (Sorrell et al., 1988a). Notably, 7D4 is expressed in transitional tissues, particularly in regions undergoing morphogenetic changes, such as the superficial zone of articular cartilage (Sorrell et al., 1988b). Similarly, 4C3 and 6C3 have been implicated in perichondrial and interzone regions of developing joints, potentially facilitating stem cell migration and differentiation (Candela et al., 2014). Furthermore, these CS sulphation motifs have been linked to the sequestration and regulation of key growth factors, such as members of the TGF-β and IGF families, within the cartilage matrix (Hayes et al., 2008). This interaction is essential for maintaining the chondrocyte phenotype and guiding the differentiation of stem cells into the chondrocyte lineage. Given the selective expression patterns of CS motifs 7D4, 6C3, and 4C3, and their functional associations between them and stem cells, these motifs may serve as critical molecular markers for chondrogenesis and cartilage homeostasis, offering valuable insights into chondrocyte/stem cell-based cartilage repair strategies (Hayes et al., 2018b). To determine the influence of free CS chains on chondrogenesis of BMSCs, the overall aim of this chapter was to purify and characterise the free CS molecules from bovine articular cartilage PGs with a view to identify CS chains enriched for 7D4, 6C3 and 4C3 epitopes in which the core peptide had been removed as shown in figure 3.1.

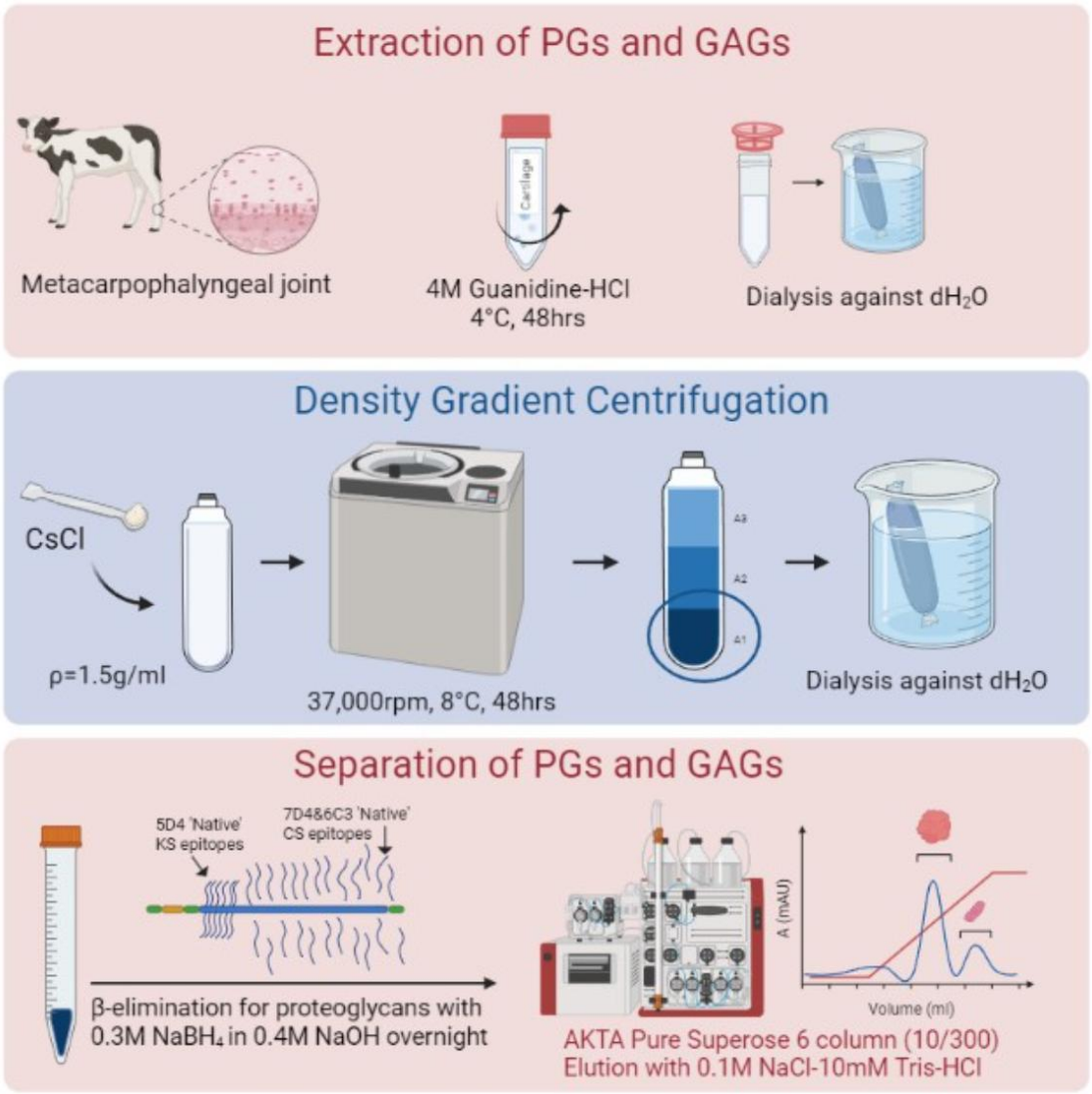

Figure 3.1 Illustration for free CS chain purification methodology from bovine joint cartilage. *4M Gu-HCl was employed to extract PGs from 3-week-old bovine metacarpophalyngeal joint before a CsCl density gradient centrifugation at 120,000 g for 48 hours at 8°C. The bottom one third fraction containing aggrecans was dialysed against water to get rid of salts. CS chains were released from aggrecan core proteins with alkaline treatment of β-elimination and then separated by anion-exchange chromatography and size-exclusion chromatography successively.*

3.1.1 Source of Chondroitin Sulphate

Bovine cartilage is an abundant source of CS, as well as its easy access from abattoirs, making it a suitable model for extraction and study of CS. Free CS chains are not naturally occurring but are typically a constituent of proteoglycans, such as aggrecan, where they are covalently attached to a core protein (Bains et al., 2023). Therefore, the traditional isolation process to free CS chains requires the enzymatic or chemical cleavage of the proteoglycan structure (Sundaresan et al., 2018, Ruensodsai et al., 2021), followed by purification to remove other biomolecules like proteins, DNA and other GAGs (Nakano et al., 2010). However, the methods involved use papain and other proteinases which often cleave the core proteins of PGs leaving behind a peptide segment on the end of the CS chains (Bai et al., 2018, Ticar et al., 2020). Hence, to explore specific bioactivities of CS chains and effects on BMSCs chondrogenesis, it is necessary to purify and characterise high-purity free CS chains without damaging their structure or biological properties.

In the context of this study, 3-week-old calves were selected as the source of PGs for CS isolation. In skeletally immature cartilage, particularly in calves at this age, there is a high concentration of GAGs, primarily CS (Collin et al., 2017). Immature cartilage has a larger proportion of CS compared to other GAGs, like KS (Sharma et al., 2007, Caterson and Melrose, 2018), making it an ideal source for extracting CS in its most abundant form. This high GAG content, combined with a relatively simpler ECM structure compared to skeletally mature animals (Sophia Fox et al., 2009, Lotz and Loeser, 2012), facilitates the extraction and purification process. Additionally, neonatal cartilage has less structural modifications and degradation compared to adult cartilage, resulting in a more homogeneous population of PGs (Bayliss et al., 1999, Shibata et al., 2024). This is particularly important when studying intact CS chains, as the lower level of post-translational modifications makes the isolation process more straightforward, ensuring the integrity of the CS chains is preserved for downstream analyses. In contrast, mature cartilage tends to contain a higher proportion of KS (Caterson and Melrose, 2018), has reduced total GAG content (Kobayashi-Miura et al., 2022) and is more prone to degradation (Li et al., 2013c), making it less suitable for this research. Furthermore, given that 3-week-old calves are not skeletally mature,

their chondrocytes are likely still undergoing active differentiation. It is therefore plausible that CS composition contributes to phenotypic changes in these immature chondrocytes, potentially affecting their maturation trajectory and ECM composition. The dynamic expression of CS epitopes of 7D4 and 6C3 during embryonic development, as demonstrated in the developing chicken bursa of Fabricius and chick cartilage (Caterson et al., 1990b), suggests that CS chains play a crucial role in tissue-specific and age-dependent regulation of chondrocyte differentiation. In particular, the differential localisation of native CS epitopes, such as 7D4, 6C3 and 3B3(-), within specific chondrocyte populations of the growth plate and hypertrophic zones, highlights the potential for CS chains to influence cartilage maturation . Therefore, the cartilage from 3-week-old calves provided an optimal balance of GAG richness, structural simplicity, and ease of processing, making it a reliable source for obtaining high-purity CS suitable for subsequent characterisation.

3.1.2 Methodology Optimisation for Chondroitin Sulphate Purification

The chaotropic agent of 4M GuHCl was employed in this study to extract PGs (Section 2.2.2). GuHCl is a powerful chaotropic agent that disrupts the non-covalent interactions between PGs, collagen and other matrix components within the ECM (Pramanick et al., 1976). This disruption is crucial for solubilising PGs, allowing them to be extracted efficiently while preserving their native structure, including the attached GAG chains (Tatara et al., 2015). One of the key benefits of using 4M GuHCl is its ability to maintain the integrity of PGs by minimizing enzymatic degradation during the extraction process. The high concentration of GuHCl denatures proteins and deactivates proteolytic enzymes, preventing the breakdown of the PG core protein or CS chains (Chang et al., 1983). This ensures that the extracted proteoglycans remain intact, which is vital for subsequent steps and characterisation of free CS chains. This method is commonly used in cartilage research as it provides a reliable and efficient means of extracting high-quality proteoglycans while maintaining the biological and structural properties necessary for detailed downstream analyses, such as GAGs profiling and molecular characterisation.

Once the PGs have been extracted by 4M Gu-HCl and CsCl density-gradient centrifugation (Section 2.3.1), the next step involves releasing the CS chains from the core protein. This is achieved through β-elimination, a chemical reaction carried out under alkaline conditions that cleaves the tetra-saccharide linker between the core protein and the CS chain (Conrad, 2001). This method is particularly advantageous because it selectively breaks the bond at the core protein linkage site without degrading the CS chain itself (Perez et al., 2023). $NaBH_4$ was employed in this process because it acts as a reducing agent, which helps stabilise the released GAG chains; it also prevents unwanted side reactions that could degrade the structure of the CS by protecting the newly formed reducing ends of the GAG chains during β-elimination (Laremore et al., 2010). Without this protection, the released CS chains could undergo further degradation or side reactions, potentially altering their molecular integrity. By reducing the aldehyde groups formed at the reducing ends of the GAG chains, $NaBH_4$ ensures that the CS chains remain intact and structurally stable (Huang et al., 2002). Moreover, $NaBH_4$ enhances the overall efficiency of the β-elimination process by ensuring a complete release of the GAG chains from the proteoglycan core. This allows for a higher yield of pure, intact CS, which is essential for obtaining reliable data in subsequent analytical procedures (Zauner et al., 2012). By preserving the native structure of the CS chains, β-elimination allows for the recovery of free CS in a form suitable for detailed analysis.

Following the release of CS chains, purification is necessary to remove any residual proteins, nucleic acids and other impurities. Chromatographic techniques are commonly employed for this purpose (Krichen et al., 2018a). In this study, anion-exchange chromatography was used to separate CS chains based on their charge properties. As a polyanionic molecule, CS binds strongly to positively charged resins, allowing for the selective elution of the purified chains under controlled conditions (Silva, 2006). Additional purification steps including size-exclusion chromatography was also employed to ensure that only CS chains of the desired molecular weight range were collected (Vázquez et al., 2018).

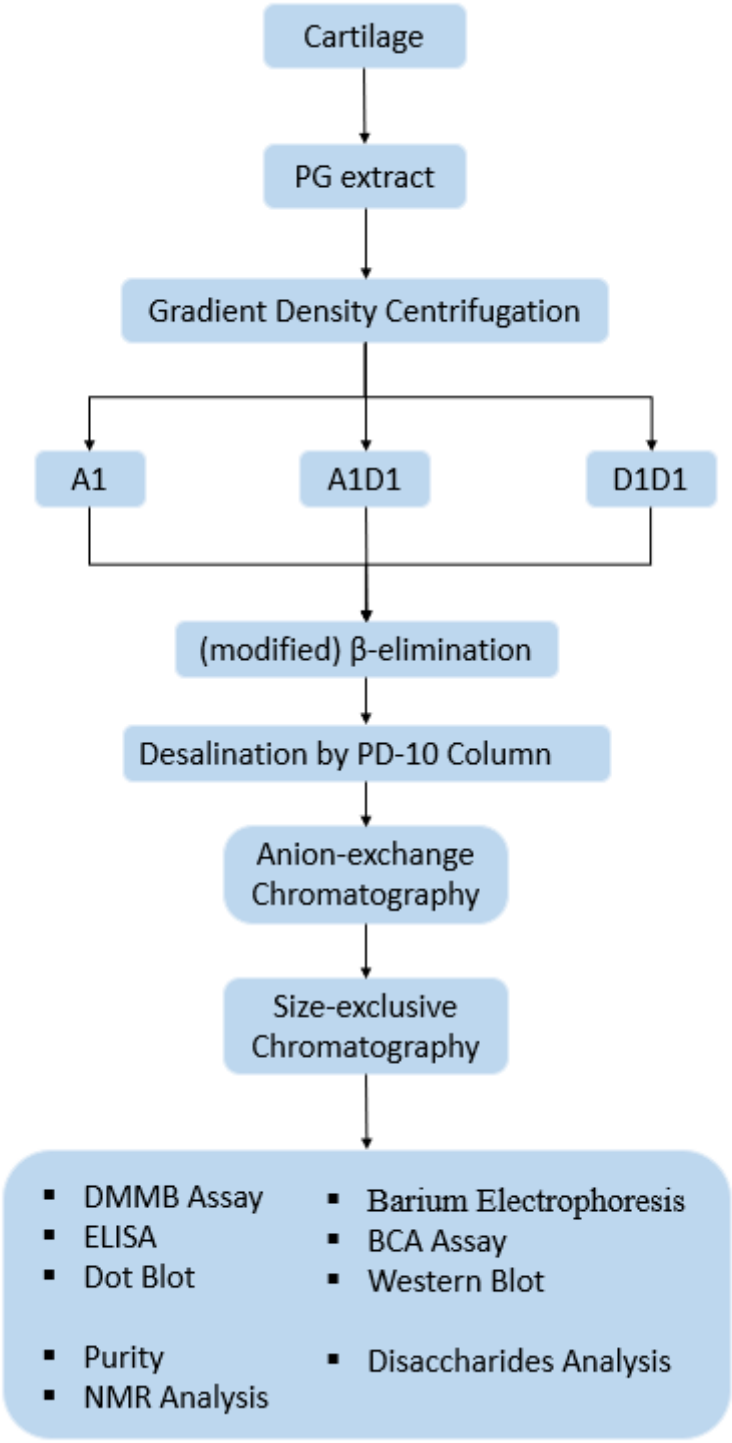

Figure 3.2 Flowchart illustrating the process for purifying CS in current study. *Cartilage was subject to 4M GuHCl and density gradient centrifugation with CsCl to extract aggrecan aggregates (associative centrifugation: A) and aggrecan monomers (dissociative centrifugation: D). With modified alkaline treatment (β-elimination) to release CS from core protein, extracts were then applied to anion-exchange chromatography and size-exclusion chromatography to separate CS from other molecules and contaminants. A series of tests were conducted to characterise purified CS.*

3.1.3 Characteristics of Free Chondroitin Sulphate epitopes using antibodies 7D4, 6C3, 4C3 and CS-56

CS is a sulphated GAG that plays a vital role in various biological processes, including cell signalling, ECM organisation, and tissue repair (Mellai et al., 2020). Its diverse structural forms, arising from specific sulphation patterns, contribute to its functional heterogeneity and interaction with a wide array of biomolecules (Lin et al., 2020a). This structural variability can be characterised using in-house monoclonal antibodies, such as 7D4 and 6C3 (Hayes et al., 2016) , as shown in figure 3.3.

These epitopes, defined by unique sulphation patterns and structural configurations, have been instrumental in advancing our understanding of CS's role in immune responses and tissue physiology (du Souich et al., 2009). For instance, the 7D4 epitope is typically associated with acute joint injuries, where 7D4 was reported to increase two- to threefold and even higher in the first 3 months after injury (Bautch et al., 2000). Furthermore, CS sulphation motifs recognised by both 7D4 and 6C3 antibodies were reported to identify stem cells and stem cell niches, which were also found in transitional areas in foetal human elbow development (Ashworth et al., 2021).

By characterising these epitopes, researchers have uncovered critical insights into the functions of CS, including its involvement in inflammation, wound healing, and immune regulation (Hayes et al., 2018b). This study utilised characteristics of CS, focusing on key epitopes, including 7D4 and 6C3, and KS native epitope 5D4 for KS contamination probing (Caterson and Melrose, 2018), highlighting their structural features and functional significance in health and disease.

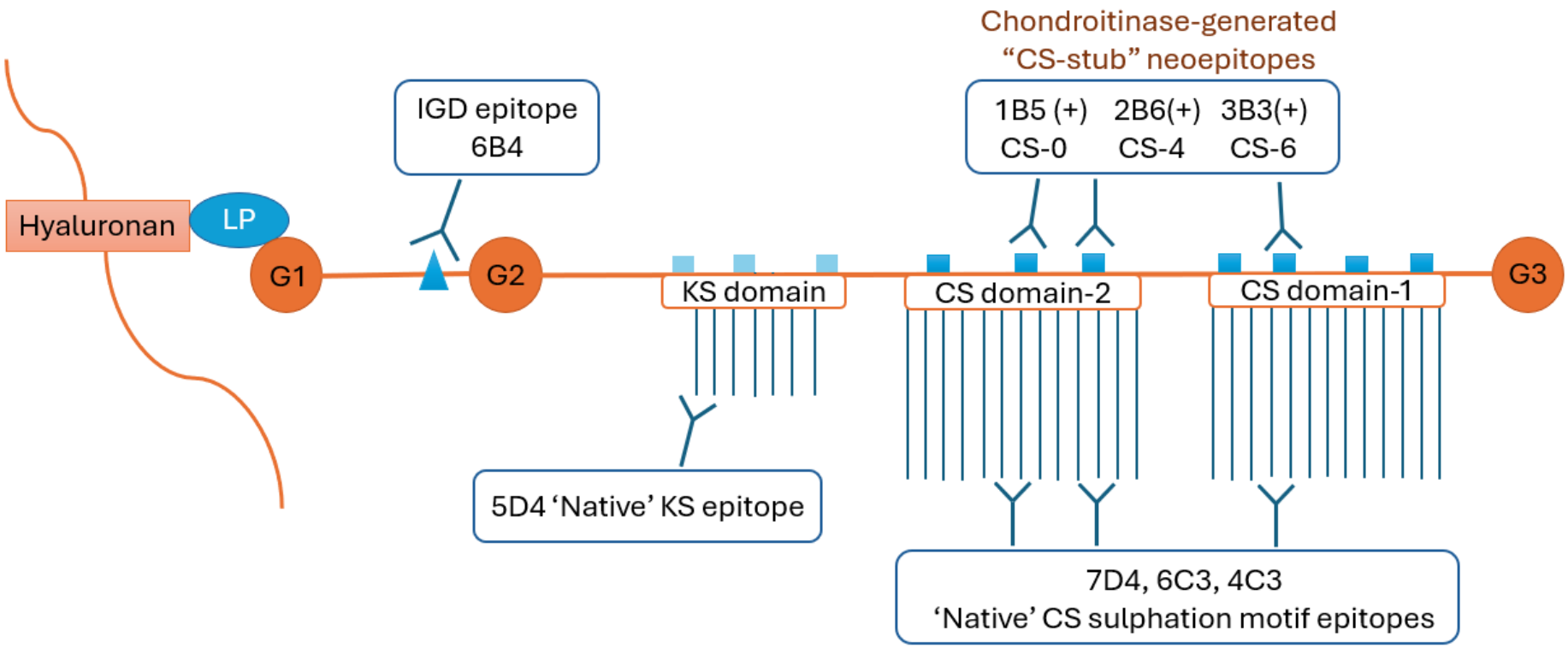

Figure 3.3 Monoclonal antibodies against metabolites of aggrecan. *Aggrecan molecule presents IGD epitope 6B4 and native CS epitopes, including 7D4, 6C3 and 4C3. CS subtypes of CS-0, CS-4 and CS-6 can be digested by chondroitinase and generate neoepitopes of 1B5(+), 2B6(+) and 3B3(+). Our in-house antibodies of 7D4 and 6C3 were used to detect native CS epitopes. Native KS presents 5D4 motif, which was used in this study to probe any potential KS contaminants in CS preparation.*

3.1.4 Characterisation of Free Chondroitin Sulphate

After purification, the free CS chains were subjected to a series of analytical techniques to determine their structural properties, including overall purity, sulphation pattern and disaccharide composition. These characteristics are critical for understanding the biological activity of CS, as variations in sulphation can influence its interaction with proteins, enzymes and other components of the ECM (Nandini and Sugahara, 2006a, Bayliss et al., 1999). High-performance liquid chromatography (HPLC) is commonly used to analyse the composition and sulphation pattern of CS, providing detailed information about the specific disaccharide units and their sulphation positions (Tian et al., 2024).

Spectroscopic techniques, such as nuclear magnetic resonance (NMR) spectroscopy, were also employed to further characterise the structure of the CS chains (Mucci et al., 2000). NMR provides detailed information about the position and configuration of sulphate groups and allows for the identification of subtle structural variations between different CS isoforms (Gardini et al., 2023). These structural details are essential for understanding how variations in CS structure affect its interactions with proteins, growth factors and enzymes, and how these interactions contribute to the overall function of cartilage.

3.2 Results

3.2.1 Barium electrophoresis demonstrates free GAG chains after β-elimination.

PGs were isolated from sources by using 4M GuHCl, which was labelled with A1 if it underwent density gradient centrifugation under associative conditions for pooling aggrecan aggregates at the bottom one third fraction as described in section 2.3.1.1, and was labelled with A1D1 with dissociative centrifugation as described in section 2.3.1.2. A1D1 from chick sterna (Chick-A1D1), A1fraction from bovine articular cartilage (BAC-A1), and BAC-D1D1 (kindly gifted by Prof. Clare Hughes) were subject to β-elimination as described in section 2.3.2 and barium gel electrophoresis was performed to ascertain if free GAG chains had been liberated by the reaction as described in section 2.16.6.

After separation, membranes were either stained with Toluidine Blue (Figure 3.4A) or immunoblotted with 7D4 to detect CS (Figure 3.4B). Sigma CS standards were used for reference. In figure 3.4A, the separation of ChickA1D1 (lane 1), BAC-A1 (lane 2) and β-eliminated BAC-A1 (lane 3) showed that the migration of the β-eliminated BAC-A1 (lane 3) was further than those of Chick-A1D1 and BAC-A1 (lanes 1 and 2, respectively) indicative of the generation of free GAG chains. The 7D4 immunoblot (figure 3.4B) showed that the staining was faint and the migration of CS for β-eliminated BAC-A1 (lane 5) could not be detected. It was suspected that the 7D4 epitope was below detection threshold after β-elimination.

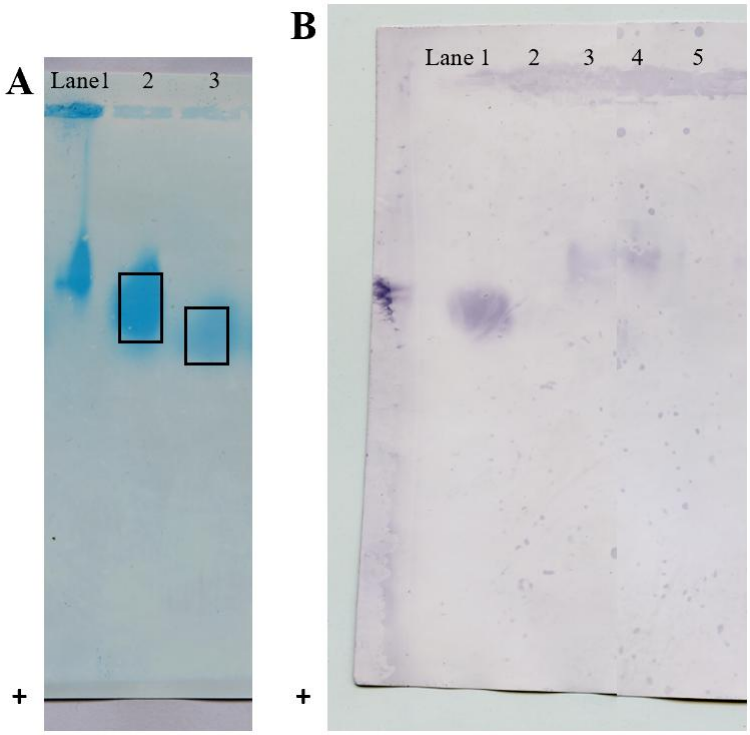

Figure 3.4 The visualisation of barium electrophoresis with Toluidine Blue staining and immunological staining of 7D4 antibody. [A] *Chick sterna dry extract A1D1 (lane 1), BAC-A1 (lane 2) and β-eliminated BAC-A1 (lane 3) were stained by Toluidine Blue, which showed further migration of GAGs after β-elimination.* ***[B]*** *Immunological staining of 7D4 antibody after barium electrophoresis for Sigma CS standards (lanes 1 and 2), chick sterna dry extract A1D1 (lane 3), BAC-A1 (lane 4), β-eliminated BAC-A1 (lane 5). Migration shift was detected after β-elimination on the barium electrophoresis.*

3.2.2 SDS-PAGE and Western Blotting demonstrates the removal of GAG chains following β-elimination.

PGs were isolated from bovine articular cartilage (BAC) by using 4M GuHCl, which underwent density gradient centrifugation under associative conditions for pooling aggrecan at the bottom one third fraction (A1). Chondroitinase ABC digested samples of BAC-A1 before and after β-elimination (as described in section 2.3.2) as well as β-eliminated chick sterna extract (kindly gifted by Prof. Clare Hughes), and 10μg of GAGs from samples were then separated by SDS-PAGE and Western blotted with monoclonal antibody 2B6 as described in section 2.16.7 recognising CS-4 'stubs' (Figure 3.5A).

Following chondroitinase ABC treatment, the neo-epitope of CS was exposed and can be detected by monoclonal antibody 2B6. Notably, a smear of positive staining (MW range 75-150 kDa) was seen in the β-eliminated chick sterna preparation (lane 1), indicating fragments of A1 were present in the initial extract. As for the digested BAC-A1 (lane 2), there was a positive staining above 250 kDa and a smear between 75-150 kDa, indicating the presence of aggrecan core protein and the CS-4 'stubs' detected by 2B6. Furthermore, a faint band was revealed at approximately 38 kDa (arrow in figure 3.5A), which is most likely decorin core protein with 2B6 epitopes. The β-eliminated BAC-A1 (lane 3) showed comparable staining, and interestingly, the 75-150 kDa smear showed reduced staining, possibly indicating the loss of GAG chains through β-elimination resulting in reduced 2B6 epitope. The strong staining above 250 kDa in both BAC-A1 (lane 2) and β-eliminated BAC-A1 (lane 3) should be the aggrecan core protein, the size of which does not allow the migration into 4-12% SDS-PAGE gel. Similarly, 5D4 staining was detected in the β-eliminated sample above 250 kDa (figure 3.5B).

The β-eliminated chick sterna extract, BAC-A1 and β-eliminated BAC-A1 were then separated by SDS-PAGE and blotted by KS antibody 5D4 as described in section 2.16.7 to examine the presence of KS in A1 before and after β-elimination, and the KS samples purified from pig cornea in our lab underwent SDS-PAGE at the same

time as the positive controls. Figure 3.5B shows the positive controls formed a smear from bottom to up (MW range 15-250 kDa), where β-eliminated chick sterna extract (lane 1) has been separated to form a smear in the range of 75-250 kDa. BAC-A1 (lane 2) and β-eliminated BAC-A1 (lane 3) exhibits a band above 250kDa, and a smear for BAC-A1 (lane 2) extends from 75 kDa to 250 kDa while the smear of β-eliminated BAC-A1 (lane 3) ranges from 50kDa to 250 kDa, which shows a further migration of β-eliminated BAC-A1 and demonstrates the presence of KS in smaller molecular size. It is noteworthy that the 5D4 antibody is highly sensitive and there is an excessively contrast between the intensity of positive controls and that of BAC-A1 samples (both before and after β-elimination). The smears and bands for β-eliminated chick sterna extract (lane 1), BAC-A1 (lane 2) and β-eliminated BAC-A1 (lane 3) can only demonstrate trace level of KS.

The further migration of β-eliminated BAC-A1 in barium electrophoresis and western blot (5D4 staining) demonstrated the β-elimination partially removed CS from core protein so that the xylosyl-serine linkage between CS and core proteins was destroyed.

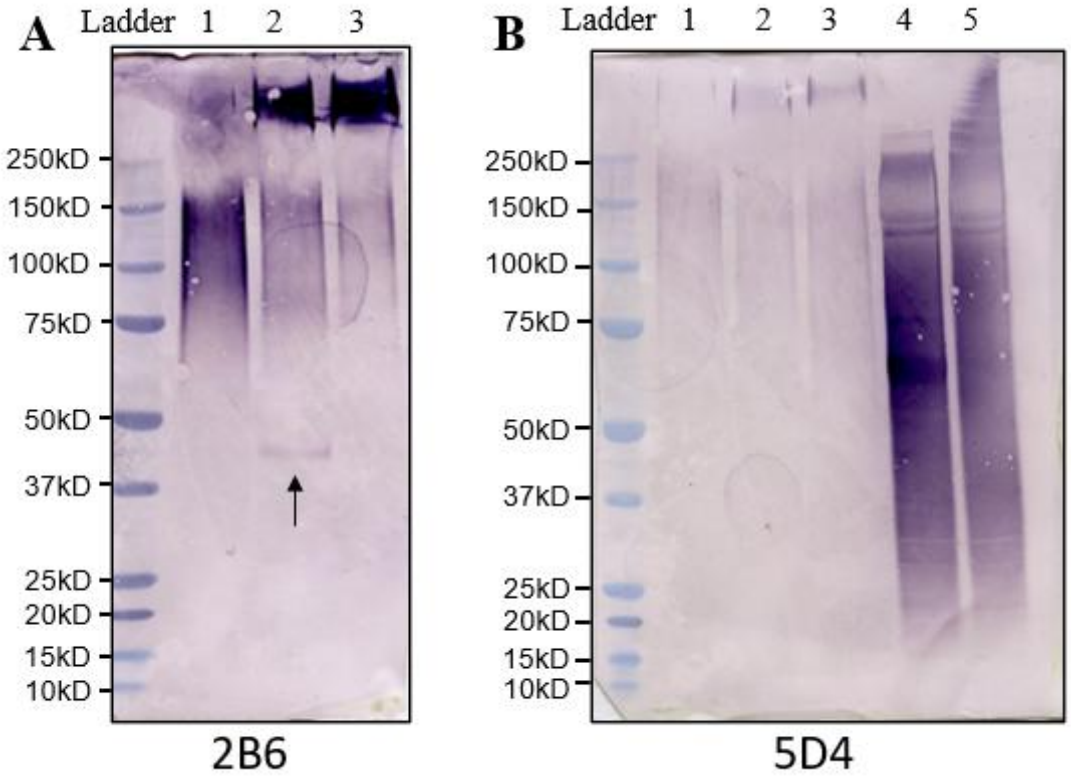

Figure 3.5 Verification of the liberation of the GAG chains using Western Blot analysis. [A] *After chondroitinase ABC treatment, the β-eliminated chick sterna extract (lane 1), A1 (lane 2) and β-A1 (lane 3) were all probed with 2B6 antibody which can detect chondroitinase-generated "CS-stub" neoepitopes, and a band with smaller molecular weight showed in the lane of BAC A1.* ***[B]*** *The β-eliminated chick sterna extract (lane 1), A1 (lane 2), β- A1 (lane 3) and along with the KS positive controls purified from pig cornea in our lab (lanes 4 and 5) were analysed with the KS antibody 5D4.*

3.2.3 Purification of β-eliminated A1 free CS chains by anion-exchange chromatography

The barium electrophoresis and Western Blot results showed release of CS chains from core protein was not fully completed with KS contamination, hence the alkaline treatment was modified to optimise the outcomes as described in section 2.3.3. A1 was β-eliminated with the addition of $NaBH_4$ and desalted with PD-10 column, and then the sGAG content in PD-10 column fractions was determined using the DMMB assay (Section 2.16.2). From this, 1 mg of sGAGs from peak fraction was lyophilised prior to reconstitution in 0.1M NaCl (pH 7.5). The sample was separated by anion-exchange chromatography as described in section 2.5 to purify CS from other molecules, such as KS and core protein. Figure 3.6A shows the absorbance profiles obtained from the elution of the sample. Three peaks were detected at wavelengths of 280nmand 214 nm reflecting protein and peptides. The first peak was unbound material, the second (major) peak eluted at 10-16ml with a salt concentration of 0.825M-1.202M NaCl and a smaller peak eluted at 16-20ml with a salt concentration of 1.26M-1.521M NaCl. The chromatography profile indicates that almost all the molecules were primarily eluted within the 10-20ml elution buffer, so they were mainly pooled by the elution of 0.825M-1.521M NaCl gradient.

The DMMB assay was then applied to examine the sGAGs content in the fractions across the elution profile (Figure 3.6B), where only a single peak was detected, and the peak fractions were used for subsequent experiments.

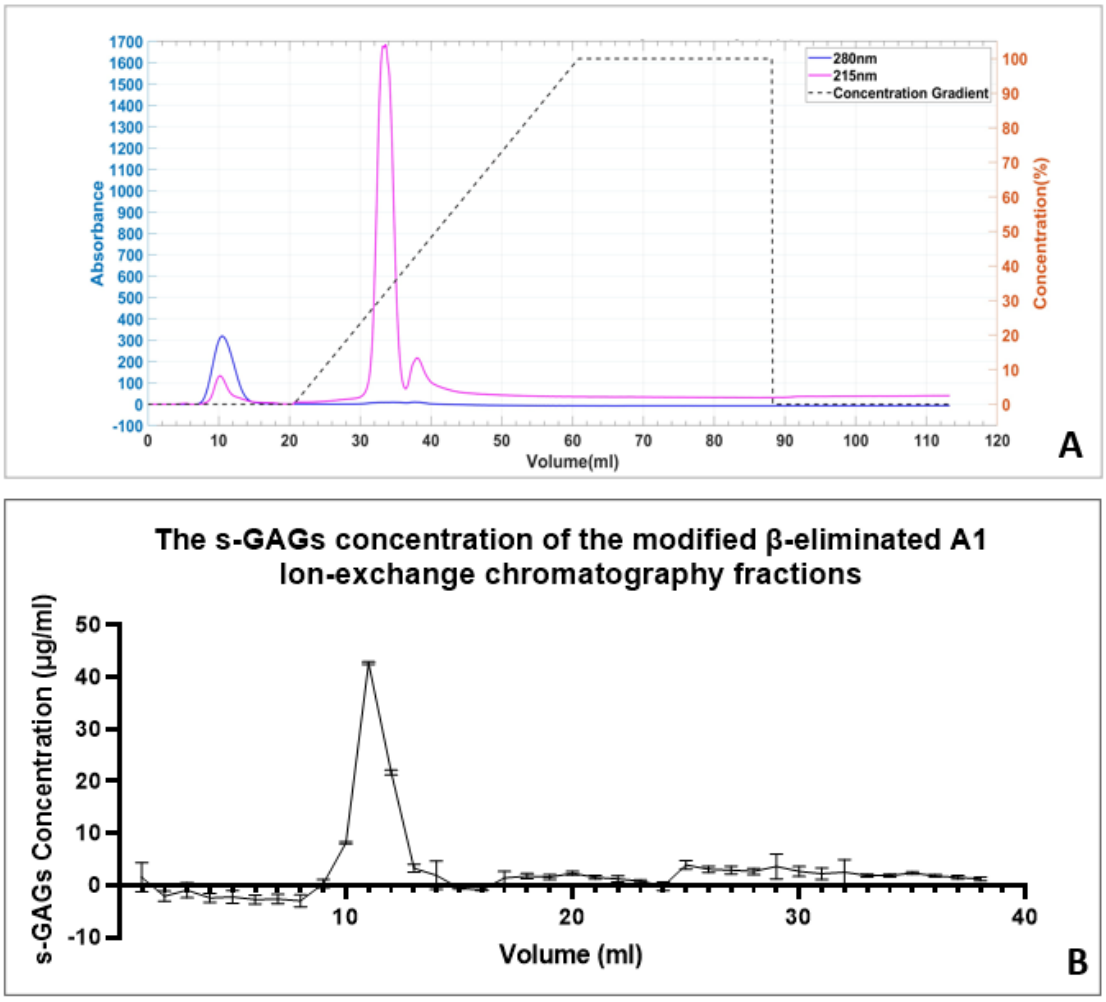

Figure 3.6 Anion-exchange chromatography of β-eliminated A1 and the DMMB concentration of eluted fractions. ***[A]*** *β-eliminated A1 was mainly pooled at 10-20ml elution buffer by 0.825M-1.521M NaCl gradient.* ***[B]*** *sGAGs concentration of all eluted fractions were determined by DMMB assay and plotted. sGAGs concentration peak is consistent with the chromatography profile where the elution peaks happened between the 9-15ml of the elution buffer. Concentration was plotted by mean value, and error bar represents standard deviation (n=3, N=3).*

3.2.3.1 ELISA analysis of anion-exchange fractions for CS and KS epitopes.

ELISA plates were coated with 2µg/ml sGAG (as determined using the DMMB assay) with A1, β-eliminated A1 and selected fractions of β-eliminated A1 after anion-exchange chromatography. Detection of CS epitopes (7D4, 6C3 and 4C3), KS epitopes (5D4) and the inter-globular domain (IGD) of aggrecan (6B4) was subsequently performed (Figure 3.7). As expected, BAC-A1 was positive for 7D4 (Abs 450 nm, mean=0.304, n=3, N=3), 6C3 (mean=1.183) and 5D4 epitopes (mean=3.473). Under the ELISA conditions used, the absorbances recorded for 4C3 and 6B4 (anti IGD) were just above that of the background control. Detection of CS and the anti IGD epitope was reduced after β-eliminated of A1, flow-through fractions (β-A1-F1, β-A1-F2) and peak elution fractions (β-A1-10,11,12 and 13). However, detection of the KS epitope was reduced in the β-eliminated A1 relative to the A1 sample but was detected in fraction β-A1-12 and β-A1-13. These results suggest that sample binding after β-elimination either masks the epitopes or there is less binding of the antigen to the plastic surface of the ELISA wells.

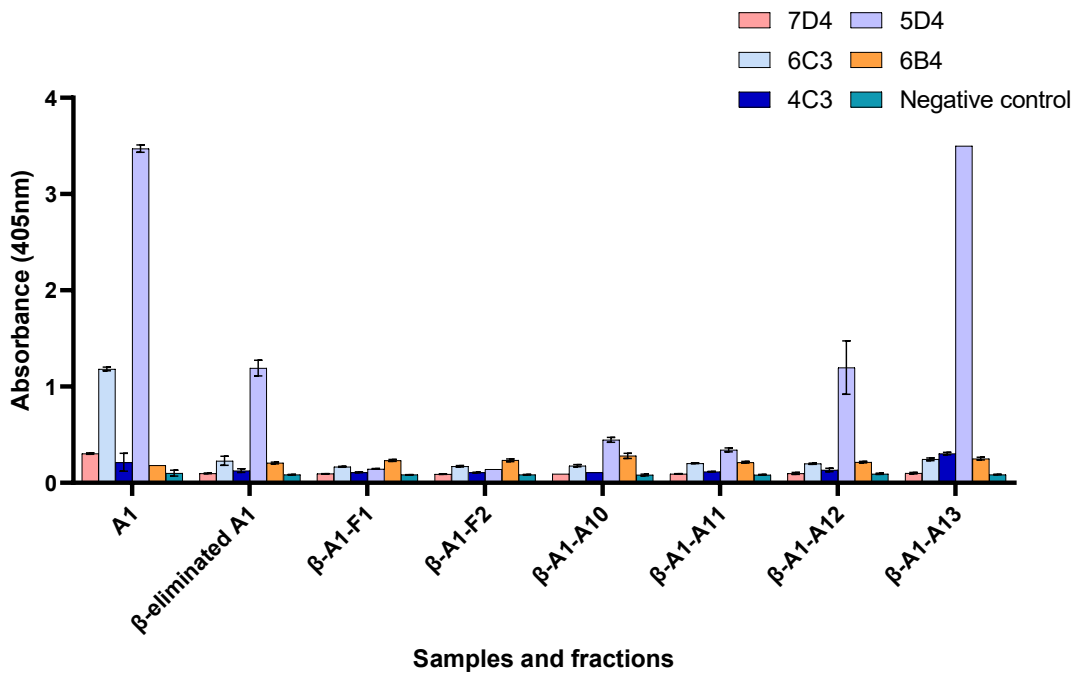

Figure 3.7 Immunological characterisation of A1, modified β-eliminated A1, and modified β-eliminated A1 anion-exchange peak fractions. *Comparison of immunological epitope characterisation via ELISA of pre- and post- β-elimination fractions, and post anion-exchange chromatography by the monoclonal antibodies of CS epitopes (7D4, 6C3 and 4C3), KS epitopes (5D4) and the inter-globular domain (IGD) of aggrecan (6B4). Absorbance values are mean ± standard deviation, n=3, N=3.*

3.2.3.2 Dot Blot analysis of anion-exchange fractions for CS and KS epitopes

Dot blots were performed to detect the presence of CS epitopes (7D4 and 6C3) and KS epitopes (5D4) in elution fractions (1-38) after anion-exchange chromatography (Figure 3.8).

Both CS epitopes for 7D4 and 6C3 were negative, but the KS epitope 5D4 was positive in fractions 9 to 14 (Figure 3.8C, arrows) with the most intense staining in β-A1-11 to β-A1-13 consistent with the ELISA data (Figure 3.7). This staining correlated with the fractions containing the highest concentrations of sGAGs as measured using the DMMB assay (Figure 3.6B).

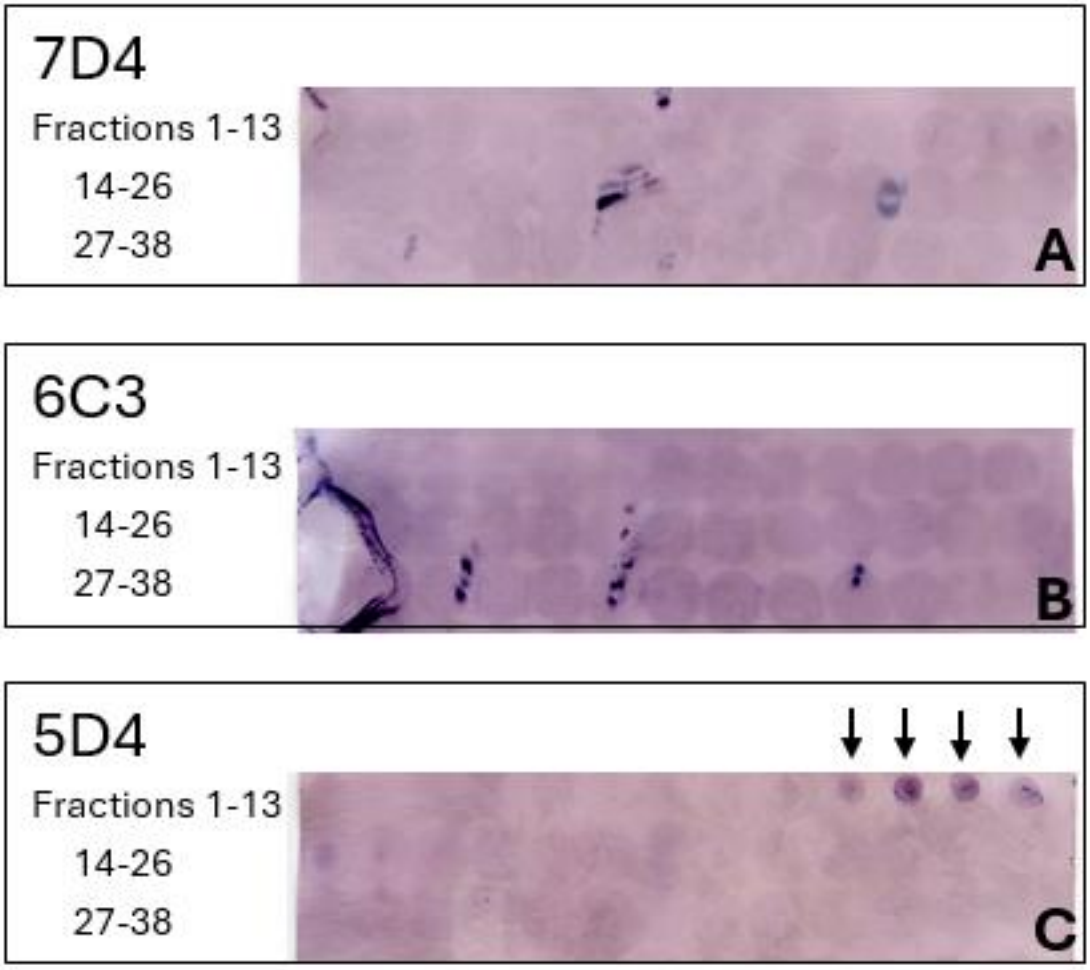

Figure 3.8 Dot blot for the β-eliminated A1 anion-exchange chromatography fractions. *Neither the 7D4 epitope nor 6C3 epitope was detected in the anion-exchange chromatography fractions, whilst the fractions with a DMMB measurement presented with positive 5D4 epitope staining.*

3.2.4 The free chains liberated using the modified β-elimination method did not inhibit the binding of PGs with CS antibody

The epitopes of interest with antibodies 7D4, 6C3 and 4C3 demonstrated reduced signal intensity in ELISA and Dot Blot after modified β-elimination, therefore, the modified β-eliminated BAC-A1 and BAC-D1D1 were desalted with a PD-10 column as described in section 2.3.2. The desalted samples were collected into 1ml fractions and the sGAGs concentrations determined using a DMMB assay (Section 2.15.2.) The sGAGs concentration of PD-10 column fractions are shown in figure 3.9. Peak fractions were pooled and used in competitive ELISA (Section 2.16.5) to ascertain if this methodology could be used to measure 6C3 epitope.

ELISA plates were coated with 5µg/ml of the BAC-D1D1. A standard curve of BAC-D1D1was prepared in the range of 0- 20µg/ml in microcentrifuge tubes to which primary antibody (6C3) was added to give a final dilution of 1:100. In a second set of tubes beta-eliminated BAC-A1and BAC D1D1 were prepared in a concentration range of 0- 20 µg/ml and antibody 6C3 added as above. Tubes were incubated for one hour before adding to the ELISA wells coated with 5µg/ml BAC-D1D1. Samples were incubated for 1 hour, washed and processed as described in section 2.16.5. As expected, the absorbance declined with increasing concentrations of D1D1. However, fractions of desalted free CS chains derived from beta elimination of BAC-A1 failed to inhibit binding of 6C3 to the BAC-D1D1 coated plates (Figure 3.10) and even improved the absorbance with an increase of its concentration.

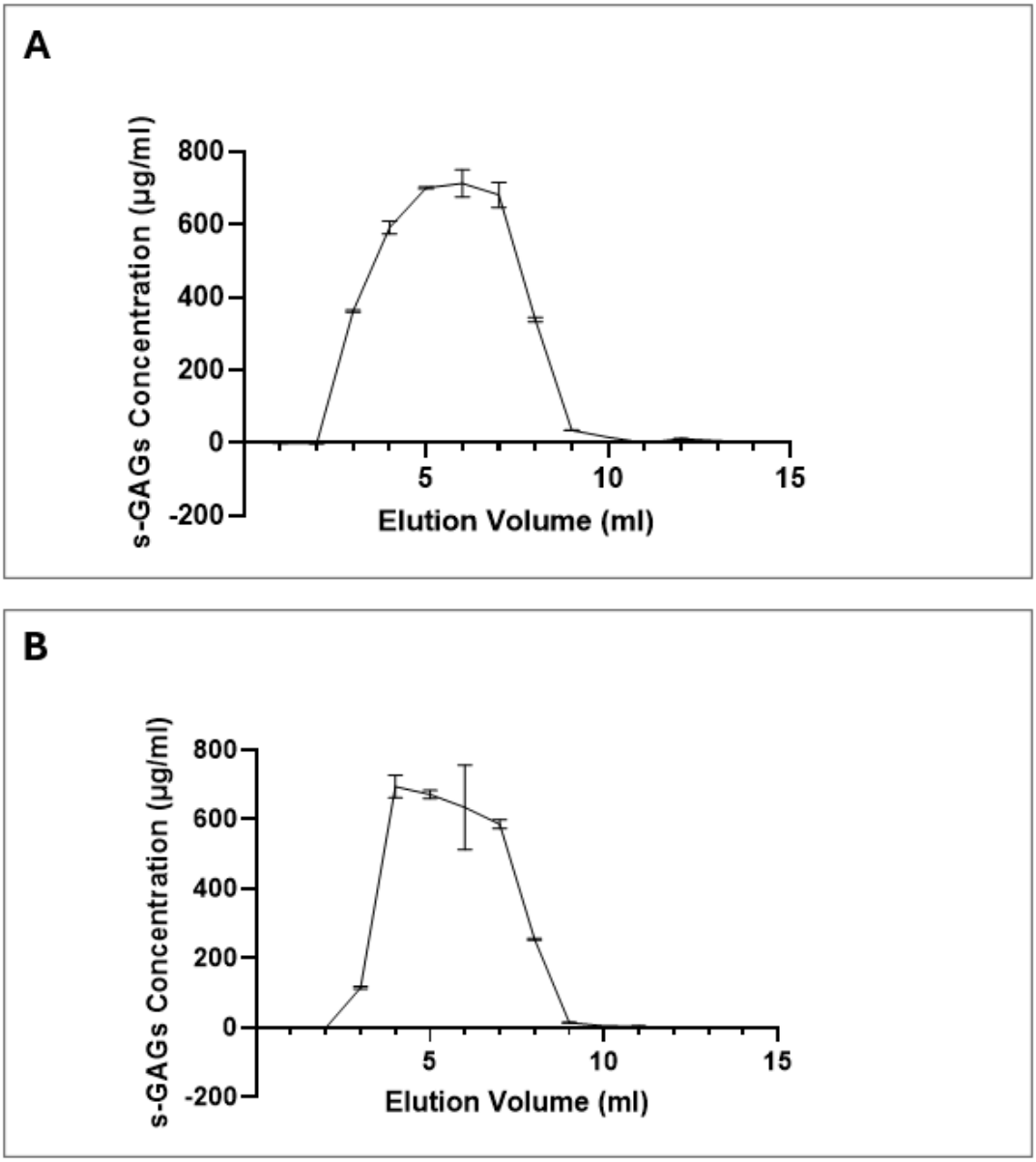

Figure 3.9 The DMMB results for PD-10 fractions of modified β-eliminated BAC-A1 and BAC-D1D1. [A] *sGAGs concentration for PD-10 column fraction of modified β-eliminated A1 was plotted by DMMB result. Only the 3rd, 4th and 5th fractions were employed for competitive ELISA.* ***[B]*** *sGAGs concentration for PD-10 column fraction of modified β-eliminated D1D1 was plotted by DMMB result. (Values are mean ± standard deviation, n=3, N=3)*

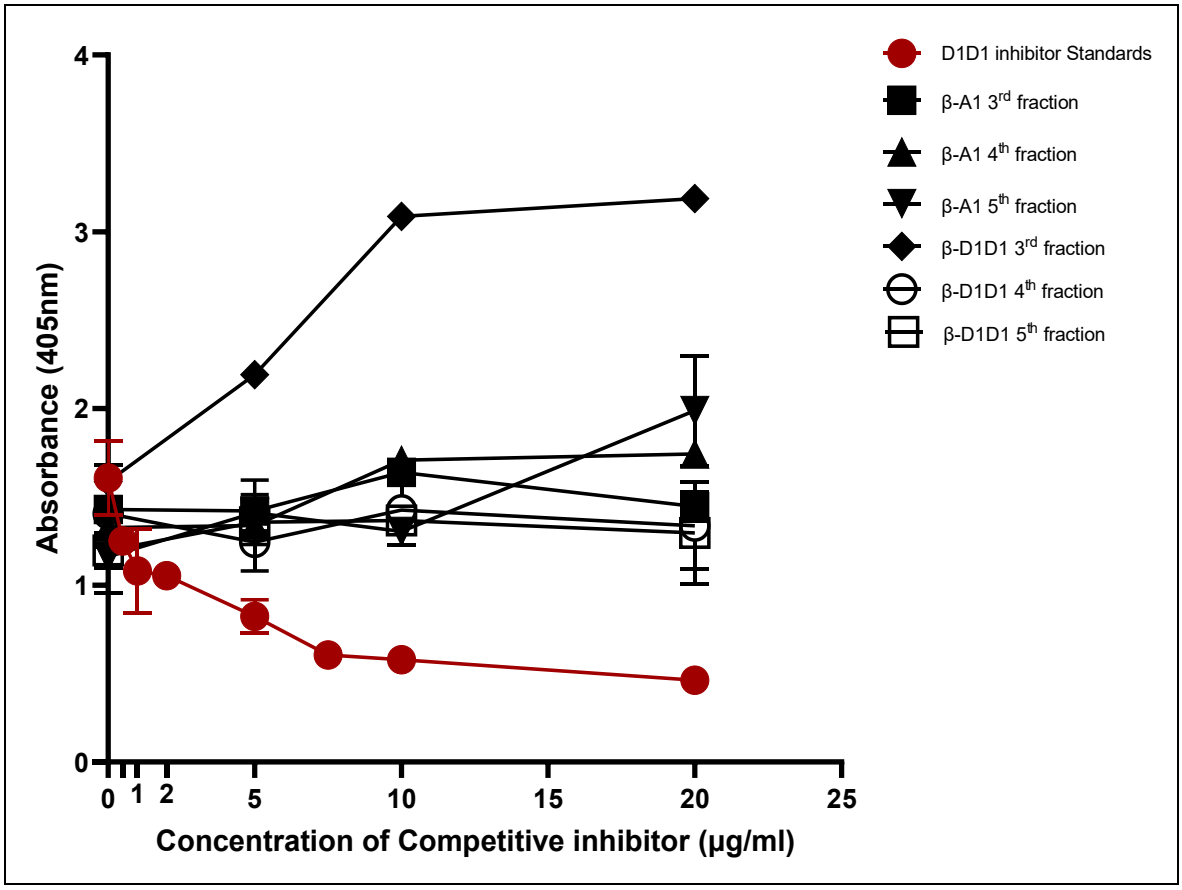

Figure 3.10 The absorbance plot of competitive ELISA for the detection of 6C3*. The red plot curve is the standards between D1D1 and a gradient concentration of inhibitor of D1D1, where the absorbance of standards declined with the increase of the standard inhibitor concentration. The black plot lines are the competitive effects of the 3rd, 4th, and 5th PD-10 fractions of β-eliminated A1/D1D1 against the coated D1D1. None of the tested samples successfully reduced the absorbance, indicating that they were unable to inhibit the binding of the primary antibody 6C3 to the coated PGs in D1D1. The third PD-10 fraction of β-eliminated D1D1 exhibited an opposite effect, with absorbance increasing as its concentration increased. Absorbance at 405nm represents mean ± standard deviation, n=3, N=3.*

3.2.5 CS purification from modified β-eliminated A1 using size-exclusion chromatography.

Peak fractions from anion-exchange chromatography were then applied to size exclusion chromatography for further CS purification. Size exclusion chromatography (Superose 6) showed the absorbance profiles (280nm and 214nm) of A1 and β-eliminated A1 after separation.

The β-eliminated A1 anion-exchange chromatography peak fractions were eluted as three peaks detected at 214nm (Figure 3.11A) by size-exclusion chromatography. sGAGs concentration of each fraction was measured by DMMB assay and presented as figure 3.11B, from which most of sGAGs was found to be pooled into fraction 9 to fraction 14 after size-exclusion chromatography. The recovery of starting sGAGs was 90% after size-exclusion chromatography by summing the sGAGs content in each fraction based on the DMMB results.

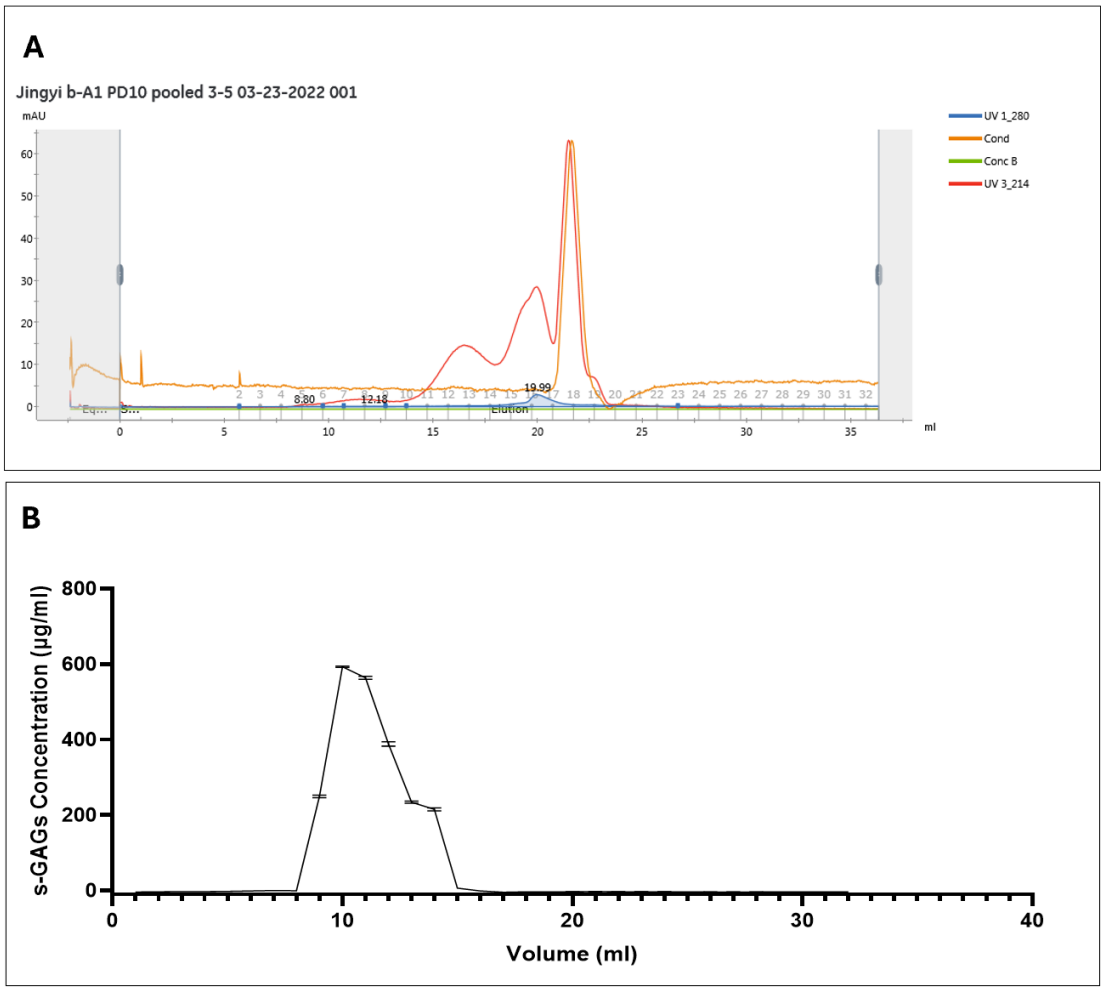

Figure 3.11 The modified β-eliminated A1 size-exclusion chromatography profile and the DMMB curve of the size-exclusive chromatography fractions. [A] *β-eliminated A1 was eluted as 3 overlapped peaks within 25ml of elution buffer.* ***[B]*** *sGAGs concentration confirmed by DMMB for all size-exclusive chromatography fractions were plotted by means ± standard deviation, n=3, N=3.*

3.2.5.1 Dot Blot analysis of CS and KS epitopes after size-exclusion chromatography (Superose 6)

To validate in-house antibody affinity, to confirm the presence of target CS motifs and to ensure the validity of experimental method, A1 and β-eliminated A1 underwent anion-exchange chromatography and the CS in peak fractions was then separated by size-exclusive chromatography before DMMB assay was applied to determine CS concentration of all of the size-exclusive fractions and Dot Blot was conducted to examine the epitopes of 6C3, CS-56 and 5D4 in peak fractions. Dot Blot analysis was performed to detect KS (5D4 epitope) and CS epitopes (CS-56 and 6C3) in the fractions which contained pooled sGAGs from the size-exclusion chromatography (Figure 3.12).

The positive staining was detected for KS in fractions 3-6 for A1 and fractions10-14 for modified β-eliminated A1 (Figure 3.12A). However, CS epitopes were strongly detected in fractions 3-6 for A1 (Figure 3.12B-C) and very faintly detected in fractions 10 and 11 for modified β-eliminated A1 (Figure 3.12B-C, arrows). This lack of detection of CS epitopes after β-elimination is consistent with the ELISA and Dot Blot analysis carried out in sections 3.2.3 above.

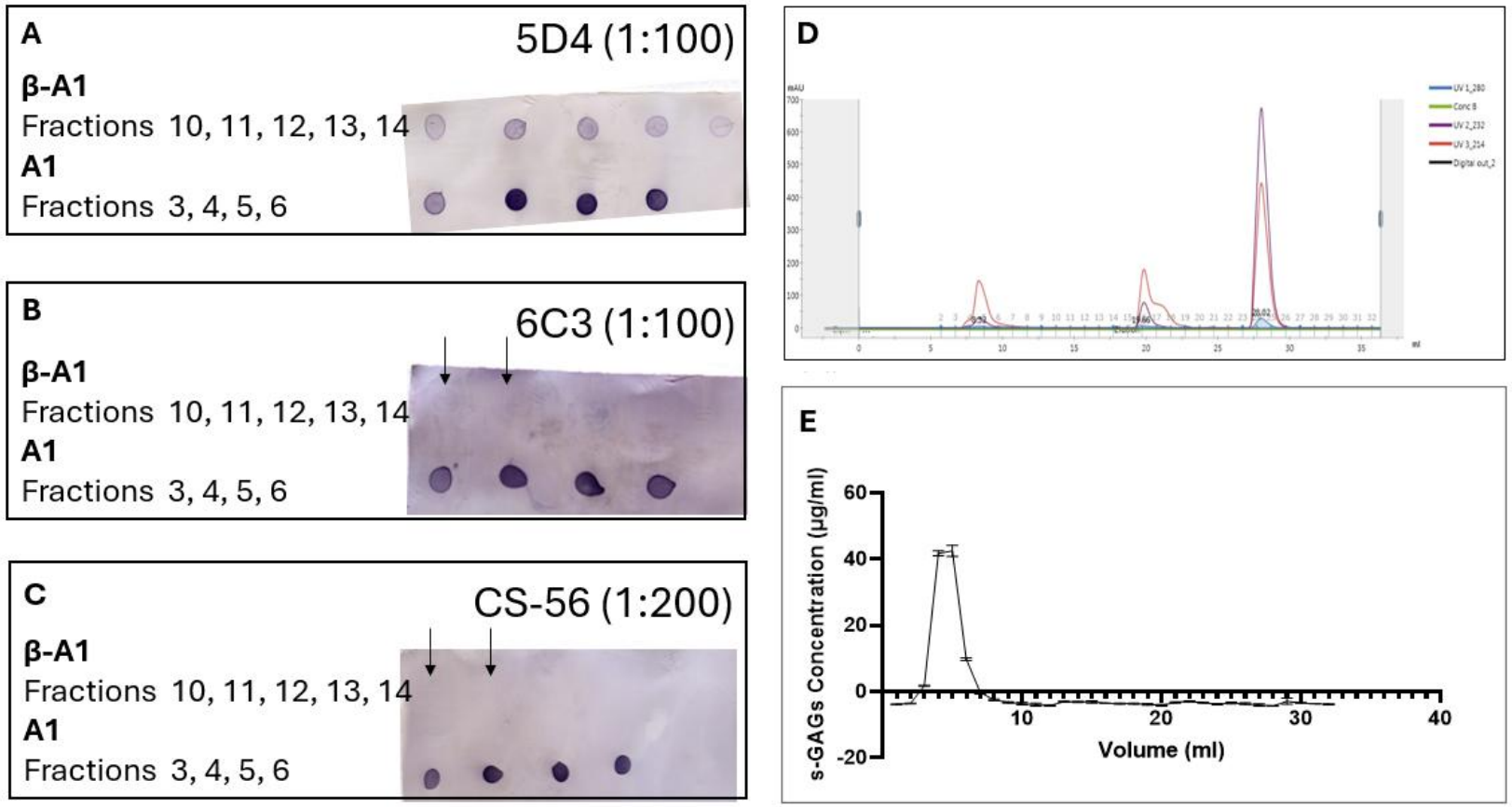

Figure 3.12 Dot Blot results for the A1 and modified β-eliminated A1 size-exclusion chromatography peak fractions with the monoclonal antibodies of 5D4 (A), 6C3 (B), and CS-56 (C), and the A1 size-exclusion chromatography profile (D) and the DMMB curve of the fractions (E). *5D4, 6C3, and CS-56 epitopes are all detected in the A1 size-exclusion peak fractions with intense blotting. Modified β-eliminated A1 size-exclusion fractions were all 5D4-epitope positive. Moreover, both 6C3 and CS-56 epitopes were probed in the 10^{th} and 11^{th} in the modified β-eliminated A1 size-exclusion fractions (arrows in B and C). DMMB values are mean ± standard deviation, n=3, N=3.*

3.2.6 Chondroitinase digestion of fractions from size-exclusion chromatography demonstrated the proportion of purified CS in peak size-exclusive chromatography fractions.

As CS epitopes were undetectable by the CS antibodies following β-elimination of A1 by ELISA and Dot Blot, digestion with 5mU chondroitinase ABC for each milligram of GAGs was used to identify β-eliminated samples that contained CS chains. A1 and commercially available CS from Sigma were used as positive controls. The percentage of CS in the samples was calculated using sGAGs measurements before and after digestion with chondroitinase ABC since the enzyme cleaves CS chains into disaccharides or oligosaccharides, disrupting the large polyanionic structure and retaining fewer sulphate groups which have weaker or no binding to DMMB dye, which has been used previously (Nandini et al., 2004). The concentration of sGAGs was measured at time points of 0 min, 10 mins and 19 hours after the addition of chondroitinase ABC (Figure 3.13). 0 min as an undigested control, 10 min to observe early-stage degradation, and 19 hours to ensure complete digestion. The 19-hour time point was also selected for practical reasons, aligning with an overnight incubation from the previous afternoon to the next morning for convenient handling.

Interestingly, the concentration of sGAGs decreased more rapidly in A1, shark and bovine tracheal CS preparations in the first 10 minutes, perhaps indicating the presence of a protein core influencing digestion of the CS chains with chondroitinase ABC. Free chains appear to digest at a slower rate in the first 10 mins.

The percentage of digested sGAGs in each sample/fraction following chondroitinase ABC treatment was calculated to reflect the percentage of CS present (Table 3.1). The Sigma commercially available CS extracted from bovine trachea was found to have a purity of 99.82% ±0.98%. In comparison, the 11^{th} fraction obtained from size-exclusion chromatography using the bovine cartilage contained the highest proportion of CS chains with 96.47%±1.90% purity; however, it was only detected with a relatively faint stain using the CS antibodies CS-56 and 6C3 (Figure 3.12 A, B and C). This can be regarded as further evidence that the CS chains do exist in the size-exclusion fractions, but the free chains have limited binding ability to the plastic

surfaces and membranes, resulting in the faint staining in the Dot Blot (Figure 3.8 and figure 3.12 A, B and C) and reduced signal in the ELISA after β-elimination (Figure 3.7).

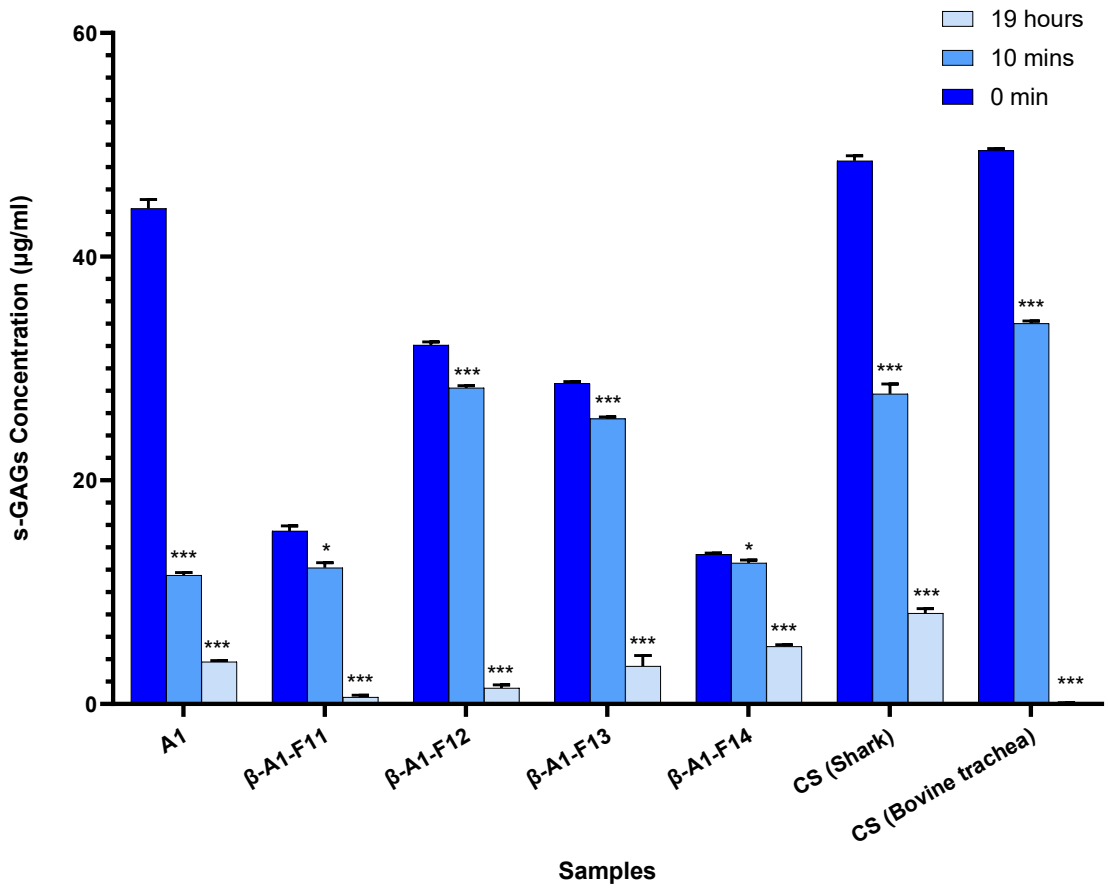

Figure 3.13 The amount of sGAG detected by DMMB before and after Chondroitinase ABC treatment. *The GAGs content in all the pre- and post- β-eliminated and size-exclusive chromatography A1/D1D1 and the Sigma CS products decreased after chondroitinase ABC digestion. Absorbance values are means ± standard deviation, n=3, N=3. (*p<0.05, **p<0.01, ***p<0.001)*

Table 3.1 The digested percentage of the fractions. *The size-exclusive fractions treated with chondroitinase ABC and the concentration of s-GAGs before and after enzymatic treatment were measured by DMMB assay. The percentage of digested by chondroitinase ABC refers to the proportion of CS in the fractions. β-A1 represents the A1 prep has been treated with β-elimination before it was loaded on size-exclusive chromatography; and the F refers to the size-exclusive chromatography fractions and the number represents their elution position. A1 prep contains 91.43% CS and after the enzymatic treatment and the size-exclusive chromatography, CS was enriched in the 11th 1-ml fraction with a purity of 96.47%, 95.96% for the 12th 1-ml fraction.*

Fractions	**Digested percentage (Mean+SD %)**
A1	91.43±3.52%
β-A1-F11	96.47±1.90%
β-A1-F12	95.96±2.14%
β-A1-F13	87.25±2.04%
β-A1-F14	61.87±2.09%
CS (shark)	83.43±2.94%
CS (bovine trachea)	99.82±0.98%

3.2.7 Characterisation of purified CS obtained from bovine cartilage

3.2.7.1 Measurement of CS purity

PGs from bovine cartilage were isolated by 4M GuHCl and density gradient centrifugation, after β-elimination, which underwent anion-exchange chromatography and size-exclusive chromatography for CS purification.

CS preparation purity was 87% as determined by a carbazole reaction, with 5.3% nucleic acid impurity and other minor impurities.

To investigate whether the CS preparation contained other sGAGs i.e. DS and Hep/HS, the CS fractions were treated with chondroitinase AC, chondroitinase B or Hepases mixture of Hepases I, II and III, respectively, as described in section 2.6.2. When treated with chondroitinase AC, most of the CS preparation was digested to mono-sulphated disaccharides (Figure 3.14). By calculating the chromatographic peak area and determining the amount of disaccharide units produced by CS preparation digestion, it was demonstrated that 95% of GAGs in CS preparation is CS-4 and CS-6. No significant oligosaccharide peak was observed in CS preparations when it was treated with Hepases mixture of Hepases I, II and III or chondroitinase B, indicating that the CS preparation contained no heparinoid or DS contaminants.

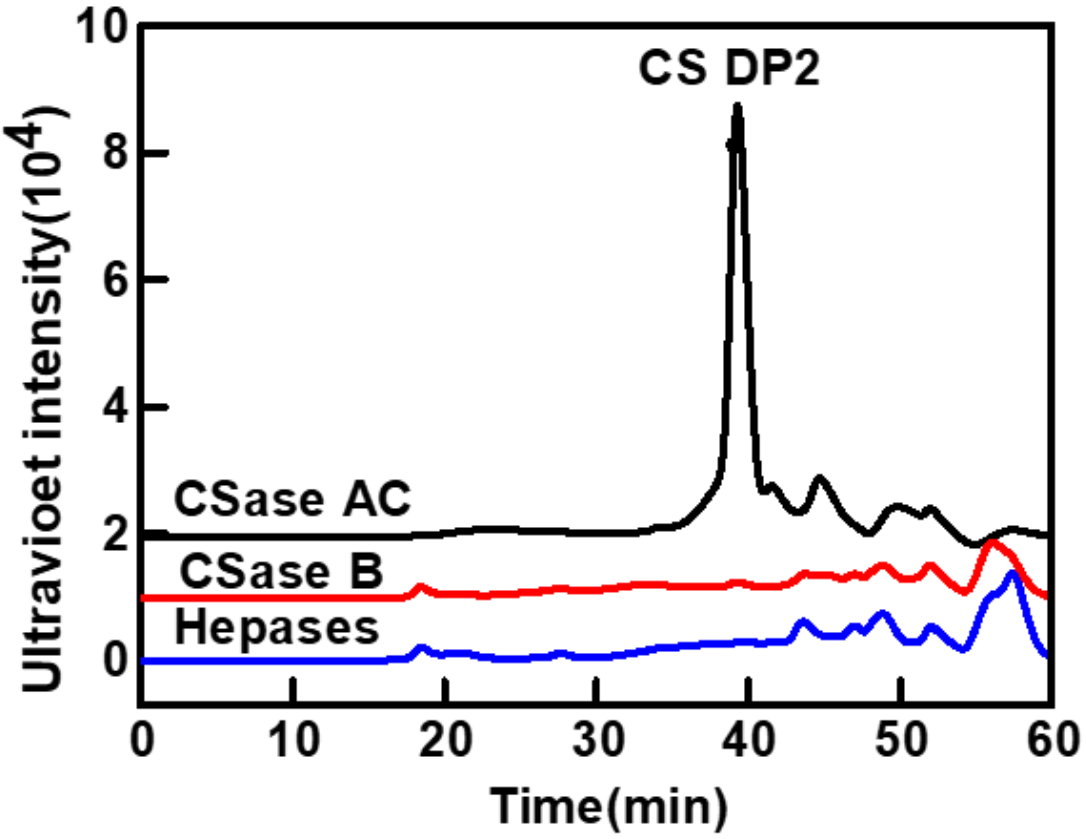

Figure 3.14 GAGs components analysis for the purified bovine articular cartilage CS preparation. *After the treatment of chondroitinase AC, with the calculation by peak area percentage method as previously described in section 2.6.2, more than 95% of the purified CS was digested to mono-sulphated disaccharides. When treated with Hepases mixture or chondroitinase B, there was not a detection absorbance peak, confirming the CS preparation does not contain heparinoid or DS contaminants.*

3.2.7.2 Disaccharide composition assay of purified CS

To further characterise the CS preparation, the disaccharide composition and disaccharides located at the non-reducing and reducing end of purified CS were determined (Figure 3.15); this was performed using an enzymatic digestion with Chondroitinase ABC followed by analysis using anion-exchange HPLC with the elution of NaH_2PO_4 solution as described in section 2.6.3. All purified CS showed the presence of $\Delta^{4,5}$HexUα1–3GalNAc (ΔO unit), in which $\Delta^{4,5}$HexUA represents unsaturated uronic acid, $\Delta^{4,5}$HexUα1–3GalNAc(6S) (ΔC unit), and $\Delta^{4,5}$HexUα1–3GalNAc(4S) (ΔA unit) (Figure 3.15). This illustrates the proportion of CS subtypes in the CS preparation, with predominantly (78.3%) CS-A (CS-4), 16.5% CS-C (CS-6) and 5.2% of $\Delta^{4,5}$HexUα1–3GalNAc (ΔO unit) (CS-0) (Table 3.2).

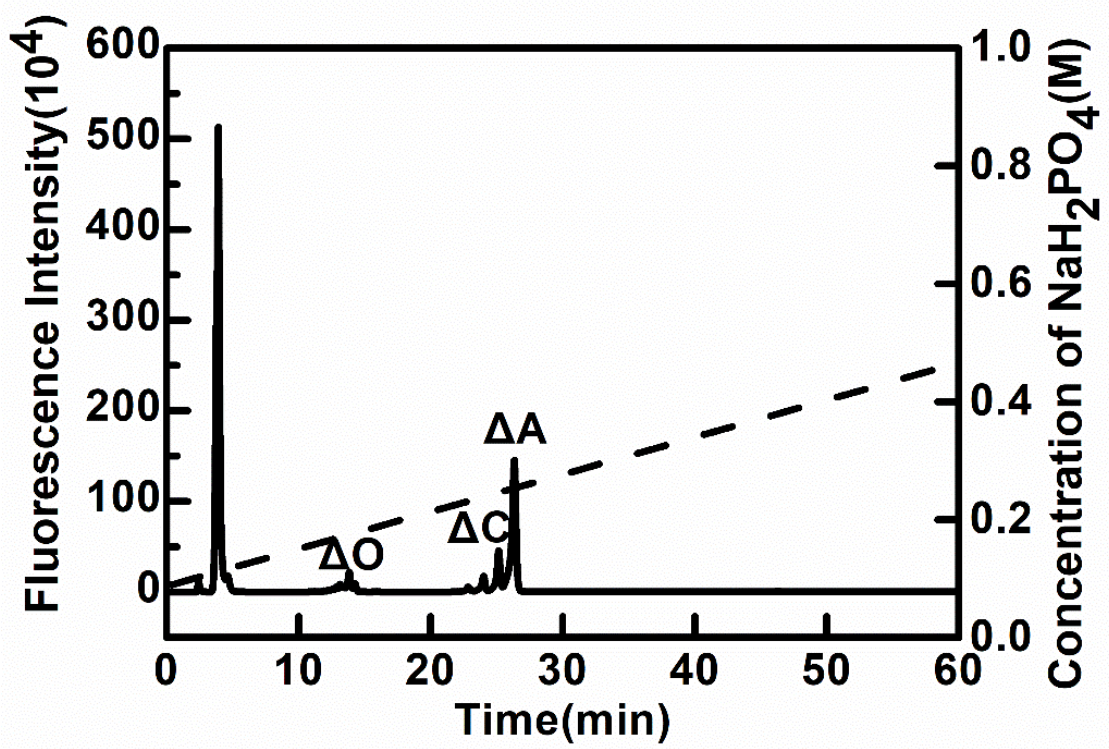

Figure 3.15 Disaccharide composition of purified CS by anion-exchange HPLC. *Purified CS was degraded with chondroitinase ABC and then analysed by anion-exchange HPLC. The elution positions of the following standard disaccarides are indicated $\Delta^{4,5}$HexUα1–3GalNAc (ΔO unit), $\Delta^{4,5}$HexUα1–3GalNAc(6S) (ΔC unit), and $\Delta^{4,5}$HexUα1–3GalNAc(4S) (ΔA unit). In the bovine cartilage sGAG preparation, CS-A is the predominant isoform compared with CS-C and CS-0.*

Table 3.2 Disaccharide composition of bovine cartilage CS following chondroitinase ABC digestion and anion-exchange HPLC.

Composition	Proportion (%)
$\Delta^{4,5}$HexUAα1-3GalNAc（ΔO）	5.20
$\Delta^{4,5}$HexUAα1-3GalNAc(4S)（ΔA）	78.30
$\Delta^{4,5}$HexUAα1-3GalNAc(6S)（ΔC）	16.50

3.2.7.3 1H NMR analysis of CS preparation

The ^{1}H spectroscopy of purified CS from bovine cartilage was recorded in the National Glycoengineering Research Centre at Shandong University, China, and the chemical shifts were assigned based on previous studies (Figure 3.15). The methyl protons of GalNAc were distributed in 2.02 ppm and the signals at 4.53 ppm and 4.48 ppm were attributed to H-1 of GalNAc and GlcA, respectively. The signals of 4.25 ppm and 3.26 ppm were assigned to the protons of the carbon rings. The resonances at 4.10 ppm were characteristic of H6 of GalNAc(6S) residues, which demonstrated the presence of sulphation at the C-6 position of GalNAc. Alpha hexopyranose residues, such as alpha-iduronic acid or alpha-glucosamine, did not exist in the purified CS since no recorded signals in the 5.0-6.0 ppm region were observed.

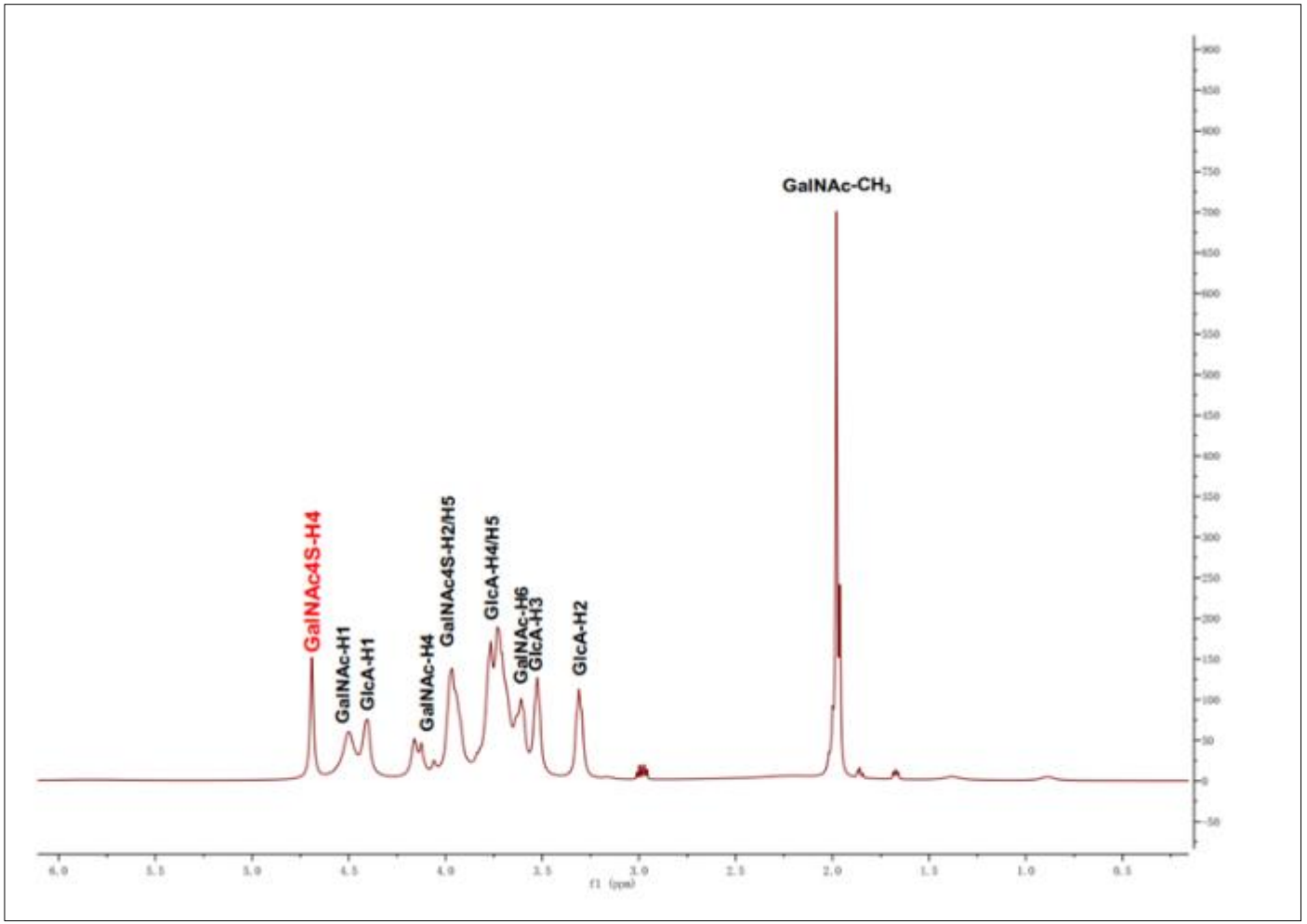

Figure 3.16 ^{1}H NMR spectra of purified CS for key structural assignments. *Methyl protons of GalNAc at 2.02 ppm, H-1 signals of GalNAc and GlcA at 4.53 ppm and 4.48 ppm, respectively, and carbon ring protons at 4.25 ppm and 3.26 ppm. The characteristic resonance at 4.10 ppm corresponds to H6 of GalNAc(6S), confirming sulphation at the C-6 position of GalNAc.*

3.3 Discussion

The overall objective of this chapter was successfully achieved in its attempt to purify CS chains and characterise their sulphate pattern from bovine articular cartilage. The novelty of this study was in its ability to obtain the free CS chains without the presence of the core peptide. The CS products produced commercially are typically purified using papain or trypsin digestion and are not exclusively free of core protein remnants; purifying free CS molecules is essential for use in examining the effects of CS on joint protection. Following adaptation of currently published protocols, the purified product demonstrated the highest purity at 96.47±1.90% (chondroitinase ABC digestion method) and 87% (carbazole reaction), which is highly desirable in terms of purity compared to commercial products.

3.3.1 Optimisation of Purification Strategy

The purification of CS is critical for its use in cartilage tissue engineering, where high-purity CS is required to maintain biological activity, structural integrity, and reproducibility across applications (Ullah et al., 2023). While this study achieved successful extraction and purification of CS from bovine cartilage, several aspects of the purification process have been optimised to improve purity, structural integrity, and scalability.

The first step in CS purification involves the extraction of PGs (e.g., aggrecan) from the dense ECM of cartilage. Many researchers are employing enzymatic digestion before extraction or purification with protease, etc (Wang et al., 2022c). However, in current study, traditional extraction methods using 4M GuHCl effectively solubilise PGs by breaking non-covalent bonds. And then, the density gradient centrifugation separated aggrecans from other molecules into A1 fraction or D1 fraction (Kuijer et al., 1986, Heinegård et al., 1981). In this way, PGs were extracted from cartilage without the breakdown of core protein as enzymatic purification strategy so that the CS chains were purified with minimal peptide contamination from core protein.

The second step in CS purification is the release of CS chains from the PG core protein, typically achieved using chemical methods such as β-elimination. This method, involving alkaline treatment in the presence of reducing agents like $NaBH_4$, effectively cleaves the glycosidic bonds while protecting the CS chains from degradation (Fukuda, 2001). Since prolonged exposure to alkaline conditions may degrade CS, reducing molecular weight and altering sulphation patterns, which can compromise its biological function. However, the addition of $NaBH_4$ can prevent unexpected alkaline reaction from CS digestion (Conrad, 2001). Meanwhile, the concentration of the alkaline reagent, the reaction temperature and reaction time should be precisely controlled to balance efficient CS release and minimal degradation. 0.4M NaOH was applied to release CS with mild alkali to minimise unwanted structural modifications. Higher temperatures (35℃ to 50℃) were reported to increase the reaction rate (Ogata and Lloyd, 1982). To control the reaction rate and avoid over-reaction, reaction in this study was taken place at room temperature. 24 hours of incubation time is sufficient for complete reaction (Conrad, 1995).

3.3.2 Detection and characterisation of free CS chains using 7D4 and 6C3

The CS antibodies employed in this study, including 4C3, 6C3 and 7D4, had been demonstrated to identify native CS chain motifs in previous studies according to their specific disaccharide compositions (Hayes et al., 2016, Hayes et al., 2018b). In this study it was the intention to purify free CS chains and obtain some measure of the abundance of epitopes for 7D4 and/or 6C3. However, after β-elimination resulting in the generation of free CS chains detection of 7D4 and 6C3 was reduced or indeed undetectable by ELISA and Dot Blotting. DMMB analysis showed no loss of sGAG throughout the purification process as demonstrated by recovery calculations after each step. Reasons for this loss of detection remain unresolved and further analysis of the CS chains is required such as size. However, since the CS chains were not detected after the β-elimination stage, it was assumed that the CS chains were not being detected by the antibodies, as opposed to loss of the CS moieties. The modified β-elimination step was employed to improve the structural integrity of the CS products by the addition of $NaBH_4$, however CS failed to be detected by the antibodies after this modified β-elimination step too.

It is likely that β-elimination cleaves the O-linked glycosidic bond between the core protein and the GAG chain, which can disrupt the native structure and expose or eliminate charged groups critical for antibody recognition. Since many antibodies against chondroitin sulphate rely not only on the disaccharide sequence but also on specific sulphation patterns and electrostatic interactions, even subtle changes in charge distribution or epitope accessibility may reduce binding affinity. Similar observations have been reported in earlier studies, where enzymatic or chemical modifications of GAGs led to diminished antibody binding due to the loss of key structural or electrostatic features (Lee and Lander, 1991, Zhang et al., 2014). Hence, after refining the CS purification strategy, this study also examined the effects of purified CS on phenotype maintenance of chondrocytes and chondrogenesis of BMSCs on 2D and 3D environments (Chapter 4 and 5).

In this study, GAG analysis was performed to assess the degree of sulphation and disaccharide composition of the purified CS chains. This is a crucial step in determining the functional properties of CS, as the pattern and extent of sulphation have a direct impact on the biological roles of the molecule (Kawamura et al., 2014). Enzymatic digestion with chondroitinase AC (specifically digest CS-4 and CS-6) and chondroitinase B (specifically digest most commonly CS preparation contaminant, dermatan sulphate), which cleave CS into their constituent disaccharides, followed by chromatographic or spectrometric analysis, enables the precise identification of the sulphated and non-sulphated disaccharide units present in the sample (Tao et al., 2017, Michel et al., 2004).

Therefore, verification of the presence of free CS in the preparation and analysis of disaccharide composition was subsequently performed via an enzymatic method and ^{1}H NMR respectively. ^{1}H NMR spectroscopy analysed the hydrogen atoms in the purified CS, providing a fingerprint of the product based on the specific chemical environment of these protons, indicating the presence and location of sulphate groups and confirming the structural identity of CS by comparing the spectrum with known standards (Wang et al., 2020). The disaccharide composition analysis identified the specific disaccharide units that comprise these CS chains, in addition to detailed information on the types and distribution of sulphation patterns. Since the sulphation pattern of CS is associated with diverse biological properties and activities, for

example, CS-4 and CS-6 have different roles in cellular behaviours including signalling, cell adhesion and tissue repair (Kawamura et al., 2014). As the spectra of ^{1}H NMR, CS-4 is the predominant constituent in the CS preparation. The CS sulphation pattern takes important roles in cartilage metabolism, including providing growth factor binding point, engaging with cell division and facilitating cell adhesion (Nandini and Sugahara, 2006b). The sulphation pattern of the purified CS product provides a better understanding in assessing the impacts of CS on chondrogenesis in the following chapters.

The successful isolation and characterisation of free CS chains are not only important for basic research into cartilage biology but also for the development of CS-based therapeutics (Reginster and Veronese, 2021b). The quality and purity of CS are critical factors in determining its efficacy in clinical applications, particularly in the treatment of osteoarthritis and other joint disorders (Bruyère et al., 2019). By obtaining a high-purity product and performing detailed structural analysis, this study provides valuable insights into the properties of CS derived from calf cartilage and highlights the importance of careful purification and characterisation techniques in both research and industrial contexts.

3.4 Conclusion

The overall aim of this chapter was to extract and purify free CS chains from PGs derived from bovine articular cartilage to enable assessment of the influence of free CS chains on chondrogenesis of BMSCs. With the various analytical methods employed, the purity of free CS product was determined to exceed 97%, and the sulphation pattern of CS fully characterised, with the predominant isoform being CS4, although the presence and proportion of epitopes 7D4 and 6C3 haven't been detected with in-house monoclonal antibodies due to limited binding ability of free CS chains. This was achieved by adapting previously published protocols to enhance the recovery of these CS moieties; the generation and characterisation of a pure CS preparation was then utilised in the subsequent experimental chapters to investigate its role in supporting chondrogenesis.

Summary of Findings:

- The methodology for CS purification has been refined and optimised to isolate free CS chains.
- CS purity of 96.47±1.90% (chondroitinase ABC digestion method) and 87% (carbazole reaction) has been achieved.
- CS-4 predominantly presented in purified CS preparation.

Chapter 4

The Cellular Behaviour of Chondrocytes and Bone Marrow Stem Cells in 2D culture with and without Chondroitin Sulphate

4.1 Introduction

Having purified and characterised highly pure free CS (Chapter 3), the objective of this chapter was to examine the effects of CS on the cellular behaviours of bovine chondrocytes and BMSCs seeded in monolayer cultures. CS is reported to play important roles in cell adhesion, proliferation and tissue repair (Hsu et al., 2022), thus the purified CS was believed to mimic the natural ECM to promote a supportive environment for chondrocytes and the native ECM in promoting and/or maintaining the chondrogenic phenotype. The overarching aim of this chapter was to determine the impact of free CS chains on the cellular behaviours of chondrocytes and BMSCs; this was achieved by applying purified CS for chondrocytes as a substrate and for bBMSCs in chondrogenic medium and examining chondrogenic marker gene expression (Figure 4.1).

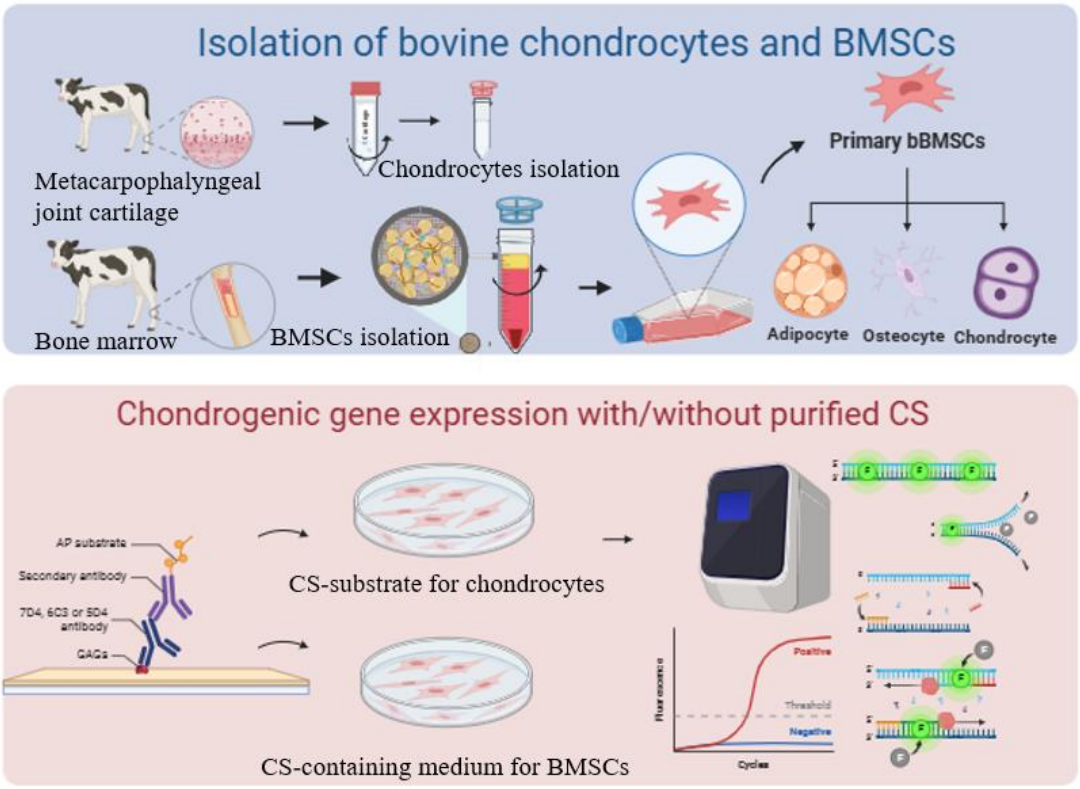

Figure 4.1 Illustration for cell culture strategy on 2D models with purified CS. *Bovine joint cartilage-derived chondrocytes were harvested from 3-week-old calves' metacarpophalyngeal joint cartilage. BMSCs were isolated from 3-week-old bovine bone marrow and authenticated by trilineage differentiation into adipocytes, osteocytes and chondrocytes. Then the purified CS was either coated on 24-well plate for chondrocytes or added into chondrogenic medium for BMSCs chondrogenesis before the expression of chondrogenic gene markers were examined by RT-qPCR.*

4.1.1 Utilisation of CS-coated substrate for supporting chondrocyte phenotype

CS is an essential component of the native cartilage ECM, where it interacts with other ECM molecules and cell surface receptors, promoting chondrocyte adhesion, survival and functionality (du Souich et al., 2009). Cellular receptor CD44 can recognise CS in the ECM and can activate cytoskeletal reorganisation and adhesion stabilisation (Fujimoto et al., 2001). CS has been demonstrated to enhance focal adhesion kinase (FAK) and extracellular signal-regulated kinase (ERK) activity to promote cell proliferation and survival while preventing chondrocyte apoptosis under stress conditions (Yang et al., 2004).

Evaluating gene markers such as *col2a1*, *acan*, and *sox-9* is essential to determine whether CS-coated substrates successfully maintain the chondrocyte phenotype. High expression levels of these markers would indicate that the chondrocytes have retained their cartilage-specific identity, emphasising the suitability of CS-coated surfaces for cartilage tissue engineering applications.

4.1.2 Utilisation of CS-coated substrate for facilitating BMSCs chondrogenic differentiation

BMSCs hold significant promise for cartilage repair due to their capacity for chondrogenic differentiation. In the presence of appropriate cues, BMSCs can differentiate into chondrocyte-like cells, expressing cartilage-specific ECM components and markers (Uzieliene et al., 2021). However, inducing and maintaining chondrogenic differentiation is highly dependent on the biochemical and physical properties of the culture environment (Zhou et al., 2023). A CS coating offers a bioactive surface that can promote the differentiation of BMSCs into chondrocytes by providing biochemical signals similar to those found in the native cartilage ECM (Zhao et al., 2021). This was endorsed by Eldeen et al. (2024b) who showed that a CS-coated nanofilm can stimulate the proliferation of human dental pulp stem cells and their chondrogenic differentiation, as assessed using scanning electron microscopy and RT-PCR. The interaction of BMSCs with CS-coated substrates may activate signalling pathways that are crucial for chondrogenesis, such as the TGF-β

pathway, which is a well-known regulator of chondrogenic differentiation (Goude et al., 2014). CS from bovine trachea was encapsulated into MSC-embedded microparticles for a 21-day chondrogenic culture, where CS and TGF-β exert synergistic effects on chondrogenesis by enhancing ECM deposition and chondrogenic gene markers expression, including *SOX-9*, *ACAN* and *COL-II* (Goude et al., 2014). Additionally, the ability of CS to bind growth factors and present them to cells in a bioavailable form can further enhance the differentiation process, Vandrovcová et al. (2011) reported CS from bovine trachea, especially CS-4, improved the proliferation of osteoblast-like MG63 cell line after 3 days of culture on a CS-coated biofilm with a more spread cellular morphology and spreading area. Compared with CS-embedded microparticles and CS-coated biofilm, the CS-coated substrate and CS in medium were expected to enhance the bioavailability with the provision of more immersive CS environment with more direct and diffusible contact to promote CS-cell interactions (Yeh et al., 2023). By mimicking the native cartilage microenvironment, the presence of exogenous CS could be postulated to improve the likelihood of differentiating BMSCs down the chondrogenic lineage; it has been previously demonstrated that CS coated scaffolds encouraged human BMSCs to express *COL2A1* and *ACAN*, and continue producing corresponding ECM components, both of which are critical for cartilage function (Han et al., 2020).

4.2 Results

4.2.1 CS-coated substrate altered chondrocyte morphology

Chondrocytes isolated from 3-week-old calves (Section 2.7) were seeded at 1×10^6 cells/well into 24-well culture plate coated with purified CS at concentration of $5\mu g/cm^2$ (prepared according to section 2.8.1); cells were cultured for 7 days, during which time the cells were imaged using an optical microscope every 3 days before medium change.

Within 1-day of chondrocytes being cultured on the CS substrate, cells started to clump together (Figure 4.2A). The chondrocytes on this 2D CS-coated surface appeared to dedifferentiate over time by losing their spherical shape and adopting a flattened, fibroblast-like morphology (Figure 4.2B-C).

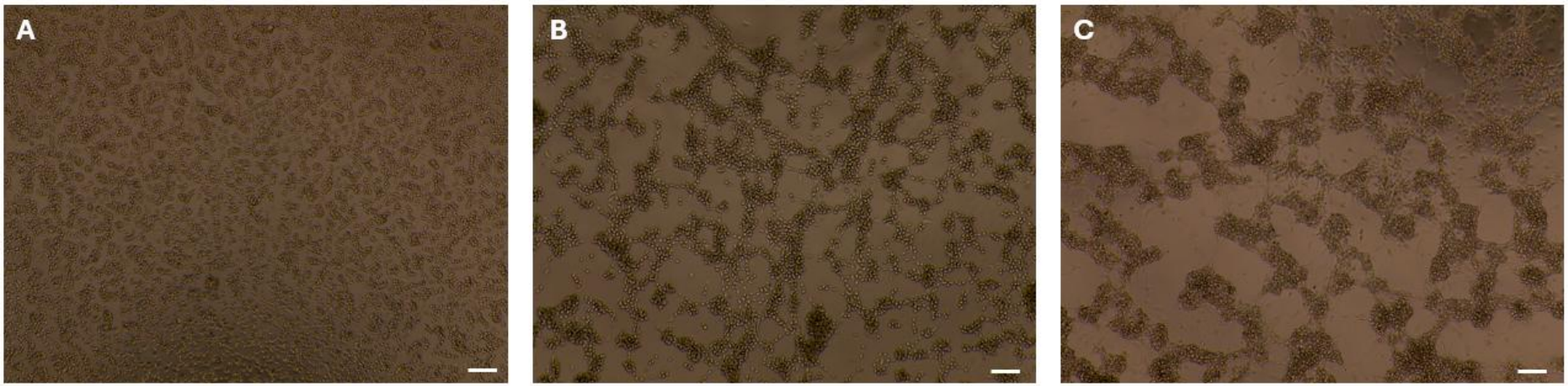

Figure 4.2 Cell morphology of bovine chondrocytes on CS-coated substrate over a 7-day culture period. *After 1-day culture on CS-coated substrate, the chondrocytes began to clump together, which was further evidenced over the 7-day culture period. Images were from the 0.5μg/cm^2 CS-coated substrate. (Scale bar = 100μm).*

4.2.2 Purified CS demonstrated biocompatibility as measured by chondrocyte viability

Chondrocytes isolated from 3-week-old calves (Section 2.7) were seeded at 1×10^6 cells/well into 24-well tissue culture plates containing an increasing concentration, ranging from 0μg/cm^2 (control) to 5μg/cm^2, of CS coated as a substrate (prepared according to section 2.8.1); cells were cultured for 7 days, during which an MTT assay was carried out to examine the viability of chondrocytes before each medium-change. The MTT absorbance was plotted for 0, 1, 4 and 7 days (Figure 4.3). The effect of increasing the concentration of CS coating on cell viability was analysed by comparing responses to the baseline of cells seeded onto non-coated tissue culture plate plastic and expressed as a percentage of the baseline cell viability.

On day 1 and day 4, there was no significant difference in cell viability across all CS-coating concentrations. By day 7, a significant increase in cell viability was observed for 0.1μg/cm^2 CS group ($p<0.001$, figure 4.3). When comparing the effect of CS-coating concentrations on cell viability, there was a statistically significant difference at day 7 of treatment ($p<0.001$), which was found in the comparison between 0.1μg/cm^2 coating relative to the control group. This suggests that the treatment has both a time-dependent and concentration-dependent effect on cell proliferation or survival, as indicated by the statistically significant results.

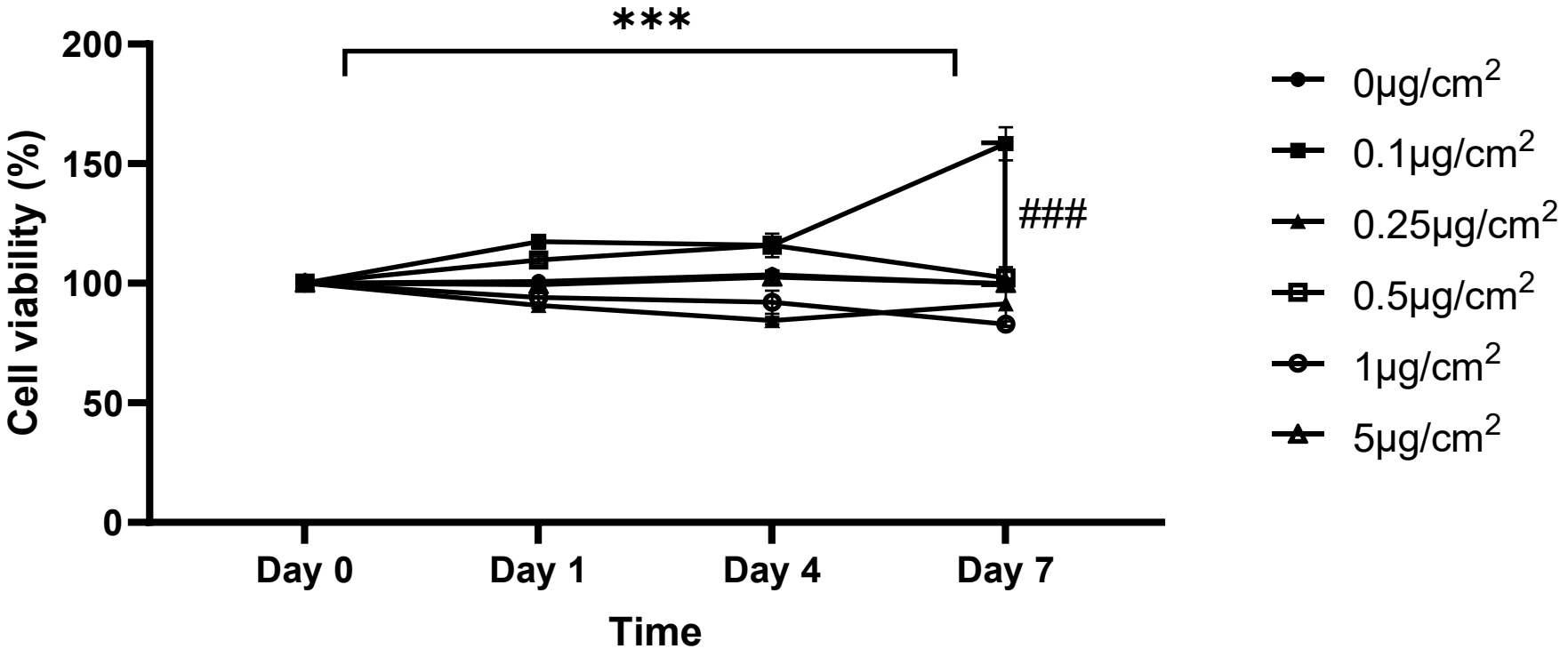

Figure 4.3 Percentage viability of chondrocytes seeded onto a concentration gradient of CS-coated substrate over a 7-day culture period; cell viability was assessed using the MTT assay and data normalised to the untreated chondrocytes at day 0 (arbitrarily assigned as 100%). *There was a significant increase in the viability of chondrocytes seeded onto 0.1µg/cm^2 CS-coated substrate after 7-days of culture; the other CS-coating concentrations had no observable effect when 2-way ANOVA (Dunnett's multiple comparison) was employed. Data is presented as mean ± standard deviation (n=3, N=3). [*** $p<0.001$ as a function of time, ### $p<0.001$ as a function of CS concentration].*

4.2.3 Purified CS-coated substrate enhanced expression of chondrogenic markers in chondrocytes

Chondrocytes (1×10^6) were seeded into wells coated with different CS concentrations and cultured for 5 days, RT-PCR was carried out to examine the expression level of chondrogenic gene markers, *col2a1, sox-9 and acan*. The CS concentration, ranging from 0μg/cm^2 (control) to 5μg/cm^2, used to coat the wells had no effect on expression of *col2a1* mRNA in the 5-day chondrocyte monolayer cultures (Figure 4.4A); expression levels remained similar to those of cells seeded directly onto tissue culture plastic (Control group). In contrast, the expression of *acan* was more variable with significant suppression observed when cells were seeded onto the 5μg/cm^2 CS substrate (2-fold decrease, $p<0.001$, figure 4.4B). However, *sox-9* transcription was consistently affected by seeding onto CS-coated wells (Figure 4.4C); compared to uncoated wells, *sox-9* mRNA expression significantly increased when cells were seeded onto 0.1μg/cm^2 (10-fold, $p<0.001$), 0.5μg/cm^2 (5-fold, $p<0.001$) and 5μg/cm^2 CS-coated substrate (3-fold, $p<0.001$). Surprisingly, there was no obvious effect of either the 0.25μg/cm^2 or 1μg/cm^2 CS-coatings.

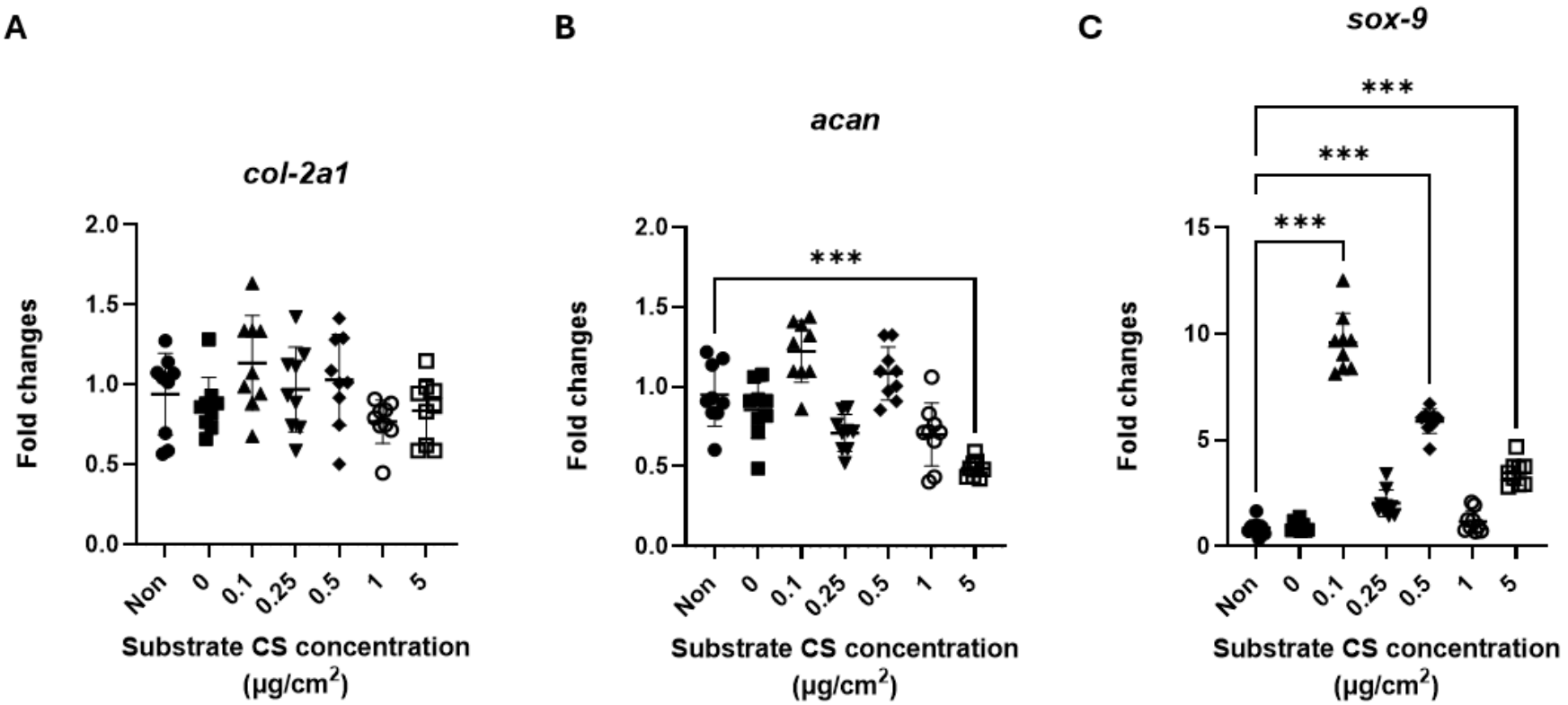

Figure 4.4 The expression of chondrogenic gene markers in the chondrocytes seeded onto a range of CS concentrations from 0-5 µg/cm²of purified CS on the coating substrate for 5 days. *The addition of purified CS did not affect the expression of* ***[A]*** *collagen II (col2a1) or* ***[B]***

aggrecan (acan). ***[C]*** *0.1μg/cm^2 CS induced 10-fold increase in SOX-9 expression($p<0.001$), Data is presented as mean ± standard deviation (n=3, N=3, 2-way ANOVA test). [*** $p<0.001$].*

4.2.4 Multipotency of bovine BMSCs were authenticated by trilineage differentiation

Multipotency of BMSCs, isolated from 3-week-old bovine calves bone marrow (Section 2.9), was assessed by culturing under specific conditions to induce differentiation into osteogenic and adipogenic lineages over 21 days (Sections 2.10 - 2.11) and a chondrogenic lineage over 28 days (Section 2.13). Using histological stains, the BMSCs were demonstrated to commit to the trilineage differentiation into osteoblasts (Figure 4.5A), adipocytes (Figure 4.5B) and chondrocytes (Figure 4.5C) with the specific staining of Alizarin Red S (osteogenesis), Oil Red O (adipogenesis) and Toluidine Blue (chondrogenesis), respectively.

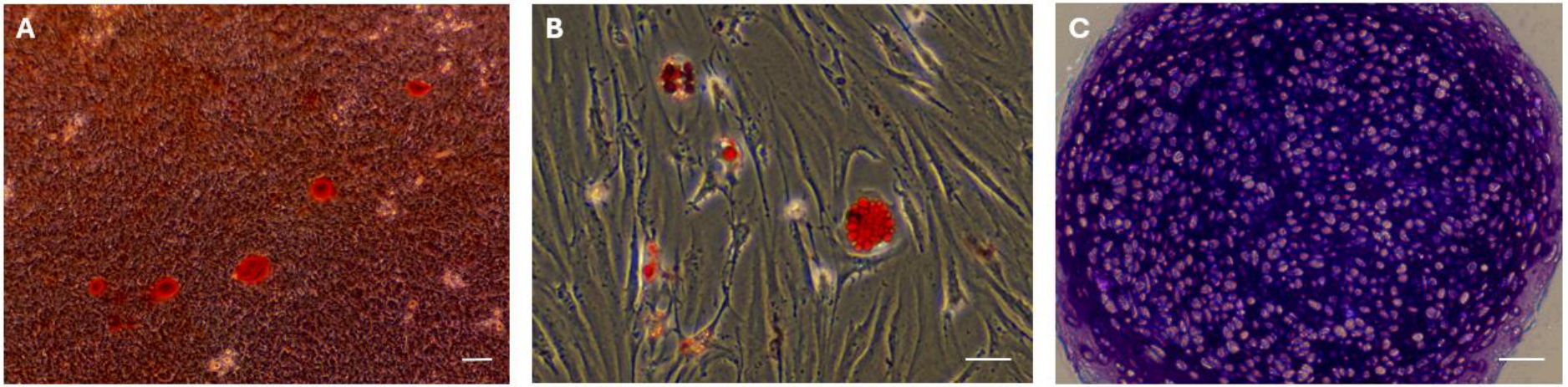

Figure 4.5 Specific staining for trilineage differentiation of BMSCs. ***[A]*** *Alizarin red S staining confirmed osteogenesis of BMSCs after 21-day culture;* ***[B]*** *Oil red O staining confirmed adipogenesis with 21-day culture,* ***[C]*** *Toluidine Blue staining demonstrated chondrogenesis with 28-day culture. (n=3, N=3, Scale bar=100μm)*

4.2.5 bBMSCs clumped together during chondrogenic differentiation in CS-containing medium

When the purified CS was reconstituted in chondrogenic medium, a CS concentration of 100μg/ml was employed as in a previous study it had been shown to promote musculoskeletal regeneration (Stabler et al., 2015); hence, bBMSCs were cultured in chondrogenic medium with or without 100μg/ml of CS (purified from bovine cartilage) for 14 days.

The bBMSCs were observed under a light microscope before the medium change every three or four days (Figure 4.6); bBMSCs were found to start to clump together as early as 4 days after seeding, in the same manner as observed for the chondrocytes on the CS-coated substrate (figure 4.2). bBMSCs with or without exogenous CS added to the culture medium formed into cellular aggregates, with bBMSCs exposed to CS forming cellular aggregates earlier (Figure 4.6A, E).

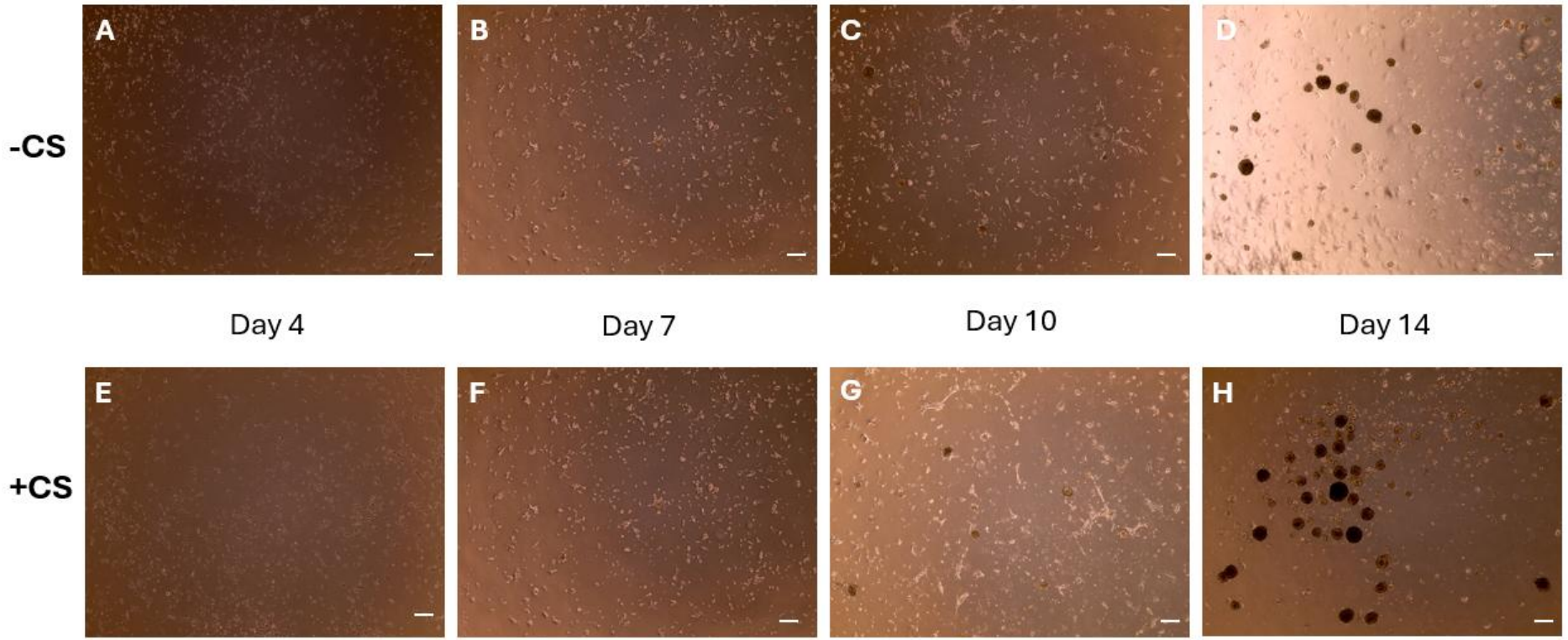

Figure 4.6 Images of BMSCs in chondrogenic medium with or without purified CS over a 14-day culture. [A-D] *Images of chondrogenic differentiation without purified CS.* ***[E-H]*** *Treatment group with 100µg/ml purified CS in chondrogenic medium. The stem cells, plated as 2D on tissue culture plastic, started to clump together within 4-days of culture, and those in CS-containing medium formed more and bigger clumps after 14 days. (n=3, N=3, Scale bar =100µm)*

4.2.6 Purified CS did not affect bovine BMSC viability during chondrogenesis

The MTT assay was conducted on the bBMSCs cultured in chondrogenic media for 14 days to determine the biocompatibility of 100µg/ml purified CS on cell viability (Figure 4.7). Overall, there was a modest 4% increase in cell viability over the time course, both in the presence ($p<0.01$) and absence of CS in the culture media ($p<0.01$) likely due to cell proliferation. However, this confirmed that addition of the purified CS to the chondrogenic media is not cytotoxic to the BMSCs.

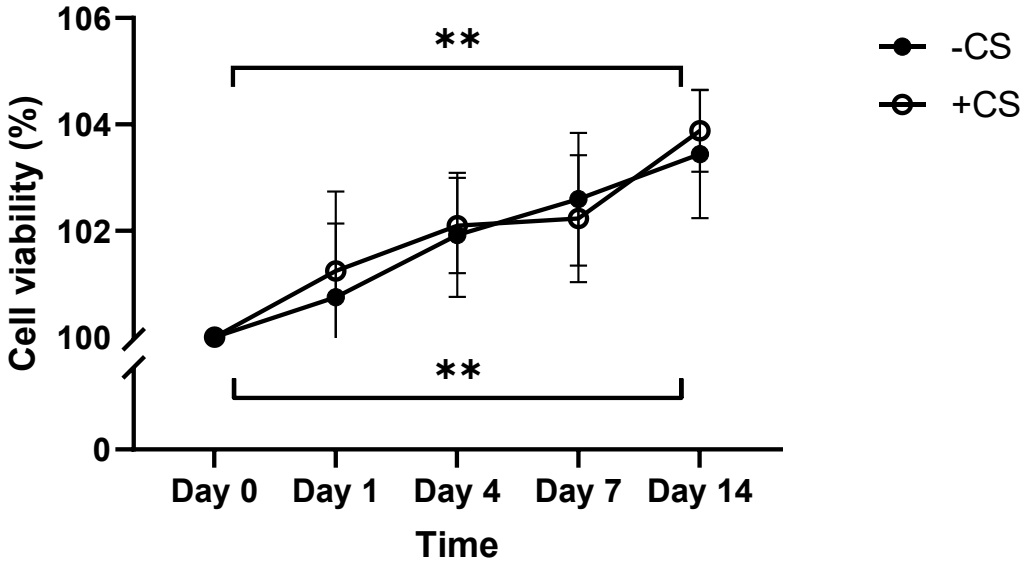

Figure 4.7 Cell viability of bBMSCs cultured in chondrogenic medium with/without 100µg/ml of purified CS as assessed using the MTT assay; data was normalised to the viability of untreated bBMSCs at day 0. BMSCs were viable over the 14-day chondrogenic culture irrespective of the presence of purified CS demonstrating it did not suppress cell viability. Data is presented as *mean ± standard deviation (n=3, N=3, 2-way ANOVA test) [** p<0.01].*

4.2.7 Inclusion of purified CS in the media increased sGAG deposition during bBMSC chondrogenesis

To better investigate the influence of CS on the chondrogenic process, bBMSCs were either cultured in basal growth medium or chondrogenic medium, for 14 days, with or without 100µg/ml purified CS in the medium; bBMSCs were stained with Alcian Blue (Section 2.13) to assess sGAG deposition (Figure 4.8). bBMSCs grown in basal growth media for 14 days showed no sGAG production either in the absence (Figure 4.8A) or presence of purified CS (Figure 4.8B). In contrast and as expected, positive 7Alcian Blue staining was observed in the bBMSCs grown in chondrogenic media alone (Figure 4.8C), and this effect was increased when bBMSCs were cultured in CS-containing chondrogenesis medium (Figure 4.8D).

To quantify the staining intensity, medium was removed followed by washing of the cells to eliminate exogenous purified CS; 4M guanidine-HCl was then used to extract the GAGs deposited by the cells. Absorbances were subsequently measured at 600nm, and it was found that chondrogenic media alone significantly increased sGAG production by 10-fold compared to cells cultured in basal growth media ($p<0.001$, Figure 4.8E). An even greater production of ECM sGAGs was observed when cultured in the presence of purified CS increasing from an absorbance of 1.163 ± 0.0159 to 1.526 ± 0.0462 ($p < 0.001$, figure 4.8E).

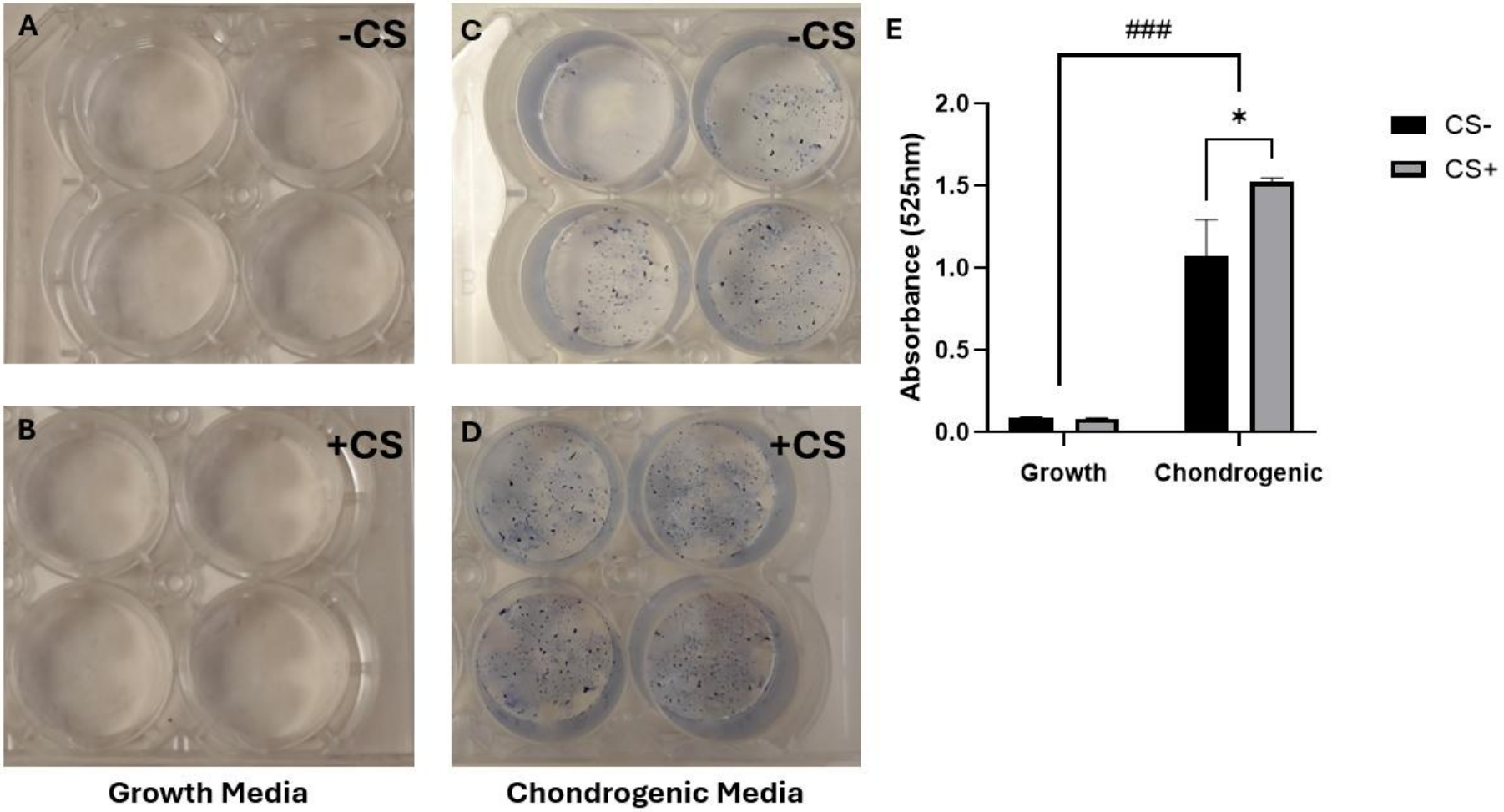
A
-CS
C
-CS
B
+CS
D
+CS
Growth Media
Chondrogenic Media
E
###
*
Absorbance (525nm)
2.0
1.5
1.0
0.5
0.0
Growth
Chondrogenic
CS-
CS+

Figure 4.8 Alcian blue staining for BMSCs cultured in [A, B] basal growth medium (with/out 100µg/ml purified CS) and in [C, D] chondrogenic medium (with/out 100µg/ml purified CS), and [E] quantitative analysis of the staining. *More intense Alcian Blue staining i.e. enhanced GAG synthesis was observed in the bBMSCs cultured in chondrogenic media containing CS compared to chondrogenic medium without CS ($p<0.0001$). Data is presented as mean ± standard deviation (n=3, N=3, 2-way ANOVA) [### $p<0.001$ comparing basal media to chondrogenic media, *** $p<0.001$ comparing presence or absence of CS].*

4.2.8 Transcriptional markers of the chondrogenic phenotype were increased in bBMSCs cultured in CS-containing chondrogenic medium

Transcriptional expression of chondrogenic markers were examined using RT-qPCR in bBMSCs (1×10^6 bBMSCs as described in section 2.13) cultured in chondrogenic medium, with or without the supplementation of 100µg/ml CS, for 14 days (Figure 4.9). There was no significant effect of CS on either *col2a1* (Figure 4.9A) or *acan* transcript levels (Figure 4.9B). In contrast, it was discovered that levels of *sox-9* gene expression significantly increased in the presence of purified CS in the medium (2-fold, $p<0.05$, figure 4.9C).

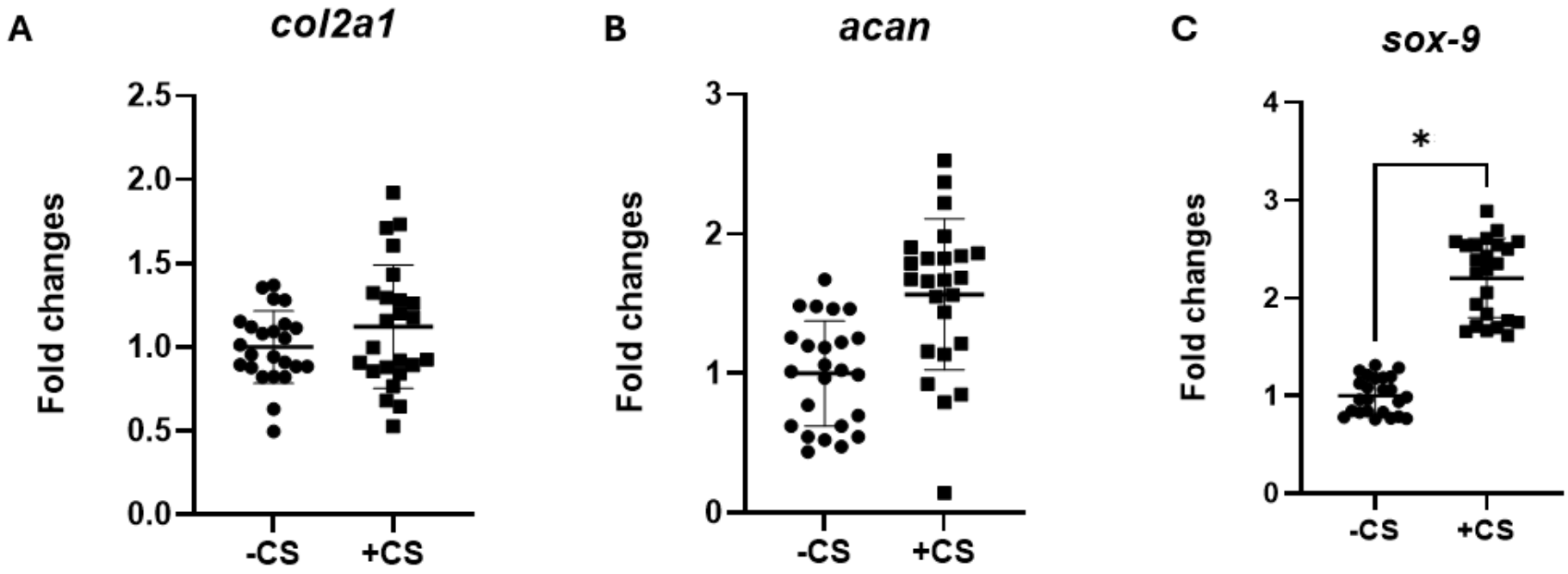

Figure 4.9 Transcriptional expression of chondrogenic gene markers in monolayer BMSCs cultured in chondrogenic medium with/out purified CS. *The expression of* ***[A]*** *col2a1,* ***[B]*** *acan and* ***[C]*** *sox-9 data are presented as mean ± standard deviation. sox-9 transcription was significantly enhanced in CS-containing chondrogenic medium. (n=3, N=6) [* $p<0.05$].*

4.3 Discussion

The aims of this chapter were to investigate the biocompatibility of purified free CS and its potential effects on (i) maintaining the chondrocyte phenotype and (ii) supporting bBMSC chondrogenic differentiation in 2D culture. By applying MTT assays, it was apparent that for the chondrocytes seeded onto a range of CS-coated substrate concentrations and for bBMSCs in CS-containing chondrogenic medium, respectively, cell viability was not adversely affected compared to the non-CS groups over the culture period. Interestingly, only the 0.1µg/cm^2 CS coating significantly affected cell behaviour with increased chondrocyte viability/proliferation after 7 days of culture, concomitant with enhanced mRNA expression of the chondrogenic marker *sox-9*. For the 2D chondrogenesis of bBMSCs cultured in chondrogenic medium, 100µg/ml CS in the media was also found to increase *sox-9* mRNA expression and sGAG deposition.

4.3.1 Utility of bovine-derived high purity CS for chondrocyte and bBMSC tissue engineering approaches

This study introduced a novel approach (CS-coated substrate) to promote maintenance of the chondrocyte phenotype and to support chondrogenic differentiation with the utilisation of high-purity free CS chains purified from bovine cartilage, which was applied to chondrocytes as a coating substrate and to bBMSCs in chondrogenic medium. Unlike the conventional CS and commercial CS products, which often contains residual protein contaminants that may influence cellular behaviour (Volpi, 2019), the CS preparation purified in this thesis provided a bioactive and biocompatible formulation with the MTT results demonstrating enhanced cell viability on CS substrate. This is the first study to systematically investigate the effects of peptide-free CS on both chondrocytes and mesenchymal stem cells, revealing enhanced ECM production and upregulation of chondrogenic markers, highlighting a role for CS as a biochemical cue for promoting and preserving the chondrogenic phenotype. While CS has been widely studied in cartilage biology, previous research primarily focused on its effects on chondrocyte metabolism,

especially under inflammatory conditions like OA (Jerosch, 2011). The findings in this chapter indicated that purified free CS preparation facilitated both chondrocyte viability/proliferation and stem cell chondrogenesis with greater matrix synthesis and higher chondrogenic marker gene expression, providing additional evidence to support its current application in CS-based cartilage engineering strategies (Wang et al., 2007).

4.3.2 Assessment of cell viability/proliferation using the MTT Assay

The results of the MTT assay are particularly important for biomaterials research as they reflect the initial compatibility of the substrate with the cells. A high level of metabolic activity observed in the MTT assay indicates a high rate of cell viability and proliferation, suggesting that the substrate is biocompatible and supports cell function (Ciapetti et al., 1993). The MTT assay is a commonly used, robust method for evaluating cell viability and proliferation (Larsson et al., 2020) and is a colorimetric assay which measures the metabolic activity of living cells by quantifying the reduction of MTT into an insoluble purple formazan product (van Meerloo et al., 2011). This reduction occurs in the cells with metabolically active mitochondria, making it a reliable indicator for assessing how well cells thrive in the microenvironment provided by the material.

For this study, the MTT assay was employed to evaluate the cellular response of both chondrocytes and BMSCs when cultured on CS-coated substrates or incorporated into the media, respectively. By measuring mitochondrial activity, the assay provides insights into whether the CS creates a supportive environment for cell growth and survival, but also helps optimise CS concentrations for cartilage tissue engineering. The novel findings from the MTT assay, particularly the indication that CS can promote bBMSC proliferation, serves as a critical foundation for correlating cell viability with chondrogenic differentiation and ultimately assessing the potential of purified CS for regenerative applications (Hsu et al., 2022). For chondrocytes, maintaining viability and proliferation is crucial to ensure their ability to maintain a chondrogenic phenotype and to produce cartilage-specific ECM components (Chu et al., 2024). For BMSCs, the assay provides insights into the cells' ability to survive

and potentially differentiate into chondrocytes on the CS-containing medium, which is essential for their use in cartilage repair and regenerative applications (Seo and Na, 2011).

4.3.3 Transcriptional expression of chondrogenic markers

Assessing phenotypic gene marker expression is a powerful tool for evaluating the effectiveness of biomaterials like CS-coated substrates in supporting chondrogenesis (Yi et al., 2018). These markers serve as molecular indicators of cell identity, function, and differentiation state. For chondrocytes, the expression of markers such as *col2a1*, *acan*, and *sox-9* confirms the maintenance of their phenotype and indicates a healthy, functional state suitable for cartilage regeneration (Zwickl et al., 2016). For BMSCs, the upregulation of these same markers signifies their successful progression toward a chondrogenic lineage, reflecting the potential of CS-containing media to induce differentiation (Weissenberger et al., 2020). The mRNA expression of *sox-9* was upregulated in both chondrocytes and bBMSCs exposed to the purified free CS, which is consistent with the findings reported by Ai et al. (2023) who demonstrated that addition of 6% (w/v) CS in scaffolds promoted MSC chondrogenesis through increased *sox-9* mRNA expression.

In this chapter, although *sox-9* expression was enhanced, the expression of *col2a1* and *acan* remained unaffected relative to control cultures. There are several potential reasons for this: *sox-9* is a critical transcription factor that regulates chondrogenesis by activating cartilage-specific genes, including *col2a1* and *acan*. However, increased *sox-9* expression does not always guarantee increased transcription of its target genes. Regulatory mechanisms at the transcriptional, post-transcriptional, or post-translational level may inhibit downstream effects, for example, *sox-9* often requires co-factors, such as *sox-5* and *sox-6*, to form a functional complex that can robustly activate *col2a1* and *acan* expression (Liu and Lefebvre, 2015). If these co-factors are not sufficiently expressed or functional, *sox-9* alone may not fully activate its target genes (Lefebvre and Dvir-Ginzberg, 2017). Furthermore, induction of *sox-9* is one of the earliest events in chondrogenesis, marking the commitment of progenitor cells to the chondrogenic lineage. However, downstream expression of *col2a1* and *acan*

typically requires additional signalling pathways and differentiation cues, including biochemical signals and mechanical stimuli. The insufficient or imbalanced stimuli may limit the full activation of chondrogenic differentiation despite *sox-9* induction (Aigner et al., 2003).

To figure out the potential cause, analysing the expression of *sox-5* and *sox-6* would be beneficial to determine whether they were limiting chondrogenesis. If the expression of the co-factors were not enhanced, the downstream induction of *col2a1* and *acan* would not be facilitated. Due to the lack of mechanical cues on a 2D monolayer surface, creating a 3D cell model would be a better environment to build and maintain the chondrogenic phenotype, which is addressed in chapter 5.

4.3.4 Validation of chondrogenesis by assessing sGAG deposition using Alcian Blue staining

Alcian Blue is a cationic dye widely used to detect acidic polysaccharides, including the GAGs in cartilage and chondrogenic tissues. In the chondrogenesis of BMSCs, Alcian Blue staining serves as a reliable histological method to assess chondrogenesis by highlighting the presence of sulphated GAGs, a hallmark of cartilage ECM synthesis (Rigueur and Lyons, 2014). When BMSCs are induced to undergo chondrogenic differentiation, they begin producing cartilage-specific ECM components, including PGs like aggrecan, which are rich in chondroitin sulphate and keratan sulphate. These proteoglycans bind strongly to alcian blue due to the high density of negatively charged sulphate and carboxyl groups, which makes the dye an effective tool for visualising the spatial distribution of GAGs and authenticating GAG production during chondrogenesis *in vitro* (Hu et al., 2019).

While visual observation of Alcian Blue staining provides qualitative insights into GAG synthesis during chondrogenesis, quantitative analysis is crucial for objective and reproducible evaluation. Quantifying staining intensity by using 4M guanidine-HCl offers a means to compare the extent of chondrogenesis across diverse conditions, treatments, or time points (Kawato et al., 2012). A higher number of bigger aggregates were stained by Alcian Blue in bBMSCs cultured in CS-containing chondrogenic medium compared to the group without CS, which is consistent with the results from

previous research (Li et al., 2013b). Li et al (2013a) used 0.25mM para-nitro-phenyl-b-xyloside (PNPX), a competitive acceptor of CS substitution on PGs, to disrupt CS/DS chain formation in BMSCs cultured in chondrogenic medium for 4 weeks. Addition of PNPX inhibited the spheroidal aggregation of bBMSCs on a 2D surface negatively impacting chondrogenesis.

Summary of key findings

- Purified CS was found to be biocompatible with both chondrocytes and bBMSCs and supported their viability/proliferation.
- Purified CS enhanced sGAG synthesis and deposition in bBMSCs during chondrogenic differentiation.
- Purified CS increased expression levels of *sox-9* mRNA in both chondrocytes and BMSCs undergoing chondrogenic differentiation.

Chapter 5

The Cellular Behaviour of Bovine Bone Marrow Stem Cells in 3D cell culture with and without Chondroitin Sulphate

5.1. Introduction

With the observed induction of *sox-9* gene expression in BMSCs seeded as a 2D monolayer in the presence of CS (Section 2.8), this chapter aimed to further explore the cellular behaviours of BMSCs, in a 3-dimensional (3D) environment cultured in chondrogenic media with or without purified CS. A couple of previous studies have suggested that this phenomenon might be relevant in 3D as well as 2D models. Specifically, 2.5wt.% CS (derived from shark fin cartilage) incorporated into a gelatin bio-scaffold with human MSCs to assess cartilage regeneration over a 21-day period reported significant increases in *SOX-9* gene expression (Vassallo et al., 2022). Furthermore, it had previously been shown that *sox-9* transcription was induced in rat MSCs cultured, for up to 28 days, in a scaffold comprising 0.05% (w/v) CS and collagen (Matsiko et al., 2012). As there is only limited evidence describing the influence of CS on *sox*-9 mRNA expression, this chapter aimed to investigate more broadly how CS influences cell viability and proliferation, its chondrogenic differentiation potential and ECM deposition within different 3D experimental systems. 3D culture systems have revolutionised cell biology and tissue engineering by providing an environment that better mimics the *in vivo* conditions compared to traditional 2D monolayer cultures (Kapałczyńska et al., 2018).

5.1.1 Relevance of using 3D models to investigate BMSC chondrogenesis

Unlike 2D cultures, where cells are constrained to grow on a flat surface, 3D systems allow cells to interact with their surroundings, closely resembling the native ECM (Edmondson et al., 2014). This biomimetic feature is particularly crucial for studying the chondrogenic behaviour of BMSCs, as cartilage is a 3D tissue characterized by a dense ECM and minimal cell-cell interactions (Estes and Guilak, 2011). Studies have shown that BMSCs respond to the mechanical and biochemical cues provided by a 3D microenvironment (Vining and Mooney, 2017), leading to enhanced expression of chondrogenic markers e.g. *sox-9* and *col2a1*, and production of cartilage-specific ECM components e.g. aggrecan. In conjunction, the 3D systems support the deposition and organisation of ECM components produced by differentiated BMSCs. In 2D cultures, ECM synthesis is often limited or irregular due to the lack of spatial

constraints and disrupted cell-matrix interactions (Harjanto and Zaman, 2013). In contrast, 3D systems allow BMSCs to differentiate into chondrocytes and produce ECM components in a manner that more closely resembles native cartilage (Estes and Guilak, 2011).

Additionally, 3D culture systems like agarose gels can help mitigate dedifferentiation and hypertrophy, common challenges associated with BMSC-based cartilage repair (Oliver-Ferrándiz et al., 2021). Dedifferentiation refers to the loss of chondrocyte-like characteristics during culture, often leading to the expression of fibroblastic markers such as COL-I (Yao and Wang, 2020). Hypertrophy, on the other hand, is characterized by the expression of COL-X and other markers associated with endochondral ossification (Kamakura et al., 2023). The 3D environment of agarose gels, combined with the presence of bioactive molecules like CS, can suppress these undesired pathways, promoting stable and sustained chondrogenic differentiation (Ai et al., 2023).

The study design in this chapter leverages two specific 3D culture systems to evaluate the impact of CS on BMSCs in namely the 3D agarose gel and the Transwell™ system. The agarose gel provides a spatially confined environment where cell-matrix interactions can be closely examined, mimicking the physical and biochemical conditions of native cartilage (Lee et al., 2000b). In contrast, the Transwell™ system facilitates molecular-level investigations of chondrogenic gene expression, offering a comprehensive understanding of how CS modulates cellular behaviours at the transcriptional level.

5.1.2 Utilisation of 3D agarose construct system

The use of 3D system, such as agarose gel, is widely used as a cartilage regeneration model with chondrocytes by providing multiple benefits for investigating BMSC behaviour during chondrogenesis (Huang et al., 2004). First, the encapsulation of cells in a 3D matrix enables them to establish cell-matrix interactions, which are pivotal for directing cellular responses, such as differentiation, migration, and ECM synthesis. The stiffness and porosity of the agarose gel can also be tailored to resemble the mechanical properties of cartilage, creating an environment conducive to

chondrogenic differentiation (Janaky et al., 2006, Bertula et al., 2019). Agarose gels are particularly advantageous for cartilage tissue engineering due to their inert and non-adhesive nature (Gutierrez et al., 2022). This property ensures that BMSC behaviour in agarose is primarily influenced by the biochemical composition of the culture medium rather than by unintended interactions with the gel itself (Coleman et al., 2007). When supplemented with CS, the agarose matrix provides a platform for studying the specific effects of it on BMSC viability, differentiation, and matrix deposition. The confined environment of the gel not only mimics the avascular nature of cartilage but also supports the uniform distribution of nutrients, oxygen, and signalling molecules, creating a physiologically relevant setting for cell culture.

5.1.3 Utilisation of Transwell™ culture system

The Transwell™ system is an advanced and versatile tool that enables the study of cellular behaviour and differentiation under physiologically relevant conditions (Wright et al., 2023). Its unique two-compartment design, separated by a permeable membrane, allows for the exchange of soluble factors while maintaining the physical separation of cells in each compartment. This setup is particularly advantageous for chondrogenic regeneration studies using BMSCs, as it facilitates paracrine signalling without direct cell-to-cell contact (Davidson et al., 2017). By mimicking the microenvironment of cartilage, the Transwell™ system provides insights into how soluble factors, such as CS, influence BMSC differentiation and ECM production.

Another significant advantage of the Transwell™ system is its ability to provide a controlled microenvironment for chondrogenesis (Chung et al., 2018). The semi-permeable membrane supports the diffusion of nutrients, oxygen, and growth factors while preventing direct cell-to-cell contact, replicating the diffusion-limited environment of native cartilage (Murdoch et al., 2007). It also allows for the spatial application of biochemical stimuli, such as growth factors or GAGs, in a gradient or controlled manner, creating more physiologically relevant conditions for differentiation (Sip et al., 2014). The membrane itself can also be functionalised with ECM components like collagen or CS, further enhancing the biomimicry of the system. Simultaneously, RNA or protein samples from the cells in both compartments

can be used to monitor gene and protein expression dynamics, including chondrogenic markers like *COL-II*, *SOX-9*, and *ACAN*. These features provide a temporal understanding of chondrogenic differentiation, enabling researchers to fine-tune culture conditions and better understand the underlying mechanisms (Ou et al., 2020).

The study initially employed an agarose gel to create a 3D culture system, allowing for a biomimetic environment that supports chondrogenesis and enhances the interaction between BMSCs and CS since hydrogel is a widely used system for chondrocyte studies. Previous studies based on an agarose gel model employed 3% agarose with 4×10^6 cells/ml, which provided more resilient mechanical properties for intervertebral disc regeneration (Lee et al., 2000a, Wann et al., 2012, Roberts et al., 2001). In parallel, the Transwell™ culture system was also employed in this study to investigate the effects of CS on BMSC chondrogenesis, whereby the BMSCs were seeded onto the membrane and the CS introduced into the chondrogenic media. Kabiri et al. (2012) seeded human MSCs into the Transwell™ system, induced chondrogenesis over a 14-day culture and observed significant increases in chondrogenic gene markers including *SOX-9*, *COL-II* and *ACAN*; this response was enhanced when the Transwell™ system was used in combination with exogenous growth factors added into the culture medium. Therefore, in this chapter bBMSCs were seeded into the Transwell™ system and CS added to the chondrogenic medium to investigate its effect(s) on chondrogenesis.

This chapter set out to explore the effects of CS on the chondrogenic differentiation of BMSCs in the two model systems, i.e. hydrogel incorporating CS and the Transwell™ system with CS introduced into the culture medium. Both models were then evaluated to assess how CS influence key markers of chondrogenesis, the mature chondrocyte phenotype and ECM production.

5.2 Results

5.2.1 Bovine BMSCs seeded in agarose hydrogels demonstrated limited viability following 1-week of culture

BMSCs (1×10^6 cells/cm^3) were embedded in 2% (w/v) agarose gel constructs and cultured in chondrogenic medium for up to 7 days prior to analysis. To determine cell viability, after 1, 2, 3 and 7 days of chondrogenic culture the chondrocyte-agarose constructs were stained using the live/dead assay with FDA and PI (described in section 2.8.3). Following staining, the constructs were cut into halves and imaged using an Olympus BX brightfield microscope with FITC and TRITC channels; viable cells were stained green by FDA and the nuclei of the dead cells appeared red with PI.

Following 1 day of culture, the bBMSCs showed a high viability in the agarose gel with relatively strong green staining and few cells detected under the red filter (Figure 5.1A - B). This trend remained similar up until 3 days of culture (Figure 5.1C – D), after which there seemed to be a reduction in FDA labelling concomitant with far more PI detected (Figure 5.1E – H). Surprisingly, following 7 days of culture very few viable bBMSCs were detected (Figure 5.1I) and instead the construct appeared to contain predominantly dead cells (Figure 5.1J). This effect was also observed in a repeat independent experiment (data not shown). However, there appeared to be no issue with the methodology because when bovine chondrocytes were embedded in agarose following an identical protocol, these cells remained viable over 7 days (Figure 5.2). Due to the extent of cell death incurred when bBMSCs were embedded in agarose, this 3D model system was not continued further; instead, the Transwell™ model was taken forwards in this chapter.

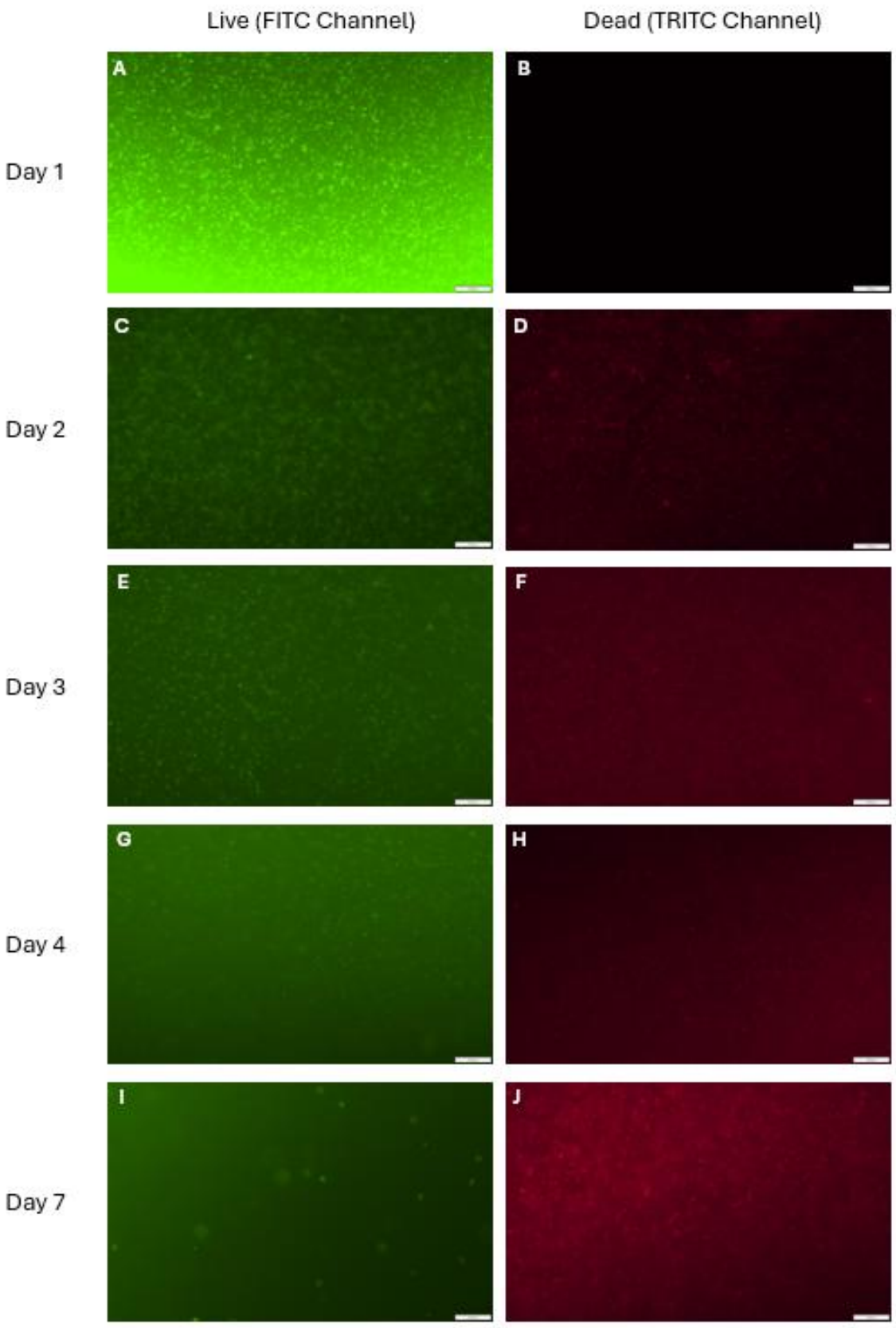

Figure 5.1 Visualisation of FDA (live cells in green)/PI (dead cells in red) staining with 2 x 10^6 bBMSCs embedded into 2% (w/v) agarose gel and cultured in

chondrogenic media for up to 7 days. *The constructs were stained using the live/dead assay (FDA/PI) on days,* ***A – B****. day 1,* ***C – D*** *day 2,* ***E – F*** *day 3,* ***G – H*** *day 4 and* ***I - J*** *day 7 after chondrogenic culture and representative fields of view imaged using appropriate channels. There was a substantial increase in bBMSC death over the culture period with very few viable cells evident at day-7. (Scale bar = 200µm)*

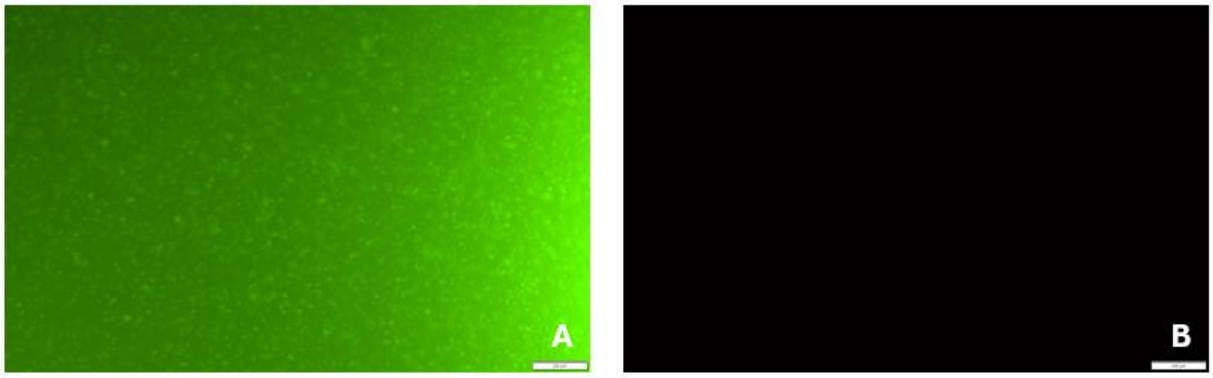

Figure 5.2 Fluorescence visualisation of cell viability of 1 x 10^6 chondrocytes encapsulated into a 2% (w/v) agarose gel and cultured for 7 days. *The constructs were stained using the live/dead (FDA/PI) assay with* ***(A)*** *strong FDA signal and* ***(B)*** *very weak PI labelling indicating chondrocyte viability in agarose. (Scale bar = 200µm)*

5.2.2 Utilisation of the Transwell™ system for bovine bone marrow stem cell (bBMSC) chondrogenesis

5.2.2.1 Chondrogenic differentiation of bBMSCs cultured in the Transwell™ system over 6 weeks produced 'cartilage-like' tissue

2×10^6 cells/well bBMSCs were seeded onto the membrane of the Transwell™ system and cultured under chondrogenic conditions for 6 weeks with different concentrations of CS (control, low CS concentration: 5μg/ml, high concentration: 100μg/ml). After 2 weeks of culture, bBMSCs in these 3 groups formed colonies visible to the naked eye (Figure 5.3, arrows), and a cartilage-like white tissue formed on the insert in one of the high CS concentration wells (Figure 5.3, green arrow); the tissue was increasingly evident over the culture period and became more resilient such that the 'cartilage-like' construct could be picked up with tweezers after 6-weeks in culture.

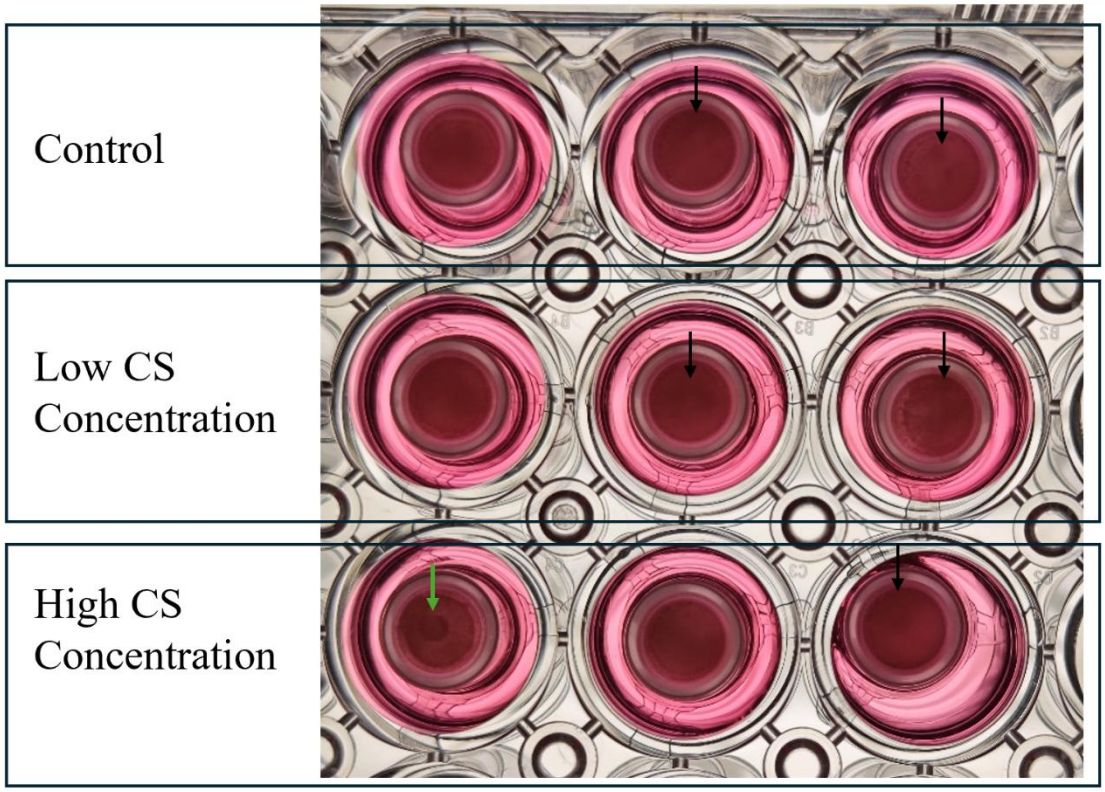

Figure 5.3 Visual observation of Transwell™ system after 2 weeks of chondrogenic culture treated with different CS concentrations. *bBMSC chondrogenic colonies formed under all three conditions (black arrows); however, it was more pronounced in the high CS concentration wells, with the formation of a tissue-like colony first (green arrow), which developed into a 'cartilage-like' tissue after another 4-weeks in culture.*

5.2.2.2 Exogenous CS induced bBMSC chondrogenesis in the Transwell™ system

After 6-weeks of chondrogenic culture, the 'cartilage-like' tissue was harvested as described (section 2.15.2), embedded in wax and sectioned prior to histological staining with H&E, Toluidine Blue and Trichrome (Figure 5.4). In the control wells, there was limited ECM deposition with less intense staining of Toluidine Blue (figure 5.4D) and Trichrome (figure 5.4G). In contrast, incorporating CS into the media of the Transwell™ system enhanced the chondrogenic capability of the bBMSCs, with this effect being more pronounced with the high CS concentration resulting in ECM formation through GAG (figure 5.4F) and collagen deposition (figure 5.4I).

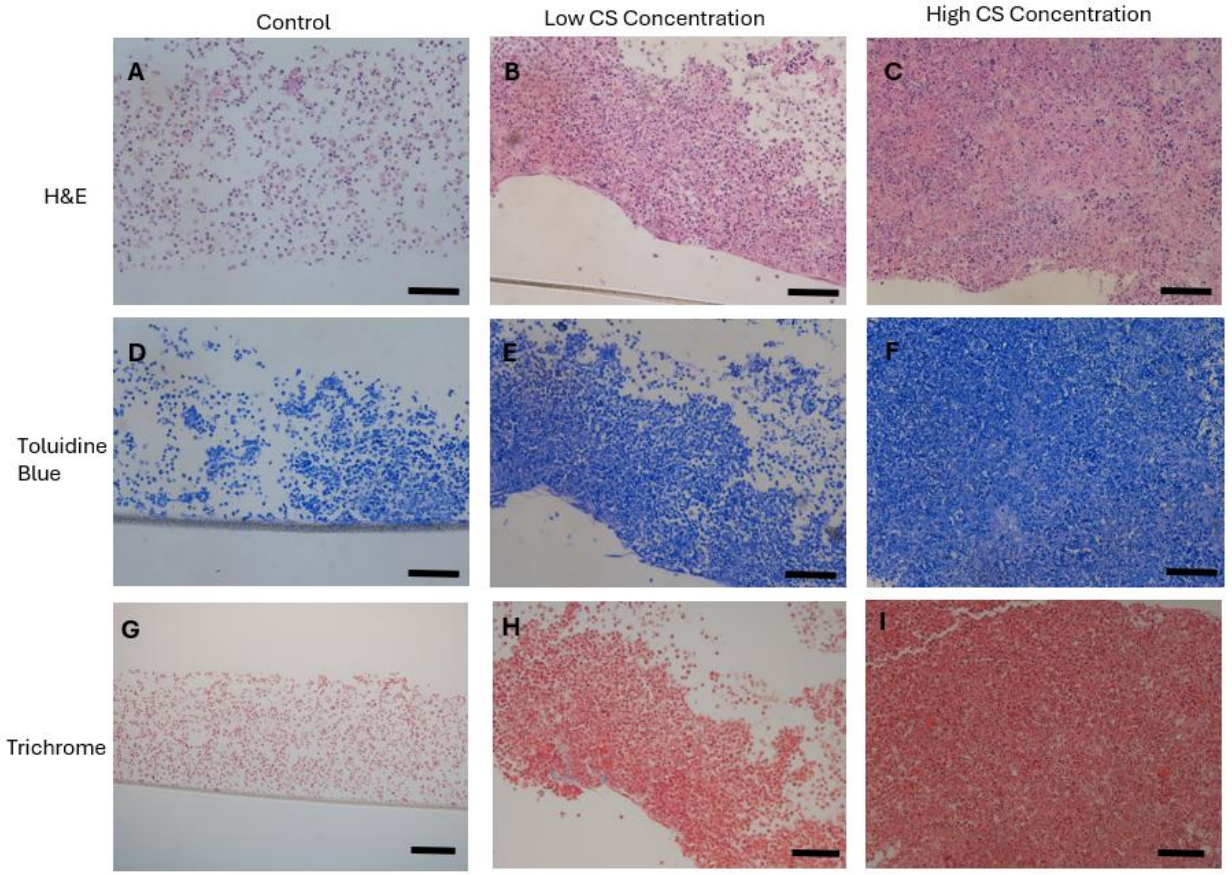

Figure 5.4 Histological imaging of chondrogenesis in the Transwell™ system with differing concentrations of CS using [A – C] H&E, [D – F] Toluidine Blue and [G – I] Trichrome. *Incorporating CS into the media enhanced the chondrogenic capability of the bBMSCs over the 6-week culture period, with this effect being more pronounced with the high CS concentration (100µg/ml) resulting in ECM formation through GAG and collagen deposition (n=3, N=3). (Scale bar = 100µm)*

5.2.2.3 Exogenous CS increased the production and deposition of type VI collagen following chondrogenic differentiation of bBMSC in the Transwell™ system

After 6-weeks in chondrogenic culture medium with and without the addition of exogenous CS, the resulting tissue was removed from the Transwell™ membrane, embedded in wax and 5µm sections prepared for immunostaining for COL-2C1 and COL-VI (figure 5.5). Correlating with the Trichrome staining observations of increased collagen deposition (figure 5.4G – I), type II collagen (COL-2C1) was evident in all of the experimental group constructs (figure 5.5A – C), however, the bBMSCs cultured in high CS concentration appeared to have a more consistent and intact ECM environment. Limited type VI collagen (COL-VI) was observed in the control constructs (figure 5.5D); however, in the presence of both low and high CS concentrations, more type VI collagen staining was seen, although some of this appeared intracellular and had not yet been secreted into the ECM (figure 5.5E – F).

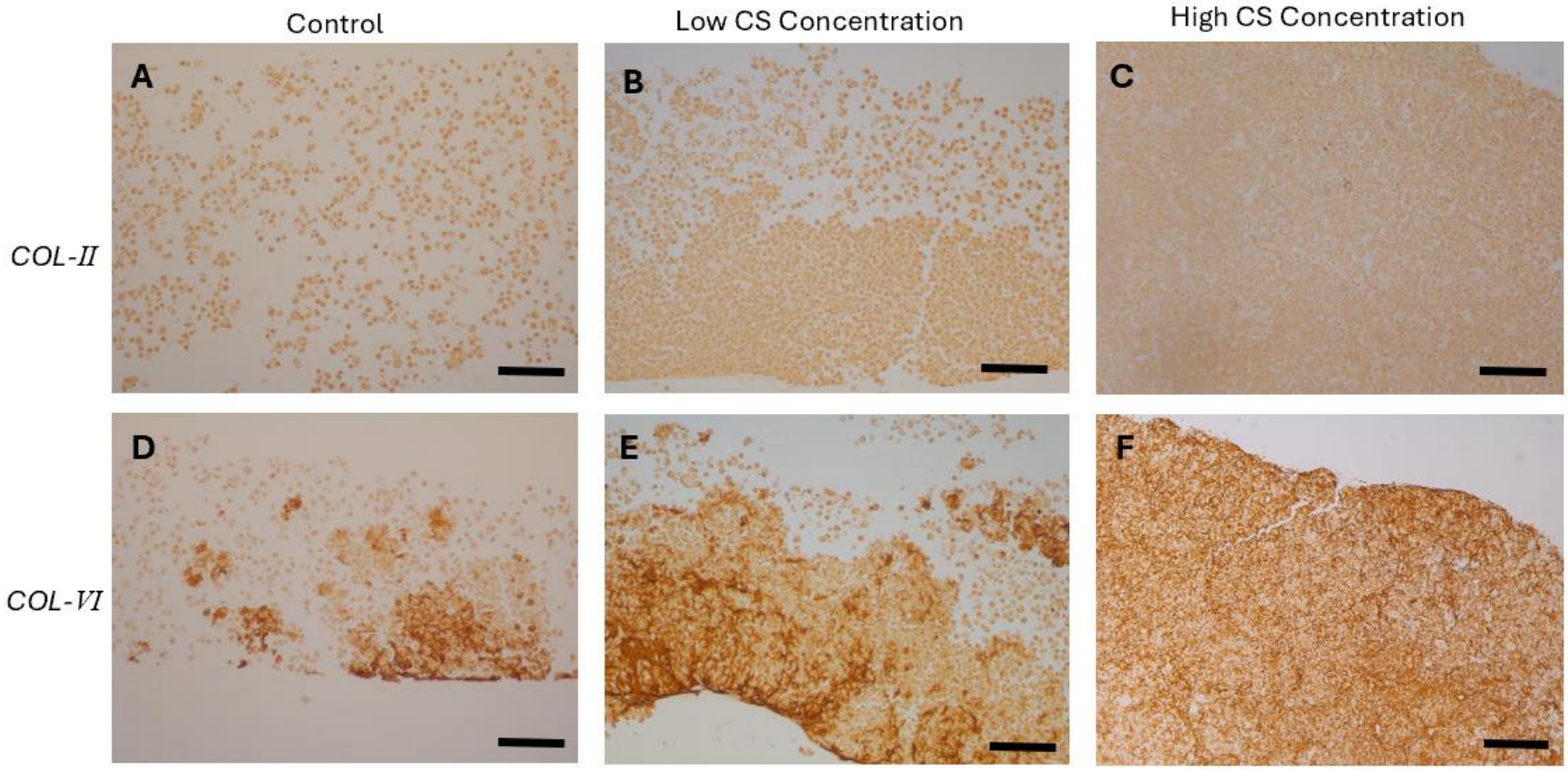

Figure 5.5 Immunohistochemical analysis of the constructs generated following chondrogenic differentiation of BMSCs in the Transwell™ system in the presence and absence of low (5µg/ml) or high CS (100µg/ml) over a 6-week period. Sections were labelled for [A – C] type II collagen (COL2-C1) and [D – F] type VI collagen. *The addition of CS into the media increased the biosynthesis and deposition of these collagens resulting in the formation of an organised ECM. (Scale bar = 100µm)*

5.2.2.4 Exogenous CS increased the production and deposition of types I and X collagen following chondrogenic differentiation of bBMSC in the Transwell™ system

In addition to types II and VI collagen (Section 5.2.2.3), the expression of types I and X collagen were also assessed to determine their distribution in the tissue constructs (Figure 5.6). Surprisingly, both collagen types were found in the control group i.e. bBMSCs cultured in chondrogenic media (Figure 5.6A, D), and this staining profile was also observed in the low (Figure 5.6B, E) and high CS concentration constructs (Figure 5.6C, F), indicating that the chondrocytes that had differentiated from the bBMSCs had begun to undergo hypertrophy.

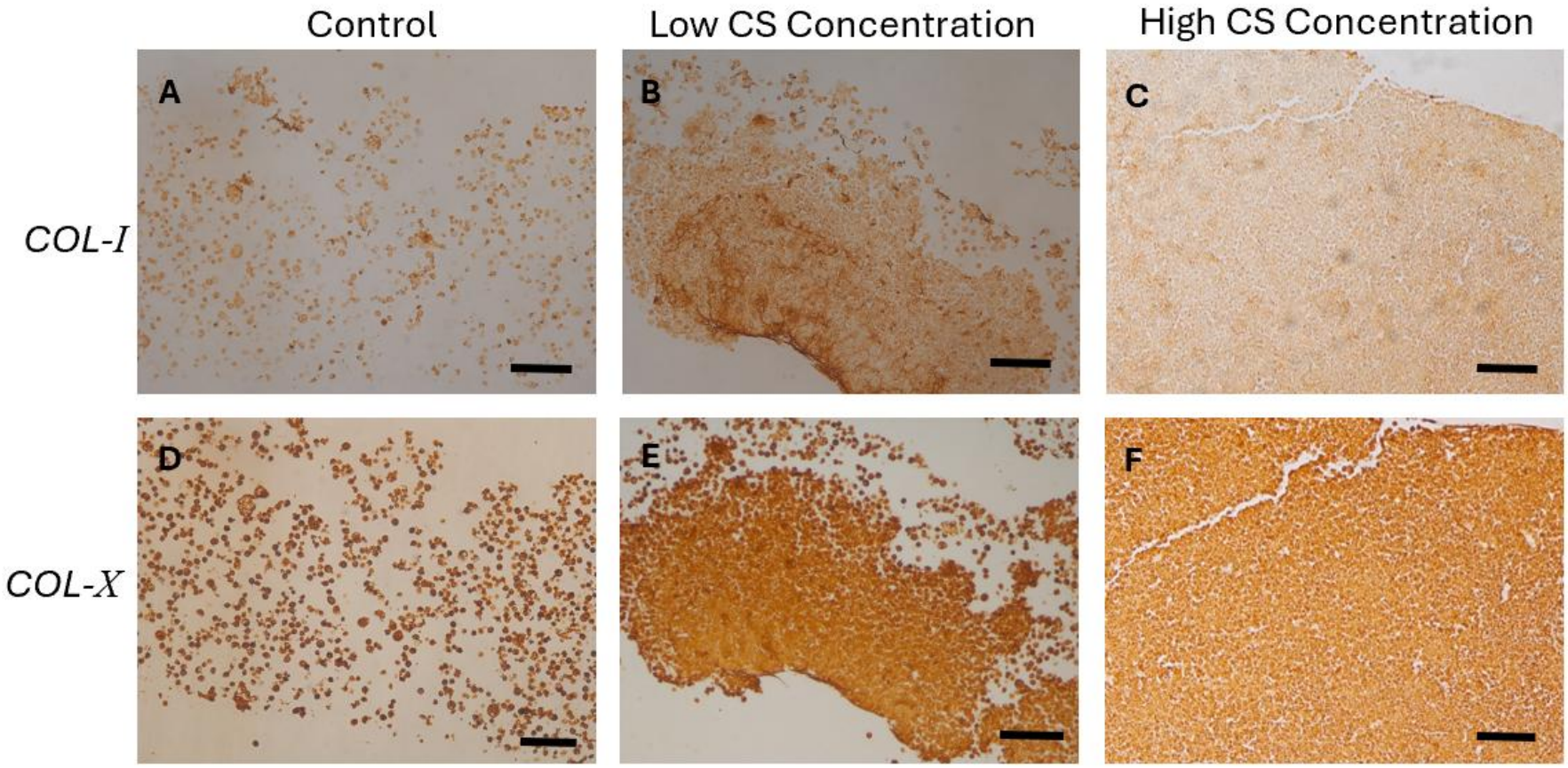

Figure 5.6 Immunohistochemical analysis of the constructs generated following chondrogenic differentiation of BMSCs in the Transwell™ system in the presence and absence of low (5µg/ml) or high CS (100µg/ml) over a 6-week period. Sections were labelled for [A – C] type I collagen and [D – F] type X collagen. *The expression of both collagen types was found in all three experimental conditions suggesting that the bBMSC-derived chondrocytes had possibly undergone hypertrophy. (Scale bar = 100µm)*

5.2.2.5 Exogenous CS increased *sox-9* mRNA levels whilst inhibiting transcription of acan following chondrogenic differentiation of bBMSCs in the Transwell™ system

The gene expression of chondrogenic markers, including *col2a1*, *sox-9* and *acan*, were determined by qRT-PCR in the bBMSCs cultured in the Transwell™ system under chondrogenic conditions for 6 weeks without (control) or with 5µg/ml CS (low) or 100µg/ml CS (high). There was no difference in the expression of *col2a1* amongst the experimental groups (Figure 5.7A). However, the addition of CS, both low (2-fold reduction, $p<0.001$) and high CS (1.33-fold reduction, $p<0.001$) depressed *acan* mRNA expression (Figure 5.7B). Interestingly, it was revealed that a high concentration of CS significantly induced *sox-9* mRNA expression (3.8-fold, $P<0.001$) compared to the control group (Figure 5.7C), an effect which was not observed when cells were treated with the low CS concentration.

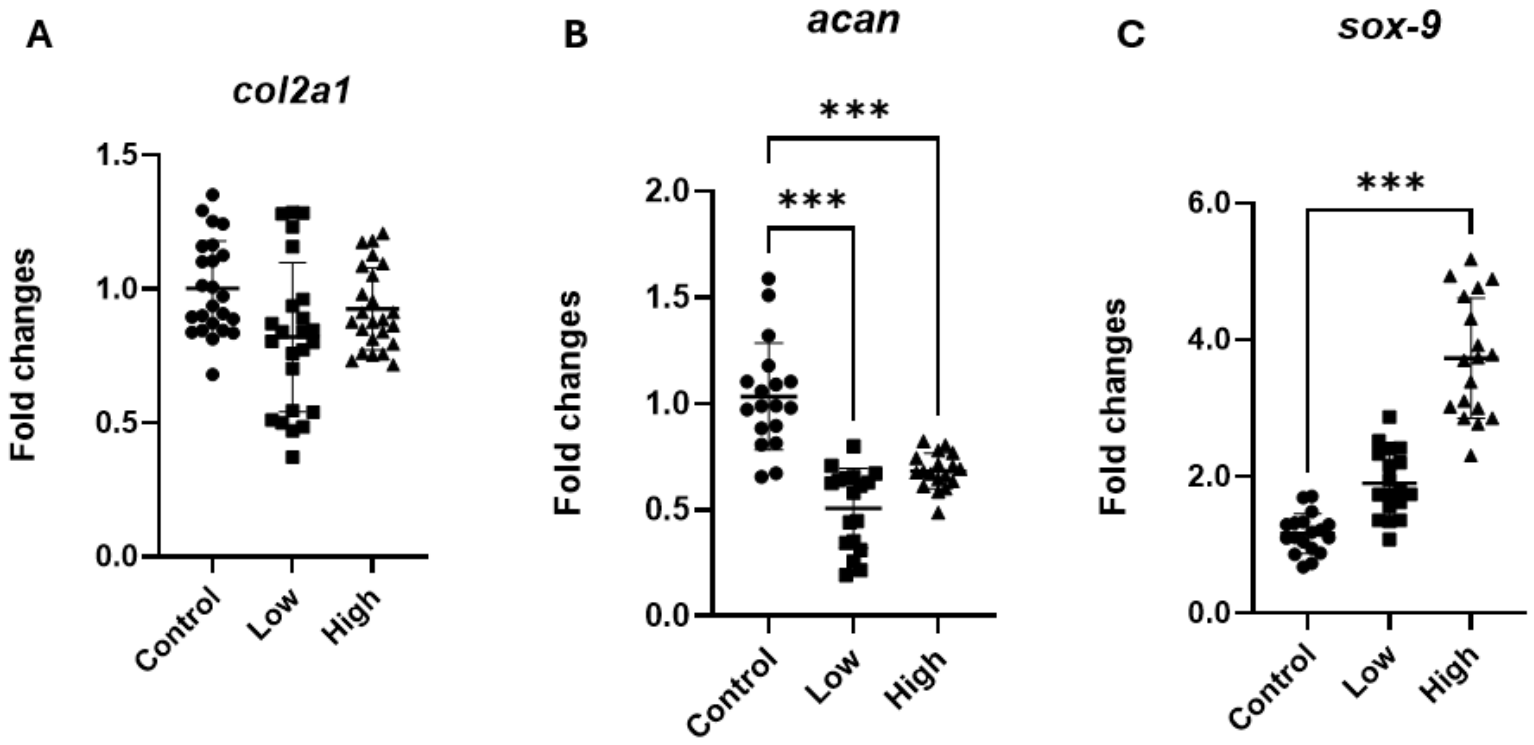

Figure 5.7 Transcript levels of chondrogenic markers expressed in bBMSCs cultured in the Transwell™ system with CS-containing medium. *qRT-PCR was used to detect the expression of* ***[A]*** *col2a1,* ***[B]*** *acan and* ***[C]*** *sox-9 mRNA levels. Data is presented as mean fold-change ± standard deviation following normalisation to the housekeeping genes and relative to the control group. Although col2a1 levels did not change, acan mRNA levels consistently decreased in both low and high CS concentrations; in contrast, high CS (100µg/ml) induced the expression of sox-9.(n=6, N=3, 1-way ANOVA) [* $p<0.05$, *** $p<0.001$].*

5.3 Discussion

The primary objective of this chapter was to investigate how the addition of purified CS into chondrogenic medium would influence chondrogenesis of bBMSCs in a 3D culture, including agarose gel and Transwell™ system, by observing the appearance of the regenerated "constructs", examining the expression of chondrogenic markers and probing for key ECM molecules present in native cartilage. The 3D agarose model did not support bBMSC viability; it is unclear why this is the case, as chondrocytes embedded into agarose remained viable over a 7-day testing window. As a consequence, the Transwell™ system was taken forward to investigate the interplay of a 3D environment with low or high CS added into the medium. The bBMSCs underwent chondrogenesis and, particularly in response to the high CS generated a 'cartilage-like' tissue which was robust to handle. Histological staining indicated the deposition of GAGs and collagen in response to CS, with increased type VI collagen following both low and high CS concentrations; however, further experiments are needed to determine the localisation of this protein as some type VI collagen appeared to be intracellular and not pericellular. Perhaps surprisingly, all experimental groups including the control (no CS) had significant types I and X collagen labelling which may reflect a more hypertrophic phenotype (see section 5.3.2)

5.3.1 Agarose hydrogel model for bBMSCs

The observation that bBMSCs encapsulated in 2% agarose hydrogel constructs and cultured in chondrogenic medium supplemented with purified CS exhibited significant cell death within 7 days provides critical insights into the limitations and challenges of this experimental setup. While the initial viability indicates some compatibility between the hydrogel environment and the BMSCs, the rapid decline in cell survival highlights potential shortcomings in the culture system that warrant further investigation. As the chondrocytes remained viable in an identical experimental set-up, it is unclear why there was a consistent and reproducible increase in cell death, but it may possibly have resulted from a lack of accessibility to the growth factors necessary to sustain BMSC growth. In a study where bBMSCs were

successfully embedded in an agarose system, the cells were cultured in 10ng/ml TGFβ1 (Connelly et al., 2009) suggesting that growth factor supplementation might have been necessary.

In vivo, bBMSCs are exposed to specific biomechanical cues defined by their stem cell niche in the bone marrow; it is possible that these *in vitro* biomechanical cues were significantly different to those experienced by the cells *in vivo* and thus the mechanical properties of the 2% agarose hydrogel were not compatible with sustaining bBMSC viability. It has been reported that stiffer gels can restrict cellular spreading, proliferation, and matrix deposition (Breuls et al., 2008), and that the lack of cell-adhesive motifs in agarose can hinder cell attachment and interaction with the surrounding ECM, further impairing cellular functions critical for survival and differentiation (Piazza et al., 2024).

To address the limitations observed in this study, several modifications to the culture system and experimental design could be considered. Reducing the agarose concentration to 1.5% or lower to create softer gels could provide a more favourable mechanical environment for bBMSCs viability and ECM production (Connelly et al., 2009) (Lee et al., 2017). Functionalizing the agarose hydrogel with cell-adhesive peptides (e.g., RGD motifs) or ECM proteins such as collagen or fibronectin could also enhance cell-matrix interactions and improve survival (Arya et al., 2019). Additionally, sustained delivery of growth factors like TGF-β_3 or IGF-1 via the hydrogel matrix may provide additional support for cell viability and chondrogenic differentiation. Alternative hydrogel systems could be utilised to optimise the chondrogenesis model (Li et al., 2024), as alternative hydrogels, such as alginate, hyaluronic acid-based systems, or composite materials, may offer improved biocompatibility and diffusion properties while retaining the structural support required for 3D cultures. The findings of this study underscore the critical role of the local microenvironment in supporting bBMSC viability and chondrogenesis in 3D culture systems, and how important it is to find a suitable hydrogel to sustain cell viability.

5.3.2 Transwell™ system for bBMSCs

As a result, BMSCs were subsequently cultured in the Transwell™ system with either 5µg/ml (low) or 100 µg/ml (high) CS supplementation. Interestingly, the high CS cultures appeared to result in 'cartilage-like' tissue which is reflected in the Trichrome histology – it can be seen that in the control group, the ECM that has developed over the 6-week culture period is loose and lacks any structural organisation. However, in the presence of CS, the matrix is more compact and organised which is more clearly evidenced in the high CS constructs. Compared to the control group, there was increased type VI collagen staining highlighting a potential role of CS in promoting chondrogenic differentiation. Type VI collagen is crucial for the organisation and stabilisation of the pericellular matrix, particularly in supporting chondrocytes or chondrocyte-like cells and facilitating the transmission of mechanical cues. Its increased presence suggests that CS facilitated the establishment of a more functional and structured ECM, which is essential for replicating the biomechanical properties of cartilage (Struijk et al., 2024).

Surprisingly, type X collagen was detected in the control and both CS-supplemented groups indicating the likely presence of hypertrophic chondrocytes. Collagen X is a marker of a late-stage chondrocyte phenotype and is often associated with terminal differentiation and hypertrophy (Struijk et al., 2024). Whilst its expression can be a natural part of chondrocyte maturation, particularly in long-term culture, its presence raises questions about the stability of the differentiated phenotype and the potential risk of hypertrophic differentiation. This phenomenon is consistent with studies suggesting that while CS promotes early chondrogenic differentiation, high concentrations or extended culture periods can lead to hypertrophic changes (Knuth et al., 2019). The bBMSC cultures were taken out to 6 weeks, thus future experiments could assess the resultant phenotype at weekly intervals to determine at which point type X collagen is expressed to better understand the process of differentiation in this model system. It underscores the need for fine-tuning CS supplementation to balance ECM production with the prevention of undesired terminal differentiation. CS did not affect the extent of type II collagen staining, and this was reflected in the unaltered *col2a1* transcripts measured at the gene level.

However, strong Toluidine Blue staining was observed in the CS-supplemented group reflecting a significant increase in sGAG content, a hallmark of cartilage-like ECM. Surprisingly, this apparent increase in GAG deposition with low and high CS supplementation was not observed at the transcript level i.e. *acan* gene expression was found to be significantly inhibited in the presence of CS. As the qRT-PCR was performed at the end of the 6-week culture period, it could be that *acan* levels had subsided by this point, and if the constructs had been sampled earlier, elevated *acan* expression might have been detected. Therefore, measuring transcript levels in a temporal manner might be more informative in determining cell behaviour over the culture period. This is particularly relevant in light of recent evidence from Naven et al. (2022), who demonstrated that the circadian clock is not inherently active in undifferentiated human embryonic stem cells, but is gradually initiated during chondrogenic differentiation. In their 3D human chondrogenesis model, the activation of core clock genes (e.g., *BMAL1*, *CLOCK*, and *PER2*) occurred progressively between day 11 and day 21 of culture, alongside robust upregulation of chondrogenic markers such as *SOX-9*, *COL2A1* and *ACAN*. These findings highlight the importance of time-resolved transcriptomic analysis to capture the dynamic regulatory events that underlie lineage commitment and matrix production, which may otherwise be overlooked in static or single time-point measurements. The control group without CS supplementation exhibited weaker ECM production and reduced staining for toluidine blue and collagen markers; this is unlikely to have been due to lower cell numbers as there was only a 4% difference in cell viability between the three groups investigated.

Collectively, the data suggests a role for CS in chondrogenesis. While the results demonstrate the benefits of CS supplementation, the presence of collagen type X highlights the need to address hypertrophic differentiation. Future studies could explore strategies to mitigate this effect. Lowering CS concentration may reduce the tendency toward hypertrophy while maintaining its chondrogenic effects. Combining CS with anti-hypertrophic agents by supplementing the medium with molecules like parathyroid hormone-related protein (PTHrP) or growth factors that inhibit hypertrophy could also improve phenotype stability (Mueller et al., 2013).

The findings of this study underscore the potential of CS supplementation to enhance ECM production during BMSC-mediated chondrogenesis, offering valuable insights

for cartilage tissue engineering. Furthermore, the use of the Transwell™ system in this context demonstrates its utility as a platform for studying chondrogenesis and the effects of biochemical supplementation on the process. These results pave the way for future studies aimed at refining culture conditions to achieve stable, high-quality cartilage tissue for regenerative medicine applications.

Summary of Findings

- bBMSCs were not viable using the 2% agarose hydrogel model.
- Within the Transwell™ system, bBMSCs cultured in chondrogenic medium containing 100µg/ml purified CS had increased *sox-9* transcript levels, whilst suppressing *acan* expression; *col2a1* transcription was unaffected
- Furthermore, type VI collagen expression was enhanced in the presence of both low and high CS concentrations
- Increased expression of type X collagen observed in all experimental groups suggests that the 6-week culture period may have tipped the cells into a pro-hypertrophic phenotype which warrants further investigation.

Chapter 6

General Discussion

6.1 Summary of Data Findings

The overall aim of this thesis was to develop and optimise a defined methodology to identify CS motifs detected by monoclonal antibodies 7D4, 6C3 and 4C3 and purify enriched populations of these native free CS chains for use in proof-of-concept studies. Specifically, to assess their use in (i) the maintenance of chondrocyte phenotype and (ii) the promotion of chondrogenesis of BMSCs with a view to determine whether the exogenous application of better characterised free CS chains could enhance cartilage repair and regeneration. This was to be achieved by extracting CS from bovine *metacarpalphalyngeal* joints and using in-house monoclonal antibodies (7D4, 6C3 and 4C3) to examine and monitor specific CS motifs through the purification process and to obtain glycol-analysis of the final products. Specifically, the CS of interest that is believed to be related to cartilage repair and regeneration, were extracted and enriched with a combination of chemical (alkaline treatment) and multiple affinity purification techniques (anion-exchange chromatography and size-exclusive chromatography) before the disaccharide composition and sulphation pattern were confirmed with relevant assays. Whilst CS epitopes were able to be probed with in-house 6C3 and 7D4 monoclonal antibodies when they were attached to PG core proteins, there was reduced detection once they were released as free CS chains most likely due to a limited ability to bind to the membrane used for Western Blotting or Dot Blotting. However, a series of targeted enzymatic digestions and downstream HPLC analysis to specific GAG subtypes confirmed the purity and disaccharide composition of the purified CS product. Furthermore, these findings were validated through the ^{1}H NMR which provided a fingerprint of hydrogen atoms in the CS structure with the spectrum peaks for N-acetyl groups, glucuronic acid and galactosamine, and also identified sulphation patterns based on chemical shift changes. These analyses enabled the characterisation of the chemical structure of the purified CS preparation, ensuring the CS culture treatment is consistently sourced for reliable reproducibility and dependable conclusions.

Once purified free CS was confirmed, increasing concentrations of CS were applied to bovine chondrocytes and BMSCs, respectively, to investigate their cellular behaviours in 2D and 3D cell culture systems; CS was either employed as a coating substrate (2D) or into free medium solution (3D). Cellular behaviours of chondrocytes

and BMSCs were evaluated through morphological, immunohistochemical and gene expression analyses for any changes to chondrogenesis or maintenance of the mature phenotype. Biocompatibility of purified CS assessed using the MTT assay indicated that changes to chondrocyte and BMSC viability and/or proliferation were relatively small (only observed for 0.1µg/ml substrate coating and 100µg/ml in solution respectively), irrespective of culture time point. However, over time, both morphological and transcriptional changes were observed: in the 2D monolayer culture, chondrocytes and BMSCs were observed to clump together forming spheroid structures, likely to produce the necessary mechanical stimuli required for survival. mRNA levels of the chondrogenic marker *sox-9* were found to be upregulated in both cell types following exogenous application of CS; this correlated with enhanced Alcian Blue staining, confirming GAG deposition in the ECM was significantly increased with CS as culture substrate. In the 3D BMSC culture model with purified CS (100µg/ml) in the medium, the expression of *sox-9* mRNA was also significantly increased compared to the equivalent control cultures, correlating with greater ECM formation over the 6-week culture.

6.2 The methodology of CS purification

The purification of CS from bovine cartilage involves a series of critical steps designed to extract, isolate, and refine the GAGs while preserving their structural integrity and ensuring a high level of purity. In this study, the methodology employed was effective in obtaining CS of sufficient purity and quality, but it also revealed challenges and areas for optimisation.

6.2.1 Advances in CS extraction and purification

Significant advances have been made in the methodologies for purifying CS from multiple sources, driven by the need for high-purity products for biomedical, pharmaceutical, and research applications. These advancements have focused on improving extraction efficiency, maintaining structural integrity, and enhancing the scalability and reproducibility of the extraction and purification processes.

6.2.1.1 Previous approaches to CS extraction methods

CS purification always starts from the chemical or enzymatic extraction of PGs, after the de-lipidation process using chloroform, methanol or acetone to remove fat from the desired CS source samples, when necessary (Nogueira et al., 2019). Some organic solvents and salts are also often used in the isolation and extraction of PGs by classic means. Sodium acetate solution is always utilised in a series of elution and extraction steps since it can solubilise the cell-matrix components in PG isolation (Boas, 1949). As for the protein contamination in the mixture, chloroform and chloroform-amyl alcohol have been successively applied with agitation until jelly precipitation no long forms (Giji and Arumugam, 2014). CPC later became a popular choice for GAG extraction due to the fact that its positively charged pyridinium ion group bind strongly to the negatively charged sulphate and carboxyl groups on CS through electrostatic attraction, leading to the formation of an insoluble CPC-CS complex that is hydrophobic and precipitates from the solution (Matsumura et al., 1963); addition of NaCl solution then enables the release of CS from the CPC-CS complex (Amagai et al., 2009). However, significant disadvantages include high solvent usage and extraction inefficiency at low concentrations.

Since the advent of producing biosynthesised enzymes, it is more prevalent in this extraction process to digest PG core protein with enzymes first before purifying the GAGs for a quick and convenient extraction. The most commonly used enzymes are papain (Gargiulo et al., 2009), pepsin (Zhao et al., 2013) and trypsin (Ürgeová and Vulganová, 2016) which facilitate degradation of the tissue and proteins within. Enzymes are deactivated by boiling the mixture, which then undergoes ethanol precipitation with ethanol saturated with sodium acetate (Volpi and Maccari, 2003). This strategy is widely used to extract GAGs from mammals (Sundaresan et al., 2018, Kim et al., 2014), fowls (Luo et al., 2002), and marine animals, including salmon (Maccari et al., 2015), tilapia (Vasconcelos Oliveira et al., 2017), octopus (Higashi et al., 2015), sea snake (Bai et al., 2018), and sea cucumber (Chen et al., 2011). The methodology has been adapted; for example, Murado et al. (2010) conducted an alkaline hydroalcoholic process with ethanol and NaOH after the enzymatic digestion for cartilage. However, not only does the enzymatic digestion require specific reaction conditions, buffers and sufficient reaction time (Maccari et al., 2015), but it also

requires post reaction heating to inactivate the enzyme (Garnjanagoonchorn et al., 2007), increasing the possibility of GAG degradation. Although enzymes can digest core proteins specifically, they are incapable of cleaving the tetra-saccharide linkage between GAGs and core proteins via serine residues so that the short peptide fragments from core protein hydrolysis may remain bound to the CS chains (Isemura and Ikenaka, 1975). Nevertheless, papain digestion is still the most commonly used method in the industrial purification of CS (Gargiulo et al., 2009).

6.2.1.2 Previous approaches to CS purification methods

After PG and subsequent GAG extraction, additional processes are commonly employed to further purify CS to achieve the desired level of purity. The philosophy of final purification is to remove other molecules and the solvent used previously, such as chloroform, ethanol, by taking advantage of size differences or differential affinities of charged constituents (Vázquez et al., 2016). Hence, a membrane with certain pore size or column filter with specific features is always required. Dialysis is the easiest and most effective process and can be flexibly inserted into the extraction process. When Li et al. (2010a) purified CS from pig laryngeal cartilage, they dialysed precipitates after ethanol precipitation to remove impurities. To achieve better dialysis outcomes, ultrafiltration-diafiltration can separate CS from other impurities by size differences and concentrate the CS in the final solution (Opdensteinen et al., 2019). Vázquez et al. (2018) carried out enzyme digestion and selective precipitation before the products were passed through a membrane of 30kDa to purify CS from blackmouth catshark cartilage. Moreover, the chromatography technologies involving ion-exchange resins are highly used in the purification of CS with the elimination of proteins and other molecules (Silva, 2006).

6.2.2 Novelty of the CS purification process developed in this thesis

The methodology developed and employed in this study represents a significant advancement in the purification of high-purity CS, addressing longstanding limitations associated with traditional enzymatic extraction methods as described above. Most commercial and laboratory-purified CS products are derived from enzymatic digestion of PGs, a process that often yields products of suboptimal purity (Volpi, 2019). These conventional methods frequently result in CS products contaminated with KS (as determined by a 5D4+ KS epitope being detected in the commercially sourced Sigma CS preparation) or residual proteins and peptides, which compromise their applicability in analysing the precise role of CS in cartilage regeneration and other biological contexts. By implementing a novel, improved protocol, this study overcomes these limitations, offering a reproducible and robust approach for obtaining structurally intact, high-purity CS suitable for detailed biochemical and functional analyses.

The innovative methodology employed in this study addresses these challenges through a carefully optimized multi-step process (Figure 3.1); this ensures both the structural integrity and purity of CS molecules as confirmed by subsequent glyco-analyses and NMR structural analysis (Chapter 3). A major innovation in this study was the use of a modified alkaline treatment for the release of CS from aggrecan core proteins. Compared to enzymatic digestion methods, the approach described here achieved superior purity and structural integrity with a purity as high as 96.47±1.90% by Chondroitinase ABC digestion. Previous studies have noted the difficulty of removing KS contamination from CS preparations (Galeotti et al., 2014). By incorporating sequential chromatographic steps, this study overcame such challenges, ensuring the isolation of pure free CS chains. NMR spectroscopy analyses confirmed the structure and sulphation pattern of the purified CS (Section 6.2.3). Furthermore, the protocol was highly reproducible, with consistent yields and purity across multiple batches extracted. Its scalability makes it suitable for both small-scale research and large-scale industrial applications. The high-purity CS obtained through this methodology has broad implications for cartilage regeneration research. By ensuring the structural and functional integrity of CS, this approach enables precise investigation of its role in chondrocyte/bBMSCs behaviours, gene expression and

ECM synthesis. Furthermore, the purified CS can be used to develop bioactive substrates or scaffolds for cartilage tissue engineering, providing a reliable platform for studying the molecular mechanisms of cartilage repair and regeneration.

6.2.3 Functional Significance of the Purified CS-4 Isoform

The ^{1}H NMR spectra demonstrated the predominant presence of CS-4 in the purified CS products highlighting its significant functional role in bovine cartilage biology (López-Senra et al., 2020) and potential therapeutic applications. The proportion of CS-4 and CS-6 has been reported to change in multiple developmental or imbalanced conditions in both human cartilage and synovial fluid samples (Henrotin et al., 2010, Bayliss et al., 1999). In adult human cartilage, CS-4 is generally the predominant form (Sauerland and Steinmeyer, 2007). CS-4, characterised by the sulphation of the 4th carbon of the N-GalNAc unit, is one of the most biologically relevant GAG isoforms in bovine cartilage, influencing both its structural properties and cellular interactions. The predominance of CS-4 in the purified products provides a valuable basis for exploring its contributions to cartilage repair and regenerative medicine.

The proportion of CS isomers in cartilage is discovered to change with ageing and physiological and pathological conditions (Bayliss et al., 1999). Lin et al. (2020b) reported that CS-4 content was markedly decreased in OA cartilage with a reduction in total CS amounts. Understanding how CS-4 perform as a biological cue in cartilage still needs further investigation, but it has been shown that its expression is important in the integrin-associated adhesion between type VI collagen and chondrocytes (Midwood and Salter, 2001); furthermore, CS-4 deficiency can accelerate the development of osteoarthritis, demonstrating importance of the interactions between CS-4 and other ECM molecules as vital for maintaining cartilage integrity and facilitating repair processes. Klüppel et al. (2005) concluded the vital role of CS-4 in chondrogenesis by mutating the gene of chondroitin-4-sulfotransferase 1 in murine embryonic stem cells; homozygous mutant mice died within hours of birth exhibiting a severe chondrodysplasia restricted to bones formed through endochondral ossification. When CS-4 expression was highly supressed, the production of CS-0 and CS-6 was also downregulated, leading to the distorted distribution of CS from the ECM to intracellular localisation patterns instead. The aberrant expression of CS-4 improved the phosphorylation of smad2 and TGF-β signalling, while the BMP-2 pathway was repressed with decreased phosphorylation of smad1, which influenced the proliferation and hypertrophy of chondrocytes. This study also confirmed the anti-

inflammatory property of CS-4: limited expression of CS-4 increased ECM disruption, apoptosis and mis-orientation of chondrocytes, which shared characteristics with OA (Klüppel et al. (2005). Therefore, the predominance of CS-4 in our purified product supports its use in tissue engineering applications aimed at replicating the native cartilage microenvironment.

6.3 Biocompatibility of CS

Purified CS preparations demonstrated excellent biocompatibility, evidenced by cell viability and proliferation, due to its natural occurrence in the ECM and its role in maintaining cartilage integrity (Kiani et al., 2002). CS-coated substrates provide a microenvironment that mimics native cartilage, supporting chondrocyte attachment and survival. When the BMSCs were cultured on the CS substrate, cell mass formation and increased cell viability were observed, likely to establish the molecular cues for themselves. These findings were corroborated by another study which demonstrated that a competitive acceptor of CS (PNPX), in the chondrogenic medium of BMSC monolayers, suppressed the formation of these cell clumps (Li et al., 2013a). The negative charge of CS was believed to facilitate interactions with cell surface receptors such as integrins, promoting adhesion and activating intracellular signalling pathways to enhance cell survival and cartilage regenerative potential (Shakibaei, 1998).

In free solution, CS interacts directly with BMSCs through cell surface receptors that drive chondrogenic differentiation, allowing for a more uniform distribution and interaction with BMSCs. The sulphated nature of CS, particularly CS-4, enhances its ability to bind and present growth factors like TGF-β, which are critical for chondrogenesis (Ai et al., 2023). By stabilising these growth factors and maintaining their bioavailability in the culture microenvironment, this contributes to the synthesis and organisation of cartilage-specific ECM components. The combination of chondrocytes and BMSCs on CS-coated substrate and CS-containing medium has been explored to leverage their complementary functions. By providing a microenvironment conducive to both cell types, CS improved the expression of

phenotypic markers and ECM deposition, enhancing the potential for cartilage regeneration.

6.4 Optimising cellular models: comparative insights on key variables

6.3.1 Cell source: comparison of chondrocyte versus BMSC

In cartilage tissue engineering, the choice of cells is one of the most critical factors in designing effective regenerative strategies. Alongside scaffolds and bioactive factors, cells form one of the three essential pillars of tissue engineering (Chan and Leong, 2008). The success of cartilage repair and regeneration depends not only on the biomaterials and biochemical cues provided but also on the capacity of cells to produce functional ECM and respond to the engineered microenvironment. Among the available cell sources, chondrocytes and BMSCs are two of the most widely studied due to their complementary roles in cartilage regeneration (Vinatier and Guicheux, 2016). Understanding the distinct behaviours of these cells, particularly their responses to CS, is crucial for optimising tissue engineering approaches.

As the primary resident cells in cartilage, chondrocytes are highly specialised for producing cartilage-specific ECM. When cultured on CS-coated surfaces in this study, chondrocytes exhibited enhanced adhesion by clumping together to maintain a spherical structure. However, they exhibit limited proliferation potential, especially *in vitro*, which may lead to their dedifferentiation and loss of cartilage-specific functionality (Zhang et al., 2021).

In contrast, BMSCs demonstrate a higher capacity for proliferation, making them an attractive alternative for large-scale applications (Kwon et al., 2018). In this thesis, a CS-coated surface also promoted the clumping and adhesion of the bBMSCs as previously reported (Li et al., 2013a). This property is critical for initiating differentiation and ECM synthesis. CS is reported to enhance their chondrogenic differentiation by interacting with growth factors like TGF-β_3, stabilising them in a bioavailable form and providing a chondro-inductive microenvironment (Du et al., 2023). These interactions activate critical signalling pathways, such as SOX-9,

driving the expression of cartilage-specific genes (Du et al., 2023). These findings are corroborated by this thesis, where addition of CS by substrate coating or supplementation in the media significantly induced *sox-9* mRNA expression in bBMSCs, supporting the role of CS in driving the chondrogenic genotype/phenotype. With their high proliferative potential and differentiation versatility, BMSCs address the scalability issues associated with chondrocytes. Their immunomodulatory properties further enhance their utility in regenerative medicine (Gupta et al., 2012).

6.3.2 Temporal comparison of cellular responses to CS

The temporal behaviours of chondrocytes and BMSCs during culture is critical for understanding their roles in cartilage tissue engineering. The dynamics of cell adhesion, proliferation, differentiation, and ECM production vary significantly between the two cell types, reflecting their inherent biological properties and responses to the culture environment. Due to the limited temporal imaging suitability of the Transwell™ system, the comparison in morphology could only be conducted based on the imaging of chondrocytes and BMSCs on the 2D CS substrate using light microscopy. In the initial phase of culture on the CS-substrate coating, chondrocytes exhibited strong adhesion to the CS, before starting to form a cell mass by clumping to form spheroidal 3D structures. However, the chondrocytes exhibited limited proliferation early in the culture due to their terminally differentiated nature. Their primary function is ECM synthesis rather than expansion, making them less suited for applications requiring rapid cell proliferation (Chen et al., 2021). By the mid-stage of culture (days 3-7), chondrocytes seeded on CS substrate actively produced cartilage-specific ECM components, such as collagen type II and aggrecan. The presence of CS in the culture environment enhances ECM production, which was highly likely achieved by providing biochemical cues that support the chondrocyte phenotype (Ahmad et al., 2025).

In comparison, the bBMSCs showed robust adhesion within the first 24-48 hours, particularly on the CS-coated surface (Grottkau et al., 2013) maintaining small, rounded, or slightly elongated morphologies. Unlike chondrocytes, BMSCs have the proliferative potential during the early stages of culture, and they can expand if

needed; however, extensive proliferation was not observed in these experiments over the culture timeframe analysed. However, similar to that observed for the chondrocytes, CS induced *sox-9* transcription and GAG deposition suggesting enhanced BMSC differentiation into chondrocytes.

6.3.3 Dimensionality matters: insight from 2D and Transwell™ systems

The culture system plays a pivotal role in influencing cell behaviours, ECM production, and the overall success of tissue engineering strategies. In this study, the performance of chondrocytes and BMSCs was evaluated in both 2D (CS-coated substrates) and Transwell™-based culture systems (CS in the chondrogenic media), offering insights into how dimensionality and environmental complexity affect cellular responses. The CS-coated substrate in 2D culture provides a simplified and reproducible platform for evaluating initial cellular responses, such as adhesion, proliferation, and early ECM formation. In this thesis, preliminary studies were performed to optimise the CS concentration required for the two cell types. In the monolayer culture system with CS-coated substrates, both the chondrocytes and BMSCs exhibited clumping behaviour, respectively. This aggregation could be attributed to the known adhesion properties of CS (Gao et al., 2014) which may support the formation of cellular clusters, particularly under conditions where cell density is high or when cells seek to mimic native tissue organisation. For BMSCs, the clumping behaviour observed in this thesis could indicate the initiation of chondrogenic differentiation, as cellular condensation is a precursor to chondrogenesis during embryonic cartilage development (DeLise et al., 2000).

The Transwell™ system provides a 3D environment that more closely mimics the native cartilage microenvironment, addressing some limitations of traditional 2D culture systems. The Transwell™ system allows BMSCs to grow in a spatially unrestricted environment, encouraging cell-cell and cell-matrix interactions similar to those in native cartilage tissue (Murdoch et al., 2007). As evidenced in this thesis, bBMSCs cultured for 6-weeks in the Transwell™ system resulted in ‘cartilage-like’ tissue when supplemented with high CS, producing an established ECM; this data supports the concept that the 3D-ness of the culture setup is critical to recapitulate the

in vivo environment, resulting in a more physiologically relevant and functionally superior matrix compared to 2D cultures (Wu et al., 2011). This is critical for cartilage regeneration, as the structural organisation of ECM significantly influences its mechanical properties, which in turn regulate BMSC chondrogenesis and chondrocyte homeostasis (Jia et al., 2023).

6.3.4 Examining environmental influences: substrate coating versus free solution approaches

The environmental context in this study where CS is presented, whether as a substrate coating or in free solution, influences the behaviour of the chondrocytes and BMSCs. When CS is immobilised on a substrate as a 2D platform, it mimics the underlying natural cartilage ECM, providing localised, static biochemical cues, directly interacting with cell surfaces to enhance adhesion and early ECM production (Roncada et al., 2022). The coating promotes direct cell adhesion and creates a stable surface that supports long-term cell attachment and ECM deposition. This spatially fixed presentation of CS ensures that cells receive consistent biochemical signals, particularly beneficial for maintaining chondrocyte phenotype and inducing early chondrogenesis in BMSCs (Begum et al., 2020). However, what it does not allow for is the 3D environment that the cells typically reside in *in vivo*. It is known that substrate stiffness also serves as a mechanical signal for the cells since cells can sense and respond to the mechanical properties of their surrounding microenvironment and convert mechanical cue into biochemical signals, which may then influence maintenance of the chondrogenic phenotype or BMSC chondrogenesis (Wu et al., 2017, Asadikorayem et al., 2024). In contrast, in the 3D system, CS acted as a soluble factor, creating a biochemical cue to improve ECM synthesis and chondrogenic marker expression (Galla et al., 2022).

Interestingly, BMSCs in both systems responded similarly to CS with enhanced ECM production and *sox-9* transcription. However, the Transwell™ system with soluble CS offers a more realistic model for studying cartilage regeneration, facilitating robust ECM production and chondrogenic differentiation in a spatially organised manner resulting in the semblance of ‘cartilage-like’ tissue, an effect not observed in the 2D

CS-coated substrate model. Furthermore, the regenerated tissue formed produced more ECM and expressed significantly higher *sox-9* (3.8-fold, $P<0.001$) as one of the most important chondrogenic gene markers. The presentation of soluble CS in the media enhances CS mobility, allowing them to bind and stabilise growth factors like TGF-β_3 to promote chondrogenesis and support the chondrocyte phenotype.

6.5 Study limitations and future directions

The successful extraction and application of free CS from bovine cartilage described in this thesis represents a significant step forward in standardising materials for use in cartilage tissue engineering approaches. Specifically, CS's roles in maintaining the chondrocyte phenotype, promoting BMSC chondrogenesis and enhancing ECM production highlight its potential as a key biomaterial for cartilage repair.

However, like any novel approach, this study faced several limitations that must be addressed to fully realise its translational potential. While this study successfully extracted high-purity free CS, the inability to detect CS epitopes using in-house monoclonal antibodies posed a challenge, with a significant amount of effort invested in trying to probe specific CS motifs for validation. Without precise epitope-level identification, it would be difficult to fully characterise the structural and functional attributes of CS, limiting the understanding of its specific interactions with chondrocytes and the ECM components. Therefore, glyco-analysis and NMR were instead applied to characterise the CS preparation which was able to successfully determine the constituents in the preparation.

Although CS demonstrated positive effects on chondrocyte adhesion and BMSC chondrogenesis, the underlying molecular mechanisms remain unclear. Published studies hypothesise a role for integrins (Wang et al., 2007), but their involvement has not been experimentally confirmed in this thesis or in the literature. CS interactions, via integrins and/or cell surface receptors, might activate downstream signalling pathways essential for cell survival and ECM production, and may suggest a mechanism to explain the enhanced *sox-9* transcription observed in this thesis. To uncover the mechanisms underlying CS's effects in adhesion and signalling (Chastney et al., 2021), future work could include conducting integrin-blocking experiments to

verify their role in CS-mediated, specifically targeting integrins known to interact with CS, e.g. integrin αvβ3 and αvβ5 involved in pro-inflammatory cytokine and MMPs expression (Jin et al., 2021), α5β1, a key fibronectin receptor, may also be influenced by CS, affecting chondrocyte adhesion and downstream signalling (Sun et al., 2016). To investigate these interactions, integrin-inhibitors could be applied to chondrocytes or bBMSCs treated with CS. Genetic approaches, such as siRNA or CRISPR knockdown (Huang et al., 2016), could also be used to selectively inhibit specific forementioned integrins and verify their role in CS-mediated effects. The functional consequences of integrin inhibition could then be assessed by measuring various downstream effects. Adhesion and spreading assays would help determine whether CS enhances cell attachment via integrin-mediated pathways (Humphries, 2001), with focal adhesion formation analysed through immunostaining of proteins like vinculin, talin, and paxillin, as well as live-cell imaging to monitor cell spreading dynamics (Owen et al., 2005).

Further investigations into downstream signalling pathways could involve assessing Focal adhesion kinase (FAK) phosphorylation, a key marker of integrin activation, as well as key intracellular pathways such as the MAPK/ERK and PI3K/Akt cascades, which regulate chondrocyte survival and ECM remodelling (Reed et al., 2021). Additionally, NF-κB activation could be monitored to determine whether CS-integrin interactions contribute to inflammatory responses (Meier-Soelch et al., 2021). To obtain a broader view of the molecular pathways influenced by CS, high-throughput transcriptomic (e.g. RNA-seq) and proteomic approaches could be employed to identify differentially regulated genes and proteins (Manzoni et al., 2018).

Cell viability was suboptimal in the agarose gel scaffolds used during the study although it has been prevalent to embed BMSCs in agarose hydrogel in cartilage repair (Wei et al., 2024, Connelly et al., 2011), The decision had to revert to the Transwell™ model. It is unclear why there was such significant BMSC cell death in the agarose, particularly as parallel experiments embedding chondrocytes demonstrated excellent cell viability. bBMSCs have been previously cultured in agarose, however the constructs utilised 1.5% agarose with a seeding density of $10x10^6$cells/ml in the presence of 10ng/ml TGF-β1 (Connelly et al., 2009). Therefore, it is clear that further optimisation is required to successfully establish this model,

including modifying cell seeding density, agarose concentration and possible addition of exogenous growth factors to support cell viability.

While *sox-9* expression was significantly upregulated, other critical chondrogenic markers such as *col2a1* and *acan* did not exhibit similar increases. For bBMSCs cultured in CS-containing Transwell™, *acan* mRNA expression was suppressed when analysed at the termination of the 6-week experiment, indicating potential inhibitory effects of the culture conditions on completion of chondrogenic differentiation; this requires further investigation to determine whether there is a temporal response of bBMSCs to the addition of CS i.e. sampling at weekly intervals would provide a greater understanding of some of the mechanistic cell behaviours as the cell undergoes differentiation. To overcome the limited expression of *col2a1* and *acan*, future studies should integrate mechanical stimulation, such as compression or dynamic loading, into culture systems to mimic the *in vivo* biomechanical environment of cartilage (Suzawa et al., 2015). Kubosch et al. (2016) reported that mechanical loading enhances hMSC chondrogenesis by activating the TGF-β signalling pathway; cyclic compression combined with surface motion significantly upregulated TGF-β1 and TGF-β3 expression and promoted chondrogenic differentiation, even in the absence of exogenous TGF-β1. Inhibition of the TGF-β type I receptor blocked these effects, confirming that mechanical stimulation drives chondrogenesis through endogenous TGF-β signalling. Furthermore, refining the biochemical conditions that the cells are seeded in e.g. inclusion of growth factor combinations such as FGF-2 (Kabiri et al., 2012) or modifying the concentration of CS applied might enhance and better support chondrogenic differentiation (Stabler et al., 2015). It would also be interesting to develop a co-culture system containing chondrocytes and BMSCs to explore potential synergistic effects in cell behaviour (Kubosch et al., 2016), replicating the *in vivo* environment.

Although the Transwell™ system supported BMSC differentiation into cartilage-like tissue, the resulting constructs did not consistently form cohesive plug-shaped cartilage tissue. Additionally, the internal organisation of the tissue differed significantly from native cartilage with inconsistent ECM deposition, suggesting that the culture conditions require further optimisation to achieve functional cartilage formation. To improve tissue morphology and function in the Transwell™ system,

future directions should include optimising the cell-seeding density and distribution to ensure uniform tissue formation (Bornes et al., 2016). It was observed on some Transwell™ inserts that the tissue-like structure that formed showed interruptions across the full width (Figure 7.1). The edges appeared to cling along the culture well walls, likely due to mechanical disruption. It is likely that during medium changes, the force of the liquid flow may have caused damage to the forming tissue before it was fully 'developed', compromising its integrity. This highlights the need for gentler handling or optimised medium exchange techniques to preserve structural continuity, hence advocating for the use of dynamic bioreactor systems that provide mechanical cues and dynamic nutrient exchange simultaneously (Ruiter et al., 2023), hence, the CS translational potential to bBMSCs chondrogenesis and cartilage regeneration can be further determined.

6.6 Conclusion

In this thesis, the aim was to explore and optimise a methodology to purify free CS chain molecules from bovine articular cartilage with the intention of assessing its influence on maintenance of the chondrocyte phenotype and chondrogenic differentiation of BMSCs. The thesis demonstrates a refined methodological pipeline to successfully extract and purify high-quality CS which was predominantly the CS-4 isoform. Application of the purified CS preparation to chondrocytes and BMSCs seeded as monolayers revealed that it enhances ECM deposition and promotes *sox-9* expression in both cell types on CS-coated substrate. The purified CS preparation also improved *sox-9* gene expression, in conjunction with more ECM production, in BMSCs cultured in the Transwell™ system. The work described here reports the promising role of pure CS products in regenerative medicine and cartilage tissue engineering, where CS positively functions as a biochemical cue to facilitate chondrogenic behaviours.

Appendix

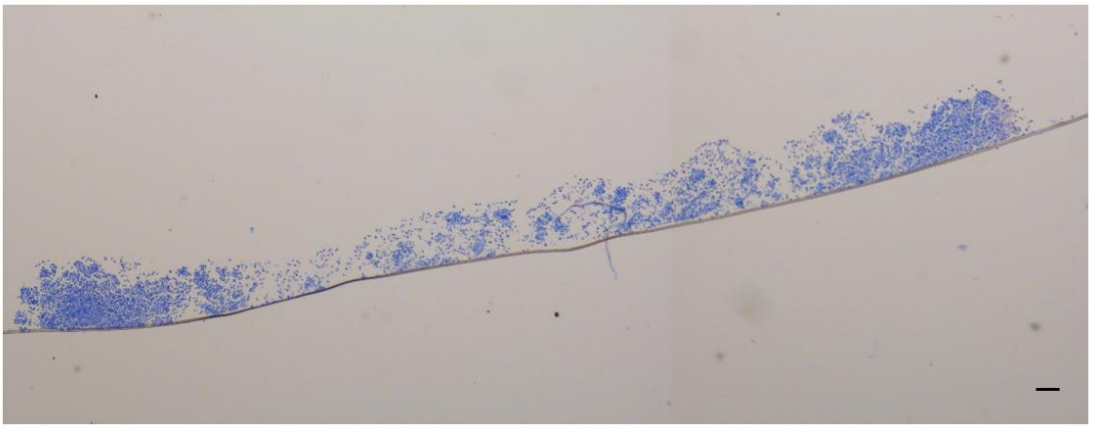

Figure 7.1 Toluidine Blue staining for a control well on Transwell system. *After 6-week differentiation culture, the imaging reported BMSCs were not able to form a full depth and width like-tissue with the interruption in the middle. The cells at the edge set together and showed a tendency to cling along the sidewall of the insert (n=3, N=3, scale bar=100μm).*

References

Ahmad, S. M.,Hameed, H.,Al-Hussain, S. A.,Khan, M. A.,Tariq, U.,Paiva-Santos, A. C.,Irfan, A. and Zaki, M. E. A. 2025. Chondroitin sulfate: An ideal biomaterial based scaffolds for cartilage regeneration and its therapeutic potential. *Carbohydrate Polymer Technologies and Applications,* 10**,** 100742, https://doi.org/https://doi.org/10.1016/j.carpta.2025.100742

Ai, C.,Liu, L.,Wong, K.,Tan, X. H. and Goh, J. C. H. 2023. The effect of chondroitin sulfate concentration and matrix stiffness on chondrogenic differentiation of mesenchymal stem cells. *Biomater Sci,* 11**,** 4557-4573, https://doi.org/10.1039/d2bm01980a

Aigner, T.,Gebhard, P. M.,Schmid, E.,Bau, B.,Harley, V. and Pöschl, E. 2003. SOX9 expression does not correlate with type II collagen expression in adult articular chondrocytes. *Matrix Biol,* 22**,** 363-72, https://doi.org/10.1016/s0945-053x(03)00049-0

Alcaide-Ruggiero, L.,Cugat, R. and Domínguez, J. M. 2023. Proteoglycans in Articular Cartilage and Their Contribution to Chondral Injury and Repair Mechanisms. *Int J Mol Sci,* 24, https://doi.org/10.3390/ijms241310824

Alcaide-Ruggiero, L.,Molina-Hernández, V.,Granados, M. M. and Domínguez, J. M. 2021. Main and Minor Types of Collagens in the Articular Cartilage: The Role of Collagens in Repair Tissue Evaluation in Chondral Defects. *Int J Mol Sci,* 22, https://doi.org/10.3390/ijms222413329

Amagai, I.,Tashiro, Y. and Ogawa, H. 2009. Improvement of the extraction procedure for hyaluronan from fish eyeball and the molecular characterization. *Fisheries Science,* 75**,** 805-810, https://doi.org/10.1007/s12562-009-0092-2

An, H.,Liu, Y.,Yi, J.,Xie, H.,Li, C.,Wang, X. and Chai, W. 2022. Research progress of cartilage lubrication and biomimetic cartilage lubrication materials. 10, https://doi.org/10.3389/fbioe.2022.1012653

Anstaett, O. L.,Brownlie, J.,Collins, M. E. and Thomas, C. J. 2010. Validation of endogenous reference genes for RT-qPCR normalisation in bovine lymphoid cells (BL-3) infected with Bovine Viral Diarrhoea Virus (BVDV). *Vet Immunol Immunopathol,* 137**,** 201-7, https://doi.org/10.1016/j.vetimm.2010.05.006

Arya, N.,Forget, A.,Sarem, M. and Shastri, V. P. 2019. RGDSP functionalized carboxylated agarose as extrudable carriers for chondrocyte delivery. *Mater Sci Eng C Mater Biol Appl,* 99**,** 103-111, https://doi.org/10.1016/j.msec.2019.01.080

Asadikorayem, M.,Brunel, L. G.,Weber, P.,Heilshorn, S. C. and Zenobi-Wong, M. 2024. Porosity dominates over microgel stiffness for promoting

chondrogenesis in zwitterionic granular hydrogels. *Biomater Sci,* 12**,** 5504-5520, https://doi.org/10.1039/d4bm00233d

Ashworth, S.,Harrington, J.,Hammond, G. M.,Bains, K. K.,Koudouna, E.,Hayes, A. J.,Ralphs, J. R.,Regini, J. W.,Young, R. D.,Hayashi, R.,Nishida, K.,Hughes, C. E. and Quantock, A. J. 2021. Chondroitin Sulfate as a Potential Modulator of the Stem Cell Niche in Cornea. 8, https://doi.org/10.3389/fcell.2020.567358

Aspden, R. M. and Hukins, D. W. 1989. Stress in collagen fibrils of articular cartilage calculated from their measured orientations. *Matrix,* 9**,** 486-8, https://doi.org/10.1016/s0934-8832(11)80018-1

Bai, M.,Han, W.,Zhao, X.,Wang, Q.,Gao, Y. and Deng, S. 2018. Glycosaminoglycans from a Sea Snake (Lapemis curtus): Extraction, Structural Characterization and Antioxidant Activity. *Mar Drugs,* 16, https://doi.org/10.3390/md16050170

Bains, K. K.,Ashworth, S.,Koudouna, E.,Young, R. D.,Hughes, C. E. and Quantock, A. J. 2023. Chondroitin Sulphate/Dermatan Sulphate Proteoglycans: Potential Regulators of Corneal Stem/Progenitor Cell Phenotype In Vitro. *Int J Mol Sci,* 24, https://doi.org/10.3390/ijms24032095

Barreto, G.,Senturk, B.,Colombo, L.,Brück, O.,Neidenbach, P.,Salzmann, G.,Zenobi-Wong, M. and Rottmar, M. 2020. Lumican is upregulated in osteoarthritis and contributes to TLR4-induced pro-inflammatory activation of cartilage degradation and macrophage polarization. *Osteoarthritis and Cartilage,* 28**,** 92-101, https://doi.org/https://doi.org/10.1016/j.joca.2019.10.011

Barreto, G.,Senturk, B.,Colombo, L.,Neidenbach, P.,Salzmann, G.,Rottmar, M. and Zenobi-Wong, M. 2018. O006 Lumican: a novel gycoprotein mediating inflammation in osteoarthritis. 77**,** A3-A4, https://doi.org/10.1136/annrheumdis-2018-EWRR2018.6 %J Annals of the Rheumatic Diseases

Barreto, G.,Soininen, A.,Ylinen, P.,Sandelin, J.,Konttinen, Y. T.,Nordström, D. C. and Eklund, K. K. 2015. Soluble biglycan: a potential mediator of cartilage degradation in osteoarthritis. *Arthritis Res Ther,* 17**,** 379, https://doi.org/10.1186/s13075-015-0902-0

Bautch, J. C.,Clayton, M. K.,Chu, Q. and Johnson, K. A. 2000. Synovial fluid chondroitin sulphate epitopes 3B3 and 7D4, and glycosaminoglycan in human knee osteoarthritis after exercise. *Annals of the Rheumatic Diseases,* 59**,** 887-891, https://doi.org/https://doi.org/10.1136/ard.59.11.887

Bayliss, M. T.,Howat, S.,Davidson, C. and Dudhia, J. 2000. The Organization of Aggrecan in Human Articular Cartilage: EVIDENCE FOR AGE-RELATED CHANGES IN THE RATE OF AGGREGATION OF NEWLY SYNTHESIZED MOLECULES*. *Journal of Biological Chemistry,* 275**,** 6321-6327, https://doi.org/https://doi.org/10.1074/jbc.275.9.6321

Bayliss, M. T.,Osborne, D.,Woodhouse, S. and Davidson, C. 1999. Sulfation of Chondroitin Sulfate in Human Articular Cartilage: THE EFFECT OF AGE,

TOPOGRAPHICAL POSITION, AND ZONE OF CARTILAGE ON TISSUE COMPOSITION*. *Journal of Biological Chemistry,* 274**,** 15892-15900, https://doi.org/https://doi.org/10.1074/jbc.274.22.15892

Bedini, E.,Corsaro, M. M.,Fernández-Mayoralas, A. and Iadonisi, A. 2019. Chondroitin, Dermatan, Heparan, and Keratan Sulfate: Structure and Functions. *In:* Cohen, E. & Merzendorfer, H. eds. *Extracellular Sugar-Based Biopolymers Matrices.* Cham: Springer International Publishing.

Begum, R.,Perriman, A. W.,Su, B.,Scarpa, F. and Kafienah, W. 2020. Chondroinduction of Mesenchymal Stem Cells on Cellulose-Silk Composite Nanofibrous Substrates: The Role of Substrate Elasticity. 8, https://doi.org/10.3389/fbioe.2020.00197

Behere, I.,Vaidya, A. and Ingavle, G. 2024. Chondroitin Sulfate and Hyaluronic Acid-Based PolyHIPE Scaffolds for Improved Osteogenesis and Chondrogenesis In Vitro. *ACS Appl Bio Mater,* 7**,** 5222-5236, https://doi.org/10.1021/acsabm.4c00393

Ben-David, U. and Benvenisty, N. 2011. The tumorigenicity of human embryonic and induced pluripotent stem cells. *Nature Reviews Cancer,* 11**,** 268-277, https://doi.org/10.1038/nrc3034

Bertolotto, A.,Agresti, C.,Castello, A.,Manzardo, E. and Riccio, A. 1998. 5D4 keratan sulfate epitope identifies a subset of ramified microglia in normal central nervous system parenchyma. *J Neuroimmunol,* 85**,** 69-77, https://doi.org/10.1016/s0165-5728(97)00251-8

Bertula, K.,Martikainen, L.,Munne, P.,Hietala, S.,Klefström, J.,Ikkala, O. and Nonappa. 2019. Strain-Stiffening of Agarose Gels. *ACS Macro Letters,* 8**,** 670-675, https://doi.org/10.1021/acsmacrolett.9b00258

Bhosale, A. M. and Richardson, J. B. 2008. Articular cartilage: structure, injuries and review of management. *Br Med Bull,* 87**,** 77-95, https://doi.org/10.1093/bmb/ldn025

Bienkowski, M. J. and Conrad, H. E. 1984. Kinetics of proteoheparan sulfate synthesis, secretion, endocytosis, and catabolism by a hepatocyte cell line. *J Biol Chem,* 259**,** 12989-96,

Bishnoi, M.,Jain, A.,Hurkat, P. and Jain, S. K. 2016. Chondroitin sulphate: a focus on osteoarthritis. *Glycoconj J,* 33**,** 693-705, https://doi.org/10.1007/s10719-016-9665-3

Blain, E. J.,Mason, D. J. and Duance, V. C. 2003. The effect of cyclical compressive loading on gene expression in articular cartilage. *Biorheology,* 40**,** 111-7,

Boas, N. F. 1949. Isolation of hyaluronic acid from the cock's comb. *J Biol Chem,* 181**,** 573-5,

Bonnet, D. 2003. Biology of human bone marrow stem cells. *Clin Exp Med,* 3**,** 140-9, https://doi.org/10.1007/s10238-003-0017-9

Bornes, T. D.,Jomha, N. M.,Mulet-Sierra, A. and Adesida, A. B. 2016. Optimal Seeding Densities for In Vitro Chondrogenesis of Two- and Three-Dimensional-Isolated and -Expanded Bone Marrow-Derived Mesenchymal Stromal Stem Cells Within a Porous Collagen Scaffold. *Tissue Eng Part C Methods,* 22**,** 208-20, https://doi.org/10.1089/ten.TEC.2015.0365

Bouffi, C.,Bony, C.,Courties, G.,Jorgensen, C. and Noël, D. 2010. IL-6-dependent PGE2 secretion by mesenchymal stem cells inhibits local inflammation in experimental arthritis. *PLoS One,* 5**,** e14247, https://doi.org/10.1371/journal.pone.0014247

Breuls, R. G.,Jiya, T. U. and Smit, T. H. 2008. Scaffold stiffness influences cell behavior: opportunities for skeletal tissue engineering. *Open Orthop J,* 2**,** 103-9, https://doi.org/10.2174/1874325000802010103

Brézillon, S.,Pietraszek, K.,Maquart, F. X. and Wegrowski, Y. 2013. Lumican effects in the control of tumour progression and their links with metalloproteinases and integrins. *Febs j,* 280**,** 2369-81, https://doi.org/10.1111/febs.12210

Brito, R.,Costa, D.,Dias, C.,Cruz, P. and Barros, P. 2023. Chondroitin Sulfate Supplements for Osteoarthritis: A Critical Review. *Cureus,* 15**,** e40192, https://doi.org/10.7759/cureus.40192

Brown, G. M.,Huckerby, T. N.,Abram, B. L. and Nieduszynski, I. A. 1996. Characterization of a non-reducing terminal fragment from bovine articular cartilage keratan sulphates containing alpha(2-3)-linked sialic acid and alpha(1-3)-linked fucose. A sulphated variant of the VIM-2 epitope. *Biochem J,* 319 (Pt 1)**,** 137-41, https://doi.org/10.1042/bj3190137

Bruyère, O.,Honvo, G.,Veronese, N.,Arden, N. K.,Branco, J.,Curtis, E. M.,Al-Daghri, N. M.,Herrero-Beaumont, G.,Martel-Pelletier, J.,Pelletier, J. P.,Rannou, F.,Rizzoli, R.,Roth, R.,Uebelhart, D.,Cooper, C. and Reginster, J. Y. 2019. An updated algorithm recommendation for the management of knee osteoarthritis from the European Society for Clinical and Economic Aspects of Osteoporosis, Osteoarthritis and Musculoskeletal Diseases (ESCEO). *Semin Arthritis Rheum,* 49**,** 337-350, https://doi.org/10.1016/j.semarthrit.2019.04.008

Burton-Wurster, N.,Liu, W.,Matthews, G. L.,Lust, G.,Roughley, P. J.,Glant, T. T. and Cs-Szabó, G. 2003. TGF beta 1 and biglycan, decorin, and fibromodulin metabolism in canine cartilage. *Osteoarthritis and Cartilage,* 11**,** 167-176, https://doi.org/https://doi.org/10.1053/S1063-4584(02)00349-7

Cai, L.,Liu, W.,Cui, Y.,Liu, Y.,Du, W.,Zheng, L.,Pi, C.,Zhang, D.,Xie, J. and Zhou, X. 2020. Biomaterial Stiffness Guides Cross-talk between Chondrocytes: Implications for a Novel Cellular Response in Cartilage Tissue Engineering. *ACS Biomater Sci Eng,* 6**,** 4476-4489, https://doi.org/10.1021/acsbiomaterials.0c00367

Campo, G. M.,Avenoso, A.,Campo, S.,D'Ascola, A.,Traina, P. and Calatroni, A. 2008. Chondroitin-4-sulphate inhibits NF-kB translocation and caspase activation in collagen-induced arthritis in mice. *Osteoarthritis Cartilage,* 16**,** 1474-83, https://doi.org/10.1016/j.joca.2008.04.002

Candela, M. E.,Yasuhara, R.,Iwamoto, M. and Enomoto-Iwamoto, M. 2014. Resident mesenchymal progenitors of articular cartilage. *Matrix Biol,* 39**,** 44-9, https://doi.org/10.1016/j.matbio.2014.08.015

Caterson, B. 2012. Fell-Muir Lecture: chondroitin sulphate glycosaminoglycans: fun for some and confusion for others. *Int J Exp Pathol,* 93**,** 1-10, https://doi.org/10.1111/j.1365-2613.2011.00807.x

Caterson, B.,Christner, J. E. and Baker, J. R. 1983. Identification of a monoclonal antibody that specifically recognizes corneal and skeletal keratan sulfate. Monoclonal antibodies to cartilage proteoglycan. *J Biol Chem,* 258**,** 8848-54,

Caterson, B.,Flannery, C. R.,Hughes, C. E. and Little, C. B. 2000. Mechanisms involved in cartilage proteoglycan catabolism. *Matrix Biology,* 19**,** 333-344, https://doi.org/10.1016/S0945-053X(00)00078-0

Caterson, B.,Griffin, J.,Mahmoodian, F. and Sorrell, J. M. 1990a. Monoclonal antibodies against chondroitin sulphate isomers: their use as probes for investigating proteoglycan metabolism. *Biochem Soc Trans,* 18**,** 820-3, https://doi.org/10.1042/bst0180820

Caterson, B.,Mahmoodian, F.,Sorrell, J. M.,Hardingham, T. E.,Bayliss, M. T.,Carney, S. L.,Ratcliffe, A. and Muir, H. 1990b. Modulation of native chondroitin sulphate structure in tissue development and in disease. *Journal of Cell Science,* 97**,** 411-417, https://doi.org/10.1242/jcs.97.3.411 %J Journal of Cell Science

Caterson, B.,Mahmoodian, F.,Sorrell, J. M.,Hardingham, T. E.,Bayliss, M. T.,Carney, S. L.,Ratcliffe, A. and Muir, H. 1990c. Modulation of native chondroitin sulphate structure in tissue development and in disease. *J Cell Sci,* 97 (Pt 3)**,** 411-7,

Caterson, B. and Melrose, J. 2018. Keratan sulfate, a complex glycosaminoglycan with unique functional capability. *Glycobiology,* 28**,** 182-206, https://doi.org/10.1093/glycob/cwy003

Cavalcante, F. S.,Ito, S.,Brewer, K.,Sakai, H.,Alencar, A. M.,Almeida, M. P.,Andrade, J. S., Jr.,Majumdar, A.,Ingenito, E. P. and Suki, B. 2005. Mechanical interactions between collagen and proteoglycans: implications for the stability of lung tissue. *J Appl Physiol (1985),* 98**,** 672-9, https://doi.org/10.1152/japplphysiol.00619.2004

Chadda, K. R. and Puthucheary, Z. 2024. Persistent inflammation, immunosuppression, and catabolism syndrome (PICS): a review of definitions, potential therapies, and research priorities. *British Journal of Anaesthesia,* 132**,** 507-518, https://doi.org/https://doi.org/10.1016/j.bja.2023.11.052

Chan, B. P. and Leong, K. W. 2008. Scaffolding in tissue engineering: general approaches and tissue-specific considerations. *Eur Spine J,* 17 Suppl 4**,** 467-79, https://doi.org/10.1007/s00586-008-0745-3

Chang, Y.,Yanagishita, M.,Hascall, V. C. and Wight, T. N. 1983. Proteoglycans synthesized by smooth muscle cells derived from monkey (Macaca nemestrina) aorta. *J Biol Chem,* 258**,** 5679-88,

Chang, Y. H.,Wu, K. C. and Ding, D. C. 2020. Induced Pluripotent Stem Cell-Differentiated Chondrocytes Repair Cartilage Defect in a Rabbit Osteoarthritis Model. *Stem Cells Int,* 2020**,** 8867349, https://doi.org/10.1155/2020/8867349

Charlier, E.,Deroyer, C.,Ciregia, F.,Malaise, O.,Neuville, S.,Plener, Z.,Malaise, M. and de Seny, D. 2019. Chondrocyte dedifferentiation and osteoarthritis (OA). *Biochem Pharmacol,* 165**,** 49-65, https://doi.org/10.1016/j.bcp.2019.02.036

Chastney, M. R.,Conway, J. R. W. and Ivaska, J. 2021. Integrin adhesion complexes. *Current Biology,* 31**,** R536-R542, https://doi.org/https://doi.org/10.1016/j.cub.2021.01.038

Chen, H.,Tan, X. N.,Hu, S.,Liu, R. Q.,Peng, L. H.,Li, Y. M. and Wu, P. 2021. Molecular Mechanisms of Chondrocyte Proliferation and Differentiation. *Front Cell Dev Biol,* 9**,** 664168, https://doi.org/10.3389/fcell.2021.664168

Chen, S. and Birk, D. E. 2013. The regulatory roles of small leucine-rich proteoglycans in extracellular matrix assembly. *Febs j,* 280**,** 2120-37, https://doi.org/10.1111/febs.12136

Chen, S.,Xue, C.,Yin, L. a.,Tang, Q.,Yu, G. and Chai, W. 2011. Comparison of structures and anticoagulant activities of fucosylated chondroitin sulfates from different sea cucumbers. *Carbohydrate Polymers,* 83**,** 688-696, https://doi.org/https://doi.org/10.1016/j.carbpol.2010.08.040

Chen, Z.,Wei, J.,Zhu, J.,Liu, W.,Cui, J.,Li, H. and Chen, F. 2016. Chm-1 gene-modified bone marrow mesenchymal stem cells maintain the chondrogenic phenotype of tissue-engineered cartilage. *Stem Cell Res Ther,* 7**,** 70, https://doi.org/10.1186/s13287-016-0328-x

Chery, D. R.,Han, B.,Zhou, Y.,Wang, C.,Adams, S. M.,Chandrasekaran, P.,Kwok, B.,Heo, S.-J.,Enomoto-Iwamoto, M.,Lu, X. L.,Kong, D.,Iozzo, R. V.,Birk, D. E.,Mauck, R. L. and Han, L. 2021. Decorin regulates cartilage pericellular matrix micromechanobiology. *Matrix Biology,* 96**,** 1-17, https://doi.org/https://doi.org/10.1016/j.matbio.2020.11.002

Cho, S. Y.,Sim, J. S.,Jeong, C. S.,Chang, S. Y.,Choi, D. W.,Toida, T. and Kim, Y. S. 2004. Effects of low molecular weight chondroitin sulfate on type II collagen-induced arthritis in DBA/1J mice. *Biol Pharm Bull,* 27**,** 47-51, https://doi.org/10.1248/bpb.27.47

Chu, Y.-Y.,Hikita, A.,Asawa, Y. and Hoshi, K. 2024. Advancements in Chondrocyte 3-Dimensional Embedded Culture: Implications for Tissue Engineering and

Regenerative Medicine. *Biomedical Journal*, 100786, https://doi.org/https://doi.org/10.1016/j.bj.2024.100786

Chung, C. and Burdick, J. A. 2008. Engineering cartilage tissue. *Adv Drug Deliv Rev,* 60, 243-62, https://doi.org/10.1016/j.addr.2007.08.027

Chung, H. H.,Mireles, M.,Kwarta, B. J. and Gaborski, T. R. 2018. Use of porous membranes in tissue barrier and co-culture models. *Lab Chip,* 18, 1671-1689, https://doi.org/10.1039/c7lc01248a

Ciapetti, G.,Cenni, E.,Pratelli, L. and Pizzoferrato, A. 1993. In vitro evaluation of cell/biomaterial interaction by MTT assay. *Biomaterials,* 14, 359-64, https://doi.org/10.1016/0142-9612(93)90055-7

Cleland, R. L. and Sherblom, A. P. 1977. Isolation and physical characterization of hyaluronic acid prepared from bovine nasal septum by cetylpyridinium chloride precipitation. *Journal of Biological Chemistry,* 252, 420-426, https://doi.org/https://doi.org/10.1016/S0021-9258(17)32732-1

Coleman, R. M.,Case, N. D. and Guldberg, R. E. 2007. Hydrogel effects on bone marrow stromal cell response to chondrogenic growth factors. *Biomaterials,* 28, 2077-2086, https://doi.org/https://doi.org/10.1016/j.biomaterials.2007.01.010

Collin, E. C.,Carroll, O.,Kilcoyne, M.,Peroglio, M.,See, E.,Hendig, D.,Alini, M.,Grad, S. and Pandit, A. 2017. Ageing affects chondroitin sulfates and their synthetic enzymes in the intervertebral disc. *Signal Transduct Target Ther,* 2, 17049, https://doi.org/10.1038/sigtrans.2017.49

Connelly, J. T.,Petrie, T. A.,García, A. J. and Levenston, M. E. 2011. Fibronectin- and collagen-mimetic ligands regulate bone marrow stromal cell chondrogenesis in three-dimensional hydrogels. *Eur Cell Mater,* 22, 168-76; discussion 176-7, https://doi.org/10.22203/ecm.v022a13

Conrad, H. E. 1995. β-Elimination for Release of O-Linked Glycosaminoglycans from Proteoglycans. 31, 17.15.1-17.15.3, https://doi.org/https://doi.org/10.1002/0471142727.mb1715as31

Conrad, H. E. 2001. Beta-elimination for release of O-linked glycosaminoglycans from proteoglycans. *Curr Protoc Mol Biol,* Chapter 17, Unit17.15A, https://doi.org/10.1002/0471142727.mb1715as31

Corano Scheri, K.,Hsieh, Y. W.,Jeong, E. and Fawzi, A. A. 2023. Limited Hyperoxia-Induced Proliferative Retinopathy (LHIPR) as a Model of Retinal Fibrosis, Angiogenesis, and Inflammation. *Cells,* 12, https://doi.org/10.3390/cells12202468

Corradetti, B.,Taraballi, F.,Minardi, S.,Van Eps, J.,Cabrera, F.,Francis, L. W.,Gazze, S. A.,Ferrari, M.,Weiner, B. K. and Tasciotti, E. 2016. Chondroitin Sulfate Immobilized on a Biomimetic Scaffold Modulates Inflammation While

Driving Chondrogenesis. *Stem Cells Transl Med,* 5**,** 670-82, https://doi.org/10.5966/sctm.2015-0233

Cortes, M.,Baria, A. T. and Schwartz, N. B. 2009. Sulfation of chondroitin sulfate proteoglycans is necessary for proper Indian hedgehog signaling in the developing growth plate. *Development,* 136**,** 1697-706, https://doi.org/10.1242/dev.030742

Couchman, J. R.,Caterson, B.,Christner, J. E. and Baker, J. R. 1984. Mapping by monoclonal antibody detection of glycosaminoglycans in connective tissues. *Nature,* 307**,** 650-652, https://doi.org/10.1038/307650a0

Darling, E. M. and Athanasiou, K. A. 2005. Rapid phenotypic changes in passaged articular chondrocyte subpopulations. *J Orthop Res,* 23**,** 425-32, https://doi.org/10.1016/j.orthres.2004.08.008

Davidson, M. D.,Kukla, D. A. and Khetani, S. R. 2017. Microengineered cultures containing human hepatic stellate cells and hepatocytes for drug development. *Integrative Biology,* 9**,** 662-677, https://doi.org/10.1039/C7IB00027H %J Integrative Biology

DeLise, A. M.,Fischer, L. and Tuan, R. S. 2000. Cellular interactions and signaling in cartilage development. *Osteoarthritis and Cartilage,* 8**,** 309-334, https://doi.org/https://doi.org/10.1053/joca.1999.0306

Desrochers, J.,Amrein, M. W. and Matyas, J. R. 2012. Viscoelasticity of the articular cartilage surface in early osteoarthritis. *Osteoarthritis and Cartilage,* 20**,** 413-421, https://doi.org/https://doi.org/10.1016/j.joca.2012.01.011

Diab, M.,Wu, J. J. and Eyre, D. R. 1996. Collagen type IX from human cartilage: a structural profile of intermolecular cross-linking sites. *Biochem J,* 314 (Pt 1)**,** 327-32, https://doi.org/10.1042/bj3140327

Dieterle, M. P.,Husari, A.,Rolauffs, B.,Steinberg, T. and Tomakidi, P. 2021. Integrins, cadherins and channels in cartilage mechanotransduction: perspectives for future regeneration strategies. *Expert Rev Mol Med,* 23**,** e14, https://doi.org/10.1017/erm.2021.16

Dilley, J. E.,Bello, M. A.,Roman, N.,McKinley, T. and Sankar, U. 2023. Post-traumatic osteoarthritis: A review of pathogenic mechanisms and novel targets for mitigation. *Bone Rep,* 18**,** 101658, https://doi.org/10.1016/j.bonr.2023.101658

Doege, K. J.,Sasaki, M.,Kimura, T. and Yamada, Y. 1991. Complete coding sequence and deduced primary structure of the human cartilage large aggregating proteoglycan, aggrecan. Human-specific repeats, and additional alternatively spliced forms. *J Biol Chem,* 266**,** 894-902,

du Souich, P.,García, A. G.,Vergés, J. and Montell, E. 2009. Immunomodulatory and anti-inflammatory effects of chondroitin sulphate. *J Cell Mol Med,* 13**,** 1451-63, https://doi.org/10.1111/j.1582-4934.2009.00826.x

Du, X.,Cai, L.,Xie, J. and Zhou, X. 2023. The role of TGF-beta3 in cartilage development and osteoarthritis. *Bone Research,* 11**,** 2, https://doi.org/10.1038/s41413-022-00239-4

Eckstein, F.,Hudelmaier, M. and Putz, R. 2006. The effects of exercise on human articular cartilage. *J Anat,* 208**,** 491-512, https://doi.org/10.1111/j.1469-7580.2006.00546.x

Edmondson, R.,Broglie, J. J.,Adcock, A. F. and Yang, L. 2014. Three-dimensional cell culture systems and their applications in drug discovery and cell-based biosensors. *Assay Drug Dev Technol,* 12**,** 207-18, https://doi.org/10.1089/adt.2014.573

Eldeen, G. N.,Elkhooly, T. A.,El Bassyouni, G. T.,Hamdy, T. M.,Hawash, A. R. and Aly, R. M. 2024a. Enhancement of the chondrogenic differentiation capacity of human dental pulp stem cells via chondroitin sulfate-coated polycaprolactone-MWCNT nanofibers. *Sci Rep,* 14**,** 16396, https://doi.org/10.1038/s41598-024-66497-w

Eldeen, G. N.,Elkhooly, T. A.,El Bassyouni, G. T.,Hamdy, T. M.,Hawash, A. R. and Aly, R. M. 2024b. Enhancement of the chondrogenic differentiation capacity of human dental pulp stem cells via chondroitin sulfate-coated polycaprolactone-MWCNT nanofibers. *Scientific Reports,* 14**,** 16396, https://doi.org/10.1038/s41598-024-66497-w

Eschweiler, J.,Horn, N.,Rath, B.,Betsch, M.,Baroncini, A.,Tingart, M. and Migliorini, F. 2021. The Biomechanics of Cartilage-An Overview. *Life (Basel),* 11, https://doi.org/10.3390/life11040302

Estes, B. T. and Guilak, F. 2011. Three-dimensional culture systems to induce chondrogenesis of adipose-derived stem cells. *Methods Mol Biol,* 702**,** 201-17, https://doi.org/10.1007/978-1-61737-960-4_15

Farrán, A.,Valverde-Franco, G.,Tío, L.,Lussier, B.,Fahmi, H.,Pelletier, J.-P.,Bishop, P. N.,Monfort, J. and Martel-Pelletier, J. 2018. In vivo effect of opticin deficiency in cartilage in a surgically induced mouse model of osteoarthritis. *Scientific Reports,* 8**,** 457, https://doi.org/10.1038/s41598-017-18047-w

Francis, S. L.,Di Bella, C.,Wallace, G. G. and Choong, P. F. M. 2018. Cartilage Tissue Engineering Using Stem Cells and Bioprinting Technology—Barriers to Clinical Translation. 5, https://doi.org/10.3389/fsurg.2018.00070

Frisch, J.,Venkatesan, J. K.,Rey-Rico, A.,Schmitt, G.,Madry, H. and Cucchiarini, M. 2014. Determination of the chondrogenic differentiation processes in human bone marrow-derived mesenchymal stem cells genetically modified to overexpress transforming growth factor-β via recombinant adeno-associated viral vectors. *Hum Gene Ther,* 25**,** 1050-60, https://doi.org/10.1089/hum.2014.091

Frye, S. R.,Yee, A.,Eskin, S. G.,Guerra, R.,Cong, X. and McIntire, L. V. 2005. cDNA microarray analysis of endothelial cells subjected to cyclic mechanical strain:

importance of motion control. *Physiol Genomics,* 21**,** 124-30, https://doi.org/10.1152/physiolgenomics.00029.2003

Fujimoto, T.,Kawashima, H.,Tanaka, T.,Hirose, M.,Toyama-Sorimachi, N.,Matsuzawa, Y. and Miyasaka, M. 2001. CD44 binds a chondroitin sulfate proteoglycan, aggrecan. *Int Immunol,* 13**,** 359-66, https://doi.org/10.1093/intimm/13.3.359

Fukuda, M. 2001. Beta-elimination for release of O-GalNAc-linked oligosaccharides from glycoproteins and glycopeptides. *Curr Protoc Mol Biol,* Chapter 17**,** Unit17.15B, https://doi.org/10.1002/0471142727.mb1715bs31

Funderburgh, J. L. 2002. Keratan sulfate biosynthesis. *IUBMB Life,* 54**,** 187-194, https://doi.org/10.1080/15216540214932

Gale, A. L.,Mammone, R. M.,Dodson, M. E.,Linardi, R. L. and Ortved, K. F. 2019. The effect of hypoxia on chondrogenesis of equine synovial membrane-derived and bone marrow-derived mesenchymal stem cells. *BMC Vet Res,* 15**,** 201, https://doi.org/10.1186/s12917-019-1954-1

Galeotti, F.,Maccari, F. and Volpi, N. 2014. Selective removal of keratan sulfate in chondroitin sulfate samples by sequential precipitation with ethanol. *Anal Biochem,* 448**,** 113-5, https://doi.org/10.1016/j.ab.2013.11.028

Galla, R.,Ruga, S.,Ferrari, S.,Saccone, S.,Saccuman, L.,Invernizzi, M. and Uberti, F. 2022. In vitro analysis of the effects of plant-derived chondroitin sulfate from intestinal barrier to chondrocytes. *Journal of Functional Foods,* 98**,** 105285, https://doi.org/https://doi.org/10.1016/j.jff.2022.105285

Gao, Y.,Liu, S.,Huang, J.,Guo, W.,Chen, J.,Zhang, L.,Zhao, B.,Peng, J.,Wang, A.,Wang, Y.,Xu, W.,Lu, S.,Yuan, M. and Guo, Q. 2014. The ECM-cell interaction of cartilage extracellular matrix on chondrocytes. *Biomed Res Int,* 2014**,** 648459, https://doi.org/10.1155/2014/648459

Gardini, C.,Boccardi, G.,Guerrini, M.,Kellenbach, E.,Lunenburg, M.,van der Meer, J. Y.,Naggi, A. and Urso, E. 2023. Quantitative 2D 1H, 13C HSQC NMR Spectroscopy for the Determination of Chondroitin Sulfate and Dermatan Sulfate Content in Danaparoid Sodium. *Thromb Haemost,* 123**,** 856-866, https://doi.org/10.1055/s-0043-1768225

Gargiulo, V.,Lanzetta, R.,Parrilli, M. and De Castro, C. 2009. Structural analysis of chondroitin sulfate from Scyliorhinus canicula: A useful source of this polysaccharide. *Glycobiology,* 19**,** 1485-1491, https://doi.org/10.1093/glycob/cwp123 %J Glycobiology

Garnjanagoonchorn, W.,Wongekalak, L. and Engkagul, A. 2007. Determination of chondroitin sulfate from different sources of cartilage. *Chemical Engineering and Processing: Process Intensification,* 46**,** 465-471, https://doi.org/https://doi.org/10.1016/j.cep.2006.05.019

Gauci, S. J.,Stanton, H.,Little, C. B. and Fosang, A. J. 2017. Proteoglycan and Collagen Degradation in Osteoarthritis. *In:* Grässel, S. & Aszódi, A. eds.

Cartilage: Volume 2: Pathophysiology. Cham: Springer International Publishing.

Ghazanfari, R.,Zacharaki, D.,Li, H.,Ching Lim, H.,Soneji, S. and Scheding, S. 2017. Human Primary Bone Marrow Mesenchymal Stromal Cells and Their in vitro Progenies Display Distinct Transcriptional Profile Signatures. *Scientific Reports,* 7**,** 10338, https://doi.org/10.1038/s41598-017-09449-x

Ghiselli, G. 2017. Drug-Mediated Regulation of Glycosaminoglycan Biosynthesis. *Med Res Rev,* 37**,** 1051-1094, https://doi.org/10.1002/med.21429

Giji, S. and Arumugam, M. 2014. Chapter Four - Isolation and Characterization of Hyaluronic Acid from Marine Organisms. *In:* Kim, S.-K. ed. *Advances in Food and Nutrition Research.* Academic Press.

Gillis, J. A. 2019. The Development and Evolution of Cartilage. *Reference Module in Life Sciences.*

Girkontaité, I.,Frischholz, S.,Lammi, P. E.,Wagner, K.,Swoboda, B.,Aigner, T. and von der Mark, K. J. M. b. j. o. t. I. S. f. M. B. 1996. Immunolocalization of type X collagen in normal fetal and adult osteoarthritic cartilage with monoclonal antibodies. 15 4**,** 231-8,

Goldring, M. B.,Otero, M.,Tsuchimochi, K.,Ijiri, K. and Li, Y. 2008. Defining the roles of inflammatory and anabolic cytokines in cartilage metabolism. *Ann Rheum Dis,* 67 Suppl 3**,** iii75-82, https://doi.org/10.1136/ard.2008.098764

Goude, M. C.,McDevitt, T. C. and Temenoff, J. S. 2014. Chondroitin sulfate microparticles modulate transforming growth factor-β1-induced chondrogenesis of human mesenchymal stem cell spheroids. *Cells Tissues Organs,* 199**,** 117-30, https://doi.org/10.1159/000365966

Grottkau, B. E.,Yang, X.,Zhang, L.,Ye, L. and Lin, Y. 2013. Comparison of Effects of Mechanical Stretching on Osteogenic Potential of ASCs and BMSCs. *Bone Research,* 1**,** 282-290, https://doi.org/10.4248/BR201303006

Guan, T.,Ding, L. G.,Lu, B. Y.,Guo, J. Y.,Wu, M. Y.,Tan, Z. Q. and Hou, S. Z. 2022. Combined Administration of Curcumin and Chondroitin Sulfate Alleviates Cartilage Injury and Inflammation via NF-κB Pathway in Knee Osteoarthritis Rats. *Front Pharmacol,* 13**,** 882304, https://doi.org/10.3389/fphar.2022.882304

Gubbiotti, M. A.,Vallet, S. D.,Ricard-Blum, S. and Iozzo, R. V. 2016. Decorin interacting network: A comprehensive analysis of decorin-binding partners and their versatile functions. *Matrix Biol,* 55**,** 7-21, https://doi.org/10.1016/j.matbio.2016.09.009

Guo, H.,Huang, J.,Liang, Y.,Wang, D. and Zhang, H. 2022. Focusing on the hypoxia-inducible factor pathway: role, regulation, and therapy for osteoarthritis. *European Journal of Medical Research,* 27**,** 288, https://doi.org/10.1186/s40001-022-00926-2

Guo, J.,Yan, P.,Qin, Y.,Liu, M.,Ma, Y.,Li, J.,Wang, R.,Luo, H. and Lv, S. 2024. Automated measurement and grading of knee cartilage thickness: a deep learning-based approach. 11, https://doi.org/10.3389/fmed.2024.1337993

Gupta, P. K.,Chullikana, A.,Rengasamy, M.,Shetty, N.,Pandey, V.,Agarwal, V.,Wagh, S. Y.,Vellotare, P. K.,Damodaran, D.,Viswanathan, P.,Thej, C.,Balasubramanian, S. and Majumdar, A. S. 2016. Efficacy and safety of adult human bone marrow-derived, cultured, pooled, allogeneic mesenchymal stromal cells (Stempeucel®): preclinical and clinical trial in osteoarthritis of the knee joint. *Arthritis Res Ther,* 18**,** 301, https://doi.org/10.1186/s13075-016-1195-7

Gupta, P. K.,Das, A. K.,Chullikana, A. and Majumdar, A. S. 2012. Mesenchymal stem cells for cartilage repair in osteoarthritis. *Stem Cell Res Ther,* 3**,** 25, https://doi.org/10.1186/scrt116

Gutierrez, R. A.,Fonseca, V. C. and Darling, E. M. 2022. Chondrogenesis of Adipose-Derived Stem Cells Using an Arrayed Spheroid Format. *Cell Mol Bioeng,* 15**,** 587-597, https://doi.org/10.1007/s12195-022-00746-8

Hallett, S. A.,Ono, W. and Ono, N. 2021. The hypertrophic chondrocyte: To be or not to be. *Histol Histopathol,* 36**,** 1021-1036, https://doi.org/10.14670/hh-18-355

Han, B.,Li, Q.,Wang, C.,Patel, P.,Adams, S. M.,Doyran, B.,Nia, H. T.,Oftadeh, R.,Zhou, S.,Li, C. Y.,Liu, X. S.,Lu, X. L.,Enomoto-Iwamoto, M.,Qin, L.,Mauck, R. L.,Iozzo, R. V.,Birk, D. E. and Han, L. 2019. Decorin Regulates the Aggrecan Network Integrity and Biomechanical Functions of Cartilage Extracellular Matrix. *ACS Nano,* 13**,** 11320-11333, https://doi.org/10.1021/acsnano.9b04477

Han, U.,Hwang, J. H.,Lee, J. M.,Kim, H.,Jung, H. S.,Hong, J. H. and Hong, J. 2020. Transmission and regulation of biochemical stimulus via a nanoshell directly adsorbed on the cell membrane to enhance chondrogenic differentiation of mesenchymal stem cell. *Biotechnol Bioeng,* 117**,** 184-193, https://doi.org/10.1002/bit.27183

Hardingham, T. E. and Fosang, A. J. 1992. Proteoglycans: many forms and many functions. 6**,** 861-870, https://doi.org/https://doi.org/10.1096/fasebj.6.3.1740236

Harjanto, D. and Zaman, M. H. 2013. Modeling extracellular matrix reorganization in 3D environments. *PLoS One,* 8**,** e52509, https://doi.org/10.1371/journal.pone.0052509

Harrell, C. R.,Markovic, B. S.,Fellabaum, C.,Arsenijevic, A. and Volarevic, V. 2019. Mesenchymal stem cell-based therapy of osteoarthritis: Current knowledge and future perspectives. *Biomed Pharmacother,* 109**,** 2318-2326, https://doi.org/10.1016/j.biopha.2018.11.099

Hascall, V. C. and Sajdera, S. W. 1969. Proteinpolysaccharide complex from bovine nasal cartilage. The function of glycoprotein in the formation of aggregates. *J Biol Chem,* 244**,** 2384-96,

Hayes, A.,Sugahara, K.,Farrugia, B.,Whitelock, J. M.,Caterson, B. and Melrose, J. 2018a. Biodiversity of CS-proteoglycan sulphation motifs: chemical messenger recognition modules with roles in information transfer, control of cellular behaviour and tissue morphogenesis. *Biochem J,* 475**,** 587-620, https://doi.org/10.1042/BCJ20170820

Hayes, A. J.,Hughes, C. E.,Smith, S. M.,Caterson, B.,Little, C. B. and Melrose, J. 2016. The CS Sulfation Motifs 4C3, 7D4, 3B3[-]; and Perlecan Identify Stem Cell Populations and Their Niches, Activated Progenitor Cells and Transitional Areas of Tissue Development in the Fetal Human Elbow. *Stem Cells Dev,* 25**,** 836-47, https://doi.org/10.1089/scd.2016.0054

Hayes, A. J. and Melrose, J. 2020. Immunolocalization of Keratan Sulfate in Rat Spinal Tissues Using the Keratanase Generated BKS-1(+) Neoepitope: Correlation of Expression Patterns with the Class II SLRPs, Lumican and Keratocan. *Cells,* 9, https://doi.org/10.3390/cells9040826

Hayes, A. J.,Smith, S. M.,Caterson, B. and Melrose, J. 2018b. Concise Review: Stem/Progenitor Cell Proteoglycans Decorated with 7-D-4, 4-C-3, and 3-B-3(-) Chondroitin Sulfate Motifs Are Morphogenetic Markers of Tissue Development. *Stem Cells,* 36**,** 1475-1486, https://doi.org/10.1002/stem.2860

Hayes, A. J.,Tudor, D.,Nowell, M. A.,Caterson, B. and Hughes, C. E. 2008. Chondroitin sulfate sulfation motifs as putative biomarkers for isolation of articular cartilage progenitor cells. *J Histochem Cytochem,* 56**,** 125-38, https://doi.org/10.1369/jhc.7A7320.2007

He, Y. and Karsdal, M. A. 2016. Chapter 9 - Type IX Collagen. *In:* Karsdal, M. A. ed. *Biochemistry of Collagens, Laminins and Elastin.* Academic Press.

Heinegård, D.,Paulsson, M.,Inerot, S. and Carlström, C. 1981. A novel low-molecular weight chondroitin sulphate proteoglycan isolated from cartilage. *Biochem J,* 197**,** 355-66, https://doi.org/10.1042/bj1970355

Henao-Murillo, L.,Pastrama, M. I.,Ito, K. and van Donkelaar, C. C. 2021. The Relationship Between Proteoglycan Loss, Overloading-Induced Collagen Damage, and Cyclic Loading in Articular Cartilage. *Cartilage,* 13**,** 1501s-1512s, https://doi.org/10.1177/1947603519885005

Henrotin, Y.,Mathy, M.,Sanchez, C. and Lambert, C. 2010. Chondroitin sulfate in the treatment of osteoarthritis: from in vitro studies to clinical recommendations. *Ther Adv Musculoskelet Dis,* 2**,** 335-48, https://doi.org/10.1177/1759720x10383076

Higashi, K.,Okamoto, Y.,Mukuno, A.,Wakai, J.,Hosoyama, S.,Linhardt, R. J. and Toida, T. 2015. Functional chondroitin sulfate from Enteroctopus dofleini

containing a 3-O-sulfo glucuronic acid residue. *Carbohydrate Polymers,* 134**,** 557-565, https://doi.org/https://doi.org/10.1016/j.carbpol.2015.07.082

Housmans, B. A. C.,Neefjes, M.,Surtel, D. A. M.,Vitík, M.,Cremers, A.,van Rhijn, L. W.,van der Kraan, P. M.,van den Akker, G. G. H. and Welting, T. J. M. 2022. Synovial fluid from end-stage osteoarthritis induces proliferation and fibrosis of articular chondrocytes via MAPK and RhoGTPase signaling. *Osteoarthritis and Cartilage,* 30**,** 862-874, https://doi.org/https://doi.org/10.1016/j.joca.2021.12.015

Hsu, H. C.,Ke, Y. L.,Lai, Y. H.,Hsieh, W. C.,Lin, C. H.,Huang, S. S.,Peng, J. Y. and Chen, C.-H. 2022. Chondroitin Sulfate Enhances Proliferation and Migration via Inducing β-Catenin and Intracellular ROS as Well as Suppressing Metalloproteinases through Akt/NF-𝜘B Pathway Inhibition in Human Chondrocytes. *The Journal of nutrition, health and aging,* 26**,** 307-313, https://doi.org/https://doi.org/10.1007/s12603-022-1752-5

Hu, N.,Gao, Y.,Jayasuriya, C. T.,Liu, W.,Du, H.,Ding, J.,Feng, M. and Chen, Q. 2019. Chondrogenic induction of human osteoarthritic cartilage-derived mesenchymal stem cells activates mineralization and hypertrophic and osteogenic gene expression through a mechanomiR. *Arthritis Res Ther,* 21**,** 167, https://doi.org/10.1186/s13075-019-1949-0

Huang, C. Y.,Reuben, P. M.,D'Ippolito, G.,Schiller, P. C. and Cheung, H. S. 2004. Chondrogenesis of human bone marrow-derived mesenchymal stem cells in agarose culture. *Anat Rec A Discov Mol Cell Evol Biol,* 278**,** 428-36, https://doi.org/10.1002/ar.a.20010

Huang, Y.,Askew, E. B.,Knudson, C. B. and Knudson, W. 2016. CRISPR/Cas9 knockout of HAS2 in rat chondrosarcoma chondrocytes demonstrates the requirement of hyaluronan for aggrecan retention. *Matrix Biol,* 56**,** 74-94, https://doi.org/10.1016/j.matbio.2016.04.002

Huang, Y.,Konse, T.,Mechref, Y. and Novotny, M. V. 2002. Matrix-assisted laser desorption/ionization mass spectrometry compatible beta-elimination of O-linked oligosaccharides. *Rapid Commun Mass Spectrom,* 16**,** 1199-204, https://doi.org/10.1002/rcm.701

Humphries, M. J. 2001. Cell-substrate adhesion assays. *Curr Protoc Cell Biol,* Chapter 9**,** Unit 9.1, https://doi.org/10.1002/0471143030.cb0901s00

Iijima, H.,Isho, T.,Kuroki, H.,Takahashi, M. and Aoyama, T. 2018. Effectiveness of mesenchymal stem cells for treating patients with knee osteoarthritis: a meta-analysis toward the establishment of effective regenerative rehabilitation. *NPJ Regen Med,* 3**,** 15, https://doi.org/10.1038/s41536-018-0041-8

Ingavle, G. C.,Dormer, N. H.,Gehrke, S. H. and Detamore, M. S. 2012. Using chondroitin sulfate to improve the viability and biosynthesis of chondrocytes encapsulated in interpenetrating network (IPN) hydrogels of agarose and poly(ethylene glycol) diacrylate. *J Mater Sci Mater Med,* 23**,** 157-70, https://doi.org/10.1007/s10856-011-4499-9

Iovu, M.,Dumais, G. and du Souich, P. 2008. Anti-inflammatory activity of chondroitin sulfate. *Osteoarthritis Cartilage,* 16 Suppl 3**,** S14-8, https://doi.org/10.1016/j.joca.2008.06.008

Isemura, M. and Ikenaka, T. 1975. Beta-Elimination and sulfite addition reaction of chondroitin sulfate peptidoglycan and the peptide structure of the linkage region. *Biochim Biophys Acta,* 411**,** 11-21, https://doi.org/10.1016/0304-4165(75)90280-9

Janaky, N.,Jun-Ying, X. and Xiang-Yang, L. 2006. Determination of agarose gel pore size: Absorbance measurements vis a vis other techniques. *Journal of Physics: Conference Series,* 28**,** 83, https://doi.org/10.1088/1742-6596/28/1/017

Janipour, M.,Soltaniesmaeili, A.,Owji, S. H.,Shahhossein, Z. and Hashemi, S. S. 2024. Auricular cartilage regeneration using chondroitin sulfate-based hydrogel with mesenchymal stem cells in rabbits. *Artif Organs*, https://doi.org/10.1111/aor.14807

Jay, G. D. and Waller, K. A. 2014. The biology of Lubricin: Near frictionless joint motion. *Matrix Biology,* 39**,** 17-24, https://doi.org/https://doi.org/10.1016/j.matbio.2014.08.008

Jerosch, J. 2011. Effects of Glucosamine and Chondroitin Sulfate on Cartilage Metabolism in OA: Outlook on Other Nutrient Partners Especially Omega-3 Fatty Acids. *Int J Rheumatol,* 2011**,** 969012, https://doi.org/10.1155/2011/969012

Jia, Y.,Le, H.,Wang, X.,Zhang, J.,Liu, Y.,Ding, J.,Zheng, C. and Chang, F. 2023. Double-edged role of mechanical stimuli and underlying mechanisms in cartilage tissue engineering. *Front Bioeng Biotechnol,* 11**,** 1271762, https://doi.org/10.3389/fbioe.2023.1271762

Jin, H.,Jiang, S.,Wang, R.,Zhang, Y.,Dong, J. and Li, Y. 2021. Mechanistic Insight Into the Roles of Integrins in Osteoarthritis. 9, https://doi.org/10.3389/fcell.2021.693484

Jørgensen, A. E. M.,Kjær, M. and Heinemeier, K. M. 2017. The Effect of Aging and Mechanical Loading on the Metabolism of Articular Cartilage. *J Rheumatol,* 44**,** 410-417, https://doi.org/10.3899/jrheum.160226

Ju, C.,Hou, L.,Sun, F.,Zhang, L.,Zhang, Z.,Gao, H.,Wang, L.,Wang, D.,Lv, Y. and Zhao, X. 2015. Anti-oxidation and Antiapoptotic Effects of Chondroitin Sulfate on 6-Hydroxydopamine-Induced Injury Through the Up-Regulation of Nrf2 and Inhibition of Mitochondria-Mediated Pathway. *Neurochem Res,* 40**,** 1509-19, https://doi.org/10.1007/s11064-015-1628-8

Jung, Y. K.,Park, H. R.,Cho, H. J.,Jang, J. A.,Lee, E. J.,Han, M. S.,Kim, G. W. and Han, S. 2019. Degrading products of chondroitin sulfate can induce hypertrophy-like changes and MMP-13/ADAMTS5 production in chondrocytes. *Sci Rep,* 9**,** 15846, https://doi.org/10.1038/s41598-019-52358-4

Kabiri, A.,Esfandiari, E.,Hashemibeni, B.,Kazemi, M.,Mardani, M. and Esmaeili, A. 2012. Effects of FGF-2 on human adipose tissue derived adult stem cells morphology and chondrogenesis enhancement in Transwell culture. *Biochemical and Biophysical Research Communications,* 424**,** 234-238, https://doi.org/https://doi.org/10.1016/j.bbrc.2012.06.082

Kadler, K. E.,Hill, A. and Canty-Laird, E. G. 2008. Collagen fibrillogenesis: fibronectin, integrins, and minor collagens as organizers and nucleators. *Curr Opin Cell Biol,* 20**,** 495-501, https://doi.org/10.1016/j.ceb.2008.06.008

Kalamajski, S.,Bihan, D.,Bonna, A.,Rubin, K. and Farndale, R. W. 2016. Fibromodulin Interacts with Collagen Cross-linking Sites and Activates Lysyl Oxidase. *J Biol Chem,* 291**,** 7951-60, https://doi.org/10.1074/jbc.M115.693408

Kamakura, T.,Jin, Y.,Nishio, M.,Nagata, S.,Fukuda, M.,Sun, L.,Kawai, S. and Toguchida, J. 2023. Collagen X Is Dispensable for Hypertrophic Differentiation and Endochondral Ossification of Human iPSC-Derived Chondrocytes. *JBMR Plus,* 7**,** e10737, https://doi.org/10.1002/jbm4.10737

Kapałczyńska, M.,Kolenda, T.,Przybyła, W.,Zajączkowska, M.,Teresiak, A.,Filas, V.,Ibbs, M.,Bliźniak, R.,Łuczewski, Ł. and Lamperska, K. 2018. 2D and 3D cell cultures - a comparison of different types of cancer cell cultures. *Arch Med Sci,* 14**,** 910-919, https://doi.org/10.5114/aoms.2016.63743

Kawamura, D.,Funakoshi, T.,Mizumoto, S.,Sugahara, K. and Iwasaki, N. 2014. Sulfation patterns of exogenous chondroitin sulfate affect chondrogenic differentiation of ATDC5 cells. *J Orthop Sci,* 19**,** 1028-35, https://doi.org/10.1007/s00776-014-0643-y

Kawato, Y.,Hirao, M.,Ebina, K.,Shi, K.,Hashimoto, J.,Honjo, Y.,Yoshikawa, H. and Myoui, A. 2012. Nkx3.2 promotes primary chondrogenic differentiation by upregulating Col2a1 transcription. *PLoS One,* 7**,** e34703, https://doi.org/10.1371/journal.pone.0034703

Kiani, C.,Chen, L.,Wu, Y. J.,Yee, A. J. and Yang, B. B. 2002. Structure and function of aggrecan. *Cell Research,* 12**,** 19-32, https://doi.org/10.1038/sj.cr.7290106

Killen, M.-C. and Charalambous, C. P. 2020. Chapter 6 - Advances in cartilage restoration techniques. *In:* Ahmed, W., Phoenix, D. A., Jackson, M. J. & Charalambous, C. P. eds. *Advances in Medical and Surgical Engineering.* Academic Press.

Kim, C. T.,Gujral, N.,Ganguly, A.,Suh, J. W. and Sunwoo, H. H. 2014. Chondroitin sulphate extracted from antler cartilage using high hydrostatic pressure and enzymatic hydrolysis. *Biotechnol Rep (Amst),* 4**,** 14-20, https://doi.org/10.1016/j.btre.2014.07.004

Kim, M. H.,Park, S. R. and Choi, B. H. 2021. Comparative Analysis of the Expression of Chondroitin Sulfate Subtypes and Their Inhibitory Effect on Axonal Growth in the Embryonic, Adult, and Injured Rat Brains. *Tissue Eng Regen Med,* 18**,** 165-178, https://doi.org/10.1007/s13770-020-00295-z

Kinoshita, A. and Sugahara, K. 1999. Microanalysis of Glycosaminoglycan-Derived Oligosaccharides Labeled with a Fluorophore 2-Aminobenzamide by High-Performance Liquid Chromatography: Application to Disaccharide Composition Analysis and Exosequencing of Oligosaccharides. *Analytical Biochemistry,* 269**,** 367-378, https://doi.org/https://doi.org/10.1006/abio.1999.4027

Klüppel, M.,Wight, T. N.,Chan, C.,Hinek, A. and Wrana, J. L. 2005. Maintenance of chondroitin sulfation balance by chondroitin-4-sulfotransferase 1 is required for chondrocyte development and growth factor signaling during cartilage morphogenesis. *Development,* 132**,** 3989-4003, https://doi.org/10.1242/dev.01948

Knudson, C. B. and Knudson, W. 2001. Cartilage proteoglycans. *Semin Cell Dev Biol,* 12**,** 69-78, https://doi.org/10.1006/scdb.2000.0243

Knuth, C. A.,Andres Sastre, E.,Fahy, N. B.,Witte-Bouma, J.,Ridwan, Y.,Strabbing, E. M.,Koudstaal, M. J.,van de Peppel, J.,Wolvius, E. B.,Narcisi, R. and Farrell, E. 2019. Collagen type X is essential for successful mesenchymal stem cell-mediated cartilage formation and subsequent endochondral ossification. *Eur Cell Mater,* 38**,** 106-122, https://doi.org/10.22203/eCM.v038a09

Kobayashi-Miura, M.,Osago, H.,Hamasaki, Y.,Takano, I.,Akiho, M.,Hiyoshi, M. and Hara, N. 2022. Decrease in Glycosaminoglycan with Aging in Normal Rat Articular Cartilage Is Greater in Females than in Males. *Cartilage,* 13**,** 19476035221102566, https://doi.org/10.1177/19476035221102566

Krichen, F.,Bougatef, H.,Capitani, F.,Ben Amor, I.,Koubaa, I.,Gargouri, J.,Maccari, F.,Mantovani, V.,Galeotti, F.,Volpi, N. and Bougatef, A. 2018a. Purification and structural elucidation of chondroitin sulfate/dermatan sulfate from Atlantic bluefin tuna (Thunnus thynnus) skins and their anticoagulant and ACE inhibitory activities. *RSC Adv,* 8**,** 37965-37975, https://doi.org/10.1039/c8ra06704j

Krichen, F.,Bougatef, H.,Sayari, N.,Capitani, F.,Ben Amor, I.,Koubaa, I.,Maccari, F.,Mantovani, V.,Galeotti, F.,Volpi, N. and Bougatef, A. 2018b. Isolation, Purification and Structural Characterestics of Chondroitin Sulfate from Smooth hound Cartilage: In vitro Anticoagulant and Antiproliferative Properties. *Carbohydr Polym,* 197**,** 451-459, https://doi.org/10.1016/j.carbpol.2018.06.040

Krichen, F.,Bougatef, H.,Sayari, N.,Capitani, F.,Ben Amor, I.,Koubaa, I.,Maccari, F.,Mantovani, V.,Galeotti, F.,Volpi, N. and Bougatef, A. 2018c. Isolation, Purification and Structural Characterestics of Chondroitin Sulfate from Smooth hound Cartilage: In vitro Anticoagulant and Antiproliferative Properties. *Carbohydrate Polymers,* 197**,** 451-459, https://doi.org/https://doi.org/10.1016/j.carbpol.2018.06.040

Krusius, T.,Finne, J.,Margolis, R. K. and Margolis, R. U. 1986. Identification of an O-glycosidic mannose-linked sialylated tetrasaccharide and keratan sulfate

oligosaccharides in the chondroitin sulfate proteoglycan of brain. *J Biol Chem,* 261**,** 8237-42,

Kubosch, E. J.,Heidt, E.,Bernstein, A.,Böttiger, K. and Schmal, H. 2016. The trans-well coculture of human synovial mesenchymal stem cells with chondrocytes leads to self-organization, chondrogenic differentiation, and secretion of TGFβ. *Stem Cell Res Ther,* 7**,** 64, https://doi.org/10.1186/s13287-016-0322-3

Kuijer, R.,van de Stadt, R. J.,van Kampen, G. P.,de Koning, M. H.,van de Voorde-Vissers, E. and van der Korst, J. K. 1986. Heterogeneity of proteoglycans extracted before and after collagenase treatment of human articular cartilage. II. Variations in composition with age and tissue source. *Arthritis Rheum,* 29**,** 1248-55, https://doi.org/10.1002/art.1780291010

Kuroda, Y.,Kitada, M.,Wakao, S. and Dezawa, M. 2011. Bone marrow mesenchymal cells: how do they contribute to tissue repair and are they really stem cells? *Arch Immunol Ther Exp (Warsz),* 59**,** 369-78, https://doi.org/10.1007/s00005-011-0139-9

Kwon, D. G.,Kim, M. K.,Jeon, Y. S.,Nam, Y. C.,Park, J. S. and Ryu, D. J. 2022. State of the Art: The Immunomodulatory Role of MSCs for Osteoarthritis. *Int J Mol Sci,* 23, https://doi.org/10.3390/ijms23031618

Kwon, S. G.,Kwon, Y. W.,Lee, T. W.,Park, G. T. and Kim, J. H. 2018. Recent advances in stem cell therapeutics and tissue engineering strategies. *Biomaterials Research,* 22**,** 36, https://doi.org/10.1186/s40824-018-0148-4

Laremore, T. N.,Leach, F. E., 3rd,Solakyildirim, K.,Amster, I. J. and Linhardt, R. J. 2010. Glycosaminoglycan characterization by electrospray ionization mass spectrometry including fourier transform mass spectrometry. *Methods Enzymol,* 478**,** 79-108, https://doi.org/10.1016/s0076-6879(10)78003-4

Larsson, P.,Engqvist, H.,Biermann, J.,Werner Rönnerman, E.,Forssell-Aronsson, E.,Kovács, A.,Karlsson, P.,Helou, K. and Parris, T. Z. 2020. Optimization of cell viability assays to improve replicability and reproducibility of cancer drug sensitivity screens. *Scientific Reports,* 10**,** 5798, https://doi.org/10.1038/s41598-020-62848-5

Lee, D. A.,Knight, M. M.,F. Bolton, J.,Idowu, B. D.,Kayser, M. V. and Bader, D. L. 2000a. Chondrocyte deformation within compressed agarose constructs at the cellular and sub-cellular levels. *Journal of Biomechanics,* 33**,** 81-95, https://doi.org/https://doi.org/10.1016/S0021-9290(99)00160-8

Lee, M. K. and Lander, A. D. 1991. Analysis of affinity and structural selectivity in the binding of proteins to glycosaminoglycans: development of a sensitive electrophoretic approach. *Proc Natl Acad Sci U S A,* 88**,** 2768-72, https://doi.org/10.1073/pnas.88.7.2768

Lee, P. S.,Eckert, H.,Hess, R.,Gelinsky, M.,Rancourt, D.,Krawetz, R.,Cuniberti, G. and Scharnweber, D. 2017. Developing a Customized Perfusion Bioreactor Prototype with Controlled Positional Variability in Oxygen Partial Pressure for

Bone and Cartilage Tissue Engineering. *Tissue Eng Part C Methods,* 23**,** 286-297, https://doi.org/10.1089/ten.TEC.2016.0244

Lee, V.,Cao, L.,Zhang, Y.,Kiani, C.,Adams, M. E. and Yang, B. B. 2000b. The roles of matrix molecules in mediating chondrocyte aggregation, attachment, and spreading. *J Cell Biochem,* 79**,** 322-33, https://doi.org/10.1002/1097-4644(20001101)79:2<322::aid-jcb150>3.0.co;2-u

Lee, Y.,Choi, J. and Hwang, N. S. 2018. Regulation of lubricin for functional cartilage tissue regeneration: a review. *Biomater Res,* 22**,** 9, https://doi.org/10.1186/s40824-018-0118-x

Lefebvre, V. and Dvir-Ginzberg, M. 2017. SOX9 and the many facets of its regulation in the chondrocyte lineage. *Connect Tissue Res,* 58**,** 2-14, https://doi.org/10.1080/03008207.2016.1183667

Legendre, F.,Baugé, C.,Roche, R.,Saurel, A. S. and Pujol, J. P. 2008. Chondroitin sulfate modulation of matrix and inflammatory gene expression in IL-1beta-stimulated chondrocytes--study in hypoxic alginate bead cultures. *Osteoarthritis Cartilage,* 16**,** 105-14, https://doi.org/10.1016/j.joca.2007.05.020

Li, A.-l.,Xiong, S.-l. J. t. I. C. o. B. and Engineering, B. 2010a. Preparation and Structure Analysis of Chondroitin Sulfate from Pig Laryngeal Cartilage. 1-5,

Li, C.,Shang, W.,Huang, Y.,Ge, J.,Ye, J.,Qu, X.,Guo, Q.,Wang, C.,Hu, P. and Liu, Y. 2024. Sodium alginate/chitosan composite scaffold reinforced with biodegradable polyesters/gelatin nanofibers for cartilage tissue engineering. *Int J Biol Macromol,* 285**,** 138054, https://doi.org/10.1016/j.ijbiomac.2024.138054

Li, F.,Nandini, C. D.,Hattori, T.,Bao, X.,Murayama, D.,Nakamura, T.,Fukushima, N. and Sugahara, K. 2010b. Structure of pleiotrophin- and hepatocyte growth factor-binding sulfated hexasaccharide determined by biochemical and computational approaches. *J Biol Chem,* 285**,** 27673-85, https://doi.org/10.1074/jbc.M110.118703

Li, S.,Hayes, A. J.,Caterson, B. and Hughes, C. E. 2013a. The effect of beta-xylosides on the chondrogenic differentiation of mesenchymal stem cells. *Histochemistry and Cell Biology,* 139**,** 59-74, https://doi.org/10.1007/s00418-012-1017-1

Li, S.,Hayes, A. J.,Caterson, B. and Hughes, C. E. 2013b. The effect of beta-xylosides on the chondrogenic differentiation of mesenchymal stem cells. *Histochem Cell Biol,* 139**,** 59-74, https://doi.org/10.1007/s00418-012-1017-1

Li, Y.,Wei, X.,Zhou, J. and Wei, L. 2013c. The age-related changes in cartilage and osteoarthritis. *Biomed Res Int,* 2013**,** 916530, https://doi.org/10.1155/2013/916530

Lin, P. P.,Buckwalter, J. A.,Olmstead, M. and Caterson, B. 1998. Expression of proteoglycan epitopes in articular cartilage repair tissue. *Iowa Orthop J,* 18**,** 12-8,

Lin, T.-S.,Hsieh, C.-H.,Kuo, C.,Juang, Y.-P.,Hsieh, Y. S. Y.,Chiang, H.,Hung, S.-C.,Jiang, C.-C. and Liang, P.-H. 2020a. Sulfation pattern of chondroitin sulfate in human osteoarthritis cartilages reveals a lower level of chondroitin-4-sulfate. *Carbohydrate Polymers,* 229**,** 115496, https://doi.org/https://doi.org/10.1016/j.carbpol.2019.115496

Lin, T. S.,Hsieh, C. H.,Kuo, C.,Juang, Y. P.,Hsieh, Y. S. Y.,Chiang, H.,Hung, S. C.,Jiang, C. C. and Liang, P. H. 2020b. Sulfation pattern of chondroitin sulfate in human osteoarthritis cartilages reveals a lower level of chondroitin-4-sulfate. *Carbohydr Polym,* 229**,** 115496, https://doi.org/10.1016/j.carbpol.2019.115496

Lindahl, A. 2015. From gristle to chondrocyte transplantation: treatment of cartilage injuries. *Philos Trans R Soc Lond B Biol Sci,* 370**,** 20140369, https://doi.org/10.1098/rstb.2014.0369

Little, C. B.,Hilbert, B. J.,Wickstrom, S. and Hedlund, B. E. 1990. Quantitative microanalysis of equine synovial fluid glycosaminoglycan concentration. *Am J Vet Res,* 51**,** 1534-9,

Liu, C.-F. and Lefebvre, V. 2015. The transcription factors SOX9 and SOX5/SOX6 cooperate genome-wide through super-enhancers to drive chondrogenesis. *Nucleic Acids Research,* 43**,** 8183-8203, https://doi.org/10.1093/nar/gkv688 %J Nucleic Acids Research

Liu, Y.,Lin, L.,Zou, R.,Wen, C.,Wang, Z. and Lin, F. 2018. MSC-derived exosomes promote proliferation and inhibit apoptosis of chondrocytes via lncRNA-KLF3-AS1/miR-206/GIT1 axis in osteoarthritis. *Cell Cycle,* 17**,** 2411-2422, https://doi.org/10.1080/15384101.2018.1526603

Livak, K. J. and Schmittgen, T. D. 2001. Analysis of relative gene expression data using real-time quantitative PCR and the 2(-Delta Delta C(T)) Method. *Methods,* 25**,** 402-8, https://doi.org/10.1006/meth.2001.1262

Loeser, R. F. 2014. Integrins and chondrocyte-matrix interactions in articular cartilage. *Matrix Biol,* 39**,** 11-6, https://doi.org/10.1016/j.matbio.2014.08.007

López-Senra, E.,Casal-Beiroa, P.,López-Álvarez, M.,Serra, J.,González, P.,Valcarcel, J.,Vázquez, J. A.,Burguera, E. F.,Blanco, F. J. and Magalhães, J. 2020. Impact of Prevalence Ratios of Chondroitin Sulfate (CS)- 4 and -6 Isomers Derived from Marine Sources in Cell Proliferation and Chondrogenic Differentiation Processes. *Mar Drugs,* 18, https://doi.org/10.3390/md18020094

Lotz, M. and Loeser, R. F. 2012. Effects of aging on articular cartilage homeostasis. *Bone,* 51**,** 241-8, https://doi.org/10.1016/j.bone.2012.03.023

Lu, J.,Shen, X.,Sun, X.,Yin, H.,Yang, S.,Lu, C.,Wang, Y.,Liu, Y.,Huang, Y.,Yang, Z.,Dong, X.,Wang, C.,Guo, Q.,Zhao, L.,Sun, X.,Lu, S.,Mikos, A. G.,Peng, J.

and Wang, X. 2018. Increased recruitment of endogenous stem cells and chondrogenic differentiation by a composite scaffold containing bone marrow homing peptide for cartilage regeneration. *Theranostics,* 8**,** 5039-5058, https://doi.org/10.7150/thno.26981

Luo, X. M.,Fosmire, G. J. and Leach, R. M., Jr. 2002. Chicken keel cartilage as a source of chondroitin sulfate. *Poult Sci,* 81**,** 1086-9, https://doi.org/10.1093/ps/81.7.1086

Maccari, F.,Galeotti, F. and Volpi, N. 2015. Isolation and structural characterization of chondroitin sulfate from bony fishes. *Carbohydrate Polymers,* 129**,** 143-147, https://doi.org/https://doi.org/10.1016/j.carbpol.2015.04.059

Mankin, H. J. and Lippiello, L. 1971. The glycosaminoglycans of normal and arthritic cartilage. *J Clin Invest,* 50**,** 1712-9, https://doi.org/10.1172/jci106660

Manzano, S.,Manzano, R.,Doblaré, M. and Doweidar, M. H. 2015. Altered swelling and ion fluxes in articular cartilage as a biomarker in osteoarthritis and joint immobilization: a computational analysis. *J R Soc Interface,* 12**,** 20141090, https://doi.org/10.1098/rsif.2014.1090

Manzoni, C.,Kia, D. A.,Vandrovcova, J.,Hardy, J.,Wood, N. W.,Lewis, P. A. and Ferrari, R. 2018. Genome, transcriptome and proteome: the rise of omics data and their integration in biomedical sciences. *Brief Bioinform,* 19**,** 286-302, https://doi.org/10.1093/bib/bbw114

Mariné-Casadó, R.,Domenech-Coca, C.,Fernández, S.,Costa, A.,Segarra, S.,López-Andreo, M. J.,Puiggròs, F.,Cerón, J. J.,Martínez-Puig, D.,Soler, C.,Sifre, V.,Serra, C. I. and Caimari, A. 2024. Effects of the oral administration of glycosaminoglycans with or without native type II collagen on the articular cartilage transcriptome in an osteoarthritic-induced rabbit model. *Genes & Nutrition,* 19**,** 19, https://doi.org/10.1186/s12263-024-00749-2

Maroudas, A.,Wachtel, E.,Grushko, G.,Katz, E. P. and Weinberg, P. 1991. The effect of osmotic and mechanical pressures on water partitioning in articular cartilage. *Biochim Biophys Acta,* 1073**,** 285-94, https://doi.org/10.1016/0304-4165(91)90133-2

Matsiko, A.,Levingstone, T. J.,O'Brien, F. J. and Gleeson, J. P. 2012. Addition of hyaluronic acid improves cellular infiltration and promotes early-stage chondrogenesis in a collagen-based scaffold for cartilage tissue engineering. *J Mech Behav Biomed Mater,* 11**,** 41-52, https://doi.org/10.1016/j.jmbbm.2011.11.012

Matsumura, F.,De Salegui, M.,Herp, A. and Pigman, W. 1963. The preparation of hyaluronic acid from bovine synovial fluid. *Biochim Biophys Acta,* 69**,** 574-6, https://doi.org/10.1016/0006-3002(63)91314-3

Mattson, J. M.,Turcotte, R. and Zhang, Y. 2017. Glycosaminoglycans contribute to extracellular matrix fiber recruitment and arterial wall mechanics. *Biomech Model Mechanobiol,* 16**,** 213-225, https://doi.org/10.1007/s10237-016-0811-4

Meier-Soelch, J.,Mayr-Buro, C.,Juli, J.,Leib, L.,Linne, U.,Dreute, J.,Papantonis, A.,Schmitz, M. L. and Kracht, M. 2021. Monitoring the Levels of Cellular NF-κB Activation States. *Cancers (Basel),* 13, https://doi.org/10.3390/cancers13215351

Mellai, M.,Casalone, C.,Corona, C.,Crociara, P.,Favole, A.,Cassoni, P.,Schiffer, D. and Boldorini, R. 2020. Chondroitin Sulphate Proteoglycans in the Tumour Microenvironment. *Adv Exp Med Biol,* 1272**,** 73-92, https://doi.org/10.1007/978-3-030-48457-6_5

Michel, G.,Pojasek, K.,Li, Y.,Sulea, T.,Linhardt, R. J.,Raman, R.,Prabhakar, V.,Sasisekharan, R. and Cygler, M. 2004. The structure of chondroitin B lyase complexed with glycosaminoglycan oligosaccharides unravels a calcium-dependent catalytic machinery. *J Biol Chem,* 279**,** 32882-96, https://doi.org/10.1074/jbc.M403421200

Michelacci, Y. M. and Horton, D. S. P. Q. 1989. Proteoglycans from the cartilage of young hammerhead shark Sphyrna lewini. *Comparative Biochemistry and Physiology Part B: Comparative Biochemistry,* 92**,** 651-658, https://doi.org/https://doi.org/10.1016/0305-0491(89)90245-9

Midwood, K. S. and Salter, D. M. 2001. NG2/HMPG modulation of human articular chondrocyte adhesion to type VI collagen is lost in osteoarthritis. *J Pathol,* 195**,** 631-5, https://doi.org/10.1002/path.985

Minina, E.,Kreschel, C.,Naski, M. C.,Ornitz, D. M. and Vortkamp, A. 2002. Interaction of FGF, Ihh/Pthlh, and BMP Signaling Integrates Chondrocyte Proliferation and Hypertrophic Differentiation. *Developmental Cell,* 3**,** 439-449, https://doi.org/https://doi.org/10.1016/S1534-5807(02)00261-7

Miosge, N.,Hartmann, M.,Maelicke, C. and Herken, R. 2004. Expression of collagen type I and type II in consecutive stages of human osteoarthritis. *Histochem Cell Biol,* 122**,** 229-36, https://doi.org/10.1007/s00418-004-0697-6

Monfort, J.,Tardif, G.,Reboul, P.,Mineau, F.,Roughley, P.,Pelletier, J.-P. and Martel-Pelletier, J. 2006. Degradation of small leucine-rich repeat proteoglycans by matrix metalloprotease-13: identification of a new biglycan cleavage site. *Arthritis Research & Therapy,* 8**,** R26, https://doi.org/10.1186/ar1873

Montreuil, J. 1980. Primary Structure of Glycoprotein Glycans Basis for the Molecular Biology of Glycoproteins. *In:* Tipson, R. S. & Horton, D. eds. *Advances in Carbohydrate Chemistry and Biochemistry.* Academic Press.

Mucci, A.,Schenetti, L. and Volpi, N. 2000. 1H and 13C nuclear magnetic resonance identification and characterization of components of chondroitin sulfates of various origin. *Carbohydrate Polymers,* 41**,** 37-45, https://doi.org/https://doi.org/10.1016/S0144-8617(99)00075-2

Mueller, M. B.,Fischer, M.,Zellner, J.,Berner, A.,Dienstknecht, T.,Kujat, R.,Prantl, L.,Nerlich, M.,Tuan, R. S. and Angele, P. 2013. Effect of parathyroid hormone-related protein in an in vitro hypertrophy model for mesenchymal

stem cell chondrogenesis. *Int Orthop,* 37**,** 945-51, https://doi.org/10.1007/s00264-013-1800-1

Mueller, M. B. and Tuan, R. S. 2011. Anabolic/Catabolic balance in pathogenesis of osteoarthritis: identifying molecular targets. *Pm r,* 3**,** S3-11, https://doi.org/10.1016/j.pmrj.2011.05.009

Murado, M. A.,Fraguas, J.,Montemayor, M. I.,Vázquez, J. A. and González, P. 2010. Preparation of highly purified chondroitin sulphate from skate (Raja clavata) cartilage by-products. Process optimization including a new procedure of alkaline hydroalcoholic hydrolysis. *Biochemical Engineering Journal,* 49**,** 126-132, https://doi.org/https://doi.org/10.1016/j.bej.2009.12.006

Murdoch, A. D.,Grady, L. M.,Ablett, M. P.,Katopodi, T.,Meadows, R. S. and Hardingham, T. E. 2007. Chondrogenic differentiation of human bone marrow stem cells in transwell cultures: generation of scaffold-free cartilage. *Stem Cells,* 25**,** 2786-96, https://doi.org/10.1634/stemcells.2007-0374

Nakano, T.,Betti, M. and Pietrasik, Z. 2010. Extraction, isolation and analysis of chondroitin sulfate glycosaminoglycans. *Recent Pat Food Nutr Agric,* 2**,** 61-74, https://doi.org/10.2174/2212798411002010061

Nandakumar, K. S. and Holmdahl, R. 2005. Efficient promotion of collagen antibody induced arthritis (CAIA) using four monoclonal antibodies specific for the major epitopes recognized in both collagen induced arthritis and rheumatoid arthritis. *Journal of Immunological Methods,* 304**,** 126-136, https://doi.org/https://doi.org/10.1016/j.jim.2005.06.017

Nandini, C. D.,Mikami, T.,Ohta, M.,Itoh, N.,Akiyama-Nambu, F. and Sugahara, K. 2004. Structural and Functional Characterization of Oversulfated Chondroitin Sulfate/Dermatan Sulfate Hybrid Chains from the Notochord of Hagfish: NEURITOGENIC AND BINDING ACTIVITIES FOR GROWTH FACTORS AND NEUROTROPHIC FACTORS*. *Journal of Biological Chemistry,* 279**,** 50799-50809, https://doi.org/https://doi.org/10.1074/jbc.M404746200

Nandini, C. D. and Sugahara, K. 2006a. Role of the sulfation pattern of chondroitin sulfate in its biological activities and in the binding of growth factors. *Adv Pharmacol,* 53**,** 253-79, https://doi.org/10.1016/s1054-3589(05)53012-6

Nandini, C. D. and Sugahara, K. 2006b. Role of the Sulfation Pattern of Chondroitin Sulfate in its Biological Activities and in the Binding of Growth Factors. *Advances in Pharmacology.* Academic Press.

Naven, M. A.,Zeef, L. A. H.,Li, S.,Humphreys, P. A.,Smith, C. A.,Pathiranage, D.,Cain, S.,Woods, S.,Bates, N.,Au, M.,Wen, C.,Kimber, S. J. and Meng, Q. J. 2022. Development of human cartilage circadian rhythm in a stem cell-chondrogenesis model. *Theranostics,* 12**,** 3963-3976, https://doi.org/10.7150/thno.70893

Nogueira, A. V.,Rossi, G. R.,Iacomini, M.,Sassaki, G. L.,Trindade, E. S. and Cipriani, T. R. 2019. Viscera of fishes as raw material for extraction of

glycosaminoglycans of pharmacological interest. *Int J Biol Macromol,* 121**,** 239-248, https://doi.org/10.1016/j.ijbiomac.2018.09.156

Ofman, D.,Slim, G. C.,Watt, D. K. and Yorke, S. C. 1997. Free radical induced oxidative depolymerisation of chondroitin sulphate and dermatan sulphate. *Carbohydrate Polymers,* 33**,** 47-56, https://doi.org/https://doi.org/10.1016/S0144-8617(97)00043-X

Ogata, S.-I. and Lloyd, K. O. 1982. Mild alkaline borohydride treatment of glycoproteins—A method for liberating both N- and O-linked carbohydrate chains. *Analytical Biochemistry,* 119**,** 351-359, https://doi.org/https://doi.org/10.1016/0003-2697(82)90597-8

Ogawa, H.,Hatano, S.,Sugiura, N.,Nagai, N.,Sato, T.,Shimizu, K.,Kimata, K.,Narimatsu, H. and Watanabe, H. 2012. Chondroitin sulfate synthase-2 is necessary for chain extension of chondroitin sulfate but not critical for skeletal development. *PLoS One,* 7**,** e43806, https://doi.org/10.1371/journal.pone.0043806

Ohnishi, T.,Tran, V.,Sao, K.,Ramteke, P.,Querido, W.,Barve, R. A.,van de Wetering, K. and Risbud, M. V. 2023. Loss of function mutation in Ank causes aberrant mineralization and acquisition of osteoblast-like-phenotype by the cells of the intervertebral disc. *Cell Death Dis,* 14**,** 447, https://doi.org/10.1038/s41419-023-05893-y

Oliver-Ferrándiz, M.,Milián, L.,Sancho-Tello, M.,Martín de Llano, J. J.,Gisbert Roca, F.,Martínez-Ramos, C.,Carda, C. and Mata, M. 2021. Alginate-Agarose Hydrogels Improve the In Vitro Differentiation of Human Dental Pulp Stem Cells in Chondrocytes. A Histological Study. *Biomedicines,* 9, https://doi.org/10.3390/biomedicines9070834

Olson, S. A.,Furman, B. and Guilak, F. 2012. Joint injury and post-traumatic arthritis. *Hss j,* 8**,** 23-5, https://doi.org/10.1007/s11420-011-9247-7

Opdensteinen, P.,Clodt, J. I.,Müschen, C. R.,Filiz, V. and Buyel, J. F. 2019. A Combined Ultrafiltration/Diafiltration Step Facilitates the Purification of Cyanovirin-N From Transgenic Tobacco Extracts. 6, https://doi.org/10.3389/fbioe.2018.00206

Ou, Y.,Zhu, L.,Wei, X.,Bai, S.,Chen, M.,Chen, H. and Zhang, J. 2020. Circular RNA circ_0111277 attenuates human trophoblast cell invasion and migration by regulating miR-494/HTRA1/Notch-1 signal pathway in pre-eclampsia. *Cell Death & Disease,* 11**,** 479, https://doi.org/10.1038/s41419-020-2679-6

Owen, G. R.,Meredith, D. O.,ap Gwynn, I. and Richards, R. G. 2005. Focal adhesion quantification - a new assay of material biocompatibility? Review. *Eur Cell Mater,* 9**,** 85-96; discussion 85-96, https://doi.org/10.22203/ecm.v009a10

Pelletier, J. P.,Raynauld, J. P.,Beaulieu, A. D.,Bessette, L.,Morin, F.,de Brum-Fernandes, A. J.,Delorme, P.,Dorais, M.,Paiement, P.,Abram, F. and Martel-Pelletier, J. 2016. Chondroitin sulfate efficacy versus celecoxib on knee

osteoarthritis structural changes using magnetic resonance imaging: a 2-year multicentre exploratory study. *Arthritis Res Ther,* 18**,** 256, https://doi.org/10.1186/s13075-016-1149-0

Perez, S.,Makshakova, O.,Angulo, J.,Bedini, E.,Bisio, A.,de Paz, J. L.,Fadda, E.,Guerrini, M.,Hricovini, M.,Hricovini, M.,Lisacek, F.,Nieto, P. M.,Pagel, K.,Paiardi, G.,Richter, R.,Samsonov, S. A.,Vivès, R. R.,Nikitovic, D. and Ricard Blum, S. 2023. Glycosaminoglycans: What Remains To Be Deciphered? *JACS Au,* 3**,** 628-656, https://doi.org/10.1021/jacsau.2c00569

Piazza, F.,Ravaglia, B.,Caporale, A.,Svetić, A.,Parisse, P.,Asaro, F.,Grassi, G.,Secco, L.,Sgarra, R.,Marsich, E.,Donati, I. and Sacco, P. 2024. Elucidating the unexpected cell adhesive properties of agarose substrates. The effect of mechanics, fetal bovine serum and specific peptide sequences. *Acta Biomaterialia,* 189**,** 286-297, https://doi.org/https://doi.org/10.1016/j.actbio.2024.09.042

Pomin, V. H.,Piquet, A. A.,Pereira, M. S. and Mourão, P. A. S. 2012. Residual keratan sulfate in chondroitin sulfate formulations for oral administration. *Carbohydrate Polymers,* 90**,** 839-846, https://doi.org/https://doi.org/10.1016/j.carbpol.2012.06.009

Poole, A. R.,Kojima, T.,Yasuda, T.,Mwale, F.,Kobayashi, M. and Laverty, S. 2001. Composition and structure of articular cartilage: a template for tissue repair. *Clin Orthop Relat Res***,** S26-33, https://doi.org/10.1097/00003086-200110001-00004

Posey, K. L.,Coustry, F. and Hecht, J. T. 2018. Cartilage oligomeric matrix protein: COMPopathies and beyond. *Matrix Biol,* 71-72**,** 161-173, https://doi.org/10.1016/j.matbio.2018.02.023

Pramanick, D.,Forstová, J. and Pivec, L. 1976. 4 M guanidine hydrochloride applied to the isolation of DNA from different sources. *FEBS Lett,* 62**,** 81-4, https://doi.org/10.1016/0014-5793(76)80021-x

Prydz, K. 2015. Determinants of Glycosaminoglycan (GAG) Structure. *Biomolecules,* 5**,** 2003-22, https://doi.org/10.3390/biom5032003

Pullig, O.,Weseloh, G. and Swoboda, B. 1999. Expression of type VI collagen in normal and osteoarthritic human cartilage. *Osteoarthritis Cartilage,* 7**,** 191-202, https://doi.org/10.1053/joca.1998.0208

Qing, C.,Wei-ding, C. and Wei-min, F. 2011. Co-culture of chondrocytes and bone marrow mesenchymal stem cells in vitro enhances the expression of cartilaginous extracellular matrix components. *Braz J Med Biol Res,* 44**,** 303-10, https://doi.org/10.1590/s0100-879x2011007500026

Radin, E. L.,Swann, D. A. and Weisser, P. A. 1970. Separation of a hyaluronate-free lubricating fraction from synovial fluid. *Nature,* 228**,** 377-8, https://doi.org/10.1038/228377a0

Rajasekaran, S.,Tangavel, C.,Djuric, N.,Raveendran, M.,Soundararajan, D. C. R.,Nayagam, S. M.,Matchado, M. S. and Anand, K. 2020. Part 1: profiling extra cellular matrix core proteome of human fetal nucleus pulposus in search for regenerative targets. *Sci Rep,* 10**,** 15684, https://doi.org/10.1038/s41598-020-72859-x

Rasoulianboroujeni, M.,Kiaie, N.,Tabatabaei, F. S.,Yadegari, A.,Fahimipour, F.,Khoshroo, K. and Tayebi, L. 2018. Dual Porosity Protein-based Scaffolds with Enhanced Cell Infiltration and Proliferation. *Scientific Reports,* 8**,** 14889, https://doi.org/10.1038/s41598-018-33245-w

Reed, D. A.,Zhao, Y.,Han, M.,Mercuri, L. G. and Miloro, M. 2021. Mechanical Loading Disrupts Focal Adhesion Kinase Activation in Mandibular Fibrochondrocytes During Murine Temporomandibular Joint Osteoarthritis. *J Oral Maxillofac Surg,* 79**,** 2058.e1-2058.e15, https://doi.org/10.1016/j.joms.2021.05.001

Reginster, J.-Y. and Veronese, N. 2021a. Highly purified chondroitin sulfate: a literature review on clinical efficacy and pharmacoeconomic aspects in osteoarthritis treatment. *Aging Clinical and Experimental Research,* 33**,** 37-47, https://doi.org/10.1007/s40520-020-01643-8

Reginster, J. Y. and Veronese, N. 2021b. Highly purified chondroitin sulfate: a literature review on clinical efficacy and pharmacoeconomic aspects in osteoarthritis treatment. *Aging Clin Exp Res,* 33**,** 37-47, https://doi.org/10.1007/s40520-020-01643-8

Rigueur, D. and Lyons, K. M. 2014. Whole-mount skeletal staining. *Methods Mol Biol,* 1130**,** 113-121, https://doi.org/10.1007/978-1-62703-989-5_9

Roberts, S. R.,Knight, M. M.,Lee, D. A. and Bader, D. L. 2001. Mechanical compression influences intracellular Ca2+ signaling in chondrocytes seeded in agarose constructs. *J Appl Physiol (1985),* 90**,** 1385-91, https://doi.org/10.1152/jappl.2001.90.4.1385

Robey, P. G.,Kuznetsov, S. A.,Riminucci, M. and Bianco, P. 2014. Bone marrow stromal cell assays: in vitro and in vivo. *Methods Mol Biol,* 1130**,** 279-293, https://doi.org/10.1007/978-1-62703-989-5_21

Roedig, H.,Nastase, M. V.,Wygrecka, M. and Schaefer, L. 2019. Breaking down chronic inflammatory diseases: the role of biglycan in promoting a switch between inflammation and autophagy. *Febs j,* 286**,** 2965-2979, https://doi.org/10.1111/febs.14791

Roggio, F.,Petrigna, L.,Trovato, B.,Di Rosa, M. and Musumeci, G. 2023. The Role of Lubricin, Irisin and Exercise in the Prevention and Treatment of Osteoarthritis. *Int J Mol Sci,* 24, https://doi.org/10.3390/ijms24065126

Ronca, F.,Palmieri, L.,Panicucci, P. and Ronca, G. 1998. Anti-inflammatory activity of chondroitin sulfate. *Osteoarthritis Cartilage,* 6 Suppl A**,** 14-21, https://doi.org/10.1016/s1063-4584(98)80006-x

Roncada, T.,Bonithon, R.,Blunn, G. and Roldo, M. 2022. Soft substrates direct stem cell differentiation into the chondrogenic lineage without the use of growth factors. *J Tissue Eng,* 13**,** 20417314221122121, https://doi.org/10.1177/20417314221122121

Roughley, P. J. and Mort, J. S. 2014. The role of aggrecan in normal and osteoarthritic cartilage. *J Exp Orthop,* 1**,** 8, https://doi.org/10.1186/s40634-014-0008-7

Ruensodsai, T.,Panakkal, E. J.,Teerapornnarong, P.,Rodiahwati, W.,Sriariyanun, M. and Rattanaporn, K. J. E. S. W. C. 2021. Optimization of Enzyme Assisted Extraction of Chondroitin Sulfate from Bohadschia argus by Response Surface Methodology. 302**,** 02012,

Ruiter, F. A. A.,King, J.,Swapnasrita, S.,Giselbrecht, S.,Truckenmüller, R.,LaPointe, V. L. S.,Baker, M. B. and Carlier, A. 2023. Optimization of Media Change Intervals through Hydrogels Using Mathematical Models. *Biomacromolecules,* 24**,** 604-612, https://doi.org/10.1021/acs.biomac.2c00961

Ruiz-Romero, V.,Toledano-Serrabona, J. and Gay-Escoda, C. 2025. Efficacy of the use of chondroitin sulphate and glucosamine for the treatment of temporomandibular joint dysfunction: A systematic review and meta-analysis. *Cranio,* 43**,** 60-69, https://doi.org/10.1080/08869634.2022.2076796

Sapra., A. N. A. 2021. *Histology, Chondrocytes* [Online]. StatPearls: Treasure Island (FL). Available: https://www.ncbi.nlm.nih.gov/books/NBK557576/ [Accessed 15/5 2021].

Sauerland, K. and Steinmeyer, J. 2007. Intermittent mechanical loading of articular cartilage explants modulates chondroitin sulfate fine structure. *Osteoarthritis and Cartilage,* 15**,** 1403-1409, https://doi.org/https://doi.org/10.1016/j.joca.2007.05.004

Sechriest, V. F.,Miao, Y. J.,Niyibizi, C.,Westerhausen-Larson, A.,Matthew, H. W.,Evans, C. H.,Fu, F. H. and Suh, J. K. 2000. GAG-augmented polysaccharide hydrogel: a novel biocompatible and biodegradable material to support chondrogenesis. *J Biomed Mater Res,* 49**,** 534-41, https://doi.org/10.1002/(sici)1097-4636(20000315)49:4<534::aid-jbm12>3.0.co;2-#

Segarra-Queralt, M.,Neidlin, M.,Tio, L.,Monfort, J.,Monllau, J. C.,González Ballester, M. Á.,Alexopoulos, L. G.,Piella, G. and Noailly, J. 2022. Regulatory network-based model to simulate the biochemical regulation of chondrocytes in healthy and osteoarthritic environments. *Scientific Reports,* 12**,** 3856, https://doi.org/10.1038/s41598-022-07776-2

Seo, S. and Na, K. 2011. Mesenchymal stem cell-based tissue engineering for chondrogenesis. *J Biomed Biotechnol,* 2011**,** 806891, https://doi.org/10.1155/2011/806891

Shakibaei, M. 1998. Inhibition of chondrogenesis by integrin antibody in vitro. *Exp Cell Res,* 240**,** 95-106, https://doi.org/10.1006/excr.1998.3933

Sharma, A.,Wood, L. D.,Richardson, J. B.,Roberts, S. and Kuiper, N. J. 2007. Glycosaminoglycan profiles of repair tissue formed following autologous chondrocyte implantation differ from control cartilage. *Arthritis Research & Therapy,* 9**,** R79, https://doi.org/10.1186/ar2278

Sharma, R.,Kuche, K.,Thakor, P.,Bhavana, V.,Srivastava, S.,Mehra, N. K. and Jain, S. 2022. Chondroitin Sulfate: Emerging biomaterial for biopharmaceutical purpose and tissue engineering. *Carbohydr Polym,* 286**,** 119305, https://doi.org/10.1016/j.carbpol.2022.119305

Shen, G. 2005. The role of type X collagen in facilitating and regulating endochondral ossification of articular cartilage. *Orthod Craniofac Res,* 8**,** 11-7, https://doi.org/10.1111/j.1601-6343.2004.00308.x

Shi, Y.-g.,Meng, Y.-c.,Li, J.-r.,Chen, J.,Liu, Y.-h. and Bai, X. 2014. Chondroitin sulfate: extraction, purification, microbial and chemical synthesis. *Journal of Chemical Technology & Biotechnology,* 89**,** 1445-1465, https://doi.org/https://doi.org/10.1002/jctb.4454

Shibata, Y.,Tanaka, Y.,Sasakura, H.,Morioka, Y.,Sassa, T.,Fujii, S.,Mitsuzumi, K.,Ikeno, M.,Kubota, Y.,Kimura, K.,Toyoda, H.,Takeuchi, K. and Nishiwaki, K. 2024. Endogenous chondroitin extends the lifespan and healthspan in C. elegans. *Scientific Reports,* 14**,** 4813, https://doi.org/10.1038/s41598-024-55417-7

Shu, C.,Hughes, C.,Smith, S. M.,Smith, M. M.,Hayes, A.,Caterson, B.,Little, C. B. and Melrose, J. 2013. The ovine newborn and human foetal intervertebral disc contain perlecan and aggrecan variably substituted with native 7D4 CS sulphation motif: spatiotemporal immunolocalisation and co-distribution with Notch-1 in the human foetal disc. *Glycoconj J,* 30**,** 717-25, https://doi.org/10.1007/s10719-013-9475-9

Silva, L. C. F. 2006. Isolation and Purification of Chondroitin Sulfate. *Advances in Pharmacology.* Academic Press.

Sim, J.-S.,Im, A. R.,Cho, S. M.,Jang, H. J.,Jo, J. H. and Kim, Y. S. 2007. Evaluation of chondroitin sulfate in shark cartilage powder as a dietary supplement: Raw materials and finished products. *Food Chemistry,* 101**,** 532-539, https://doi.org/https://doi.org/10.1016/j.foodchem.2006.02.011

Simental-Mendía, M.,Sánchez-García, A.,Vilchez-Cavazos, F.,Acosta-Olivo, C. A.,Peña-Martínez, V. M. and Simental-Mendía, L. E. 2018. Effect of glucosamine and chondroitin sulfate in symptomatic knee osteoarthritis: a systematic review and meta-analysis of randomized placebo-controlled trials. *Rheumatol Int,* 38**,** 1413-1428, https://doi.org/10.1007/s00296-018-4077-2

Sip, C. G.,Bhattacharjee, N. and Folch, A. 2014. Microfluidic transwell inserts for generation of tissue culture-friendly gradients in well plates. *Lab Chip,* 14**,** 302-14, https://doi.org/10.1039/c3lc51052b

Sommer, R. J. 2020. Phenotypic Plasticity: From Theory and Genetics to Current and Future Challenges. *Genetics,* 215**,** 1-13, https://doi.org/10.1534/genetics.120.303163

Sophia Fox, A. J.,Bedi, A. and Rodeo, S. A. 2009. The basic science of articular cartilage: structure, composition, and function. *Sports Health,* 1**,** 461-8, https://doi.org/10.1177/1941738109350438

Sorkin, R.,Kampf, N.,Dror, Y.,Shimoni, E. and Klein, J. 2013. Origins of extreme boundary lubrication by phosphatidylcholine liposomes. *Biomaterials,* 34**,** 5465-75, https://doi.org/10.1016/j.biomaterials.2013.03.098

Sorrell, J. M.,Lintala, A. M.,Mahmoodian, F. and Caterson, B. 1988a. Epitope-specific changes in chondroitin sulfate/dermatan sulfate proteoglycans as markers in the lymphopoietic and granulopoietic compartments of developing bursae of Fabricius. *J Immunol,* 140**,** 4263-70,

Sorrell, J. M.,Mahmoodian, F. and Caterson, B. 1988b. Immunochemical characterization and ultrastructural localization of chondroitin sulfates and keratan sulfate in embryonic chick bone marrow. *Cell Tissue Res,* 252**,** 523-31, https://doi.org/10.1007/bf00216639

Stabler, T.,Montell, E.,Verges, J. and Kraus, V. B. 2015. Attentuation of hyaluronan fragment induced inflammatory response in macrophages by chondroitin sulphate. *Osteoarthritis and Cartilage,* 23**,** A263-A264, https://doi.org/10.1016/j.joca.2015.02.481

Struijk, C.,Korpershoek, J.,Lydon, K. L.,Verdonk, P.,Michielsen, J.,Krych, A. J.,Vonk, L. A. and Saris, D. B. F. 2024. Identification and culture of meniscons, meniscus cells with their pericellular matrix. *Cytotherapy*, https://doi.org/10.1016/j.jcyt.2024.08.006

Sugahara, K.,Mikami, T.,Uyama, T.,Mizuguchi, S.,Nomura, K. and Kitagawa, H. 2003. Recent advances in the structural biology of chondroitin sulfate and dermatan sulfate. *Curr Opin Struct Biol,* 13**,** 612-20, https://doi.org/10.1016/j.sbi.2003.09.011

Sun, M.,Luo, E. Y.,Adams, S. M.,Adams, T.,Ye, Y.,Shetye, S. S.,Soslowsky, L. J. and Birk, D. E. 2020. Collagen XI regulates the acquisition of collagen fibril structure, organization and functional properties in tendon. *Matrix Biol,* 94**,** 77-94, https://doi.org/10.1016/j.matbio.2020.09.001

Sun, M. M. and Beier, F. 2014. Chondrocyte hypertrophy in skeletal development, growth, and disease. *Birth Defects Res C Embryo Today,* 102**,** 74-82, https://doi.org/10.1002/bdrc.21062

Sun, Z.,Guo, S. S. and Fässler, R. 2016. Integrin-mediated mechanotransduction. *J Cell Biol,* 215**,** 445-456, https://doi.org/10.1083/jcb.201609037

Sundaresan, G.,Abraham, R. J. J.,Appa Rao, V.,Narendra Babu, R.,Govind, V. and Meti, M. F. 2018. Established method of chondroitin sulphate extraction from

buffalo (Bubalus bubalis) cartilages and its identification by FTIR. *J Food Sci Technol,* 55**,** 3439-3445, https://doi.org/10.1007/s13197-018-3253-4

Suzawa, Y.,Kubo, N.,Iwai, S.,Yura, Y.,Ohgushi, H. and Akashi, M. 2015. Biomineral/Agarose Composite Gels Enhance Proliferation of Mesenchymal Stem Cells with Osteogenic Capability. *Int J Mol Sci,* 16**,** 14245-58, https://doi.org/10.3390/ijms160614245

Tallheden, T.,Dennis, J. E.,Lennon, D. P.,Sjögren-Jansson, E.,Caplan, A. I. and Lindahl, A. 2003. Phenotypic plasticity of human articular chondrocytes. *J Bone Joint Surg Am,* 85-A Suppl 2**,** 93-100, https://doi.org/10.2106/00004623-200300002-00012

Tao, L.,Song, F.,Xu, N.,Li, D.,Linhardt, R. J. and Zhang, Z. 2017. New insights into the action of bacterial chondroitinase AC I and hyaluronidase on hyaluronic acid. *Carbohydr Polym,* 158**,** 85-92, https://doi.org/10.1016/j.carbpol.2016.12.010

Tatara, Y.,Suto, S.,Sasaki, Y. and Endo, M. 2015. Preparation of proteoglycan from salmon nasal cartilage under nondenaturing conditions. *Biosci Biotechnol Biochem,* 79**,** 1615-8, https://doi.org/10.1080/09168451.2015.1044933

Theocharis, A. D.,Karamanos, N. K.,Papageorgakopoulou, N.,Tsiganos, C. P. and Theocharis, D. A. 2002. Isolation and characterization of matrix proteoglycans from human nasal cartilage. Compositional and structural comparison between normal and scoliotic tissues. *Biochim Biophys Acta,* 1569**,** 117-26, https://doi.org/10.1016/s0304-4165(01)00242-2

Tian, Z.,Jiang, F. and Zhu, S. 2024. Quantitative determination of chondroitin sulfate with various molecular weights in raw materials by pre-column derivatization with 6-aminoquinolyl-N-hydroxysuccinimidyl carbamate. *Food Chemistry,* 440**,** 138273, https://doi.org/https://doi.org/10.1016/j.foodchem.2023.138273

Ticar, B. F.,Rohmah, Z.,Neri, T. A. N.,Pahila, I. G.,Vasconcelos, A.,Archer-Hartmann, S. A.,Reiter, C. E. N.,Dobruchowska, J. M.,Choi, B. D.,Heiss, C.,Azadi, P. and Pomin, V. H. 2020. Biocompatibility and structural characterization of glycosaminoglycans isolated from heads of silver-banded whiting (Sillago argentifasciata Martin & Montalban 1935). *Int J Biol Macromol,* 151**,** 663-676, https://doi.org/10.1016/j.ijbiomac.2020.02.160

Tsang, K. Y.,Chan, D. and Cheah, K. S. 2015. Fate of growth plate hypertrophic chondrocytes: death or lineage extension? *Dev Growth Differ,* 57**,** 179-92, https://doi.org/10.1111/dgd.12203

Ullah, F.,Javed, F.,Mushtaq, I.,Rahman, L.-u.,Ahmed, N.,Din, I. U.,Alotaibi, M. A.,Alharthi, A. I.,Ahmad, A.,Bakht, M. A.,Khan, F. and Tasleem, S. 2023. Development of highly-reproducible hydrogel based bioink for regeneration of skin-tissues via 3-D bioprinting technology. *International Journal of Biological Macromolecules,* 230**,** 123131, https://doi.org/https://doi.org/10.1016/j.ijbiomac.2022.123131

Ürgeová, E. and Vulganová, K. J. N. B. e. C. 2016. Comparison of Enzymatic Hydrolysis of Polysaccharides from Eggshells Membranes. 15**,** 133 - 141,

Uzieliene, I.,Bagdonas, E.,Hoshi, K.,Sakamoto, T.,Hikita, A.,Tachtamisevaite, Z.,Rakauskiene, G.,Kvederas, G.,Mobasheri, A. and Bernotiene, E. 2021. Different phenotypes and chondrogenic responses of human menstrual blood and bone marrow mesenchymal stem cells to activin A and TGF-β3. *Stem Cell Research & Therapy,* 12**,** 251, https://doi.org/10.1186/s13287-021-02286-w

Uzieliene, I.,Bironaite, D.,Pachaleva, J.,Bagdonas, E.,Sobolev, A.,Tsai, W. B.,Kvedaras, G. and Bernotiene, E. 2023. Chondroitin Sulfate-Tyramine-Based Hydrogels for Cartilage Tissue Repair. *Int J Mol Sci,* 24, https://doi.org/10.3390/ijms24043451

Vallières, M. and du Souich, P. 2010. Modulation of inflammation by chondroitin sulfate. *Osteoarthritis Cartilage,* 18 Suppl 1**,** S1-6, https://doi.org/10.1016/j.joca.2010.02.017

van Meerloo, J.,Kaspers, G. J. and Cloos, J. 2011. Cell sensitivity assays: the MTT assay. *Methods Mol Biol,* 731**,** 237-45, https://doi.org/10.1007/978-1-61779-080-5_20

Vandrovcová, M.,Douglas, T.,Hauk, D.,Grössner-Schreiber, B.,Wiltfang, J.,Bačáková, L. and Warnke, P. H. 2011. Influence of collagen and chondroitin sulfate (CS) coatings on poly-(lactide-co-glycolide) (PLGA) on MG 63 osteoblast-like cells. *Physiol Res,* 60**,** 797-813, https://doi.org/10.33549/physiolres.931994

Vasconcelos Oliveira, A. P.,de Abreu Feitosa, V.,de Oliveira, J. M.,Coelho, A. L.,de Araújo P. Vieira, L.,de Assis Rocha da Silva, F.,de Assis Avelino Figueredo Sobrinho, F.,Duarte, E. B.,de Souza, B. W. and de sá Moreira de Souza Filho, M. 2017. Characteristics of Chondroitin Sulfate Extracted of Tilapia (Oreochromis niloticus) Processing. *Procedia Engineering,* 200**,** 193-199, https://doi.org/https://doi.org/10.1016/j.proeng.2017.07.028

Vassallo, V.,Tsianaka, A.,Alessio, N.,Grübel, J.,Cammarota, M.,Tovar, G. E. M.,Southan, A. and Schiraldi, C. 2022. Evaluation of novel biomaterials for cartilage regeneration based on gelatin methacryloyl interpenetrated with extractive chondroitin sulfate or unsulfated biotechnological chondroitin. *J Biomed Mater Res A,* 110**,** 1210-1223, https://doi.org/10.1002/jbm.a.37364

Vázquez, J. A.,Blanco, M.,Fraguas, J.,Pastrana, L. and Pérez-Martín, R. 2016. Optimisation of the extraction and purification of chondroitin sulphate from head by-products of Prionace glauca by environmental friendly processes. *Food Chemistry,* 198**,** 28-35, https://doi.org/https://doi.org/10.1016/j.foodchem.2015.10.087

Vázquez, J. A.,Fraguas, J.,Novoa-Carvallal, R.,Reis, R. L.,Antelo, L. T.,Pérez-Martín, R. I. and Valcarcel, J. 2018. Isolation and Chemical Characterization of Chondroitin Sulfate from Cartilage By-Products of Blackmouth Catshark (Galeus melastomus). *Mar Drugs,* 16, https://doi.org/10.3390/md16100344

Vinatier, C. and Guicheux, J. 2016. Cartilage tissue engineering: From biomaterials and stem cells to osteoarthritis treatments. *Annals of Physical and Rehabilitation Medicine,* 59**,** 139-144, https://doi.org/https://doi.org/10.1016/j.rehab.2016.03.002

Vining, K. H. and Mooney, D. J. 2017. Mechanical forces direct stem cell behaviour in development and regeneration. *Nat Rev Mol Cell Biol,* 18**,** 728-742, https://doi.org/10.1038/nrm.2017.108

Volpi, N. 1996. Purification of heparin, dermatan sulfate and chondroitin sulfate from mixtures by sequential precipitation with various organic solvents. *J Chromatogr B Biomed Appl,* 685**,** 27-34, https://doi.org/10.1016/0378-4347(96)00154-5

Volpi, N. 2019. Chondroitin Sulfate Safety and Quality. *Molecules,* 24, https://doi.org/10.3390/molecules24081447

Volpi, N. and Maccari, F. 2003. Purification and characterization of hyaluronic acid from the mollusc bivalve Mytilus galloprovincialis. *Biochimie,* 85**,** 619-625, https://doi.org/https://doi.org/10.1016/S0300-9084(03)00083-X

Waller, K. A.,Zhang, L. X.,Elsaid, K. A.,Fleming, B. C.,Warman, M. L. and Jay, G. D. 2013. Role of lubricin and boundary lubrication in the prevention of chondrocyte apoptosis. *Proc Natl Acad Sci U S A,* 110**,** 5852-7, https://doi.org/10.1073/pnas.1219289110

Wang, D. A.,Varghese, S.,Sharma, B.,Strehin, I.,Fermanian, S.,Gorham, J.,Fairbrother, D. H.,Cascio, B. and Elisseeff, J. H. 2007. Multifunctional chondroitin sulphate for cartilage tissue-biomaterial integration. *Nat Mater,* 6**,** 385-92, https://doi.org/10.1038/nmat1890

Wang, K.,Ma, C.,Feng, J. Q. and Jing, Y. 2022a. The Emerging Role of Cell Transdifferentiation in Skeletal Development and Diseases. *Int J Mol Sci,* 23, https://doi.org/10.3390/ijms23115974

Wang, P. and Tang, J. 2009. Solvent-free mechanochemical extraction of chondroitin sulfate from shark cartilage. *Chemical Engineering and Processing: Process Intensification,* 48**,** 1187-1191, https://doi.org/https://doi.org/10.1016/j.cep.2009.04.003

Wang, W.,Shi, L.,Qin, Y. and Li, F. 2020. Research and Application of Chondroitin Sulfate/Dermatan Sulfate-Degrading Enzymes. *Front Cell Dev Biol,* 8**,** 560442, https://doi.org/10.3389/fcell.2020.560442

Wang, W.,Ye, R.,Xie, W.,Zhang, Y.,An, S.,Li, Y. and Zhou, Y. 2022b. Roles of the calcified cartilage layer and its tissue engineering reconstruction in osteoarthritis treatment. *Front Bioeng Biotechnol,* 10**,** 911281, https://doi.org/10.3389/fbioe.2022.911281

Wang, X.,He, W.,Huang, H.,Han, J.,Wang, R.,Li, H.,Long, Y.,Wang, G. and Han, X. 2024. Recent Advances in Hydrogel Technology in Delivering Mesenchymal

Stem Cell for Osteoarthritis Therapy. *Biomolecules,* 14, https://doi.org/10.3390/biom14070858

Wang, Y.,Ahmadi, S.,Yu, C.,Zhang, L.,Hu, X.,Ye, X. and Chen, S. 2022c. A rapid method for extraction, purification and structure analysis of chondroitin sulfate from six marine tissues. *Food Quality and Safety,* 6, https://doi.org/10.1093/fqsafe/fyac057

Wann, A. K.,Zuo, N.,Haycraft, C. J.,Jensen, C. G.,Poole, C. A.,McGlashan, S. R. and Knight, M. M. 2012. Primary cilia mediate mechanotransduction through control of ATP-induced Ca2+ signaling in compressed chondrocytes. *Faseb j,* 26**,** 1663-71, https://doi.org/10.1096/fj.11-193649

Wei, B.,Xu, Y.,Tang, C.,Liu, N. Q.,Li, X.,Yao, Q. and Wang, L. 2024. An injectable active hydrogel based on BMSC-derived extracellular matrix for cartilage regeneration enhancement. *Biomaterials Advances,* 160**,** 213857, https://doi.org/https://doi.org/10.1016/j.bioadv.2024.213857

Weissenberger, M.,Weissenberger, M. H.,Gilbert, F.,Groll, J.,Evans, C. H. and Steinert, A. F. 2020. Reduced hypertrophy in vitro after chondrogenic differentiation of adult human mesenchymal stem cells following adenoviral SOX9 gene delivery. *BMC Musculoskelet Disord,* 21**,** 109, https://doi.org/10.1186/s12891-020-3137-4

Wright, C. W.,Li, N.,Shaffer, L.,Hill, A.,Boyer, N.,Alves, S. E.,Venkataraman, S.,Biswas, K.,Lieberman, L. A. and Mohammadi, S. 2023. Establishment of a 96-well transwell system using primary human gut organoids to capture multiple quantitative pathway readouts. *Sci Rep,* 13**,** 16357, https://doi.org/10.1038/s41598-023-43656-z

Wu, L.,Leijten, J. C. H.,Georgi, N.,Post, J. N.,van Blitterswijk, C. A. and Karperien, M. 2011. Trophic Effects of Mesenchymal Stem Cells Increase Chondrocyte Proliferation and Matrix Formation. 17**,** 1425-1436, https://doi.org/10.1089/ten.tea.2010.0517

Wu, M.,Chen, G. and Li, Y.-P. 2016. TGF-β and BMP signaling in osteoblast, skeletal development, and bone formation, homeostasis and disease. *Bone Research,* 4**,** 16009, https://doi.org/10.1038/boneres.2016.9

Wu, M.,Wu, S.,Chen, W. and Li, Y.-P. 2024a. The roles and regulatory mechanisms of TGF-β and BMP signaling in bone and cartilage development, homeostasis and disease. *Cell Research,* 34**,** 101-123, https://doi.org/10.1038/s41422-023-00918-9

Wu, R.,Fan, X.,Wang, Y.,Shen, M.,Zheng, Y.,Zhao, S. and Yang, L. 2022. Mesenchymal Stem Cell-Derived Extracellular Vesicles in Liver Immunity and Therapy. 13, https://doi.org/10.3389/fimmu.2022.833878

Wu, Y.,Lyu, Z.,Hu, F.,Yang, L.,Yang, K.,Chen, M. and Wang, Y. 2024b. A chondroitin sulphate hydrogel with sustained release of SDF-1α for extensive cartilage defect repair through induction of cell homing and promotion of

chondrogenesis. *J Mater Chem B,* 12**,** 8672-8687, https://doi.org/10.1039/d4tb00624k

Wu, Y.,Yang, Z.,Law, J. B.,He, A. Y.,Abbas, A. A.,Denslin, V.,Kamarul, T.,Hui, J. H. and Lee, E. H. 2017. The Combined Effect of Substrate Stiffness and Surface Topography on Chondrogenic Differentiation of Mesenchymal Stem Cells. *Tissue Eng Part A,* 23**,** 43-54, https://doi.org/10.1089/ten.TEA.2016.0123

Wu, Z.,Korntner, S. H.,Mullen, A. M. and Zeugolis, D. I. 2021. Collagen type II: From biosynthesis to advanced biomaterials for cartilage engineering. *Biomaterials and Biosystems,* 4**,** 100030, https://doi.org/https://doi.org/10.1016/j.bbiosy.2021.100030

Yamabe, D.,Murakami, H.,Chokan, K.,Endo, H.,Oikawa, R.,Sawamura, S. and Doita, M. 2017. Evaluation of Water Content in Lumbar Intervertebral Discs and Facet Joints Before and After Physiological Loading Using T2 Mapping MRI. *Spine (Phila Pa 1976),* 42**,** E1423-e1428, https://doi.org/10.1097/brs.0000000000002204

Yang, J.,Price, M. A.,Neudauer, C. L.,Wilson, C.,Ferrone, S.,Xia, H.,Iida, J.,Simpson, M. A. and McCarthy, J. B. 2004. Melanoma chondroitin sulfate proteoglycan enhances FAK and ERK activation by distinct mechanisms. *J Cell Biol,* 165**,** 881-91, https://doi.org/10.1083/jcb.200403174

Yang, K.-C.,Yang, Y.-T.,Wu, C.-C.,Hsiao, J.-K.,Huang, C.-Y.,Chen, I.-H. and Wang, C.-C. 2023. Bioinspired collagen-gelatin-hyaluronic acid-chondroitin sulfate tetra-copolymer scaffold biomimicking native cartilage extracellular matrix facilitates chondrogenesis of human synovium-derived stem cells. *International Journal of Biological Macromolecules,* 240**,** 124400, https://doi.org/https://doi.org/10.1016/j.ijbiomac.2023.124400

Yang, K. R.,Tsai, M. F.,Shieh, C. J.,Arakawa, O.,Dong, C. D.,Huang, C. Y. and Kuo, C. H. 2021. Ultrasonic-Assisted Extraction and Structural Characterization of Chondroitin Sulfate Derived from Jumbo Squid Cartilage. *Foods,* 10, https://doi.org/10.3390/foods10102363

Yang, L.,Li, W.,Zhao, Y. and Shang, L. 2024a. Magnetic Polysaccharide Mesenchymal Stem Cells Exosomes Delivery Microcarriers for Synergistic Therapy of Osteoarthritis. *ACS Nano*, https://doi.org/10.1021/acsnano.4c01406

Yang, Q.,Liu, G.,Chen, G.,Chen, G.,Chen, K.,Fan, L.,Tu, Y.,Chen, J.,Shi, Z.,Chen, C.,Liu, S.,Deng, G.,Deng, X.,Sun, C.,Li, X.,Yang, S.,Zheng, S. and Chen, B. 2024b. Novel injectable adhesive hydrogel loaded with exosomes for holistic repair of hemophilic articular cartilage defect. *Bioact Mater,* 42**,** 85-111, https://doi.org/10.1016/j.bioactmat.2024.08.018

Yao, Y. and Wang, C. 2020. Dedifferentiation: inspiration for devising engineering strategies for regenerative medicine. *npj Regenerative Medicine,* 5**,** 14, https://doi.org/10.1038/s41536-020-00099-8

Yeh, M. L.,Chang, G. M. and Juang, Y. J. 2023. Acoustofluidics-Assisted Coating of Microparticles. *Polymers (Basel),* 15, https://doi.org/10.3390/polym15194033

Yi, S. W.,Kim, H. J.,Oh, H. J.,Shin, H.,Lee, J. S.,Park, J. S. and Park, K.-H. 2018. Gene expression profiling of chondrogenic differentiation by dexamethasone-conjugated polyethyleneimine with SOX trio genes in stem cells. *Stem Cell Research & Therapy,* 9**,** 341, https://doi.org/10.1186/s13287-018-0998-7

Zauner, G.,Kozak, R. P.,Gardner, R. A.,Fernandes, D. L.,Deelder, A. M. and Wuhrer, M. 2012. Protein O-glycosylation analysis. *Biol Chem,* 393**,** 687-708, https://doi.org/10.1515/hsz-2012-0144

Zeng-Brouwers, J.,Pandey, S.,Trebicka, J.,Wygrecka, M. and Schaefer, L. 2020. Communications via the Small Leucine-rich Proteoglycans: Molecular Specificity in Inflammation and Autoimmune Diseases. *J Histochem Cytochem,* 68**,** 887-906, https://doi.org/10.1369/0022155420930303

Zeng, L.,Zhao, T. S.,Wei, L.,Jiang, H. R. and Wu, M. C. 2019. Anion exchange membranes for aqueous acid-based redox flow batteries: Current status and challenges. *Applied Energy,* 233-234**,** 622-643, https://doi.org/https://doi.org/10.1016/j.apenergy.2018.10.063

Zhang, A.,Hu, P.,MacGregor, P.,Xue, Y.,Fan, H.,Suchecki, P.,Olszewski, L. and Liu, A. 2014. Understanding the conformational impact of chemical modifications on monoclonal antibodies with diverse sequence variation using hydrogen/deuterium exchange mass spectrometry and structural modeling. *Anal Chem,* 86**,** 3468-75, https://doi.org/10.1021/ac404130a

Zhang, C.,Zhao, X.,Ao, Y.,Cao, J.,Yang, L. and Duan, X. 2021. Proliferation ability of particulated juvenile allograft cartilage. *J Orthop Surg Res,* 16**,** 56, https://doi.org/10.1186/s13018-020-02199-z

Zhang, Y.,Huang, W.,Xiao, H.,Ruan, S. and Deng, J. 2024. NGF-BMSC-SF/CS composites for repairing knee joint osteochondral defects in rabbits: evaluation of the repair effect and potential underlying mechanisms. *J Orthop Surg Res,* 19**,** 443, https://doi.org/10.1186/s13018-024-04801-0

Zhao, F.,Bai, Y.,Xiang, X. and Pang, X. 2023. The role of fibromodulin in inflammatory responses and diseases associated with inflammation. 14, https://doi.org/10.3389/fimmu.2023.1191787

Zhao, T.,Zhou, Y.,Mao, G.,Zou, Y.,Zhao, J.,Bai, S.,Yang, L. and Wu, X. 2013. Extraction, purification and characterisation of chondroitin sulfate in Chinese sturgeon cartilage. *J Sci Food Agric,* 93**,** 1633-40, https://doi.org/10.1002/jsfa.5937

Zhao, X.,Hu, D. A.,Wu, D.,He, F.,Wang, H.,Huang, L.,Shi, D.,Liu, Q.,Ni, N.,Pakvasa, M.,Zhang, Y.,Fu, K.,Qin, K. H.,Li, A. J.,Hagag, O.,Wang, E. J.,Sabharwal, M.,Wagstaff, W.,Reid, R. R.,Lee, M. J.,Wolf, J. M.,El Dafrawy, M.,Hynes, K.,Strelzow, J.,Ho, S. H.,He, T. C. and Athiviraham, A. 2021. Applications of Biocompatible Scaffold Materials in Stem Cell-Based Cartilage Tissue

Engineering. *Front Bioeng Biotechnol,* 9**,** 603444, https://doi.org/10.3389/fbioe.2021.603444

Zheng, L.,Zhang, Z.,Sheng, P. and Mobasheri, A. 2021. The role of metabolism in chondrocyte dysfunction and the progression of osteoarthritis. *Ageing Research Reviews,* 66**,** 101249, https://doi.org/https://doi.org/10.1016/j.arr.2020.101249

Zheng, Y. H.,Deng, Y. Y.,Lai, W.,Zheng, S. Y.,Bian, H. N.,Liu, Z. A.,Huang, Z. F.,Sun, C. W.,Li, H. H.,Luo, H. M.,Ma, L. H.,Chen, H. X. and Xiong, B. 2018. Effect of bone marrow mesenchymal stem cells on the polarization of macrophages. *Mol Med Rep,* 17**,** 4449-4459, https://doi.org/10.3892/mmr.2018.8457

Zhou, F.,Zhang, X.,Cai, D.,Li, J.,Mu, Q.,Zhang, W.,Zhu, S.,Jiang, Y.,Shen, W.,Zhang, S. and Ouyang, H. W. 2017. Silk fibroin-chondroitin sulfate scaffold with immuno-inhibition property for articular cartilage repair. *Acta Biomater,* 63**,** 64-75, https://doi.org/10.1016/j.actbio.2017.09.005

Zhou, J. Q.,Wan, H. Y.,Wang, Z. X. and Jiang, N. 2023. Stimulating factors for regulation of osteogenic and chondrogenic differentiation of mesenchymal stem cells. *World J Stem Cells,* 15**,** 369-384, https://doi.org/10.4252/wjsc.v15.i5.369

Zhou, X.,Cao, H.,Yuan, Y. and Wu, W. 2020. Biochemical Signals Mediate the Crosstalk between Cartilage and Bone in Osteoarthritis. *Biomed Res Int,* 2020**,** 5720360, https://doi.org/10.1155/2020/5720360

Zhu, W.,Ji, Y.,Wang, Y.,He, D.,Yan, Y.,Su, N.,Zhang, C. and Xing, X.-H. 2018a. Structural characterization and in vitro antioxidant activities of chondroitin sulfate purified from Andrias davidianus cartilage. *Carbohydrate Polymers,* 196**,** 398-404, https://doi.org/https://doi.org/10.1016/j.carbpol.2018.05.047

Zhu, X.,Sang, L.,Wu, D.,Rong, J. and Jiang, L. 2018b. Effectiveness and safety of glucosamine and chondroitin for the treatment of osteoarthritis: a meta-analysis of randomized controlled trials. *Journal of Orthopaedic Surgery and Research,* 13**,** 170, https://doi.org/10.1186/s13018-018-0871-5

Zimmerman, B. K.,Nims, R. J.,Chen, A.,Hung, C. T. and Ateshian, G. A. 2021. Direct Osmotic Pressure Measurements in Articular Cartilage Demonstrate Nonideal and Concentration-Dependent Phenomena. *J Biomech Eng,* 143, https://doi.org/10.1115/1.4049158

Zwickl, H.,Niculescu-Morzsa, E.,Halbwirth, F.,Bauer, C.,Jeyakumar, V.,Reutterer, A.,Berger, M. and Nehrer, S. 2016. Correlation Analysis of SOX9, -5, and -6 as well as COL2A1 and Aggrecan Gene Expression of Collagen I Implant-Derived and Osteoarthritic Chondrocytes. *Cartilage,* 7**,** 185-92, https://doi.org/10.1177/1947603515615388